

VU Research Portal

Phenotyping the right ventricle in pulmonary hypertension

van der Bruggen, Cathelijne Emma Elisabeth

2021

document version

Publisher's PDF, also known as Version of record

[Link to publication in VU Research Portal](#)

citation for published version (APA)

van der Bruggen, C. E. E. (2021). *Phenotyping the right ventricle in pulmonary hypertension*.

General rights

Copyright and moral rights for the publications made accessible in the public portal are retained by the authors and/or other copyright owners and it is a condition of accessing publications that users recognise and abide by the legal requirements associated with these rights.

- Users may download and print one copy of any publication from the public portal for the purpose of private study or research.
- You may not further distribute the material or use it for any profit-making activity or commercial gain
- You may freely distribute the URL identifying the publication in the public portal ?

Take down policy

If you believe that this document breaches copyright please contact us providing details, and we will remove access to the work immediately and investigate your claim.

E-mail address:

vuresearchportal.ub@vu.nl

PHENOTYPING THE RIGHT VENTRICLE IN PULMONARY HYPERTENSION

Cathelijne Emma Elisabeth van der Bruggen

Financial support for printing and distribution of this thesis was provided by:
Vrije Universiteit, Amsterdam

ISBN: 978-94-6416-523-4

Cover design: C.M. Happé
Lay-out & Printing: Ridderprint | www.ridderprint.nl

© C.E.E. van der Bruggen, Eindhoven 2021

All rights reserved. No part of this thesis may be reproduced, stored in a retrieval system, in any form or by any means without prior written permission by the author or from the publisher holding the copyright of the published articles

VRIJE UNIVERSITEIT

Phenotyping the right ventricle in pulmonary hypertension

ACADEMISCH PROEFSCHRIFT

ter verkrijging van de graad Doctor
aan de Vrije Universiteit Amsterdam,
op gezag van de rector magnificus
prof.dr. V. Subramaniam,
in het openbaar te verdedigen
ten overstaan van de promotiecommissie
van de Faculteit der Geneeskunde
op vrijdag 1 oktober 2021 om 11.45
in de aula van de universiteit,
De Boelelaan 1105

door

Cathelijne Emma Elisabeth van der Bruggen

geboren te Veghel

Promotor: prof.dr. A. Vonk Noordegraaf

Copromotoren: dr. F.S. Handoko - de Man
prof.dr. H.J. Bogaard

Leescommissie: Prof.dr. S.A.J. Chamuleau
Prof.dr. B.K. Velthuis
Prof.dr. S.M. Kawut
Dr. R.H.H. van Balkom
Dr. B. Bartelds
Dr. J. Altenburg

Paranimfen: Pia Trip
Gerrina Ruiter

The work presented in this thesis was performed at the department of Pulmonary Medicine of the Amsterdam UMC, location VUmc / Amsterdam Cardiovascular Sciences, Amsterdam, the Netherlands

*'Ciò che il cuore conosce oggi,
la testa comprenderà domani'*
Lucius Annaeus Seneca

Voor mijn oma's

TABLE OF CONTENTS

Chapter 1 General introduction and thesis outline

Part I: Right ventricular adaptation in pulmonary arterial hypertension

Chapter 2 Bone Morphogenetic Protein Receptor Type 2 mutation in pulmonary arterial hypertension: a view on the right ventricle
Circulation, 2016

Chapter 3 Contribution of impaired parasympathetic activity to right ventricular dysfunction and pulmonary vascular remodeling in pulmonary arterial hypertension
Circulation, 2018

Chapter 4 Interplay of sex hormones and long-term right ventricular adaptation in a Dutch pulmonary arterial hypertension cohort
Submitted

Chapter 5 Right ventricular pressure overload: From hypertrophy to failure
Cardiovascular research, 2017

Part II: Novel insights in (assessing) treatment response in pulmonary arterial hypertension

Chapter 6 The value of hemodynamic measurements or cardiac magnetic resonance imaging in the follow-up of patients with idiopathic pulmonary arterial hypertension
Chest, 2020

Chapter 7 Treatment response in patients with idiopathic pulmonary arterial hypertension and a severely reduced diffusion capacity
Pulmonary Circulation, 2017

Chapter 8 Imaging in Pulmonary Hypertension
ERS Monograph, 2016

Chapter 9 Summary and future perspectives

Addendum Nederlandse samenvatting
List of publications
Curriculum Vitae
Dankwoord

1

GENERAL INTRODUCTION AND THESIS OUTLINE

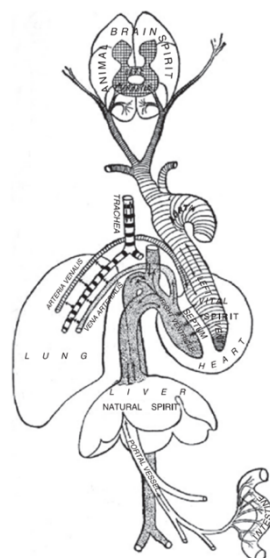
Cathelijne E.E. van der Bruggen

THE HISTORY OF THE PULMONARY CIRCULATION

The first systematic explanation of the cardiopulmonary circulation was provided in the second century AD, by the Roman scientist and philosopher Galen.(1) In his extensive theory, which would dominate and influence the Western medical science for at least 15 centuries, he claimed that blood was formed in the liver with components originating from the gut. The blood would flow into the right ventricle, from where it would divide into two blood flows. Some blood would 'nourish' the lungs via the pulmonary artery, and some blood would flow directly into the left ventricle (LV) via invisible pores in the interventricular septum. The blood that went into the LV would gain the 'vital spirit' via 'pneuma' or 'soul' which was retrieved from the inhaled air. Through the arterial system peripheral tissues could be provided with the vital spirit. After that, the blood would disappear and its waste products would travel back via the pulmonary vein to the lungs, where they could be exhaled in the expired air (Figure 1.1).(1,2)

Despite the discovery of the Persian physician, theologian and jurist Ibn al-Nafis in the 13th century that no direct pathway between the right- and left ventricle existed and blood therefore had to pass the lungs before returning to the LV, it would take the Western medical society until the 17th century to cautiously leave Galen's theory. In 1628, William Harvey published his '*Exercitatio Anatomica de Motu Cordis et Sanguinis in Animalibus*'.(3) He argued: 'If Nature does nothing in vain, she would not have added the right ventricle (RV) for the sole purpose of nourishing the lungs, but to propel blood through the lungs in the cavity of the LV!'(3) In the same century, Marcello Malpighi discovered the pulmonary capillaries and alveoli.(4) Ever since, enormous progress has been made in understanding the pulmonary circulation.

Figure 1.1 – The Cardiopulmonary system according to Galen. (2)



THE PULMONARY CIRCULATION

The main function of the pulmonary circulation is to transport deoxygenated blood from the RV into the lungs, where oxygen uptake and carbon dioxide elimination takes place through the alveolar-capillary membrane. After that, the oxygenated blood is transported to the LV and is distributed to all organs by the systemic circulation. The pulmonary circulation is characterized as a low pressure, high flow system. The RV, generating this low pressure, is characterized by a crescent shape and thin muscular wall when compared to the LV. (5–7) The present thesis focuses on a disease affecting the pulmonary circulation; pulmonary hypertension.

PULMONARY HYPERTENSION AND THE RIGHT VENTRICLE

Pulmonary hypertension (PH) is a hemodynamic condition characterized by an elevated mean pulmonary artery pressure (mPAP). During the first World Symposium on PH in 1973 in Geneva, PH has been defined as a mPAP ≥ 25 mmHg measured during a right heart catheterization (RHC).(8) In 2018, this definition was revised after Kovacs et al. demonstrated in a systematic review that healthy individuals had a resting mPAP of 14.0 ± 3.3 mmHg, leading to an upper limit of normal of >20 mmHg.(8,9)

The pathophysiological process behind the development of PH is dependent of the underlying etiology. Despite the fact that all PH entities are characterized by an increased mPAP and pulmonary vascular resistance (PVR), prognosis and treatment strategies vary significantly. Therefore, PH is categorized in five main subtypes based their clinical, pathophysiological and therapeutic characteristics, as can be observed in *Table 1.1*. (8) The most common forms are PH due to left heart diseases and PH due to lung diseases. Regardless of the underlying entity, patients with PH present with non-specific symptoms such as exertional dyspnea, exercise intolerance, palpitations and syncope. As a result, patients are often diagnosed by the time their disease is already in an advanced state. Even in the modern treatment era, survival rates are still unsatisfactorily low in all groups.(10–13)

Pulmonary arterial hypertension (PAH, group 1) is a diagnosis per exclusionem and cannot coexist with the other PH subtypes. PAH is characterized by excessive pulmonary vascular remodeling and proliferation, resulting in a progressive increase in PVR. To maintain stroke volume and cardiac output, the RV has to undergo morphological and functional adaptation. As a comparison, the LV has to cope with a 50% increase in pressure in systemic hypertension, while the RV in PAH has to cope with a 400-500% increase in pressure.(14) When faced with this increased load, the RV initially adapts by increasing its contractility via the enhancement of intrinsic contractile properties of the cardiomyocyte and via muscular hypertrophy.(14,15) However, as the load progressively increases, the hypertrophic response will be hampered and a vicious circle of RV dilatation, RV systolic dysfunction and RV diastolic dysfunction is

entered (Figure 1.2). Right heart failure is the main cause of death in PAH, and markers of RV adaptation and failure are of great prognostic value in PAH-patients.(16–19)

Intriguingly, the response to rather than the amount of pressure overload determines the fate of the RV in PAH patients.(17) Although it is currently unknown what the transition from an adaptive to failing RV triggers, several mechanisms could play a role. In this thesis, we focus on the possible roles of genetics, the neurohormonal system and sex.

Table 1.1 – Clinical classification of pulmonary hypertension as proposed on the Sixth World Symposium on Pulmonary Hypertension (8)

1. Pulmonary Arterial Hypertension
1.1 Idiopathic PAH
1.2 Heritable PAH
1.3 Drugs and toxins induced
1.4 Associated with:
1.4.1 Connective tissue disease
1.4.2 Human immunodeficiency virus (HIV) infection
1.4.3 Portal hypertension
1.4.4 Congenital heart disease
1.4.5 Schistosomiasis
1.5 PAH long-term responders to calcium channel blockers
1.6 PAH with over features of venous/capillaries (PVOD/PCH) involvement
1.7 Persistent PH of the newborn syndrome
2. Pulmonary Hypertension due to left heart disease
3. Pulmonary Hypertension due to lung diseases and/or hypoxia
4. Chronic Thromboembolic Pulmonary Hypertension and other pulmonary artery obstructions
5. Pulmonary hypertension with unclear and/or multifactorial mechanisms

THE GENETICS OF PULMONARY ARTERIAL HYPERTENSION

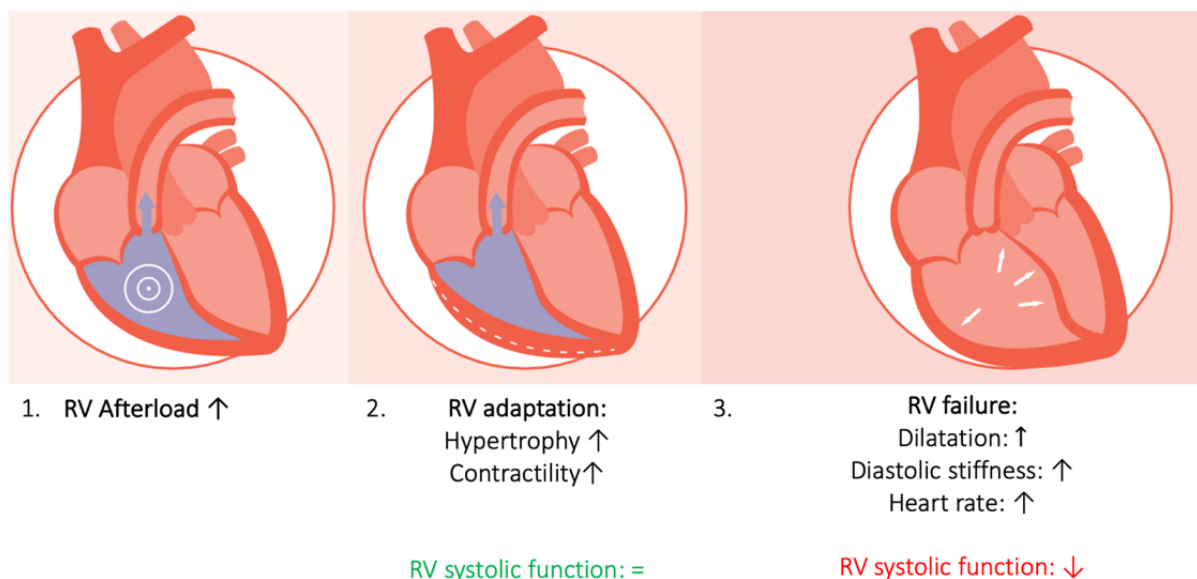
Hereditary PAH-patients (Group 1.2) have a younger age at diagnosis, often present with worse hemodynamic features and have a worse prognosis compared to idiopathic PAH-patients.(20,21) In 2000, Deng et al. and Thomson et al. identified the first gene to cause pulmonary hypertension: the Bone Morphogenetic Protein Receptor type 2 (BMPR2), a member of the Transforming Growth Factor β (TGF- β) superfamily.(22,23) To date, the BMPR2 mutation remains the most common mutation, with mutations in 53-86% of patients with a family history and in 14-35% of patients with IPAH.(24,25) Transmission occurs in an autosomal dominant manner. Interestingly, BMPR2 mutations have incomplete penetrance, estimated to be 14% for males and 42% for females.(26) In recent years, sixteen additional genes in which mutation may cause PAH are identified. Remarkably, the vast majority of these genes participate in the TGF- β /BMPR2 pathway and lead to a relative increase in TGF- β activity. It is known that TGF- β activity is pivotal to protect the heart against dilatation and matrix

degeneration in case of a pressure-overload. However, it is unknown what the effects of the BMPR2 mutation is on RV function and adaptation. Excessive TGF- β signaling might be detrimental in case of a pressure-overloaded RV, because of maladapted hypertrophy and myocardial dysfunction.(27,28)

THE NEUROHORMONAL SYSTEM IN PULMONARY ARTERIAL HYPERTENSION

To maintain cardiac output and enhance contractility and hypertrophy in the short term, the sympathetic nervous system is upregulated and overstimulated in PAH.(29,30) However, in the long term, overstimulation of the sympathetic nervous system proved to be detrimental. In preclinical studies, a partial restoration of the sympathetic overdrive by beta-blocker therapy led to an improved systolic and diastolic RV function and thereby a survival benefit.(31,32)

Figure 1.2 – The Right Ventricle in Pulmonary Arterial Hypertension, adapted from Vonk Noordegraaf et al.(14)



Unfortunately, a randomized, placebo-controlled trial did not favor the use of bisoprolol in IPAH.(33) Less studied is the counterpart of the sympathetic nervous system, the parasympathetic nervous system. The both systems are connected in such a way that increased activity in one will result in reduced activity in the other. In PAH-patients, markers of parasympathetic activity are strong predictors of prognosis.(34) However, it is currently unknown whether enhancing the parasympathetic activity might play a beneficial role in preventing the transition from RV adaptive remodeling to RV failure.

THE ROLE OF SEX IN PULMONARY ARTERIAL HYPERTENSION

The prevalence of PAH in females is known to be two times higher than in males. However, survival of female patients is significantly higher than in males. (11,35,36) Previous studies

suggest that this survival benefit might be explained by a differential response of the RV to the altering afterload. (35) Estrogens, androgens and their precursors (dehydroepiandrosterone sulfate, DHEAs), are known to be involved in RV adaptation and maladaptation to a pressure overload. Due to fluctuating sex hormones, specifically estrogen, in premenopausal women, clinical studies and analyses are challenging. Therefore, the exact interplay between sex hormones and RV adaptation and maladaptation currently remains elusive.

TREATMENT RESPONSE IN PULMONARY ARTERIAL HYPERTENSION

Conventionally, management of PAH-patients is based on functional (i.e. six-minute walking distance, New York Heart Association (NYHA) -classification) and invasive measurements obtained during right heart catheterization (RHC). However, as previously mentioned, non-invasive measurements obtained via CMR are of great predictive value in PAH-patients. (16–18,37,38). The non-invasive character of CMR may provide a more patient-friendly routine follow-up in PAH-patients with minimal risks. Whether CMR is a suitable modality to monitor idiopathic PAH-patients in comparison to invasive and/or functional measurements remains to be established.

OUTLINE OF THIS THESIS

In Part I, we aimed to identify possible factors affecting the transition of RV adaptation towards RV failure in PAH. In **Chapter 2**, we investigated RV function in PAH-patients with and without the BMPR2 mutation by combining in vivo measurements with molecular and histological analysis of human RV and LV tissue. In **Chapter 3**, the relationship between parasympathetic activity and RV function in PAH-patients was studied. In addition, the potential therapeutic effects of pyridostigmine were studied in experimental PH. Pyridostigmine is an oral drug stimulating the parasympathetic activity via acetylcholinesterase inhibition, and is currently prescribed to patients with Myasthenia Gravis. Whether sex and age influence the RV response to pressure-overload was studied in **Chapter 4**. In **Chapter 5**, we provide a perspective on the mechanisms of RV adaptation in PAH and discuss which mechanisms play a role in the transition from RV adaptation to RV failure by comparing different etiologies of RV pressure overload.

In Part II of this thesis we focus on novel insights in (assessing) treatment response in PAH. In **Chapter 6**, we aimed to compare non-invasive and invasive follow-up in PAH-patients. In **Chapter 7**, we investigated whether the hemodynamic and cardiac responses to PAH-specific therapy are different between patients with IPAH patients and a severely reduced diffusion capacity of the lung for carbon monoxide compared to IPAH patients with a more preserved diffusion capacity of the lung for carbon monoxide. Lastly, in **Chapter 8**, we discuss the different imaging modalities used during the diagnosis and follow-up of PH patients.

REFERENCES

1. West J. The Human Pulmonary Circulation: Historical Introduction. In: Textbook of Pulmonary Vascular Disease. 2011.
2. Singer C. A short history of anatomy and physiology from the Greeks to Harvey. Dover, New York; 1957.
3. Harvey W. The works of William Harvey. Philadelphia: University of Pennsylvania Press; 1989.
4. Young J. Malphigi's De Pulmonibus. In: R Soc Med Proc 23:1: 1-11. 1929.
5. Vonk Noordegraaf A, Chin KM, Haddad F, Hassoun PM, Hemnes AR, Hopkins SR, e.a. Pathophysiology of the right ventricle and of the pulmonary circulation in pulmonary hypertension: an update. *Eur Respir J*. januari 2019;53(1).
6. Naeije R, Vanderpool R, Peacock A, Badagliacca R. The Right Heart-Pulmonary Circulation Unit: Physiopathology. *Heart Fail Clin*. juli 2018;14(3):237-45.
7. Haddad F, Doyle R, Murphy DJ, Hunt SA. Right ventricular function in cardiovascular disease, part II: pathophysiology, clinical importance, and management of right ventricular failure. *Circulation*. 1 april 2008;117(13):1717-31.
8. Simonneau G, Montani D, Celermajer DS, Denton CP, Gatzoulis MA, Krowka M, e.a. Haemodynamic definitions and updated clinical classification of pulmonary hypertension. *Eur Respir J* [Internet]. 1 januari 2018 [geciteerd 19 november 2019]; Beschikbaar op: <https://erj.ersjournals.com/content/early/2018/10/11/13993003.01913-2018>
9. Kovacs G, Berghold A, Scheidl S, Olschewski H. Pulmonary arterial pressure during rest and exercise in healthy subjects: a systematic review. *Eur Respir J*. 1 oktober 2009;34(4):888-94.
10. Benza RL, Miller DP, Barst RJ, Badesch DB, Frost AE, McGoon MD. An evaluation of long-term survival from time of diagnosis in pulmonary arterial hypertension from the REVEAL Registry. *Chest*. augustus 2012;142(2):448-56.
11. Humbert M, Sitbon O, Chaouat A, Bertocchi M, Habib G, Gressin V, e.a. Survival in patients with idiopathic, familial, and anorexigen-associated pulmonary arterial hypertension in the modern management era. *Circulation*. 13 juli 2010;122(2):156-63.
12. Gall H, Felix JF, Schneck FK, Milger K, Sommer N, Voswinckel R, e.a. The Giessen Pulmonary Hypertension Registry: Survival in pulmonary hypertension subgroups. *J Heart Lung Transplant Off Publ Int Soc Heart Transplant*. september 2017;36(9):957-67.
13. Wijeratne TD, Lajkosz K, Brogly SB, Loughheed MD, Jiang L, Housin A, e.a. Increasing Incidence and Prevalence of WHO Groups 1-4 Pulmonary Hypertension: A Population-Based Cohort Study in Ontario, Canada. *Circ Cardiovasc Qual Outcomes*. februari 2018;11(2):e003973.
14. Vonk Noordegraaf A, Westerhof BE, Westerhof N. The Relationship Between the Right Ventricle and its Load in Pulmonary Hypertension. *J Am Coll Cardiol*. 17 januari 2017;69(2):236-43.
15. van der Bruggen CEE, Tedford RJ, Handoko ML, van der Velden J, de Man FS. RV pressure overload: from hypertrophy to failure. *Cardiovasc Res*. 1 oktober 2017;113(12):1423-32.
16. van Wolferen SA, Marcus JT, Boonstra A, Marques KMJ, Bronzwaer JGF, Spreeuwenberg MD, e.a. Prognostic value of right ventricular mass, volume, and function in idiopathic pulmonary arterial hypertension. *Eur Heart J*. mei 2007;28(10):1250-7.
17. van de Veerdonk MC, Kind T, Marcus JT, Mauritz G-J, Heymans MW, Bogaard H-J, e.a. Progressive right ventricular dysfunction in patients with pulmonary arterial hypertension responding to therapy. *J Am Coll Cardiol*. 6 december 2011;58(24):2511-9.
18. Swift AJ, Capener D, Johns C, Hamilton N, Rothman A, Elliot C, e.a. Magnetic Resonance Imaging in the Prognostic Evaluation of Patients with Pulmonary Arterial Hypertension. *Am J Respir Crit Care Med*. 15 2017;196(2):228-39.

19. Courand P-Y, Pina Jomir G, Khouatra C, Scheiber C, Turquier S, Glérant J-C, e.a. Prognostic value of right ventricular ejection fraction in pulmonary arterial hypertension. *Eur Respir J*. januari 2015;45(1):139–49.
20. Sztrymf B, Coulet F, Girerd B, Yaici A, Jais X, Sitbon O, e.a. Clinical outcomes of pulmonary arterial hypertension in carriers of BMPR2 mutation. *Am J Respir Crit Care Med*. 15 juni 2008;177(12):1377–83.
21. BMPR2 mutations and survival in pulmonary arterial hypertension: an individual participant data meta-analysis. - PubMed - NCBI [Internet]. [geciteerd 19 november 2019]. Beschikbaar op: <https://www.ncbi.nlm.nih.gov/pubmed/26795434>
22. Deng Z, Morse JH, Slager SL, Cuervo N, Moore KJ, Venetos G, e.a. Familial primary pulmonary hypertension (gene PPH1) is caused by mutations in the bone morphogenetic protein receptor-II gene. *Am J Hum Genet*. september 2000;67(3):737–44.
23. Thomson JR, Machado RD, Pauciulo MW, Morgan NV, Humbert M, Elliott GC, e.a. Sporadic primary pulmonary hypertension is associated with germline mutations of the gene encoding BMPR-II, a receptor member of the TGF-beta family. *J Med Genet*. oktober 2000;37(10):741–5.
24. Southgate L, Machado RD, Gräf S, Morrell NW. Molecular genetic framework underlying pulmonary arterial hypertension. *Nat Rev Cardiol*. 12 augustus 2019;1–11.
25. Machado RD, Southgate L, Eichstaedt CA, Aldred MA, Austin ED, Best DH, e.a. Pulmonary Arterial Hypertension: A Current Perspective on Established and Emerging Molecular Genetic Defects. *Hum Mutat*. december 2015;36(12):1113–27.
26. Larkin EK, Newman JH, Austin ED, Hemnes AR, Wheeler L, Robbins IM, e.a. Longitudinal analysis casts doubt on the presence of genetic anticipation in heritable pulmonary arterial hypertension. *Am J Respir Crit Care Med*. 1 november 2012;186(9):892–6.
27. Koitabashi N, Danner T, Zaiman AL, Pinto YM, Rowell J, Mankowski J, e.a. Pivotal role of cardiomyocyte TGF- β signaling in the murine pathological response to sustained pressure overload. *J Clin Invest*. juni 2011;121(6):2301–12.
28. Dobaczewski M, Chen W, Frangogiannis NG. Transforming growth factor (TGF)- β signaling in cardiac remodeling. *J Mol Cell Cardiol*. oktober 2011;51(4):600–6.
29. Bristow MR, Ginsburg R, Umans V, Fowler M, Minobe W, Rasmussen R, e.a. Beta 1- and beta 2-adrenergic-receptor subpopulations in nonfailing and failing human ventricular myocardium: coupling of both receptor subtypes to muscle contraction and selective beta 1-receptor down-regulation in heart failure. *Circ Res*. september 1986;59(3):297–309.
30. Ciarka A, Doan V, Velez-Roa S, Naeije R, van de Borne P. Prognostic significance of sympathetic nervous system activation in pulmonary arterial hypertension. *Am J Respir Crit Care Med*. 1 juni 2010;181(11):1269–75.
31. de Man FS, Handoko ML, van Ballegoij JJM, Schalij I, Bogaards SJP, Postmus PE, e.a. Bisoprolol delays progression towards right heart failure in experimental pulmonary hypertension. *Circ Heart Fail*. januari 2012;5(1):97–105.
32. Bogaard HJ, Natarajan R, Mizuno S, Abbate A, Chang PJ, Chau VQ, e.a. Adrenergic receptor blockade reverses right heart remodeling and dysfunction in pulmonary hypertensive rats. *Am J Respir Crit Care Med*. 1 september 2010;182(5):652–60.
33. van Campen JSJA, de Boer K, van de Veerdonk MC, van der Bruggen CEE, Allaart CP, Raijmakers PG, e.a. Bisoprolol in idiopathic pulmonary arterial hypertension: an explorative study. *Eur Respir J*. 2016;48(3):787–96.
34. Minai OA, Gudavalli R, Mummadi S, Liu X, McCarthy K, Dweik RA. Heart rate recovery predicts clinical worsening in patients with pulmonary arterial hypertension. *Am J Respir Crit Care Med*. 15 februari 2012;185(4):400–8.
35. Jacobs W, van de Veerdonk MC, Trip P, de Man F, Heymans MW, Marcus JT, e.a. The right ventricle explains sex differences in survival in idiopathic pulmonary arterial hypertension. *Chest*. juni 2014;145(6):1230–6.

36. Shapiro S, Traiger GL, Turner M, McGoon MD, Wason P, Barst RJ. Sex differences in the diagnosis, treatment, and outcome of patients with pulmonary arterial hypertension enrolled in the registry to evaluate early and long-term pulmonary arterial hypertension disease management. *Chest*. februari 2012;141(2):363–73.
37. van de Veerdonk MC, Marcus JT, Westerhof N, de Man FS, Boonstra A, Heymans MW, e.a. Signs of right ventricular deterioration in clinically stable patients with pulmonary arterial hypertension. *Chest*. april 2015;147(4):1063–71.
38. Swift AJ, Rajaram S, Campbell MJ, Hurdman J, Thomas S, Capener D, e.a. Prognostic value of cardiovascular magnetic resonance imaging measurements corrected for age and sex in idiopathic pulmonary arterial hypertension. *Circ Cardiovasc Imaging*. januari 2014;7(1):100–6.

PART I

RIGHT VENTRICULAR ADAPTATION IN
PULMONARY ARTERIAL HYPERTENSION

2

BONE MORPHOGENETIC PROTEIN RECEPTOR TYPE II MUTATION IN PULMONARY ARTERIAL HYPERTENSION: A VIEW ON THE RIGHT VENTRICLE

CEE van der Bruggen & CM Happé, P Dorfmueller, P Trip, OA Spruijt, N Rol, FP Hoevenaars, AC Houweling, B Girerd, JT Marcus, O Mercier, M Humbert, ML Handoko, J van der Velden, A Vonk Noordegraaf, HJ Bogaard, MJ Goumans, FS de Man

Circulation, 2016

ABSTRACT

Background: The effect of a mutation in the *bone morphogenetic protein receptor 2 gene (BMPR2)* on right ventricular (RV) pressure overload in patients with pulmonary arterial hypertension (PAH) is unknown. Therefore, we investigated RV function in PAH-patients with and without *BMPR2* mutation by combining in vivo measurements with molecular and histological analysis of human RV and left ventricular (LV) tissue.

Methods & Results: In total, 95 idiopathic or familial PAH patients were genetically screened for the presence of a *BMPR2* mutation: 28 patients had a *BMPR2* mutation, 67 patients did not have a *BMPR2* mutation. In vivo measurements were assessed using right heart catheterization (RHC) and cardiac magnetic resonance imaging. Despite a similar mean pulmonary artery pressure (non-carriers 54 ± 15 vs. mutation carriers 55 ± 9 mmHg) and pulmonary vascular resistance (755 (483 - 1043) vs. 931 (624 - 1311) dynes*s/cm⁵), mutation carriers presented with a more severely compromised RV function (RV ejection fraction: 37.6 ± 12.8 vs. 29.0 ± 9 %: $p < 0.05$, cardiac index 2.7 ± 0.9 vs. 2.2 ± 0.4 l/min/m²). Differences continued to exist after treatment. To investigate the role of TGF- β and BMPRII signaling, human RV and LV tissue were studied in controls ($n=6$), mutation carriers ($n=5$) and non-carriers ($n=11$). However, TGF- β and BMPRII signaling, as well as hypertrophy, apoptosis, fibrosis, capillary density, inflammation and cardiac metabolism were similar between mutation carriers and non-carriers.

Conclusion: Despite a similar afterload, RV function is more severely affected in mutation carriers compared to non-carriers. However, these differences cannot be explained by a differential TGF- β , BMPRII signaling or cardiac adaptation.

INTRODUCTION

Pulmonary arterial hypertension (PAH) is a rapidly progressive and lethal disease, characterized by an increase in resistance of the pulmonary arterioles, causing an increased right ventricular (RV) afterload.¹⁻³ The RV adapts to this increased load via several compensatory mechanisms but these are not sufficient to prevent progression to RV dysfunction and failure, which is the predominant cause of death in PAH.⁴ Intriguingly, this clinical observation suggests that the *response* to rather than the *amount of* pressure overload determines the fate of the RV in PAH-patients.

Patients with PAH may have an underlying genetic predisposition, in particular a mutation in the *bone morphogenetic protein receptor type 2 (BMPR2)* gene.⁵⁻¹¹ *BMPR2* mutations are an autosomal dominant cause of PAH with reduced penetrance (14% in men, 42% in women) clinically characterized by a younger age and a more severe hemodynamic compromise at presentation compared to idiopathic PAH patients.^{10,12-15} The bone morphogenetic protein receptor II (BMPRII) encoded by the *BMPR2* gene belongs to the transforming growth factor β (TGF- β) superfamily and mutations have been shown to result in a disturbed BMP/TGF- β balance.¹⁶⁻¹⁸ Decreased BMPRII activity leads to an overactivated TGF- β signaling, which stimulates vasculogenesis, intimal hyperplasia and medial smooth muscle growth in the pulmonary vasculature.^{19,20} In addition, growing evidence suggests a key role for TGF- β signaling in the response to pressure overload of the heart.²¹⁻²³

While TGF- β signaling is necessary to protect the heart against uncontrolled matrix degradation and dilatation, excessive TGF- β signaling might be detrimental due to maladapted hypertrophy and myocardial dysfunction, as previously described in left heart failure.²¹⁻²³ Furthermore, a recent study by Hemnes et al. showed that the RV hypertrophic response was disturbed in pulmonary hypertensive mice carrying a *BMPR2* mutation.²⁴ However, whether RV function and adaptation in PAH-patients carrying a *BMPR2* mutation differs from PAH-patients without identified *BMPR2* mutation remains currently elusive. Therefore, the aim of this study was two-fold: 1) to determine the effects of a *BMPR2* mutation on RV function in PAH patients and 2) to compare the histological and morphological characteristics of RV tissue samples from PAH-patients with and without a *BMPR2* mutation.

METHODS

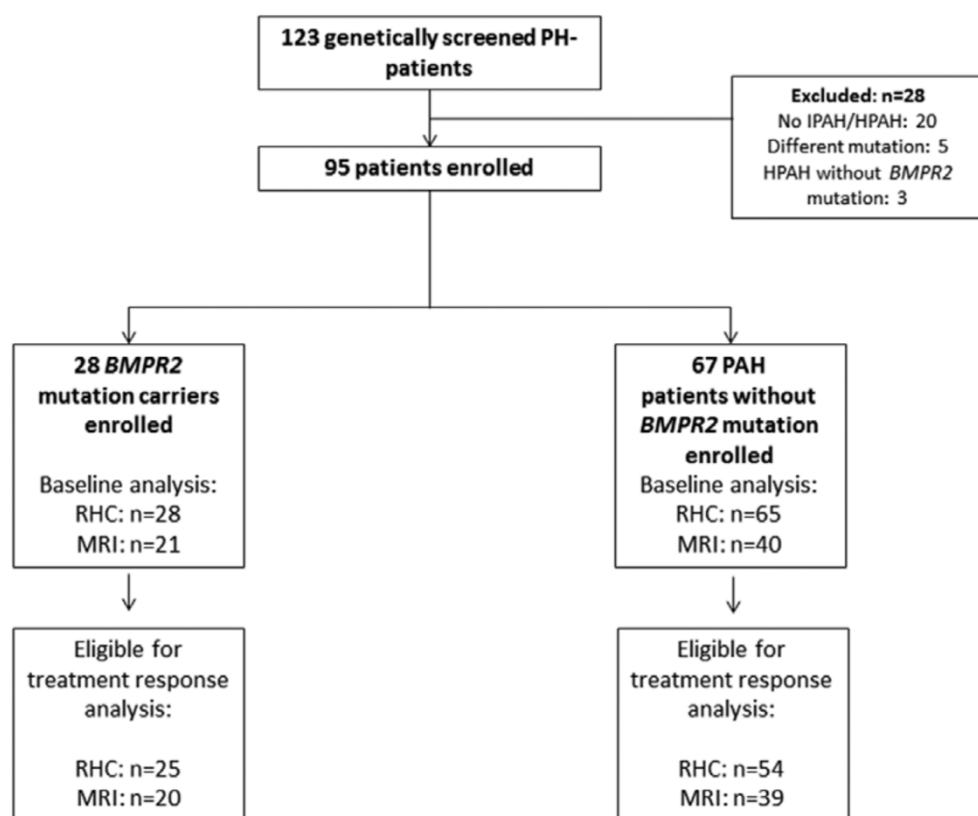
Study population

Clinical study: We retrospectively reviewed PAH patients seen at the VU University Medical Center (Amsterdam, the Netherlands) between March 1995 and October 2014. Patients were eligible for this study when the results from *BMPR2* mutation analysis were available. In total, 123 PAH-patients were genetically screened for the presence of a *BMPR2* mutation. After the exclusion of 28 patients, 95 patients were included in this study. 28 patients were carriers of a *BMPR2* mutation (mutation carriers) and no *BMPR2* mutation was identified in 67 sporadic

PAH patients (non-carriers). Patients with a family history of PAH with no evidence of a *BMPR2* mutation (n=3) or patients with a genetic mutation linked to pulmonary hypertension other than the *BMPR2* mutation (n=5) were excluded from the analysis to avoid the risk of misclassification in the *BMPR2* non-carriers group. For comparison a group of 15 control subjects without PAH family history was included in this study. Controls were selected from referred patients suspected with PAH but in whom the condition was ruled out after right heart catheterization (RHC). A subset of patients was eligible for treatment response analysis. (Figure 2.1) Patients were diagnosed with idiopathic PAH according to current clinical guidelines, by means of RHC and by ruling out all associated conditions of PH by a multidisciplinary team.²⁵ All genetically tested patients signed written informed consent and received genetic counseling.

Because the MRI and RHC data were obtained for clinical purposes and analyzed retrospectively, the Medical Ethics Review Committee of the VU University Medical Center did not consider this study to fall within the scope of the Medical Research Involving Human Subjects Act. Therefore, no additional approval was acquired.

Figure 2.1 – Flow chart



Schematic overview of study populations. PH: pulmonary hypertension; IPAH: idiopathic pulmonary arterial hypertension, HPAH; hereditary pulmonary arterial hypertension, *BMPR2*: bone morphogenetic protein receptor 2, RHC: right heart catheterization, MRI: magnetic resonance imaging.

Cardiac tissue samples: Explanted RV and LV tissue samples were collected from PAH patients undergoing heart/lung transplantation in the French Referral Centre for Pulmonary Hypertension (Université Paris-Sud, France) (mutation carriers n=5, non-carriers n=11). Control RV and LV tissue was obtained from non-failing donors (n=6). Human cardiac tissue collection and use by collaborating universities (VU Medical Center, Amsterdam) was approved by the Human Research Ethics Committee of the Université Paris-Sud - Inserm U999 (ID RBC 2008-A00485-50). Written informed consent was obtained. All samples were stored in paraffin.

Genetic analysis of the *BMPR2* gene

Genomic DNA was extracted from peripheral blood samples after the patients gave informed consent. The coding sequences and the surrounding splice sites of the *BMPR2* gene were amplified by polymerase chain reaction (PCR). PCR amplification was performed using a PE9700 thermocycles (Applied Biosystems, Forster City, CA, USA). Sequencing reactions were performed using the Big Dye Terminator system (Applied Biosystems, Forster City, CA, USA) and run on an ABI 3100XL or ABI3730 genetic analyzer (Applied Biosystems, Forster City, CA, USA). To detect deletions and duplications of one or more exons MLPA analysis was performed using MLPA kit P093-A (MRC-Holland, Amsterdam, The Netherlands).

Hemodynamic measurements

A 7-F balloon-tipped Swan Ganz catheter (131HF7, Baxter Healthcare Corp., Irvine, CA, USA) was inserted via the jugular or femoral vein and brought into position under local anesthesia during continuous electrocardiographic monitoring. The following variables were recorded: mean pulmonary artery pressure (mPAP), right atrial pressure (RAP), pulmonary arterial wedge pressure (PAWP), mixed venous oxygen saturation (SvO₂) and heart rate (HR). PVR was calculated via the following formula: $80 \times (\text{mPAP} - \text{PAWP}) / \text{cardiac output (CO)}$. CO was determined by either the Fick method or thermodilution and stroke volume (SV) was calculated as CO divided by HR. Both CO and SV were indexed for body surface area (BSA), shown as respectively cardiac index (CI) and SV index (SVI).

Cardiac magnetic resonance imaging

Cardiac magnetic resonance imaging (MRI) was performed on a Siemens 1.5-Tesla Avanto or 1.5-Tesla Sonato scanner (Siemens Medical Solutions, Erlangen, Germany), equipped with a 6-element phased-array coil. A stack of short-axis images were obtained at breath-hold per slice, with a slice thickness and interslice gap of 5 mm, fully covering both ventricles from base to apex.

On end-diastolic images (first cine after R-wave trigger) and end-systolic images (cine with visually the smallest cavity area), endocardial and epicardial contours were manually drawn using MASS software (Department of Radiology, Leiden University Medical Center, Leiden, The Netherlands) to obtain RV end-diastolic volume (RVEDV), RV end-systolic volume (RVESV) and RV mass. Volume measurements and RV mass were indexed for BSA. Papillary muscles

and trabeculae were included in RV mass. RV ejection fraction (RVEF) is calculated as $(RVEDV - RVESV)/RVEDV \times 100\%$.

Histology and morphometry

Paraffin embedded cardiac sections (5 μ m) were histochemically stained with Hematoxylin-Eosin (HE) and Picrosirius Red using standard methods. Analysis of the cross sectional area (CSA) was performed by randomly selecting 20 transversally cut cardiomyocytes (CMC) in RV and LV (40x magnification) and tracing the exterior of the cell with image analysis software. (Image J 1.45S, National institute of Health, USA). Collagen content was expressed as a percentage collagen positive tissue-area per total field of view, as measured in 5 randomly selected fields (40x magnification).

Immunofluorescent staining was performed using standard methods. Briefly, sections were deparaffinized followed by epitope retrieval with antigen unmasking solution (H3300, Vector Laboratories, USA). Blocking steps with 3% H₂O₂ for endogenous peroxidase and 1% bovine serum albumin (BSA) were performed before labeling with the primary antibodies O/N; phosphorylated (p) SMAD1,5,8 (CS9511, 1:200), p-SMAD2 (CS8828s, 1:100), Von Willebrand Factor (VWf) (used for capillary density analysis) (A0082, DAKO, 1:100), CD45+ (used for inflammation analysis) (M0701, DAKO, 1:200). Subsequent labeling with appropriate FITC-conjugated secondary antibody followed VWf and CD45 labeling. Both p-SMAD1,5,8 and p-SMAD2 sections were labeled with appropriate HRP-conjugated secondary antibodies followed by tyramide signal amplification (TSA) (NEL700A001KT, Perkin Elmer, USA). All sections were counterstained with wheat germ agglutinin (W32464, Life technologies, USA) and 4',6-diamidino-2 phenylindole (DAPI) (H-1200, Vector labs, USA). Image acquisition was performed on a ZEISS Axiovert 200M Marianas inverted microscope. A minimum of 5 fields per section was randomly acquired for analysis. Slidebook 5.5 imaging analysis software (Intelligent Imaging Innovations, Denver, CO) was used to quantify for positive p-SMAD1,5,8 and p-SMAD2 nuclei and expresses as total number of p-SMAD-positive nuclei vs. total nuclei count. CD45+ cells positive cells were expressed as number of positive cells per area. Capillaries (VWF staining) and CMC were semi-automatically counted and expressed as a number of capillaries per CMC.

RNA analysis

RNA was isolated from paraffin embedded RV and LV tissues according to the manufacturer's protocol (73504, Qiagen, Venlo, The Netherlands) followed by purification (74204, Qiagen, Venlo, The Netherlands). Subsequently RNA concentration and purity was assessed using a Nanodrop spectrophotometer (Nanodrop 1000, Thermo Scientific, Breda, The Netherlands). Equal concentrations of RNA of all individual samples was reversely transcribed and amplified (3312-48, NuGEN, Leek, The Netherlands). Differential gene expression was assessed by qRT-PCR using Takyon PCR mastermix (UF-LSMT-B0705, Eurogentec, Maastricht, The

Netherlands) and the CFX96 Touch detection system (Bio-Rad, Veenendaal, The Netherlands). Relative levels of gene expression were obtained using 18s rRNA as reference gene. Data is shown as fold change \pm standard error of the mean (SEM). Target genes, primers sequences and annealing temperatures are shown in Table 2.1.

Statistical analysis

Statistical analyses was performed using Prism 5 for Windows (GraphPad Software Inc, San Diego, CA). The data are presented as means \pm SEM or median (25-75%), dependent on normal distribution. Normal distribution was tested using the D'Agostino and Pearson omnibus normality test. Values of $p < 0.05$ were considered significant.

Differences in patient characteristics, hemodynamics, RV function and RV histology were tested using a one-way ANOVA or Kruskal-Wallis test with proper post-hoc comparison, depending on normal distribution. To compare categorical variables, a chi-squared test was used. Linear regression analysis was used to correct differences in RV function for PVR. Treatment response analysis was performed using a two-way analysis of variance with Bonferroni's multiple comparison test.

Cross sectional area was analyzed using multilevel analysis to correct for nonindependence of successive measurements per patients (MLwiN 2.02.03, Center for Multilevel Modeling, Bristol, UK).

Table 2.1 - Primers used

Genes	Forward Primer 5'–3'	Reverse Primer 5'–3'	Temp (°C)
<i>BMPR2</i>	GTCCTGGATGGCAGCAGTAT	CCAGCGATTCAAGTGGAGATGA	55
<i>TGFbR1</i>	AAGAACGTTCTGGTTCGGT	CTGACACCAACCAGAGCTGA	55
<i>FAS</i>	TTGGTGGACCGCTCAGTA	TGATGTCAGTCACTTGGGCA	55
<i>Caspase 3</i>	CTCTGGTTTTCGGTGGGTGT	CGCTTCCATGTATGATCTTTGGTT	55
<i>ANP</i>	GCAGGATGGACAGGATTGGAG	CTTGTCCTCCCTGGCTGTTAT	60
<i>GLUT1</i>	TTGGCTCCGGTATCGTCAAC	GGCCACGATGCTCAGATAGG	55
<i>Hexokinase 2</i>	CCTGAGGACATCATGCGAGG	TGGACTTGAATCCCTTGGTCC	55
<i>FABP3</i>	CGCCTGCTCTCTTGTAGCTT	GTGGTAGGCTTGGTCATGCT	63
<i>Hexokinase 1</i>	CGCAGCTCCTGGCCTATTAC	GAGCCGCATGGCATAGAGAT	63
<i>CD36</i>	CTGAGGACTGCAGTGTAGGAC	TCACAAATCAACAGCAAGACATGA	63
<i>CPT1B</i>	GGAGCCCTCTCATGGTGAAC	CGGTCCAGTTTACGGCGATA	55
<i>CPT2</i>	CTCCAAGTACCATGGCCAGC	CCGCAGAGCAAACAAGTGTC	55

Abbreviations: *Bmpr2*, bone morphogenetic protein receptor 2; *TgfbR1*, transforming growth factor beta receptor 1; *Fas*, Fas cell surface death receptor; *ANP*, atrial natriuretic peptide; *Glut1*, glucose transporter 1; *Fabp3*, fatty acid binding protein 3; *cpt*, carnitine almitoyltransferase

RESULTS

Patient characteristics

Clinical characteristics of patients seen at the VU University Medical Center are presented in Table 2.2 and supplementary Table 1. No differences between carriers and non-carriers were found in sex or 6 minute walking distance (6MWD). Mutation carriers tended to present at a younger age compared to non-carriers.

BMPR2 mutations

BMPR2 mutations were identified in 15 of 82 (18%) sporadic PAH patients and 13 of 21 (61%) familial PAH patients. Familial patients without *BMPR2* mutation were excluded. Twenty different germline *BMPR2* mutations were identified in the mutation carriers, including three large rearrangements (corresponding to an exon 1 deletion, a deletion from exon 4 to 12 and a deletion of exon 10 to 13) and one duplication of exon 8. (Table 2.3)

Table 2.2 - General characteristics and hemodynamics at baseline

	Controls (n=15)	PAH – Noncarriers (n=67)	PAH – Mutation Carriers (n=28)	P Value*
General characteristics				
Age, y	47±15	49±16	42±14	0.05
Male, %	20	26	20	0.49
6MWD, %pred	–	69.8±26.1	73.4±14.0	0.62
Follow-up time, y	–	1.9 (1.0–4.7)	1.2 (0.8–5.1)	0.34
Hemodynamics				
HR, beats/min	78±14	77±12	86±17	<0.05
mPAP, mm Hg	14±2	54±15	55±9	0.64
mRAP, mm Hg	4 (3–5)	7 (4–12)	7 (5–10)	0.95
SvO ₂ , %	75±6	65±9	63±7	0.32
PAWP, mm Hg	8 (5–11)	10 (7–13)	9 (7–11)	0.55
PVR, dynes·s ⁻¹ ·cm ⁻⁵	69 (49–80)	755 (483–1043)	931 (624–1311)	0.11
CI, L·min ⁻¹ ·m ⁻²	4.1±1.1	2.7±0.9	2.2±0.4	<0.01
SVI, mL/m ²	52.7±12.7	34.5±11.2	26.4±7.8	<0.01
Cardiac MRI				
RVEDVI, mL/m ²	63.8±12.7	77.4±20.1	79.3±21.4	0.74
RVESVI, mL/m ²	25.4±8.4	51.3±21.0	57.0±19.2	0.33
RVEF (%)	62.0±7.4	37.6±12.8	29.0±9.0	0.01
RV mass index, g/m ²	21.6±3.9	54±17	51±11	0.08
LVEDVI, mL/m ²	57.4±11.3	45.4±13.1	40.0±12.9	0.14
LVESVI, mL/m ²	16.1 (15.6–18.0)	15.5 (10.7–20.8)	17.9 (9.2)	0.89
LVEF, %	69.3±10.9	63.9±10.7	61.1±10.9	0.36
LV mass index, g/m ²	56.2±8.6	55.9±13.4	54.5±9.7	0.90

Data are presented as mean \pm SD or median (25-75%), dependent on normal distribution. 6MWD: 6 minute walk distance, HR: heart rate; mPAP: mean pulmonary artery pressure; mRAP: mean right atrial pressure; SvO₂: mixed venous oxygen saturation; PAWP: pulmonary arterial wedge pressure; PVR: pulmonary vascular resistance; CI: cardiac index; SVI: stroke volume index; RVEDVI: right ventricular end-diastolic volume index; RVESVI: right ventricular end-systolic volume index; RVEF: right ventricular ejection fraction; LVEDVI: left ventricular end-diastolic volume index; LVESVI: left ventricular end-systolic volume index; LVEF: ejection fraction. P-value: comparison mutation carriers-non-carriers.

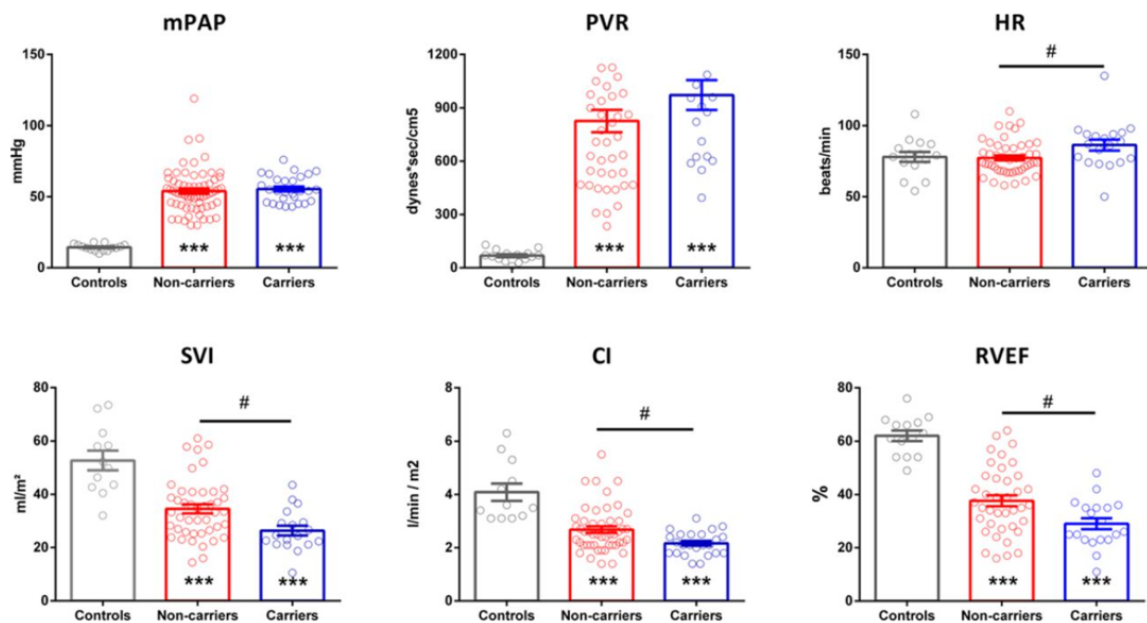
Table 2.3 – Details of BMPR2 mutations

Patient	Mutation Location	Nucleotide Change	Amino Acid Change
1	Intron 1	c.76+2T>C	
2	Exon 1	c.168delG	p.Thr57fs
3	Exon 3	c.350G>C	p.Cys117Ser
4	Exon 3	c.350G>C	p.Cys117Ser
5	Exon 3	c.399delT	p.Pro133fs
6	Exon 3	c.399delT	p.Pro133fs
7	Exon 5	c.619dupG	p.Glu207fs
8	Exon 5	c.619dupG	p.Glu207fs
9	Exon 6	c.637C>T	p.Arg213X
10	Exon 6	c.690delA	p.Val231fs
11	Exon 10	c.1281A>T	p.Glu427Asp
12	Exon 11	c.1454A>G	p.Asp485Gly
13	Exon 11	c.1454A>G	p.Asp485Gly
14	Exon 11	c.1454A>G	p.Asp485Gly
15	Exon 11	c.1454A>G	p.Asp485Gly
16	Exon 11	c.1471C>T	p.Arg491Trp
17	Exon 11	c.1471C>T	p.Arg491Trp
18	Exon 11	c.1525G>T	p.Glu509X
19	Exon 12	c.1978G>T	p.Glu660X
20	Exon 12	c.2413dupA	p.Thr805fs
21	Exon 12	c.2752C>T	p.Gln918X
22	Exon 12	c.2752C>T	p.Gln918X
23	Exon 12	c.2752C>T	p.Gln918X
24	Exon 12	c.2695C>T	p.Arg899X
25		Deletion of exon 1	Large rearrangement
26		Deletion of exon 4–12	Large rearrangement
27		Deletion of exon 10–13	Large rearrangement
28		Duplication of exon 8	Large rearrangement

Treatment response

To assess whether initial changes between mutation carriers and non-carriers at baseline remain after PAH-specific treatment, we performed a treatment response analysis in a subgroup of patients (Supplementary Table 2). Median time between baseline and follow-up was similar for non-carriers and mutation carriers (1.9 years (interquartile range 1.0-4.7) and 1.2 years (interquartile range 0.8-5.1) respectively). Time between RHC and MRI was 2 \pm 7 days in mutation carriers and 1 \pm 6 days in non-carriers. As can be appreciated from Supplementary Table 3, both groups were treated equally. Initial differences between mutation carriers and non-carriers found at baseline (Table 2.2, Figure 2.2) continued to exist under treatment.

Figure 2.2 – Hemodynamic measurements and cardiac function at baseline



mPAP: mean pulmonary artery pressure, PVR: pulmonary vascular resistance, HR: heart rate, CI: cardiac index, SVI: stroke volume index, RVEF: right ventricular ejection fraction. Hemodynamic measurements: controls: n=15, non-carriers: n=65, carriers n=28. RVEF: controls n=15, non-carriers n=40, carriers n=21. Data are presented as mean±SEM. Controls vs. non-carriers or carriers: *, p<0.05, **, p<0.01, ***, p<0.001, non-carriers vs. carriers: #: p<0.05

The effects *BMPR2* mutations on TGF- β /BMP signaling, RV adaptation and cardiac metabolism

To investigate whether the differences observed in the clinical data could be explained by differences in TGF- β or BMP signaling in cardiomyocytes, immunofluorescent stainings and RNA analyses were performed in LV and RV tissue obtained from controls, mutation carriers and non-carriers. Hemodynamic characteristics of tissue samples donors can be observed in Table 2.4. Tissue samples of mutation carriers and non-carriers were matched on pulmonary vascular resistance (PVR) in order to avoid load-dependent differences.

TGF- β /BMP signaling

To assess BMP signaling, the first downstream effector of the BMP signaling cascade was stained, phosphorylated SMAD1,5,8 (p-SMAD1,5,8) (Figure 2.3A). No difference was observed in p-SMAD1,5,8 expression in RV tissue of PAH and controls or between *BMPR2* mutation carriers and non-carriers. However, expression of p-SMAD1,5,8 was significantly reduced in LV tissue of PAH-patients in comparison to controls, although again no difference was found between *BMPR2* mutation carriers and non-carriers.

To assess TGF- β activity, the expression of phosphorylated SMAD2 (p-SMAD2) was determined (Figure 2.3B). Expression of p-SMAD2 was significantly reduced in PAH in

comparison in both RV and LV tissue. However, no differences in p-SMAD2 activity were observed between *BMPR2* mutation carriers and non-carriers.

No differences were observed in RNA expression of *BMPR2* and the TGF- β type I receptor (T β RI) (Figure 2.4A), indicating that TGF- β and BMP activity is similar in cardiomyocytes in *BMPR2* mutation carriers and non-carriers and that other factors may play a role in the different RV adaptation in mutation carriers and non-carriers.

Table 2.4 – Cardiac tissue samples – Patient characteristics RV tissue samples

	Controls (n=6)	PAH – Noncarriers (n=11)	PAH – Mutation Carriers (n=5)	<i>P</i> Value*
Age at death/transplantation, y	67 (46–83)	31 (21–39) \ddagger	44 (29–54)	0.07
Male, %	83	18 \ddagger	40	0.03
NYHA class (I/II/III/IV)	–	0/25/25/50	0/40/60/0	0.16
mPAP, mm Hg	–	68 (47–94)	57 (55–61)	0.57
PVR, dynes·s ⁻¹ ·cm ⁻⁵	–	1200 (774–1974)	1424 (1290–1600)	0.57
CI, L·min ⁻¹ ·m ⁻²	–	1.7 (1.5–2.8)	1.5 (1.4–1.8)	0.21
Heart weights, g	465 (453–553)	403 (330–500)	360 (283–450)	0.07
Cause of death				
Cerebral hemorrhage	2			
Accident	2			
Pneumonia	1			
Acute respiratory distress syndrome	1			

Data are presented as mean \pm SD or median (25–75%), dependent on normal distribution. NYHA class: New York Heart Association Functional class, mPAP: mean arterial pressure, PVR: pulmonary vascular resistance, CI: cardiac index. *P*-value: comparison mutation carriers – non-carriers. Comparison to controls: $\ddagger p < 0.05$, $\ddagger\ddagger p < 0.01$.

RV adaptation

To obtain more insight into the mechanisms of RV and LV adaptation, morphological characteristics of both non-carriers and mutation carriers were assessed. RV hypertrophy and LV atrophy was observed in all PAH-patients in comparison to controls, without differences between mutation carriers and non-carriers (Figure 2.5A). In line with these data, increased expression of ANP was observed in PAH-patients compared to controls, while expression was similar in carriers and non-carriers (Figure 2.4B).

RV fibrosis was increased in PAH-patients in comparison to control (Figure 5B). However, no differences were observed in RV fibrosis, capillary density, or CD45 expression in both RV and LV tissue of mutation carriers and non-carriers. (Figure 2.5B, 2.6).

In addition, apoptotic rate (expression of caspase 3 and fas cell surface death receptor) was increased in PAH-patients to controls, but similar in between carriers and non-carriers (Figure 2.4C).

Cardiac metabolism

To determine whether changes in metabolism may explain the differences in RV function between mutation carriers and non-carriers, we subsequently assessed RNA expression of key-components of glucose metabolism (GLUT1, hexokinase 1/2) and fatty acid oxidation (fatty acid binding protein 3 (FABP3), CD36, carnitine palmitoyltransferase 1/2). Although significant increases in expression of GLUT 1, FABP3 and CPTB1 were observed in PAH tissue in comparison to control, no differences were identified between mutation carriers and non-carriers. (Figure 2.7)

DISCUSSION

By combining in vivo measurements of RV function with molecular and histological analyses of unique RV and LV tissue of PAH-patients and controls, we were able to demonstrate that:

- 1) Despite a similar afterload, RV function is more severely compromised in *BMPR2* mutation carriers compared to non-carriers. Differences continue to exist after PAH-specific treatment.
- 2) TGF- β and BMP signaling is similar in LV and RV cardiomyocytes of *BMPR2* mutation carriers and non-carriers.
- 3) The amount of RV hypertrophy, LV atrophy, fibrosis, apoptosis, inflammation, capillary density and cardiac metabolism is similar between *BMPR2* mutation carriers and non-carriers, indicating an equal RV and LV adaptation.

Impaired RV function in *BMPR2* mutation carriers

Previous large retrospective studies have demonstrated the increased hemodynamic burden in PAH-patients carrying a *BMPR2* mutation, accompanied by a shorter time to death or lung transplantation.^{13,14,26–28} Until now, differences in survival and disease severity were mainly explained by a more severe pulmonary vascular involvement, leading to a more severe and faster disease trajectory. However, combining the fact that RV function is the main determinant of prognosis and disease severity and that the *BMPR2* gene is also expressed in the RV, it can be speculated that RV function plays a role in the differential clinical phenotypes of mutation carriers and non-carriers.^{4,9,29,30} Accordingly, a recent study by Brittain et al. revealed an out of proportion RV dysfunction in HPAH patients at baseline.²⁷ However, these differences should be interpreted with caution, as the afterload of mutation carriers was significantly higher in comparison to non-carriers.

An interesting finding in our present study is the comparable afterload of *BMPR2* mutation carriers and non-carriers, suggesting a distinct clinical phenotype of *BMPR2* mutation carriers in the Netherlands. A possible explanation is the relatively high percentage of cytoplasmic tail mutation carriers in our cohort, which is 25%, compared to 13% in the French PAH registry.

³¹ As cytoplasmic tail mutations carriers present hemodynamically similar to non-carriers, this may have contributed to the observed phenotype of our patient cohort. Despite these similarities, we observed a decreased RV function in mutation carriers. This reduction was not

explained by differences in PVR or a more severe state of disease at presentation. These findings suggest a negative effect of *BMPR2* mutations on RV function in PAH-patients.

TGF- β /BMP balance in PAH

Significant progress in the knowledge about the role of TGF- β in the response to pressure overload has been achieved by studies in left heart failure. Whilst it is known that TGF- β is associated with maladaptive hypertrophy, inflammation and fibrosis in various models and diseases, the study of Koitabashi et al was the first to show that TGF- β plays a central role in the cardiac maladaptive response to pressure-overload.^{32–36} However, as the left ventricle has a different embryological origin and the amount of pressure overload in right and left heart failure is not comparable, these results cannot directly be extrapolated.^{37,38}

Until recently, little was known about the effects of *BMPR2* mutations on RV adaptation in PAH. First, Megalou et al. showed the importance of TGF- β in the hypertrophic response in the myocardium of pulmonary hypertensive monocrotaline rats, and more recently Hemnes et al. demonstrated impaired hypertrophy due to an altered cardiac energy metabolism in the RV of a transgenic mice model expressing mutant BMPRII.^{24,39} However, the effects of *BMPR2* mutations in human cardiomyocytes remain elusive. Therefore, we studied the TGF- β -BMP signaling in cardiomyocytes of PAH patients with and without *BMPR2* mutation and characterized hypertrophy, capillarization, inflammation and fibrosis. Surprisingly, our study did not reveal any differences in neither TGF- β nor BMP signaling between carriers and non-carriers, although it corresponds to a previous study of Atkinson et al., in which they show a decreased BMPRII receptor expression in the pulmonary vasculature of both mutation carriers and non-carriers.¹⁶ Interestingly, we were able to demonstrate significant differences in *BMPR2* expression and metabolic adaptation between non-carriers and controls, suggesting a potential dysfunctional compensatory signaling underlying the functional differences between mutation carriers and non-carriers.

We were not able to confirm the previous observed RV maladaptive response in *BMPR2* mice in our human RV tissue. One explanation might be the difference between rodents and human cardiac physiology. Another explanation could be the end-stage right heart failure of the patient samples used for our histomorphological analysis of the RV. There may be important differences in myocardial structure of failing and adapting RV, but due to the inherent difficulties of obtaining biopsies (reported high complication rates) from adapted patients this is problematic to assess.

Study limitations

We were only able to include a small number of RV and LV tissue samples of PAH-patients and controls. This may have limited our statistical power to identify differences between mutation carriers and non-carriers. However, we were able to confirm known differences in hypertrophy, fibrosis and cardiac metabolism, which were described previously in animal models.^{40–42} These findings suggest, that although the number of subjects was small, it was sufficient to identify differences between PAH and control subjects.

Clinical implications

Although a direct relation between RV function and a *BMPR2* mutation was not revealed in this study, our findings suggest that *BMPR2* mutations lead to an impaired RV function in symptomatic PAH. Our results raise the question whether clinical status and time to death or lung transplantation in *BMPR2* mutation carriers could be improved using the RV as a therapeutic target. Furthermore, our results provide rationale for closely monitoring RV function in *BMPR2* mutation carriers in PAH referral centers and subsequently timely referral for lung transplantation. Further therapeutic studies targeting the disturbed TGF- β /BMP pathway will reveal the clinical implications of this disturbed balance in the RV of PAH patients.

Conclusions

We demonstrated that PAH patients carrying a *BMPR2* mutation have a decreased RV function compared to PAH patients without *BMPR2* mutation at presentation, which persisted after PAH specific treatment. We revealed that there are no alterations in TGF- β and BMP induced SMAD phosphorylation in cardiomyocytes of PAH patients with or without mutation. Furthermore, we demonstrated that RV and LV adaptation is not different between *BMPR2* mutation carriers and non-carriers.

Figure 2.3 - Expressions of p-SMADs in the right and left ventricle, legend page 44

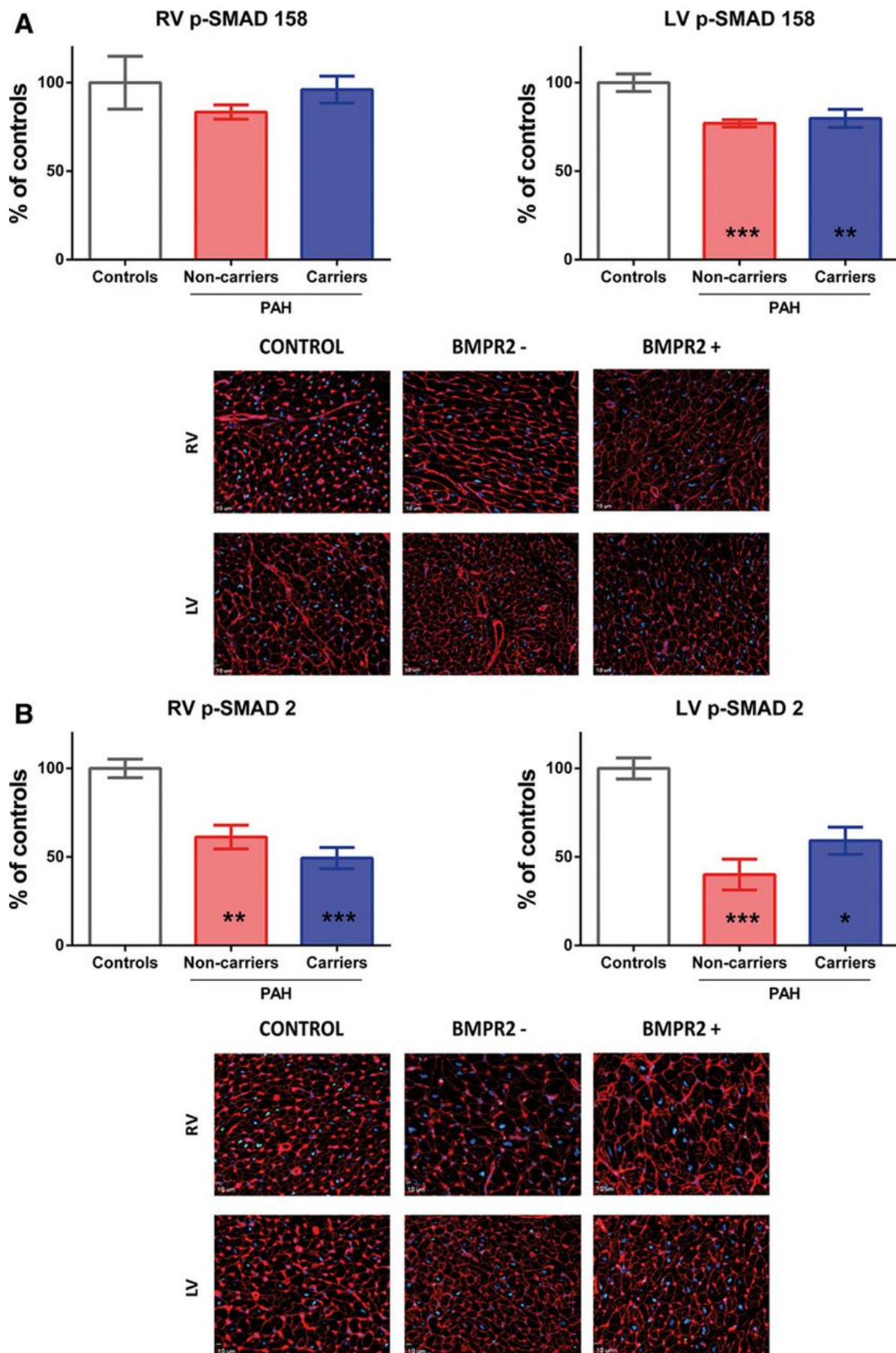


Figure 2.4 – Hypertrophy, apoptosis and the TGF- β /BMP axis, legend page 44

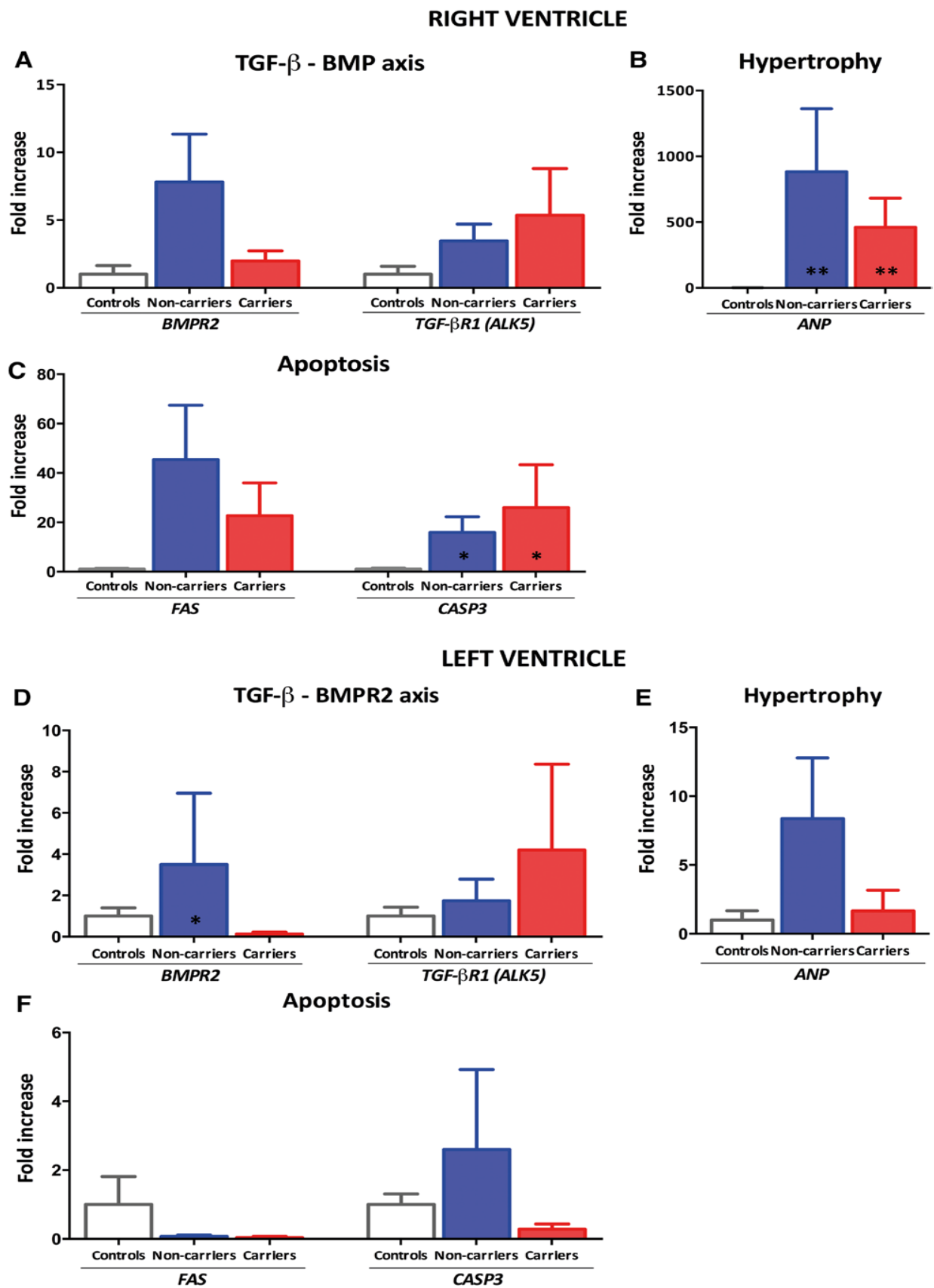


Figure 2.5 – Cross-sectional area (A) and fibrosis (B) in the LV and RV, legend page 44

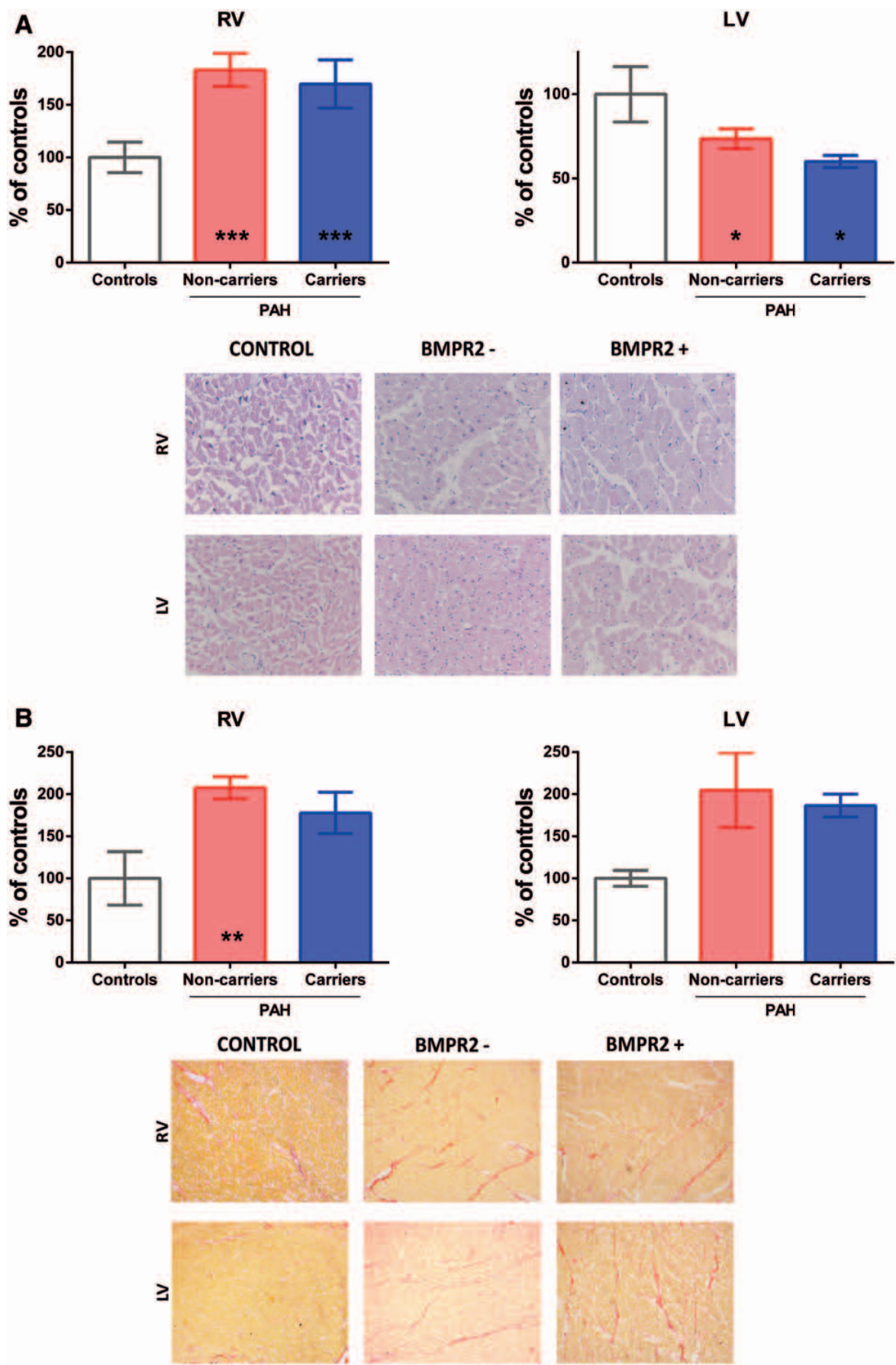


Figure 2.6 – CD-45 expression (A) and capillary density (B) in the RV and LV – legend page 44

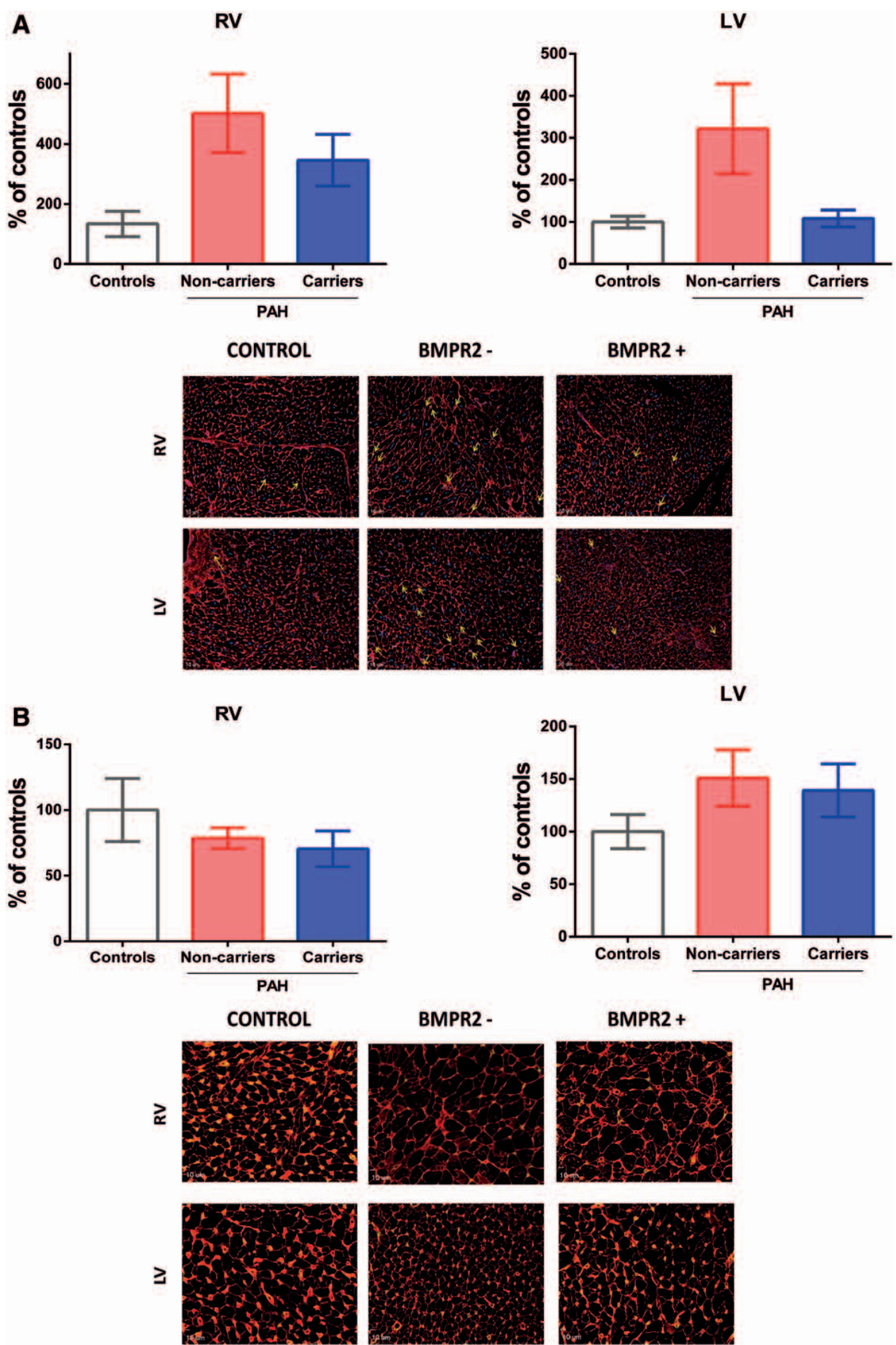


Figure 2.7 – RNA-expression of metabolic markers – legend page 44

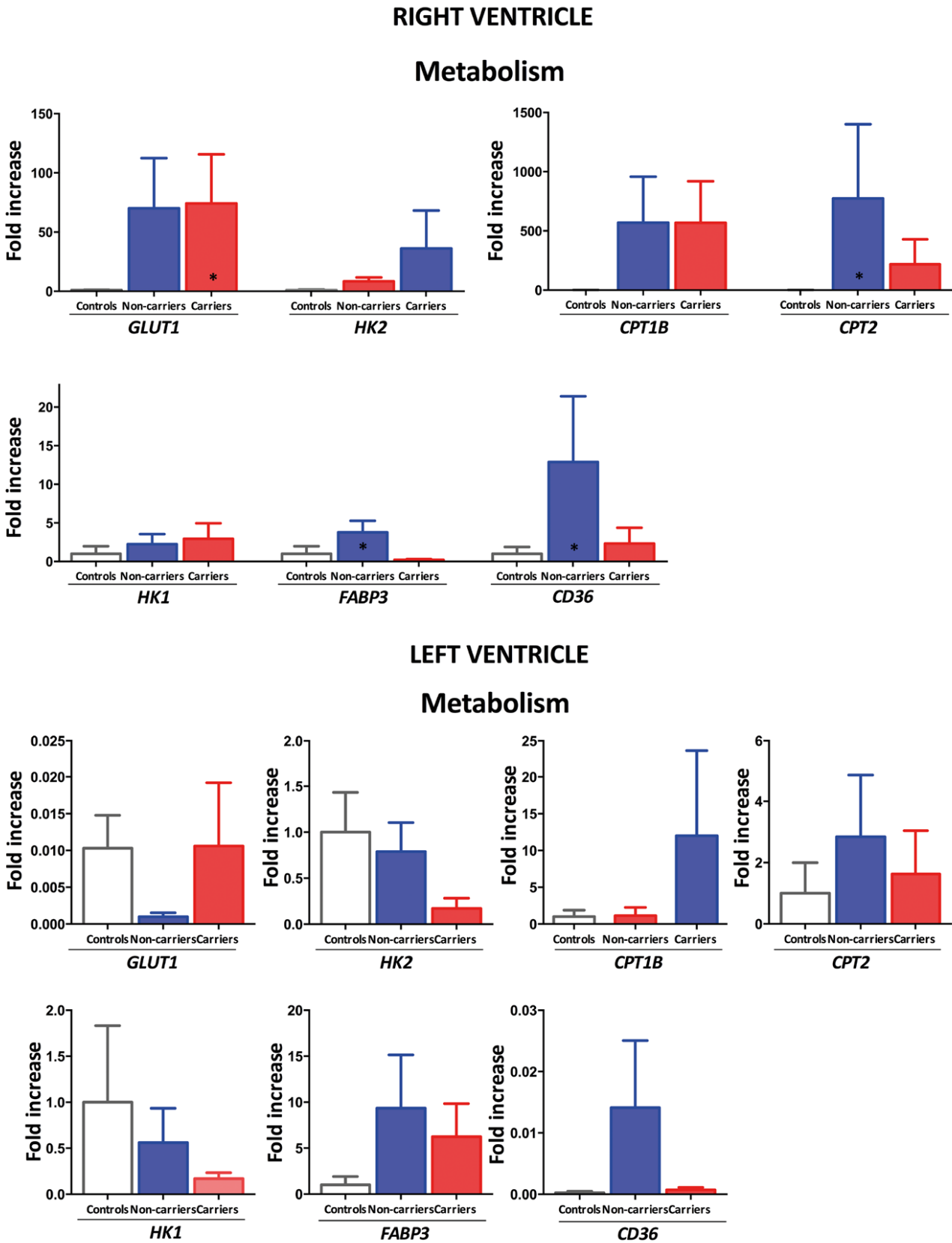


Figure 2.3:

Percentage of a) p-SMAD1,5,8 activated nuclei per total nuclei in the left ventricle (LV) and right ventricle (RV), b) percentage of p-SMAD2 activated nuclei per total nuclei in the LV and RV. Controls n=6, non-carriers n=11, carriers n=5. Control values are normalized to 100%. Data are presented as mean±SEM. *: p<0.05, **: p<0.01, ***: p<0.001

Figure 2.4:

RNA-expression of RV a) the TGF-β/BMP axis, b) hypertrophy and c) apoptosis and LV d) TGF-β/BMP axis, e) hypertrophy and f) apoptosis. BMPR2: Bone Morphogenetic Protein Receptor 2, TGF-βR1: Transforming Growth Factor -β1, ANP: atrial natriuretic peptide, FAS: Fas Cell Surface Death Receptor, CASP3: Caspase 3. Controls n=6, non-carriers n=11, carriers n=5. Data are presented as mean±SEM. Control values are normalized to 1. *<0.05, **<p<0.01

Figure 2.5:

Percentage of a) cross-sectional area and b) fibrosis in both the LV and RV. Control values are normalized to 100%. Controls n=6, non-carriers n=11, carriers n=5. Data are presented as mean±SEM. *:p<0.05, **: p<0.01, ***: p<0.001

Figure 2.6:

Percentage of a) CD45 expression and b) capillary density in both LV and RV. Control values are normalized to 100%. Controls n=6, non-carriers n=11, carriers n=5. Data are presented as mean±SEM.

Figure 2.7:

RNA expression of metabolic markers. GLUT1: glucose transporter 1; HK2: hexokinase 2, HK1: hexokinase 1, FABP3: fatty acid binding protein 3, CPT: carnitine palmitoyltransferase. Controls n=6, non-carriers n=11, carriers n=5. Data are presented as mean±SEM. Control values are normalized to 1. *p<0.05.

REFERENCES

- Humbert M, Sitbon O, Chaouat A, Bertocchi M, Habib G, Gressin V, Yaïci A, Weitzenblum E, Cordier J-F, Chabot F, Dromer C, Pison C, Reynaud-Gaubert M, Haloun A, Laurent M, Hachulla E, Cottin V, Degano B, Jaïs X, Montani D, Souza R, Simonneau G. Survival in patients with idiopathic, familial, and anorexigen-associated pulmonary arterial hypertension in the modern management era. *Circulation*. 2010;122:156–163.
- Simonneau G, Gatzoulis MA, Adatia I, Celermajer D, Denton C, Ghofrani A, Gomez Sanchez MA, Krishna Kumar R, Landzberg M, Machado RF, Olschewski H, Robbins IM, Souza R. Updated clinical classification of pulmonary hypertension. *J Am Coll Cardiol*. 2013;62:D34–41.
- Runo JR, Loyd JE. Primary pulmonary hypertension. *Lancet*. 2003;361:1533–1544.
- van de Veerdonk MC, Kind T, Marcus JT, Mauritz G-J, Heymans MW, Bogaard H-J, Boonstra A, Marques KMJ, Westerhof N, Vonk-Noordegraaf A. Progressive right ventricular dysfunction in patients with pulmonary arterial hypertension responding to therapy. *J Am Coll Cardiol*. 2011;58:2511–2519.
- Cogan JD, Pauciulo MW, Batchman AP, Prince MA, Robbins IM, Hedges LK, Stanton KC, Wheeler LA, Phillips JA, Loyd JE, Nichols WC. High frequency of BMPR2 exonic deletions/duplications in familial pulmonary arterial hypertension. *Am J Respir Crit Care Med*. 2006;174:590–598.
- Deng Z, Morse JH, Slager SL, Cuervo N, Moore KJ, Venetos G, Kalachikov S, Cayanis E, Fischer SG, Barst RJ, Hodge SE, Knowles JA. Familial primary pulmonary hypertension (gene PPH1) is caused by mutations in the bone morphogenetic protein receptor-II gene. *Am J Hum Genet*. 2000;67:737–744.
- International PPH Consortium, Lane KB, Machado RD, Pauciulo MW, Thomson JR, Phillips JA, Loyd JE, Nichols WC, Trembath RC. Heterozygous germline mutations in BMPR2, encoding a TGF-beta receptor, cause familial primary pulmonary hypertension. *Nat Genet*. 2000;26:81–84.
- Newman JH, Wheeler L, Lane KB, Loyd E, Gaddipati R, Phillips JA, Loyd JE. Mutation in the gene for bone morphogenetic protein receptor II as a cause of primary pulmonary hypertension in a large kindred. *N Engl J Med*. 2001;345:319–324.
- Thomson JR, Machado RD, Pauciulo MW, Morgan NV, Humbert M, Elliott GC, Ward K, Yacoub M, Mikhail G, Rogers P, Newman J, Wheeler L, Higenbottam T, Gibbs JS, Egan J, Crozier A, Peacock A, Allcock R, Corris P, Loyd JE, Trembath RC, Nichols WC. Sporadic primary pulmonary hypertension is associated with germline mutations of the gene encoding BMPR-II, a receptor member of the TGF-beta family. *J Med Genet*. 2000;37:741–745.
- Soubrier F, Chung WK, Machado R, Grünig E, Aldred M, Geraci M, Loyd JE, Elliott CG, Trembath RC, Newman JH, Humbert M. Genetics and genomics of pulmonary arterial hypertension. *J Am Coll Cardiol*. 2013;62:D13–21.
- Machado RD, Eickelberg O, Elliott CG, Geraci MW, Hanaoka M, Loyd JE, Newman JH, Phillips JA, Soubrier F, Trembath RC, Chung WK. Genetics and genomics of pulmonary arterial hypertension. *J Am Coll Cardiol*. 2009;54:S32–42.
- Girerd B, Montani D, Eyries M, Yaici A, Sztrymf B, Coulet F, Sitbon O, Simonneau G, Soubrier F, Humbert M. Absence of influence of gender and BMPR2 mutation type on clinical phenotypes of pulmonary arterial hypertension. *Respir Res*. 2010;11:73.
- Rosenzweig EB, Morse JH, Knowles JA, Chada KK, Khan AM, Roberts KE, McElroy JJ, Juskiw NK, Mallory NC, Rich S, Diamond B, Barst RJ. Clinical implications of determining BMPR2 mutation status in a large cohort of children and adults with pulmonary arterial hypertension. *J Heart Lung Transplant Off Publ Int Soc Heart Transplant*. 2008;27:668–674.
- Sztrymf B, Coulet F, Girerd B, Yaici A, Jais X, Sitbon O, Montani D, Souza R, Simonneau G, Soubrier F, Humbert M. Clinical outcomes of pulmonary arterial hypertension in carriers of BMPR2 mutation. *Am J Respir Crit Care Med*. 2008;177:1377–1383.
- Larkin EK, Newman JH, Austin ED, Hemnes AR, Wheeler L, Robbins IM, West JD, Phillips JA, Hamid R, Loyd JE. Longitudinal Analysis Casts Doubt on the Presence of Genetic Anticipation in Heritable Pulmonary Arterial Hypertension. *Am J Respir Crit Care Med*. 2012;186:892–896.
- Atkinson C, Stewart S, Upton PD, Machado R, Thomson JR, Trembath RC, Morrell NW. Primary pulmonary hypertension is associated with reduced pulmonary vascular expression of type II bone morphogenetic protein receptor. *Circulation*. 2002;105:1672–1678.
- Akhurst RJ. TGF beta signaling in health and disease. *Nat Genet*. 2004;36:790–792.
- Machado RD, Pauciulo MW, Thomson JR, Lane KB, Morgan NV, Wheeler L, Phillips III JA, Newman J, Williams D, Galie N, Manes A, McNeil K, Yacoub M, Mikhail G, Rogers P, Corris P, Humbert M, Donnai D, Martensson G, Tranebjaerg L, Loyd JE, Trembath RC, Nichols WC. BMPR2 Haploinsufficiency as the Inherited Molecular Mechanism for Primary Pulmonary Hypertension. *Am J Hum Genet*. 2001;68:92–102.

19. Morrell NW. Pulmonary hypertension due to BMPR2 mutation: a new paradigm for tissue remodeling? *Proc Am Thorac Soc*. 2006;3:680–686.
20. Stacher E, Graham BB, Hunt JM, Gandjeva A, Groshong SD, McLaughlin VV, Jessup M, Grizzle WE, Aldred MA, Cool CD, Tudor RM. Modern age pathology of pulmonary arterial hypertension. *Am J Respir Crit Care Med*. 2012;186:261–272.
21. Dobaczewski M, Chen W, Frangogiannis NG. Transforming growth factor (TGF)- β signaling in cardiac remodeling. *J Mol Cell Cardiol*. 2011;51:600–606.
22. Koitabashi N, Danner T, Zaiman AL, Pinto YM, Rowell J, Mankowski J, Zhang D, Nakamura T, Takimoto E, Kass DA. Pivotal role of cardiomyocyte TGF- β signaling in the murine pathological response to sustained pressure overload. *J Clin Invest*. 2011;121:2301–2312.
23. Rosenkranz S. TGF-beta1 and angiotensin networking in cardiac remodeling. *Cardiovasc Res*. 2004;63:423–432.
24. Hemnes AR, Brittain EL, Trammell AW, Fessel JP, Austin ED, Penner N, Maynard KB, Gleaves L, Talati M, Absi T, Disalvo T, West J. Evidence for right ventricular lipotoxicity in heritable pulmonary arterial hypertension. *Am J Respir Crit Care Med*. 2014;189:325–334.
25. Galiè N, Humbert M, Vachiery J-L, Gibbs S, Lang I, Torbicki A, Simonneau G, Peacock A, Vonk Noordegraaf A, Beghetti M, Ghofrani A, Gomez Sanchez MA, Hansmann G, Klepetko W, Lancellotti P, Matucci M, McDonagh T, Pierard LA, Trindade PT, Zompatori M, Hoeper M. 2015 ESC/ERS Guidelines for the diagnosis and treatment of pulmonary hypertension: The Joint Task Force for the Diagnosis and Treatment of Pulmonary Hypertension of the European Society of Cardiology (ESC) and the European Respiratory Society (ERS): Endorsed by: Association for European Paediatric and Congenital Cardiology (AEPC), International Society for Heart and Lung Transplantation (ISHLT). *Eur Respir J*. 2015;46:903–975.
26. Kabata H, Satoh T, Kataoka M, Tamura Y, Ono T, Yamamoto M, Huqun null, Hagiwara K, Fukuda K, Betsuyaku T, Asano K. Bone morphogenetic protein receptor type 2 mutations, clinical phenotypes and outcomes of Japanese patients with sporadic or familial pulmonary hypertension. *Respirol Carlton Vic*. 2013;18:1076–1082.
27. Brittain EL, Pugh ME, Wheeler LA, Robbins IM, Loyd JE, Newman JH, Larkin EK, Austin ED, Hemnes AR. Shorter survival in familial versus idiopathic pulmonary arterial hypertension is associated with hemodynamic markers of impaired right ventricular function. *Pulm Circ*. 2013;3:589–598.
28. Evans JDW, Girerd B, Montani D, Wang X-J, Galiè N, Austin ED, Elliott G, Asano K, Grünig E, Yan Y, Jing Z-C, Manes A, Palazzini M, Wheeler LA, Nakayama I, Satoh T, Eichstaedt C, Hinderhofer K, Wolf M, Rosenzweig EB, Chung WK, Soubrier F, Simonneau G, Sitbon O, Gräf S, Kaptoge S, Di Angelantonio E, Humbert M, Morrell NW. BMPR2 mutations and survival in pulmonary arterial hypertension: an individual participant data meta-analysis. *Lancet Respir Med*. 2016;4:129–137.
29. Wolferen SA van, Marcus JT, Boonstra A, Marques KMJ, Bronzwaer JGF, Spreeuwenberg MD, Postmus PE, Vonk-Noordegraaf A. Prognostic value of right ventricular mass, volume, and function in idiopathic pulmonary arterial hypertension. *Eur Heart J*. 2007;28:1250–1257.
30. Vonk-Noordegraaf A, Haddad F, Chin KM, Forfia PR, Kawut SM, Lumens J, Naeije R, Newman J, Oudiz RJ, Provencher S, Torbicki A, Voelkel NF, Hassoun PM. Right heart adaptation to pulmonary arterial hypertension: physiology and pathobiology. *J Am Coll Cardiol*. 2013;62:D22–33.
31. Girerd B, Coulet F, Jaïs X, Eyries M, Van Der Bruggen C, De Man F, Houweling A, Dorfmueller P, Savale L, Sitbon O, Vonk-Noordegraaf A, Soubrier F, Simonneau G, Humbert M, Montani D. CHaracteristics of pulmonary arterial hypertension in affected carriers of a mutation located in the cytoplasmic tail of bmprii. *Chest [Internet]*. 2014 [cited 2015 Feb 26];Available from: <http://dx.doi.org/10.1378/chest.14-0880>
32. Ying X, Lee K, Li N, Corbett D, Mendoza L, Frangogiannis NG. Characterization of the Inflammatory and Fibrotic Response in a Mouse Model of Cardiac Pressure Overload. *Histochem Cell Biol*. 2009;131:471–481.
33. Koitabashi N, Danner T, Zaiman AL, Pinto YM, Rowell J, Mankowski J, Zhang D, Nakamura T, Takimoto E, Kass DA. Pivotal role of cardiomyocyte TGF- β signaling in the murine pathological response to sustained pressure overload. *J Clin Invest*. 2011;121:2301–2312.
34. Dobaczewski M, Chen W, Frangogiannis NG. Transforming Growth Factor (TGF)- β signaling in cardiac remodeling. *J Mol Cell Cardiol*. 2011;51:600–606.
35. Rosenkranz S. TGF-beta1 and angiotensin networking in cardiac remodeling. *Cardiovasc Res*. 2004;63:423–432.
36. Akhurst RJ. TGF beta signaling in health and disease. *Nat Genet*. 2004;36:790–792.
37. Voelkel NF, Quaife RA, Leinwand LA, Barst RJ, McGoon MD, Meldrum DR, Dupuis J, Long CS, Rubin LJ, Smart FW, Suzuki YJ, Gladwin M, Denholm EM, Gail DB, National Heart, Lung, and Blood Institute Working Group on Cellular and Molecular Mechanisms of Right Heart Failure. Right ventricular function and failure: report of a National Heart, Lung, and Blood Institute working group on cellular and molecular mechanisms of right heart failure. *Circulation*. 2006;114:1883–1891.
38. Rain S, Handoko ML, Vonk Noordegraaf A, Bogaard HJ, van der Velden J, de Man FS. Pressure-

overload-induced right heart failure. *Pflüg Arch Eur J Physiol.* 2014;466:1055–1063.

39. Megalou AJ, Glava C, Oikonomidis DL, Vilaeti A, Agelaki MG, Baltogiannis GG, Papalois A, Vlahos AP, Kolettis TM. Transforming growth factor- β inhibition attenuates pulmonary arterial hypertension in rats. *Int J Clin Exp Med.* 2010;3:332–340.

40. Piao L, Fang Y-H, Cadete VJJ, Wietholt C, Urboniene D, Toth PT, Marsboom G, Zhang HJ, Haber I, Rehman J, Lopaschuk GD, Archer SL. The inhibition of pyruvate dehydrogenase kinase improves impaired cardiac function and electrical remodeling in two models of right

ventricular hypertrophy: resuscitating the hibernating right ventricle. *J Mol Med Berl Ger.* 2010;88:47–60.

41. Fang Y-H, Piao L, Hong Z, Toth PT, Marsboom G, Bache-Wiig P, Rehman J, Archer SL. Therapeutic inhibition of fatty acid oxidation in right ventricular hypertrophy: exploiting Randle's cycle. *J Mol Med Berl Ger.* 2012;90:31–43.

42. Sutendra G, Dromparis P, Paulin R, Zervopoulos S, Haromy A, Nagendran J, Michelakis ED. A metabolic remodeling in right ventricular hypertrophy is associated with decreased angiogenesis and a transition from a compensated to a decompensated state in pulmonary hypertension. *J Mol Med Berl Ger.* 2013;91:1315–1327.

2

BONE MORPHOGENETIC PROTEIN RECEPTOR TYPE II MUTATION IN PULMONARY ARTERIAL HYPERTENSION: A VIEW ON THE RIGHT VENTRICLE

Supplemental material

Table S1 – Clinical study – ethnicities

	PAH – Non-carriers n=67	PAH- Mutation carriers n=28
Caucasian (%)	90.0	93.0
Asian (%)	3.0	4.0
Asian-Caucasian (%)	1.5	0.0
Carribean (%)	1.5	0.0
African Carribean (%)	1.5	0.0
Hindustanian Carribean (%)	3.0	0.0
North-African (%)	0.0	4.0

Table S2 – Treatment response

	Non-carriers		Mutation carriers		P-interaction
	Baseline	FU	Baseline	FU	
Hemodynamics	n=54		n=25		
HR (beats/min)	78±13	76±14	87±17†	81±15	ns
mPAP (mmHg)	55±17	47±17*	56±10	49±13*	ns
mRAP (mmHg)	7 (4-11)	5 (3-9)*	7 (5-11)	5 (3-6)*	ns
SvO2 (%)	67±8	70±8	63±7	69±11*	ns
PAWP (mmHg)	10±5	10±3	9±4	7±3	ns
PVR (dynes*s/cm ⁵)	723 (466-1010)	405 (232-619)*	972 (608-1311)	585 (484-795)*	ns
CI (l/min/m ²)	2.7±0.9	3.4±1.2*	2.1±0.4†	2.8±0.6*	ns
SVI (ml/m ²)	35.1±11.9	44.8±15*	25.5±7.7†	36.2±13.8*	ns
Cardiac MRI	n=39		n=20		
RVEDVI (ml/m ²)	79±21	80±22	89±38	79±27	ns
RVESVI (ml/m ²)	54±21	58±20	62±38	47±26	ns
RVEF (%)	34±12	29±10	35±14	43±13*	ns
RV mass index	58±17†	48±11	53±24	52±22	0.05

Table S3 – PAH-specific therapy at follow-up

	Non-carriers n=54	Carriers n=26	P-value
Prostanoids	15%	23%	0.36
PDE5-inhibitors	11%	8%	0.63
ERAs	23%	4%	0.11
Calcium-channel blockers	4%	0%	0.32
Combination therapy	39%	50%	0.35
Triple therapy	9%	8%	0.82
Unknown (study medication)	2%	4%	0.97

PAH=pulmonary arterial hypertension, PDE-5-inhibitors: phosphodiesterase type 5 inhibitors; ERAs: endothelin receptor antagonists

3

CONTRIBUTION OF IMPAIRED PARASYMPATHETIC ACTIVITY IN RIGHT VENTRICULAR DYSFUNCTION AND PULMONARY VASCULAR REMODELING IN PULMONARY ARTERIAL HYPERTENSION

D da Silva Gonçalves Bos, CE van der Bruggen, K Kurakula, XQ Sun, KR Casali, AG Casali, N Rol, R Szulcek, C dos Remedios, C Guignabert, L Tu, P Dorfmueller, M Humbert, PJM Wijnker, DWD Kuster, J van der Velden, MJ Goumans, HJ Bogaard, A Vonk Noordegraaf, FS de Man & ML Handoko

Circulation, 2018

ABSTRACT

Background: Beneficial effects of parasympathetic stimulation have been reported in left heart failure, however, whether it would be beneficial for pulmonary arterial hypertension (PAH) remains to be explored. Here, we investigated the relationship between parasympathetic activity and right ventricular (RV) function in PAH-patients, and the potential therapeutic effects of pyridostigmine (PYP), an oral drug stimulating the parasympathetic activity through acetylcholinesterase (AChE) inhibition, in experimental pulmonary hypertension (PH).

Methods: Heart rate recovery (HRR) after maximal cardiopulmonary exercise test was used as a surrogate for parasympathetic activity. RV ejection fraction (RVEF) was assessed in 112 PAH-patients. Expression of nicotinic (α -7nAChR) and muscarinic (m2AChR) receptors, and AChE activity were evaluated in RV (n=11) and lungs (n=7) from PAH-patients undergoing heart/lung transplantation and compared with tissue obtained from controls. In addition, we investigated the effects of PYP (40 mg/kg/day) in experimental PH. PH was induced in male rats by SU5416 (25 mg/kg; s.c.) injection followed by 4 weeks of hypoxia. In a subgroup sympathetic/parasympathetic modulation was assessed by power spectral analysis. At week 6, PH status was confirmed by echocardiography, and rats were randomized to vehicle or treatment (both n=12). At the end-of-study, echocardiography was repeated, with additional RV pressure-volume measurements, along with lung, RV histological and protein analyses.

Results: PAH-patients with lower RVEF (<41%) had a significantly reduced HRR in comparison to patients with higher RVEF. In PAH RV-samples, α -7nAChR was increased and AChE activity was reduced versus controls. No difference in m2AChR expression was observed. Chronic PYP-treatment in PH-rats normalized the cardiovascular autonomic function, demonstrated by an increase in parasympathetic activity and baroreflex sensitivity. PYP improved survival, increased RV contractility, and reduced RV stiffness, RV hypertrophy, RV fibrosis, RV inflammation, as well as RV α -7nAChR and m2AChR expression. Furthermore, PYP reduced pulmonary vascular resistance, RV afterload and pulmonary vascular remodeling, which was associated with reduced local and systemic inflammation.

Conclusion: RV dysfunction is associated with reduced systemic parasympathetic activity in PAH-patients, with an inadequate adaptive response of the cholinergic system in the right ventricle. Enhancing parasympathetic activity by PYP improved survival, RV function and pulmonary vascular remodeling in experimental-PH.

INTRODUCTION

Pulmonary arterial hypertension (PAH) is characterized by progressive pulmonary vascular remodeling and increased right ventricular (RV) afterload, which eventually leads to right heart failure.¹ Despite the significant progress in the treatment of PAH, its prognosis remains grim.^{2,}

³

Cardiovascular autonomic dysfunction, or more specifically, increased sympathetic nervous system activity^{4, 5}, parasympathetic nervous system withdrawal⁶ and blunted baroreflex sensitivity^{7, 8} are associated with disease progression and poor prognosis in PAH. It has however, never been directly related with RV function.^{7, 9} We and others have demonstrated that targeting the sympathetic nervous system could be a promising therapy to improve RV function and pulmonary vascular remodeling.¹⁰⁻¹² Hypothetically, autonomic function can also be restored via parasympathetic stimulation. However, this has not been investigated yet in the context of PAH.

Local cardiac parasympathetic activity is mediated via two types of receptors, the nicotinic receptors (at the preganglionic level) and the muscarinic receptors (postganglionic level). Nicotinic receptors are activated by acetylcholine released from parasympathetic nerve terminals at the preganglionic level, and subsequently the muscarinic receptors are activated at organ level.¹³ Increased expression of the nicotinic receptor was observed in the left ventricle in a pressure-overload rat model.¹⁴ This finding suggests a compensatory cholinergic response to reduced parasympathetic activity. Another study in experimental left heart failure provided evidence that pyridostigmine (PYR), an oral drug which stimulates the parasympathetic nervous system through acetylcholinesterase inhibition, was able to improve autonomic and left ventricular function.^{15, 16} Furthermore, donepezil, a different acetylcholinesterase inhibitor which crosses the blood-brain barrier, was also shown to improve cardiac function in left heart failure¹⁷ and attenuated the development of hypertension in spontaneously hypertensive rats.¹⁸ In the present study we choose to use PYR, a long approved drug for myasthenia gravis, with a more favorable pharmacological profile compared to donepezil, to activate the parasympathetic nervous system.

Here, we aim to investigate the relationship between parasympathetic activity and RV function in idiopathic/hereditary PAH-patients. In addition, we aim to determine the potential therapeutic effects of parasympathetic activity stimulation by pyridostigmine in an experimental pulmonary hypertension.

METHODS

Parasympathetic nervous system activity and RV function in pulmonary arterial hypertension patients

We retrospectively reviewed 112 idiopathic and hereditary PAH-patients seen at the VU University Medical Center (Amsterdam, the Netherlands) between 2002 and 2015, who underwent a maximal cardiopulmonary exercise test and cardiac magnetic resonance imaging (CMR) for clinical reasons. Eight healthy volunteers who underwent a maximal cardiopulmonary exercise test were used as a control group. Heart rate recovery (HRR) was used as a surrogate of parasympathetic activity.¹⁹ HRR was defined as the difference in heart rate at the maximum workload and at 30 seconds, 60 seconds and 120 seconds after completion of the cardiopulmonary exercise test. RV ejection fraction (RVEF) was used as a parameter of RV function, and the cutoff value of 41% was selected based on the median.

Table 3.1 – General characteristics and hemodynamics

Characteristic	RVEF<41% <i>n</i> =56	RVEF≥41% <i>n</i> =56	<i>P</i> Value*
Age, y	45±13	53±16	<0.01
Female, %	69.6	76.8	0.39
Body mass index, kg/m ²	25.0±4.6	26.1±4.9	0.30
N-terminal prohormone of brain natriuretic peptide, pmol/L	1025 (536–2071)	156 (95–367)	<0.0001
6-min walking distance, m	407±123	476±133	<0.01
Cardiopulmonary exercise test			
Maximum work, W	65±29	92±44	<0.001
Heart rate at maximum work, beats/min	138±21	140±24	0.66
Hemodynamics			
Heart rate at rest, beats/min	84±14	74±12	<0.001
Mean pulmonary artery pressure, mm Hg	54±16	42±11	<0.0001
Mean right atrial pressure, mm Hg	7 (4–11)	5 (2–8)	<0.01
Mixed venous oxygen saturation, %	63±11	71±6	<0.0001
Pulmonary arterial wedge pressure, mm Hg	9 (6–11)	10 (7–11)	0.89
Pulmonary vascular resistance, dynes·s ⁻¹ ·cm ⁻⁵	684 (468–864)	376 (288–519)	<0.0001
Cardiac output, L·min ⁻¹	4.9±1.4	6.6±1.9	<0.0001
Stroke volume, mL	61±20	91±24	<0.0001
Cardiac magnetic resonance imaging, mL			
Right ventricular end-diastolic volume	186±79	131±33	<0.0001
Right ventricular end-systolic volume	111 (91–162)	64 (52–74)	<0.0001

Data are presented as mean±SD or median (25%–75%), dependent on normal distribution. RVEF indicates right ventricular ejection fraction. Compares RVEF<41% and RVEF≥41%.

Human RV and Lung samples

Explanted RV tissue samples were collected from PAH-patients undergoing heart/lung transplantation (PAH-patient; *n*=11) and compared with RV tissue obtained from non-failing controls (control; *n*=9).²⁰ Human cardiac tissue collection was approved by the Human Research Ethics Committee of The University of Sydney (AU/1/961515) and the Université Paris-Sud-Inserm U999 (ID RBC 2008-A00485-50). Control lung tissues and pulmonary arteries were obtained from patients undergoing surgery for lung carcinoma (control; *n*=4). Samples

were obtained distant from the malignant lesion and were dissected by a pathologist. Lung tissues and pulmonary arteries were also obtained from PAH-patients undergoing lung transplantation (PAH-patient; n=7). Lung sample collection was approved by the local ethics committees (Comité de Protection des Personnes, Sud-Ouest et Outre-mer III, Bordeaux, France; and Comité de Protection des Personnes, Ile de France, VII, Le Kremlin Bicêtre, France).

Cholinergic system in human samples

Acetylcholinesterase (AChE) activity (supplemental methods) and protein expression of cholinergic receptors were evaluated in RV, pulmonary artery and lung homogenates from PAH and control patients by Western blot analyses. In the current study, we evaluated the expression of the following cholinergic receptors: the α -7 nicotinic acetylcholine receptor (α -7nAChR; 1:1000; AB24644; Abcam), a receptor which can activate the anti-inflammatory cholinergic pathway²¹, and muscarinic acetylcholine type 2 receptor (m2AChR; 1:1000; MA3-044; Thermo Scientific), a receptor related to negative inotropic effects via inhibition of adenylate cyclase.²² Moreover, α -7nAChR was evaluated by immunofluorescence in lung sections from PAH and control patients.

Cell proliferation assay of PAH-patients

Pulmonary microvascular endothelial cells (MVECs) were isolated from patients that underwent lobectomy. The study was approved by the Institutional Review Board of the VU University Medical Center (Amsterdam, the Netherlands). Endothelial cell isolation and culture of the smallest pulmonary vessels were performed as previously described.²³ Cell proliferation was assessed by the MTT (3-[4, 5-dimethylthiazol-2-yl]-2, 5-diphenyltetrazolium bromide) (Sigma-Aldrich) assay as described previously.²⁴ Cells were seeded in a 96-well plate at a density of 3×10^3 cells/well and incubated overnight. Cells were made quiescent by incubation in medium without fetal calf serum (FCS) for 2 h. Cells were then treated with vehicle or various concentrations of PYR for 2 h followed by FCS (10 % v/v) stimulation for 24 h. After the incubation, cells were incubated with 10 μ L of MTT reagent (5 mg/ml) for 2.5 h at 37°C. The MTT reagent was removed and 100 μ L of isopropanol was added to each well. Plate was wrapped in an aluminium foil and incubated for 15 min on a shaker. Colorimetric analysis was performed with an ELISA plate reader. This experiment (in quadruplicate) was repeated at least three times.

Human 3D-engineered heart tissue

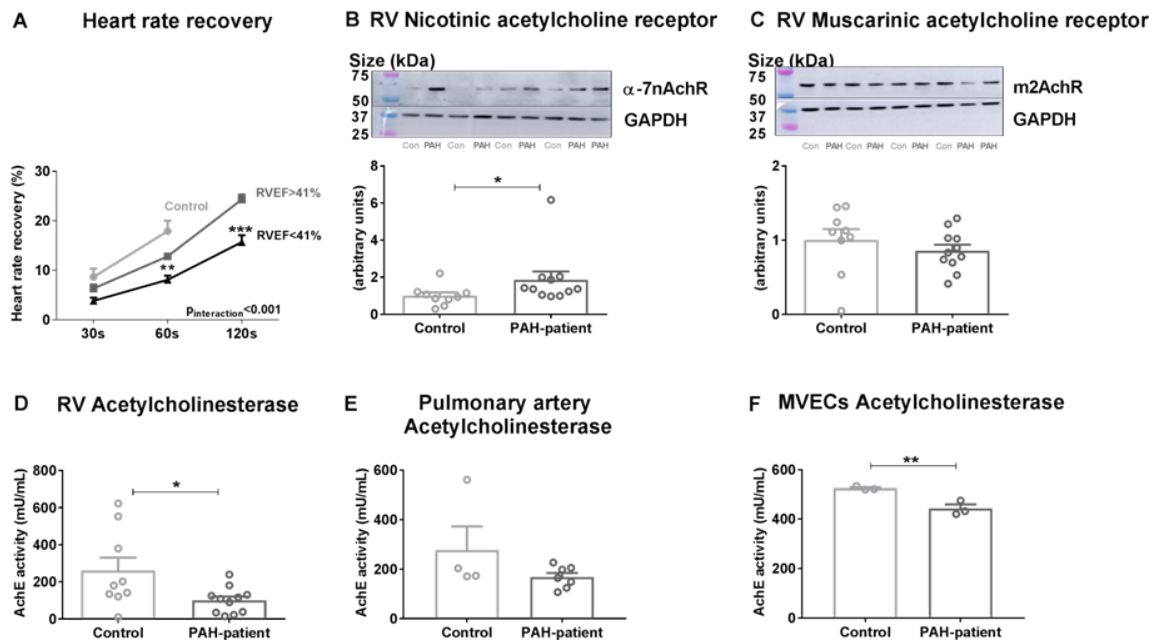
For regulatory reasons, we were not permitted to include a PYR-control group in the main experimental study. Therefore, we included a study on the effects of PYR on 3D-engineered heart tissue (EHT), generated from iCell® cardiomyocytes² (Cellular Dynamics International), which are human induced pluripotent stem cell-derived cardiomyocytes, mixed with

Matrigel™ (Corning, 354234), bovine fibrinogen (Sigma, F8630) plus aprotinin (Sigma, A1153), and thrombin (Sigma, T7513) (for details see Supplement).²⁵

Experimental pulmonary hypertension

All animal experiments were approved by the Institutional Animal Care and Use Committee of the VU University, Amsterdam, the Netherlands.

Figure 3.1 - Heart rate recovery and local change in the cholinergic system in PAH-patients



(A) Heart rate recovery (HRR) after the cardiopulmonary exercise test at 30, 60 and 120 seconds. PAH-patients with lower right ventricle (RV) function (RV ejection fraction or RVEF <41%) had a significant reduced HRR in comparison to patients with higher RV function (RVEF >41%). Control: n=8, PAH RVEF >41% (n=56), PAH RVEF <41% (n=56). **p<0.01, ***p<0.001, versus PAH RVEF >41%. RVEF=right ventricle ejection fraction. (B) Representative RV protein expression from alpha-7 nicotinic acetylcholine receptor (α-7nAChR) and (C) muscarinic acetylcholine receptor (m2AChR). (D) Acetylcholinesterase (AChE) activity in RV homogenates from PAH-patients. Control: n=9 and PAH-patients: n=11. (E) AChE activity in pulmonary artery homogenates. Control: n=4 and PAH-patients: n=7. (F) AChE activity in microvascular endothelial cells from Control: n=3 and PAH-patients: n=3. *p<0.05, **p<0.01 versus Control.

Sugen/hypoxia-rat model of pulmonary hypertension

Male Sprague Dawley rats were used (n=31, 125-150 g; Charles River, Sulzfeld, Germany). One week before PH-induction, a pressure telemetry device (TA11PA-C40, Data Science International, St. Paul, MN) was implanted in the abdominal aorta in a subgroup of rats (n=4-6) for heart rate and blood pressure variability analysis.²⁶ PH was induced by a single subcutaneous injection of a vascular endothelial growth factor inhibitor (SU5416, 25 mg/kg body mass; Tocris Bioscience, Bristol, UK) dissolved in 0.5% carboxymethylcellulose, followed by 4 weeks of hypoxia exposure (10% oxygen; Biospherix Ltd, New York, NY) maintained by

a nitrogen generator (Avilo, Dirksland, The Netherlands) and re-exposed to normoxia for maximally 10 weeks. The control group (controls; n=7) received a carboxymethylcellulose injection and was housed in normoxic condition until the end-of-study (Supplement Figure S1).²⁷

Pyridostigmine treatment and hemodynamic measurements

Pyridostigmine (PYR) dose (Sigma Aldrich, 40 mg/kg) was determined in a pilot study as the minimal dose able to reduce heart rate by 10% and increase parasympathetic activity, with minimal effects on systolic arterial pressure or animal activity (Supplement Figure S2). At week 6, PH status was confirmed by echocardiography, and animals were randomized into: PH (n=12) or PH-PYR (n=12). PYR was delivered in drinking water. At the end-of-study, week 10, or earlier when animals developed signs of right heart failure, defined as > 10% of body weight reduction, cyanosis, dyspnea and/or lethargy, echocardiography and RV catheterization with pressure-volume analyses were performed as described before (see also Supplement, Figure S1).^{12, 28}

Heart rate and blood pressure variability analysis

Cardiovascular autonomic function was assessed by power spectral analysis, applied to pulse interval (PI) and systolic arterial pressure (SAP) series. Heart rate variability (HRV) and blood pressure variability (BPV) were evaluated at spectral domain using an autoregressive algorithm on stationary sequences of 200 beats. The low-frequency (0.25-0.75 Hz) and high-frequency (0.75-3.0 Hz) bands, represented the sympathetic and parasympathetic modulation and were expressed in both absolute (HRV: ms², BPV: mmHg²) and normalized units. The ratio between low-frequency and high-frequency components (low-frequency/high-frequency index) was considered a synthetic expression of the sympathovagal balance.^{29, 30} The alpha-index was obtained from the square root of the ratio between the PI interval and the SAP variability within the low-frequency ranges,³¹ and it was used to estimate spontaneous baroreflex sensitivity.^{32, 33}

Histology of heart and lungs

After hemodynamic evaluation, rats were euthanized under isoflurane by exsanguination (by dissecting the abdominal aorta and inferior vena cava) with immediate removal of the vital organs. Heart and lungs were harvested and frozen. Cardiomyocyte cross-sectional area, cardiac fibrosis and relative wall thickness of pulmonary arterioles, were determined (see Supplement). Furthermore, RV capillary density, leukocytes infiltration, α -7nAChR and m2AChR were measured by immunofluorescence (see Supplement).

Cholinergic system in experimental-PH

RV tissue of the rats was homogenized in radioimmunoprecipitation assay (RIPA) buffer containing phosphatase and protease inhibitors (Sigma-Aldrich). The protein concentration

was quantified by the Pierce 660 nm protein assay kit (Thermo Scientific, Rockford, USA). 10µg of protein was used to detect the expression of cholinergic receptors: α -7nAChR (1:1000; AB24644; Abcam) and m2AChR (1:1000; MA3-044; Thermo Scientific). The protein amount was normalized by GAPDH as loading control (1:50000; G9295, Sigma-Aldrich). In addition, AchE activity (supplemental methods) was measured in plasma and RV homogenates.

Statistical analysis

Statistical analyses were performed using Prism for Windows (GraphPad 6 Software). Data are presented as mean±SEM, p-values < 0.05 were considered significant. Normality of data was checked and either log-transformation or non-parametric testing was performed if data was not normally distributed. Unpaired t-test was used to compare the general characteristics of PAH-patients and to compare acetylcholinesterase levels and cholinergic receptors expression between control and PAH-patients. The χ^2 test was used for categorical variables. The survival estimates were performed by Kaplan-Meier analysis, with post-hoc comparison by log rank (Mantel-Cox) test between PH rats with/without PYR treatment. Two-way ANOVA for repeated measurements followed by Bonferroni post-hoc test was used for: heart rate recovery, echocardiography and cell proliferation assay. One-way ANOVA with Bonferroni post-hoc comparison between PH and PH-PYR was used for: pressure-volume relationships, autopsy data, histology data and protein analyses. Kruskal-wallis test followed by Dunn's multiple comparison test was used for: heart rate variability and blood pressure variability analyses. The heart rate and blood pressure variability data are presented in delta percentage before and after the treatment.

RESULTS

Reduced parasympathetic activity was associated with reduced RV function in PAH-patients

To investigate whether parasympathetic activity is associated with RV function in idiopathic/hereditary PAH patients, we assessed heart rate recovery after the cardiopulmonary exercise test as a measure of parasympathetic activity and RVEF as a measure of RV function assessed by cardiac magnetic resonance imaging (CMR). General patient characteristics and hemodynamics are presented in (Table 1). The median RVEF was 41%. Patients with lower RVEF had increased NT-proBNP levels, lower exercise capacity, higher resting heart rate, increased mean pulmonary artery pressure and pulmonary vascular resistance (Table 3.1).

PAH-patients had an impaired HRR at 30 and 60 seconds after maximal exercise, in comparison to control subjects (Figure 3.1A). Importantly, in patients with low RVEF, heart rate recovery (at both 60 and 120 seconds) was lower compared to patients with higher RVEF (Figure 3.1A). These results indicate that reduced parasympathetic activity in PAH-patients is associated with a reduced RV function.

Local changes in the cholinergic system in PAH-patients

Acetylcholine is the main parasympathetic nerve neurotransmitter and exerts its effect by binding to its nicotinic and muscarinic receptors. To investigate the local changes in the cholinergic system in the right ventricle, expression of the nicotinic (α -7nAChR), muscarinic receptors (m2AChR) and acetylcholinesterase (AChE) activity were assessed in RV tissue of PAH-patients and controls. We observed that α -7nAChR expression was upregulated in RV tissue from PAH-patients versus controls (Figure 3.1B), whereas no difference in m2AChR expression was found (Figure 3.1C). In addition, AChE activity was reduced in RV tissue of PAH-patients (Figure 3.1D).

To determine the local changes in the cholinergic system in the lung, we assessed the expression of α -7nAChR, m2AChR and AChE activity in whole lung tissue and pulmonary artery of PAH-patients and controls. Both α -7nAChR and m2AChR expression were similar in lung homogenates of control and PAH-patients (Figure S3A-B). However, because our immunofluorescence staining suggested higher α -7nAChR expression around the pulmonary arteries from PAH-patients (Figure S3C), we further investigated the expression of α -7nAChR in pulmonary artery homogenates from PAH-patients versus controls, and again no significant difference was observed (Figure S3D). In addition, m2AChR expression was also not significant different in pulmonary artery homogenates from PAH-patients in comparison to controls (Figure S3E). Moreover reduced AChE activity was observed in MVECs and pulmonary arteries of PAH-patients (Figure 3.1E,F).

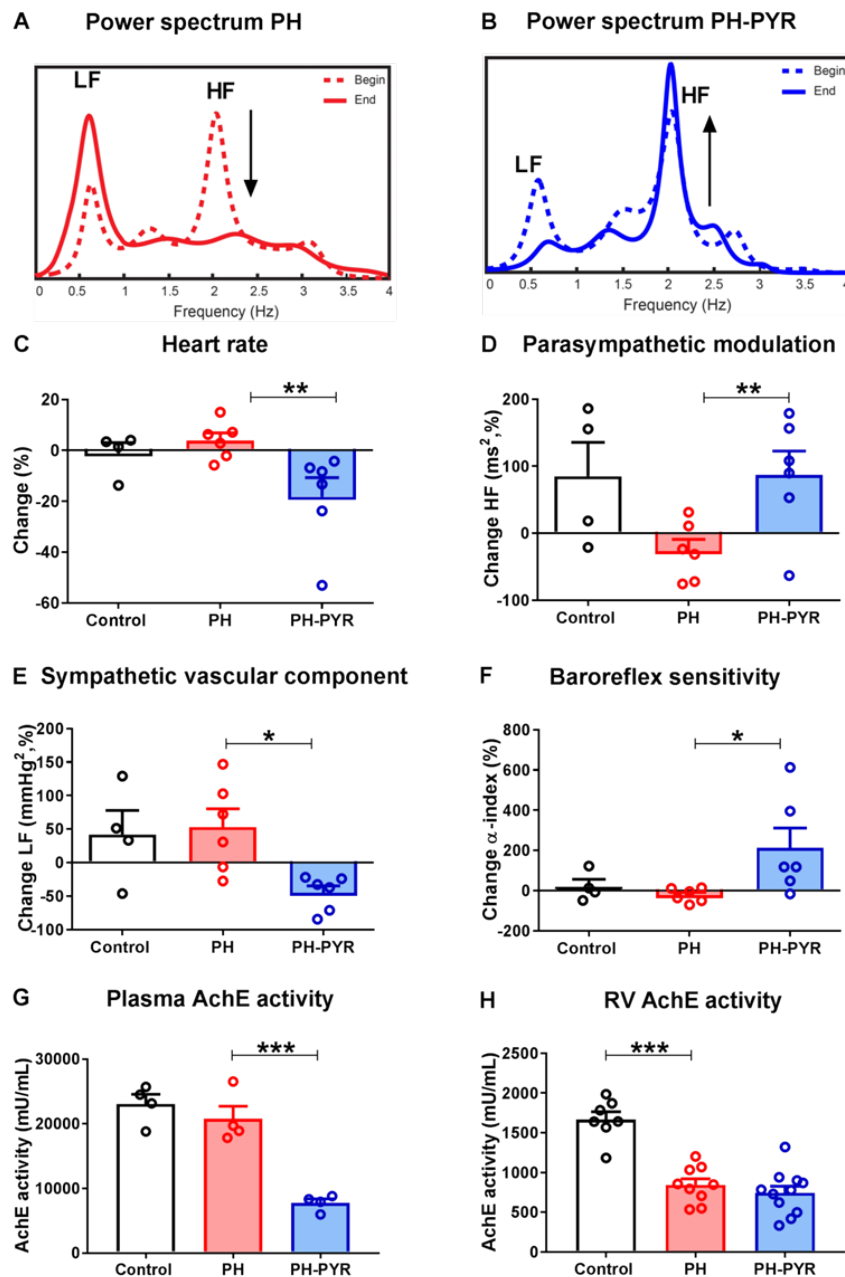
Based on these data we hypothesize that the observed reduction in AChE activity may be an adaptive mechanism to the known autonomic imbalance observed in PAH-patients. However, as patients still suffer from an autonomic imbalance, this adaptation can be regarded as insufficient. The association of reduced parasympathetic activity with RV dysfunction and local changes in cholinergic signaling in the RV and lungs in PAH-patients were the rationale to study the role of parasympathetic activity in more detail in an experimental model of PH.

Effects of PYR in control animals and in human 3D-engineered heart tissue

In a pilot study (supplemental material and methods, pilot dose finding), we found that PYR-treatment at 40 mg/kg had no significant effects in RV end-systolic and end-diastolic pressures (Figure S4) in healthy rats. In addition, no relevant differences on dP/dt maximum or dP/dt minimum was observed after PYR-treatment (Figure S4). Furthermore, the effects of PYR were investigated in human engineered 3D-heart tissue (EHT, supplemental material and methods). Functional measurements in EHT were obtained at baseline, 15 and 60 minutes after acetylcholine or PYR treatment. As observed in (Figure S4E) we confirmed that PYR and acetylcholine significantly reduced the heart rate on spontaneous beating EHTs. PYR also reduced the relaxation velocity after 60 min (Figure S4F). In addition, no significant effects of

PYR-treatment on maximum force and contraction velocity were observed (Figure S4G-H). These results confirmed that PYR had no relevant hemodynamics effect in controls.

Figure 3.2 - Pyridostigmine improved cardiovascular autonomic function and reduced acetylcholinesterase activity in rats



Relative changes at end-of-study (week 10) compared to baseline (week 6) on heart rate (HRV) and blood pressure variability (BPV). In summary, PYR restores the sympathovagal balance and thus (partially) normalized the cardiovascular autonomic function in experimental PH. (**A-B**) Typical examples of a power spectrum (amplitude by heart rate frequency domains) that is the basis for the HRV analysis: the low frequency (low-frequency) component is a reflection of sympathetic activity and the high frequency (high-frequency) component reflects parasympathetic activity. The dashed lines represent the data at start of treatment and the continuous lines indicate the data at the end-of-study. As can be appreciated, high-frequency-component increases after PYR (arrow in Figure 2B). PYR reduced heart

rate (**C**) and increased the parasympathetic activity (high-frequency-component) after the treatment (**D**). (**E-F**) Data derived from the BPV analysis; the sympathetic vascular component is the low-frequency-component from the BPV (in analogy of the low-frequency-component of HRV), and the lowering effect of PYR in PH on this parameter is demonstrated (**E**); Spontaneous baroreflex sensitivity (\bar{a} -index) is calculated by the square root of the ratio between the pulse interval and the systolic arterial pressure variability within the low-frequency-components (sympathetic), the lowering effect of PYR on this parameter is demonstrated in (**F**). Biochemical analysis confirmed that PYR intervention reduced plasma acetylcholinesterase (AChE) activity (**G**) and no effect in RV AChE activity (**H**). Control: n=4, PH: n=4-6, PH-PYR: n=4-6; * $p < 0.05$, ** $p < 0.01$, *** $p < 0.001$ versus PH.

Pyridostigmine improved cardiovascular autonomic function in experimental PH

To establish that PYR effectively stimulated parasympathetic activity in our PH-rat model, the cardiovascular autonomic function was assessed by heart rate and blood pressure variability analysis (Supplement: Table S1). Typical power spectrum before and after the treatment from PH and PH-PYR groups can be appreciated at (Figure 3.2A,B), the low-frequency-component represents sympathetic activity and high-frequency-component represents parasympathetic activity. PYR significantly reduced the heart rate in comparison to vehicle (Figure 3.2C and significantly increased the parasympathetic activity, measured by the high-frequency-component of the heart rate variability obtained by spectral analysis (Figure 3.2D). Moreover, no significant changes in systemic arterial pressure (Supplement: Figure S5A) and daily activity (Supplement: Figure S5B) were observed with the dose used. Through the blood pressure variability analysis we observed that PYR reduced the sympathetic vascular component (Figure 3.2E) and improved the spontaneous baroreflex sensitivity (Figure 3.2F). In addition, PYR effectively reduced plasma AChE activity in our experimental-PH (Figure 3.2G). No significant effects on AChE activity after PYR-treatment was observed in RV homogenates (Figure 3.2H). These results confirmed that PYR-treatment reduced plasma AChE activity and partially normalized cardiovascular autonomic function in our PH-rat model, without adverse side effects.

Pyridostigmine delayed progression towards right heart failure

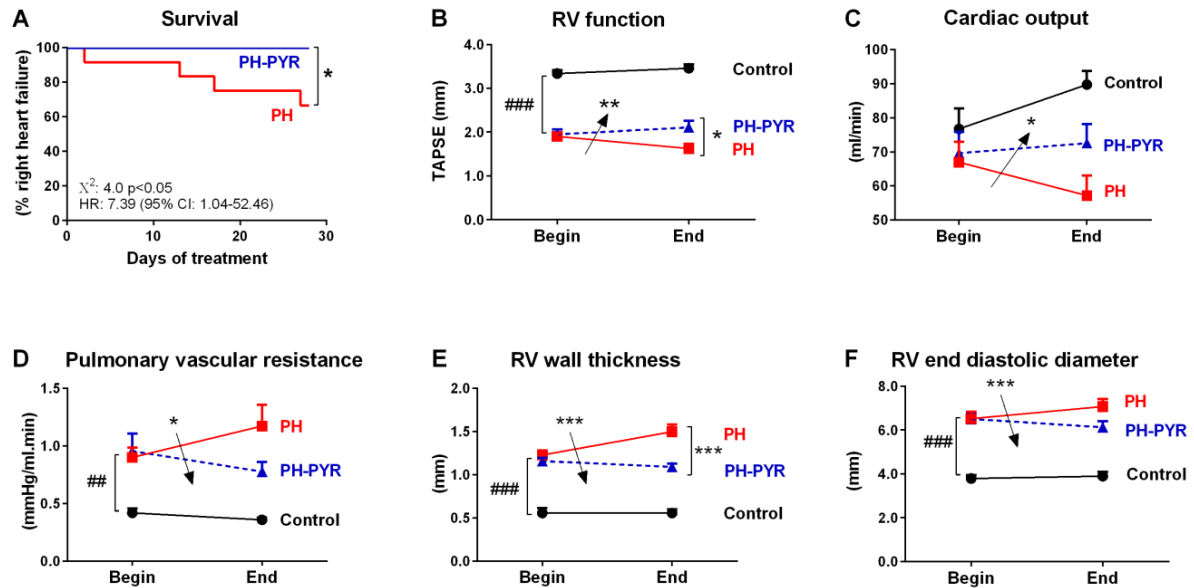
PH was confirmed before the start of PYR-treatment in all PH-rats (Supplement: Table S2). Survival analysis demonstrated that PYR significantly delayed the time to manifest right heart failure in comparison to PH-rats (Figure 3.3A). This finding was confirmed by serial echocardiographic analysis, where PYR-treatment maintained RV systolic function, measured by TAPSE, stroke volume (Supplement: Table S3) and cardiac output (Figure 3.3B,C). In addition, PYR reduced the pulmonary vascular resistance, RV wall thickness and RV end-diastolic diameter (Figure 3.3D-F).

Pyridostigmine improved RV function

To determine the effect of PYR on load-independent parameters of RV function, RV pressure-volume analyses were performed at the end-of-study (representative examples: Figure 3.4A-C). PYR significantly increased RV contractility (Ees), reduced RV diastolic stiffness (Eed) and

also reduced RV afterload (Ea, Figure 3.4D-F), resulting in a partial normalization of RV-arterial coupling (E_{es}/E_a : 0.86 ± 0.09 vs. 0.37 ± 0.09 ; $p < 0.05$).

Figure 3.3 - Pyridostigmine delayed progression towards right heart failure



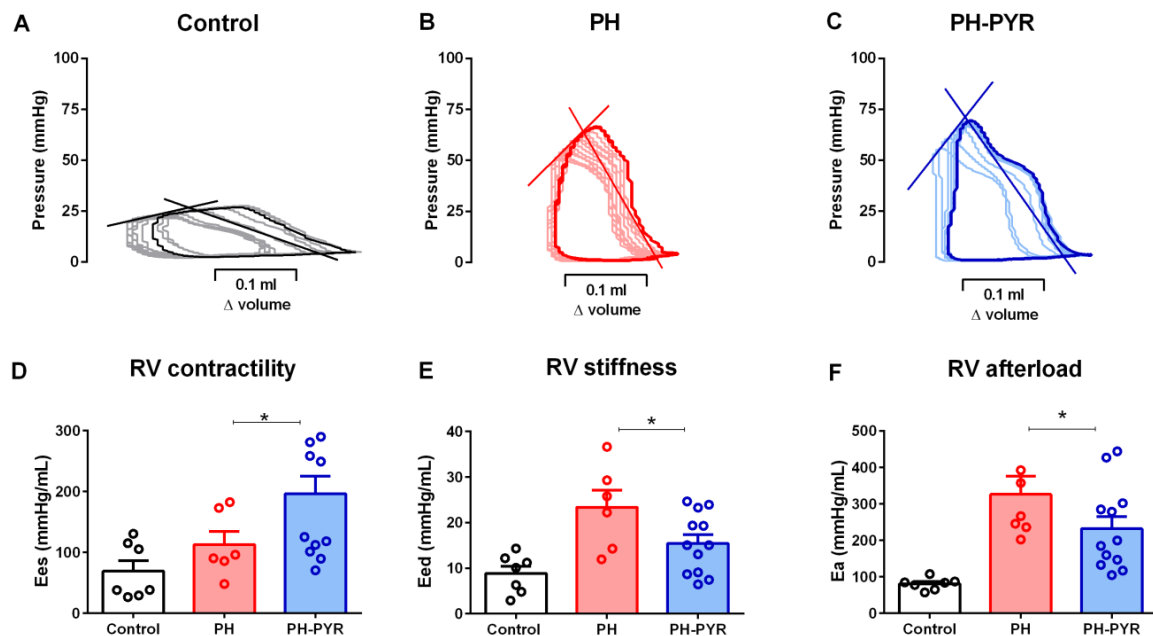
Pyridostigmine (PYR) treatment delayed time to manifest right heart failure (**A**). PYR treatment improved RV function (**B**) and cardiac output (**C**). PYR reduced significantly the pulmonary vascular resistance (**D**), RV wall thickness (**E**), RV end-diastolic diameter (**F**). Data presented as mean \pm SEM. Control: $n=7$, PH: $n=8$, PH-PYR: $n=12$; Arrows represent significant interaction of the two way ANOVA. ## $p < 0.01$, ### $p < 0.001$, versus control; * $p < 0.05$, ** $p < 0.01$, *** $p < 0.001$, versus PH. TAPSE= tricuspid annular plane systolic excursion, CO= cardiac output, PVR= pulmonary vascular resistance, RVWT= right ventricle wall thickness, RVEDD=right ventricle end-diastolic diameter.

Pyridostigmine reduced RV remodeling and inflammation

RV histological analyses were performed to analyze structural changes in the right ventricle. RV cardiomyocyte cross-sectional area (Figure 3.5A,E,I) and RV fibrosis were decreased with PYR (Figure 3.5B,F,J). Although RV myocardial capillary density was reduced in PH-rats in comparison to controls, it was not significantly different after PYR (Figure 3.5C,G,K). RV myocardial leukocyte infiltration was observed in PH-rats, which was not present in the left ventricle (Supplement: Table S4). PYR significantly reduced RV myocardial leukocyte infiltration (Figure 3.5D,H,L).

Furthermore, we evaluated changes in the cholinergic receptors after PYR. Western blot and immunofluorescent analysis revealed that PYR reduced α -7nAChR and m2AChR expression in the RV (Figure 3.6A-D). These findings suggest that the improvement in RV function by increased parasympathetic activity may be related to a decreased expression of cholinergic receptors and dampening of RV inflammation.

Figure 3.4 - Pyridostigmine improved RV function

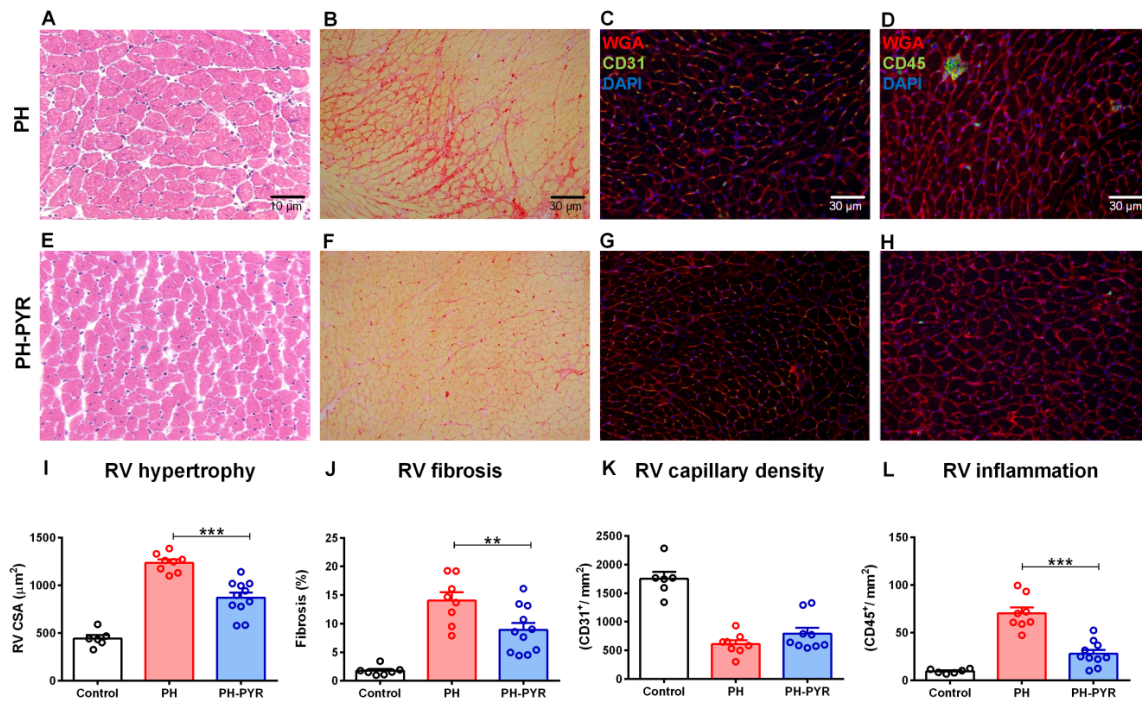


Representative examples of pressure-volume relationship for control, PH and PH-pyridostigmine (PYR) groups. By preload reduction, multiple end-systolic pressure/volume points were obtained, from which the RV end-systolic pressure-volume relationship was derived (depicted by the solid rising line). Its slope is a load-independent measure for RV contractility (Ees). Similarly, by preload reduction RV end-diastolic pressure-volume relationship and RV stiffness (Eed) were derived. RV afterload (Ea) was measured by RV end-systolic pressure at steady state divided by stroke volume (descending solid line; A-C). PYR significantly improved the RV contractility (D) and reduced RV stiffness (E). Moreover, PYR reduced RV afterload (F) Control: n=7, PH: n=8, PH-PYR: n=12. * $p < 0.05$ versus PH

Pyridostigmine reduced pulmonary vascular remodeling

Pulmonary histology was subsequently performed to study structural changes that may explain the observed reduction in RV afterload. Histological analyses from pulmonary arterioles indicated a significant reduction in media and intima wall thickness after PYR treatment (Figure 3.7A-E). Moreover, PYR decreased the formation of occlusive vascular lesions (Figure 3.7F). To further investigate the effects of PYR on intima proliferation, we evaluated different PYR concentrations on proliferation of microvascular endothelial cells (MVECs) derived from control and PAH-patients. Our *in vitro* study confirmed that PYR reduced the MVECs proliferation (Figure 3.7G, Supplement: Figure S6). Taken together, these data suggest that PYR may have direct anti-proliferative effects.

Figure 3.5 - Pyridostigmine reduced right ventricle hypertrophy and fibrosis

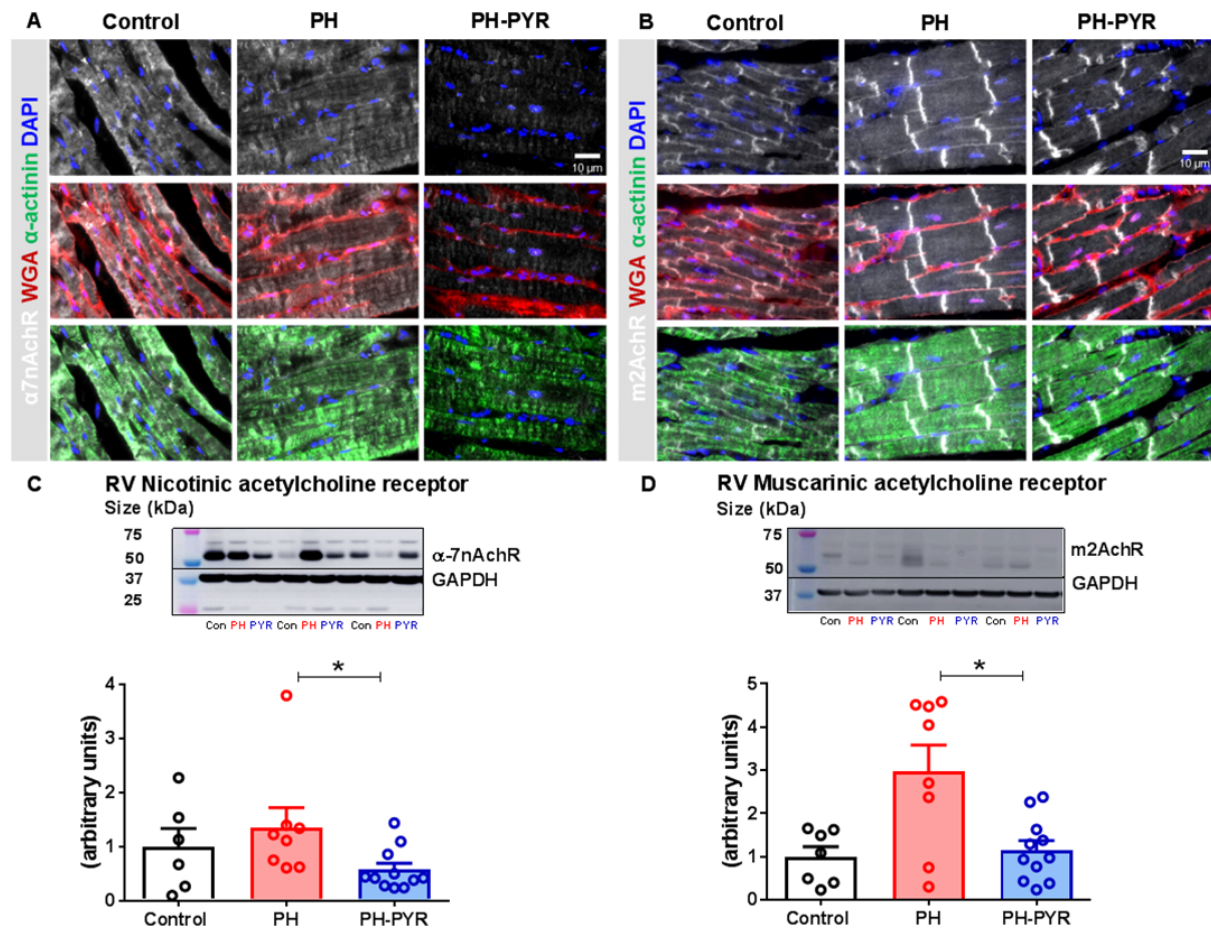


Representative examples for control, PH and PH-PYR groups of right ventricle (RV) cross sectional area (hematoxylin and eosin, 400X magnification, **A,D**), fibrosis (picrosirius red, 100X magnification, **B,E**) and CD31 (myocardial capillary density, 100X magnification, **C,F**). CD31 (green), WGA (red), nuclei (DAPI). Scale bar 20 μm . PYR reduced significantly the RV cross sectional area (**G**) and RV fibrosis (**H**). No difference was observed in RV capillary density (**I**). Data presented as mean \pm SEM. Control: $n=7$, PH: $n=8$ and PH-PYR: $n=12$. ** $p<0.01$, *** $p<0.001$, versus PH.

Pyridostigmine reduced systemic and pulmonary inflammation

To assess the anti-inflammatory effects of PYR, we measured systemic and local inflammation in the lung. In plasma, lower levels of IL-6 (730 ± 24 vs. 843 ± 42 , $p=0.01$; pg/ml) and MCP-1 (1913 ± 273 vs. 3646 ± 542 , $p=0.002$; pg/ml) were observed in PH-PYR compared to the PH-group. In addition, we observed a reduction in lung perivascular CD45⁺ cells infiltration in PH-PYR group (293 ± 44 vs. 439 ± 37 , $p=0.02$; CD45⁺/mm²). To assess whether the changes on pulmonary vasculature and inflammation could be explained by changes in the cholinergic signaling, the expression levels of α -7nAChR and m2AChR were measured by immunofluorescence in the pulmonary vasculature. However, no significant changes in α -7nAChR and m2AChR expression were observed (Figure 3.7H-I, Supplement: Figure S7) after PYR. Downstream signaling of α -7nAChR was further analyzed.³⁴ Western blot analysis revealed no significant differences on phosphorylated-ERK, total-ERK and NF- κ B p65 expression in lung homogenates by PYR (Supplement: Figure S8). These findings suggest that PYR has direct anti-proliferative and anti-inflammatory effects that seems to be independent of α -7nAChR.

Figure 3.6 - Pyridostigmine improved cholinergic system in RV



Representative RV immunofluorescence staining for alpha-7 nicotinic acetylcholine receptor (α -7nAChR; **A**) and muscarinic acetylcholine type 2-receptor (m2AChR; **B**) for control, PH and PH-PYR groups. α -7nAChR and m2AChR (white), WGA (red), α -actinin (green) and nuclei (DAPI). Scale bar 20 μ m. Western blot analyses revealed significant reduction of cholinergic α -7nAChR (**C**) and m2AChR (**D**) expression in the right ventricle (RV) homogenates after PYR-treatment. Protein expression was normalized by GAPDH, as a loading control. Control: n=7, PH: n=8 and PH-PYR: n=12. *p<0.05, **p<0.01 versus PH.

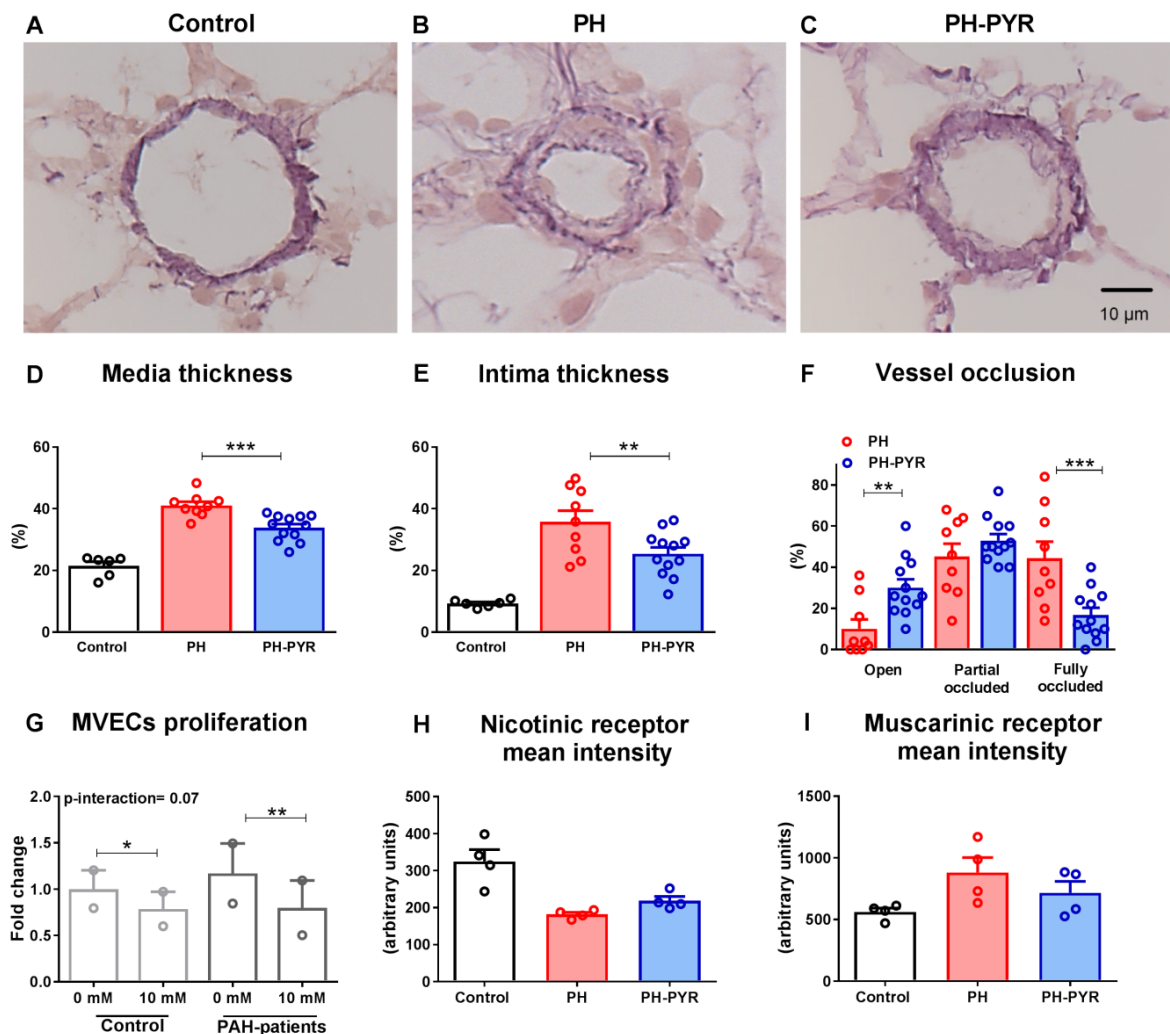
DISCUSSION

In this translational study we demonstrated the clinical relevance of impaired parasympathetic activity in RV dysfunction and pulmonary vascular remodeling in pulmonary arterial hypertension.

We were able to provide evidence that:

1. In PAH-patients, reduced parasympathetic activity was associated with reduced RV function;
2. In our PAH-rat model, increase in parasympathetic activity by PYR delayed the progression towards right heart failure;
3. PYR improved RV function, which was related to a reduction of inflammation, fibrosis and normalization of cholinergic receptors in the right ventricle;
4. PYR also reduced RV afterload and pulmonary vascular remodeling, which was associated with direct anti-proliferative and -inflammatory effects of PYR.

Figure 3.7 - Pyridostigmine effects on pulmonary vascular remodeling, MVECs proliferation and cholinergic receptors in pulmonary vasculature



Representative images of pulmonary arterioles (elastica von Gieson, 40X magnification) for control, PH and PH-PYR groups (A-C). PYR improved significantly the wall thickness of the pulmonary arterioles, as observed by media (D), intima thickness reduction (E) and formation of occlusive vascular lesions (F). In addition PYR reduced human microvascular endothelial cells (MVECs) proliferation *in vitro* from control and pulmonary arterial hypertension (PAH) cells (G). Data presented as mean \pm SEM. PO: partially obliterated vessels; FO: fully obliterated vessels. * $p < 0.05$, ** $p < 0.01$ comparison between 0 mM dose versus 10 mM. $n = 2$ in each condition. Control: $n = 7$, PH: $n = 8$ and PH-PYR: $n = 12$. ** $p < 0.01$, *** $p < 0.001$, versus PAH. Immunofluorescence quantification for α -7 nicotinic acetylcholine receptor (α -7nAChR; H) and muscarinic acetylcholine type 2-receptor (m2AChR; I). There was no difference on receptors density after PYR-treatment. Control: $n = 4$, PH: $n = 4$ and PH-PYR: $n = 4$.

Sympathovagal imbalance and RV dysfunction in PAH

Previous studies have demonstrated impaired cardiovascular autonomic function and reduced parasympathetic nerve system activity in PAH-patients.^{7, 35} Evaluation of parasympathetic activity in patients is challenging, but it can be indirectly assessed by heart rate variability spectral analysis, heart rate recovery after exercise and by evaluating the reflexes involved in heart rate changes, such as baroreflex sensitivity.¹⁹ Lower high-frequency-component of

spectral analysis⁷, impaired heart rate recovery^{6,35} and depressed baroreflex sensitivity^{7,8} have been described in PAH-patients. In addition, these parameters have been related to worse exercise capacity⁷ and prognosis.⁶ In the present study, we demonstrated that patients with reduced parasympathetic activity had a lower RVEF. In addition, we provide direct evidence that local parasympathetic activity of the RV is significantly changed. These findings suggest an important pathophysiological role of the parasympathetic nervous system. However, until now no systematic evaluation in the context of PAH has been performed.

In (right) heart failure, an autonomic nervous system imbalance develops characterized by sympathetic over-activity and parasympathetic withdrawal. At the tissue level, the RV responds by reducing beta-adrenergic receptor expression, and increasing nicotinic and/or muscarinic receptor expression. The preganglionic part of the parasympathetic system is mainly mediated by nicotinic receptors and the postganglionic part is mainly mediated by muscarinic receptor, while the pre- and postganglionic neurons are connected in series. Our finding that nicotinic receptor expression was increased and AchE activity were reduced in the right ventricle in PAH (Figure 3.1) is consistent with an adaptive, albeit inadequate, response to reduced parasympathetic signaling (Figure 3.8). This is further supported by the finding that treatment with PYR in PH-rats resulted in a further reduction of AchE activity in plasma (Figure 3.2G).

The involvement of the α -7nAChR in the 'cholinergic anti-inflammatory pathway' is well-described. Via this pathway, the vagal nerve exerts its anti-inflammatory effects by release of acetylcholine and the activation of this specific receptor. Vang *et al.* also found evidence of increased α -7nAChR expression in a cigarette smoke model. Furthermore, they observed that increased cardiac fibroblast proliferation and collagen content in RV of this mouse model was mediated via α -7nAChR.³⁶ This is in line with our observations and suggests that the improvement in RV remodeling and RV inflammation by PYR could be mediated via the α -7nAChR.

It would be of interest to explore potential differences in RV α -7nAChR expression, local AchE activity and RVEF efficiency in PAH-patients with an adapted right ventricle (RVEF>40%) *versus* patients with right heart failure (RVEF <40%). Unfortunately, the hemodynamic data from the RV tissue were not available. Also, all RV tissue samples were obtained from PAH-patients with end-stage right heart failure and a RVEF far below 40%, as they were all eligible for heart-lung transplantation.

In a recent paper by DeMazumder *et al.*, a relationship between the muscarinic receptor and beta-adrenergic receptor at myocardial level was described.²² As an (initial) compensatory mechanism, the downstream effect of the beta-adrenergic receptor was attenuated by the upregulation of the muscarinic receptors in their model of pacing-induced heart failure, which resulted in less calcium influx. Even though this protected the heart from arrhythmias; it also resulted in impaired contractility due to reduced PKA-mediated phosphorylation. We

previously demonstrated that PKA-phosphorylation is impaired in experimental and clinical PAH.^{12, 37}

Based on these studies, we propose that impaired parasympathetic activity observed in the present study may be a consequence of increased sympathetic nervous system and renin angiotensin-aldosterone system activities, which were previously described in PAH-patients.^{5, 28, 38} Sympathetic and parasympathetic activities are linked in such a way that increased sympathetic activity results in reduced parasympathetic activity. Increased RV wall stress and reduced RV function are triggers for the increased neurohormonal activation observed in PAH-patients. Thus, reduced parasympathetic activity may be a direct consequence of the increased sympathetic activation in PAH-patients. We postulate that PYR not only enhances parasympathetic activity, but also reduces sympathetic activity, and therefore may restore the autonomic imbalance in PAH.

Sympathovagal imbalance, inflammation and pulmonary vascular remodeling in PAH

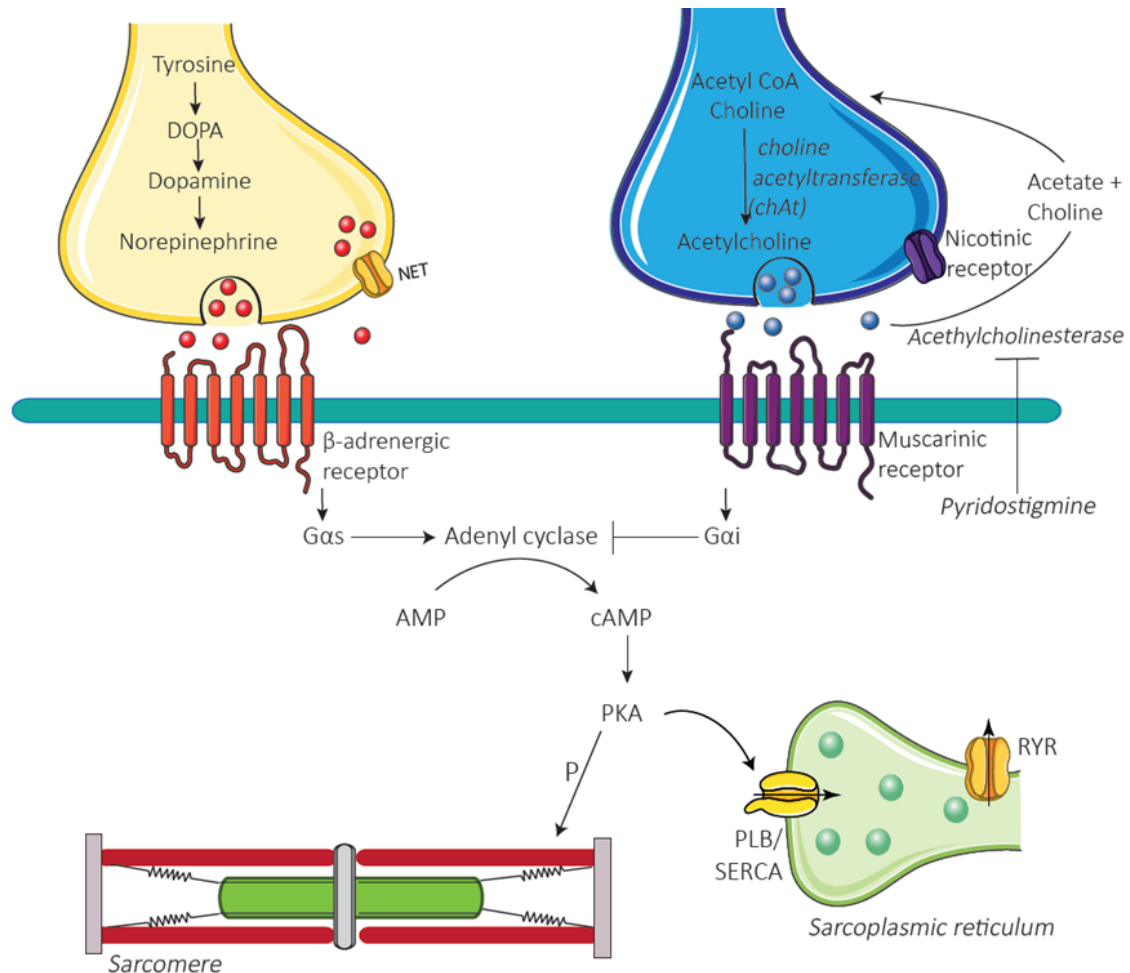
Increased levels of pro-inflammatory markers have been reported in PAH-patients.³⁹ In addition, these high levels of inflammatory mediators were associated with worse prognosis^{40, 41}, suggesting an important role of inflammation in PAH pathogenesis. Previous studies in animal models of inflammation and left heart failure have described the beneficial effects of vagal nerve^{42, 43} and cholinergic stimulation on the inflammatory response.^{44, 45} However, until now the anti-inflammatory effect of cholinergic stimulation in PAH was unknown. In the current study, we provided evidence that parasympathetic nervous system activation reduced systemic and local pro-inflammatory cytokine production, resulting in reduced RV and pulmonary vascular inflammation. The anti-inflammatory effect of a restoration of parasympathetic activity is mainly regulated via cholinergic stimulation mediated by nicotinic receptor activation and inhibition of NF- κ B pathway.^{46, 47} However, direct effects of acetylcholine on chemokine production in tumor necrosis factor-treated macrophages⁴² and endothelial cells have been described.⁴³ In our study, nicotinic receptor expression in the pulmonary vasculature was unaltered. Moreover, downstream signaling of α -7nAChR in lung homogenates was unchanged after PYR-treatment. Therefore, the anti-inflammatory and anti-proliferative effects of parasympathetic stimulation observed in the pulmonary vasculature are unlikely mediated via α -7nAChR.

Clinical relevance

In this study, we show that enhancing parasympathetic nervous system activity, by PYR is beneficial in experimental PH. PYR is a long-approved drug, used in myasthenia gravis patients, with a favorable pharmacological profile. Although no major side effects were observed in our experimental PH-model, the safety and efficacy of PYR in PAH-patients should be investigated. Currently, we are designing a proof-of-principle pilot study to investigate the acute effects of PYR on the pulmonary vasculature and RV function of PAH-patients. Also,

other approaches to alter parasympathetic activity, like vagal nerve stimulation or other drugs may be of interest.

Figure 3.8 – Summary of findings



(A) Parasympathetic-related abnormalities in PAH-patients; (B) Proposed mechanism for improved RV function, reduced RV afterload and improved survival after pyridostigmine treatment. PAH= pulmonary arterial hypertension, RV= right ventricular, SuHX model= Sugen/hypoxia rat model, AchE-activity= acetylcholinesterase activity.

Limitation

We did not include a PYR-control group in our main experimental study, based on evidence in prior studies that PYR does not have significant hemodynamic effects,^{15, 48} and anticipated difficulties obtaining ethical approval for use of animals in studies of this nature. We acknowledge that PYR has not been studied specifically for the right ventricle. However, our dose-finding study confirmed that PYR (40 mg/kg) did not have any relevant effect on RV function in controls. In addition, our novel data in human EHT, also revealed no relevant effect of PYR on maximal force and force development.

In addition, we acknowledge that the exact mechanism by which parasympathetic activity is reduced in PAH remains unclear. The focus of this study was on the consequences of reduced parasympathetic activity and the therapeutic potential of (pharmacologically) enhancement.

Conclusion

In this translational study, we demonstrated that reduced RV function in PAH-patients is associated with reduced parasympathetic activity. In addition, α -7nAChR is upregulated in the right ventricle from PAH-patients. Furthermore we also demonstrated reduced AchE activity in RV and MVECs from PAH-patients. These results are suggestive of an local adaptive response to reduced parasympathetic activity in PAH-patients. However, this compensatory mechanism may be insufficient, with persistence in autonomic dysfunction. Chronic parasympathetic nervous system stimulation in experimental-PH can improve survival, RV function and reduce pulmonary vascular remodeling. The beneficial effects of PYR may be associated with reduced inflammation and normalized RV cholinergic receptors expression. Our findings revealed a novel potential therapeutic target in PAH, and provide evidence that encourage further clinical investigations to evaluate the safety and efficacy of PYR in PAH-patients.

REFERENCES

1. Simonneau G, Gatzoulis MA, Adatia I, Celermajer D, Denton C, Ghofrani A, Gomez Sanchez MA, Krishna Kumar R, Landzberg M, Machado RF, Olschewski H, Robbins IM and Souza R. Updated clinical classification of pulmonary hypertension. *J Am Coll Cardiol*. 2013;62:D34-41.
2. Benza RL, Miller DP, Gomberg-Maitland M, Frantz RP, Foreman AJ, Coffey CS, Frost A, Barst RJ, Badesch DB, Elliott CG, Liou TG and McGoon MD. Predicting survival in pulmonary arterial hypertension: insights from the Registry to Evaluate Early and Long-Term Pulmonary Arterial Hypertension Disease Management (REVEAL). *Circulation*. 2010;122:164-72.
3. Humbert M, Sitbon O, Chaouat A, Bertocchi M, Habib G, Gressin V, Yaici A, Weitzenblum E, Cordier JF, Chabot F, Dromer C, Pison C, Reynaud-Gaubert M, Haloun A, Laurent M, Hachulla E, Cottin V, Degano B, Jais X, Montani D, Souza R and Simonneau G. Survival in patients with idiopathic, familial, and anorexigen-associated pulmonary arterial hypertension in the modern management era. *Circulation*. 2010;122:156-63.
4. de Man FS, Handoko ML, Guignabert C, Bogaard HJ and Vonk-Noordegraaf A. Neurohormonal axis in patients with pulmonary arterial hypertension: friend or foe? *Am J Respir Crit Care Med*. 2013;187:14-9.
5. Velez-Roa S, Ciarka A, Najem B, Vachieri JL, Naeije R and van de Borne P. Increased sympathetic nerve activity in pulmonary artery hypertension. *Circulation*. 2004;110:1308-12.
6. Minai OA, Gudavalli R, Mummadi S, Liu X, McCarthy K and Dweik RA. Heart rate recovery predicts clinical worsening in patients with pulmonary arterial hypertension. *Am J Respir Crit Care Med*. 2012;185:400-8.
7. Wensel R, Jilek C, Dorr M, Francis DP, Stadler H, Lange T, Blumberg F, Opitz C, Pfeifer M and Ewert R. Impaired cardiac autonomic control relates to disease severity in pulmonary hypertension. *Eur Respir J*. 2009;34:895-901.
8. Mar PL, Nwazue V, Black BK, Biaggioni I, Diedrich A, Paranjape SY, Loyd JE, Hemnes AR, Robbins IM, Robertson D, Raj SR and Austin ED. Valsalva Maneuver in Pulmonary Arterial Hypertension: Susceptibility to Syncope and Autonomic Dysfunction. *Chest*. 2016;149:1252-60.
9. Ciarka A, Doan V, Velez-Roa S, Naeije R and van de Borne P. Prognostic significance of sympathetic nervous system activation in pulmonary arterial hypertension *Am J Respir Crit Care Med*; 2010(181): 1269-75.
10. Bogaard HJ, Natarajan R, Mizuno S, Abbate A, Chang PJ, Chau VQ, Hoke NN, Kraskauskas D, Kasper M, Salloum FN and Voelkel NF. Adrenergic receptor blockade reverses right heart remodeling and dysfunction in pulmonary hypertensive rats. *Am J Respir Crit Care Med*. 2010;182:652-60.
11. Perros F, Ranchoux B, Izikki M, Bentebbal S, Happe C, Antigny F, Jourdon P, Dorfmueller P, Lecerf F, Fadel E, Simonneau G, Humbert M, Bogaard HJ and Eddahibi S. Nebivolol for improving endothelial dysfunction, pulmonary vascular remodeling, and right heart function in pulmonary hypertension. *J Am Coll Cardiol*. 2015;65:668-80.
12. de Man FS, Handoko ML, van Ballegoij JJ, Schalij I, Bogaards SJ, Postmus PE, van der Velden J, Westerhof N, Paulus WJ and Vonk-Noordegraaf A. Bisoprolol delays progression towards right heart failure in experimental pulmonary hypertension. *Circ Heart Fail*. 2012;5:97-105.
13. Bibevski S and Dunlap ME. Evidence for impaired vagus nerve activity in heart failure. *Heart Fail Rev*. 2011;16:129-35.
14. Ni M, Yang ZW, Li DJ, Li Q, Zhang SH, Su DF, Xie HH and Shen FM. A potential role of alpha-7 nicotinic acetylcholine receptor in cardiac angiogenesis in a pressure-overload rat model. *J Pharmacol Sci*. 2010;114:311-9.
15. Durand MT, Becari C, de Oliveira M, do Carmo JM, Silva CA, Prado CM, Fazan R, Jr. and Salgado HC. Pyridostigmine restores cardiac autonomic balance after small myocardial infarction in mice. *PLoS One*. 2014;9:e104476.
16. Lатарo RM, Silva CA, Fazan R, Jr., Rossi MA, Prado CM, Godinho RO and Salgado HC. Increase in parasympathetic tone by pyridostigmine prevents ventricular dysfunction during the onset of heart failure. *Am J Physiol Regul Integr Comp Physiol*. 2013;305:R908-16.
17. Okazaki Y, Zheng C, Li M and Sugimachi M. Effect of the cholinesterase inhibitor donepezil on cardiac remodeling and autonomic balance in rats with heart failure. *J Physiol Sci*. 2010;60:67-74.
18. Lатарo RM, Silva CA, Tefe-Silva C, Prado CM and Salgado HC. Acetylcholinesterase Inhibition Attenuates the Development of Hypertension and Inflammation in Spontaneously Hypertensive Rats. *Am J Hypertens*. 2015;28:1201-8.
19. Chappleau MW and Sabharwal R. Methods of assessing vagus nerve activity and reflexes. *Heart Fail Rev*. 2011;16:109-27.
20. Rain S, Handoko ML, Trip P, Gan CT, Westerhof N, Stienen GJ, Paulus WJ, Ottenheijm CA, Marcus JT, Dorfmueller P, Guignabert C, Humbert M, Macdonald P, Dos Remedios C, Postmus PE, Saripalli C, Hidalgo CG, Granzier HL, Vonk-Noordegraaf A, van der Velden J and de Man FS. Right ventricular diastolic impairment in patients with

pulmonary arterial hypertension. *Circulation*. 2013;128:2016-25, 1-10.

21. Zhao M, He X, Bi XY, Yu XJ, Gil Wier W and Zang WJ. Vagal stimulation triggers peripheral vascular protection through the cholinergic anti-inflammatory pathway in a rat model of myocardial ischemia/reperfusion. *Basic Res Cardiol*. 2013;108:345.

22. DeMazumder D, Kass DA, O'Rourke B and Tomaselli GF. Cardiac resynchronization therapy restores sympathovagal balance in the failing heart by differential remodeling of cholinergic signaling. *Circ Res*. 2015;116:1691-9.

23. Szulcek R, Happe CM, Rol N, Fontijn RD, Dickhoff C, Hartemink KJ, Grunberg K, Tu L, Timens W, Nossent GD, Paul MA, Leyen TA, Horrevoets AJ, de Man FS, Guignabert C, Yu PB, Vonk-Noordegraaf A, van Nieuw Amerongen GP and Bogaard HJ. Delayed Microvascular Shear Adaptation in Pulmonary Arterial Hypertension. Role of Platelet Endothelial Cell Adhesion Molecule-1 Cleavage. *Am J Respir Crit Care Med*. 2016;193:1410-20.

24. Kurakula K, Hamers AA, van Loenen P and de Vries CJ. 6-Mercaptopurine reduces cytokine and Muc5ac expression involving inhibition of NFkappaB activation in airway epithelial cells. *Respir Res*. 2015;16:73.

25. Hansen A, Eder A, Bonstrup M, Flato M, Mewe M, Schaaf S, Aksehirlioglu B, Schwoerer AP, Uebeler J and Eschenhagen T. Development of a drug screening platform based on engineered heart tissue. *Circ Res*. 2010;107:35-44.

26. Handoko ML, Schali J, Kramer K, Sebkh A, Postmus PE, van der Laarse WJ, Paulus WJ and Vonk-Noordegraaf A. A refined radio-telemetry technique to monitor right ventricle or pulmonary artery pressures in rats: a useful tool in pulmonary hypertension research. *Pflugers Arch*. 2008;455:951-9.

27. de Raaf MA, Schali J, Gomez-Arroyo J, Rol N, Happe C, de Man FS, Vonk-Noordegraaf A, Westerhof N, Voelkel NF and Bogaard HJ. SuHx rat model: partly reversible pulmonary hypertension and progressive intima obstruction. *Eur Respir J*. 2014;44:160-8.

28. de Man FS, Tu L, Handoko ML, Rain S, Ruiter G, Francois C, Schali J, Dorfmueller P, Simonneau G, Fadel E, Perros F, Boonstra A, Postmus PE, van der Velden J, Vonk-Noordegraaf A, Humbert M, Eddahibi S and Guignabert C. Dysregulated renin-angiotensin-aldosterone system contributes to pulmonary arterial hypertension. *Am J Respir Crit Care Med*. 2012;186:780-9.

29. Heart rate variability: standards of measurement, physiological interpretation and clinical use. Task Force of the European Society of Cardiology and the North American Society of Pacing and Electrophysiology. *Circulation*. 1996;93:1043-65.

30. Montano N, Porta A, Cogliati C, Costantino G, Tobaldini E, Casali KR and Iellamo F. Heart rate variability

explored in the frequency domain: a tool to investigate the link between heart and behavior. *Neurosci Biobehav Rev*. 2009;33:71-80.

31. Baselli G, Cerutti S, Badilini F, Biancardi L, Porta A, Pagani M, Lombardi F, Rimoldi O, Furlan R and Malliani A. Model for the assessment of heart period and arterial pressure variability interactions and of respiration influences. *Med Biol Eng Comput*. 1994;32:143-52.

32. Rubini R, Porta A, Baselli G, Cerutti S and Paro M. Power spectrum analysis of cardiovascular variability monitored by telemetry in conscious unrestrained rats. *J Auton Nerv Syst*. 1993;45:181-90.

33. Fazan R, Jr., de Oliveira M, da Silva VJ, Joaquim LF, Montano N, Porta A, Chappleau MW and Salgado HC. Frequency-dependent baroreflex modulation of blood pressure and heart rate variability in conscious mice. *Am J Physiol Heart Circ Physiol*. 2005;289:H1968-75.

34. Schuller HM. Is cancer triggered by altered signalling of nicotinic acetylcholine receptors? *Nat Rev Cancer*. 2009;9:195-205.

35. Dimopoulos S, Anastasiou-Nana M, Katsaros F, Papazachou O, Tzanis G, Gerovasili V, Pozios H, Roussos C, Nanas J and Nanas S. Impairment of autonomic nervous system activity in patients with pulmonary arterial hypertension: a case control study *J Card Fail*; 2009(15): 882-9.

36. Vang A, Clements RT, Chichger H, Kue N, Allawzi A, O'Connell KA, Jeong EM, Dudley S, Jr., Sakhatysky P, Lu Q, Zhang P, Rounds S and Choudhary G. Effect of alpha7 nicotinic acetylcholine receptor activation on cardiac fibroblasts: A mechanism underlying RV fibrosis associated with cigarette smoke exposure. *Am J Physiol Lung Cell Mol Physiol*. 2017:ajplung 00393 2016.

37. Rain S, Bos Dda S, Handoko ML, Westerhof N, Stienen G, Ottenheijm C, Goebel M, Dorfmueller P, Guignabert C, Humbert M, Bogaard HJ, Remedios CD, Saripalli C, Hidalgo CG, Granzier HL, Vonk-Noordegraaf A, van der Velden J and de Man FS. Protein changes contributing to right ventricular cardiomyocyte diastolic dysfunction in pulmonary arterial hypertension. *J Am Heart Assoc*. 2014;3:e000716.

38. Bristow MR, Minobe W, Rasmussen R, Larrabee P, Skerl L, Klein JW, Anderson FL, Murray J, Mestroni L and Karwande SV. Beta-adrenergic neuroeffector abnormalities in the failing human heart are produced by local rather than systemic mechanisms. *J Clin Invest*. 1992;89:803-15.

39. Humbert M, Monti G, Brenot F, Sitbon O, Portier A, Grangeot-Keros L, Duroux P, Galanaud P, Simonneau G and Emilie D. Increased interleukin-1 and interleukin-6 serum concentrations in severe primary pulmonary hypertension. *Am J Respir Crit Care Med*. 1995;151:1628-31.

40. Soon E, Holmes AM, Treacy CM, Doughty NJ, Southgate L, Machado RD, Trembath RC, Jennings S,

Barker L, Nicklin P, Walker C, Budd DC, Pepke-Zaba J and Morrell NW. Elevated levels of inflammatory cytokines predict survival in idiopathic and familial pulmonary arterial hypertension. *Circulation*. 2010;122:920-7.

41. Cracowski JL, Chabot F, Labarere J, Faure P, Degano B, Schwebel C, Chaouat A, Reynaud-Gaubert M, Cracowski C, Sitbon O, Yaici A, Simonneau G and Humbert M. Proinflammatory cytokine levels are linked to death in pulmonary arterial hypertension. *Eur Respir J*. 2014;43:915-7.

42. Borovikova LV, Ivanova S, Zhang M, Yang H, Botchkina GI, Watkins LR, Wang H, Abumrad N, Eaton JW and Tracey KJ. Vagus nerve stimulation attenuates the systemic inflammatory response to endotoxin. *Nature*. 2000;405:458-62.

43. Saeed RW, Varma S, Peng-Nemeroff T, Sherry B, Balakhaneh D, Huston J, Tracey KJ, Al-Abed Y and Metz CN. Cholinergic stimulation blocks endothelial cell activation and leukocyte recruitment during inflammation. *J Exp Med*. 2005;201:1113-23.

44. Rocha JA, Ribeiro SP, Franca CM, Coelho O, Alves G, Lacchini S, Kallas EG, Irigoyen MC and Consolim-Colombo FM. Increase in cholinergic modulation with pyridostigmine induces anti-inflammatory cell recruitment

soon after acute myocardial infarction in rats. *Am J Physiol Regul Integr Comp Physiol*. 2016;310:R697-706.

45. Feriani DJ, Souza GI, Carrozzi NM, Mostarda C, Dourado PM, Consolim-Colombo FM, De Angelis K, Moreno H, Irigoyen MC and Rodrigues B. Impact of exercise training associated to pyridostigmine treatment on autonomic function and inflammatory profile after myocardial infarction in rats. *Int J Cardiol*. 2017;227:757-765.

46. Tracey KJ. The inflammatory reflex. *Nature*. 2002;420:853-9.

47. Wang H, Yu M, Ochani M, Amella CA, Tanovic M, Susarla S, Li JH, Wang H, Yang H, Ulloa L, Al-Abed Y, Czura CJ and Tracey KJ. Nicotinic acetylcholine receptor $\alpha 7$ subunit is an essential regulator of inflammation. *Nature*. 2003;421:384-8.

48. Lu Y, Zhao M, Liu JJ, He X, Yu XJ, Liu LZ, Sun L, Chen LN and Zang WJ. Long-term administration of pyridostigmine attenuates pressure overload-induced cardiac hypertrophy by inhibiting calcineurin signalling. *J Cell Mol Med*. 2017.

3

CONTRIBUTION OF IMPAIRED PARASYMPATHETIC ACTIVITY IN RIGHT VENTRICULAR DYSFUNCTION AND PULMONARY VASCULAR REMODELING IN PULMONARY ARTERIAL HYPERTENSION

Supplemental material

SUPPLEMENTAL METHODS

Pyridostigmine pilot dose finding

5 male Sprague Dawley rats were used to identify the optimal pyridostigmine (PYR) dose. Previous to the treatment, an aorta telemetry device (TA11PA-C40, Data Science International, St. Paul, MN) was implanted for heart rate, systolic arterial pressure and animal activity measurements. After animal recovery from the telemetry surgery, PYR-treatment was initiated for 5 days, at different doses (25, 31 and 40mg/kg/day). The 40 mg/kg was the optimal dose able to reduce the heart rate by 10% and increase the parasympathetic modulation (**Figure S1**).

Hemodynamic evaluation

Echocardiography

Rats were evaluated by echocardiography prior to PYR-treatment and at the end of study. Transthoracic echocardiographic measurements (ProSound SSD-4000 system equipped with a 13-MHz linear transducer UST-5542, Aloka, Tokyo, Japan) were performed under anesthetized and spontaneously breathing rats (isoflurane 2.0% in 1:1 O₂/air mix; Pharmachemie, Haarlem, The Netherlands).¹ Analyses were performed off-line (Image-Arena 2.9.1, TomTec Imaging Systems, Unterschleissheim, Munich, Germany). Parameters for right ventricular (RV) function were: cardiac output (Doppler-derived stroke volume, heart rate), and tricuspid annular plane systolic excursion (TAPSE). Parameters for RV remodeling were: RV end diastolic diameter (RVEDD) and RV wall thickness. Pulmonary vascular resistance (PVR) was estimated by Poiseuille's law.²⁻⁴

Right ventricle catheterization

At the end of study rats were anesthetized with isoflurane (induction: 4.0% in 1:1 O₂/air mix; maintenance: 2.0% in 1:1 O₂/air mix), intubated (16G Teflon tube) and attached to a mechanical ventilator (Micro-Ventilator, UNO, Zevenaar, The Netherlands; ventilator settings: breathing frequency 75/min, pressures 9/0 cmH₂O, inspiratory/expiratory ratio 1:1). Rats were placed on a warming pad to maintain body temperature, and open-chest RV catheterization was performed. For the RV catheterization, the thorax was opened and the heart exposed, a temporary suture was placed around the inferior vena cava and a (23G needle) puncture in the right ventricle was performed. A combined pressure-volume catheter (SPR-869, Millar Instruments, Houston TX) was inserted into the right ventricle and positioned in the long axis. The signals (processed by MPVS-300, Millar Instruments), obtained at steady state (at least 10s) and during temporary vena cava occlusion were digitally recorded (2.0 kHz sampling rate; Chart 5.5.6, ADInstruments, Sydney, Australia) and analyzed off-line, using (LabChart 8, ADInstruments, Sydney, Australia) with custom-made algorithms (programmed in MATLAB R2007b, The MathWorks, Natick MA). Stroke volume (in RVU) derived from the conductance catheter was calibrated using the stroke volume (in ml) from echocardiogram as reference.⁵

RV pressure-volume relationships

Using custom made algorithms (programmed in MATLAB 2007b, The MathWorks, Natick, MA) RV (peak-) systolic pressures and RV end-diastolic pressures were automatically determined from steady state measurements, as well as arterial elastance (E_a), a measurement of RV afterload.⁶ From vena cava occlusion, end-systolic elastance (E_{es} ; RV contractility) and end-diastolic elastance (E_{ed} ; RV stiffness) were determined.⁵ These parameters represent the slope of end-systolic and end-diastolic pressure-volume relationships, and are considered load independent measurements for cardiac contractility (E_{es}) and stiffness (E_{ed}).⁷ The ratio E_{es}/E_a was calculated, and it represents the RV-arterial coupling.

Histomorphometric analyses of heart and lungs

After the hemodynamic evaluation, rats were euthanized (by exsanguination under isoflurane), and heart, lungs and other major organs were harvested. Lungs were weighted; left lobe was filled by 1:1 mix of saline and cryofixative (Tissue-Tek O.C.T. compound, Sakura, Fintek, Europe, Zoeterwolde, The Netherlands), and snap frozen in liquid nitrogen. The heart was perfused, weighted, dissected and snap-frozen in liquid nitrogen. Images were collected using a Motic microscope (BA210, Wetzlar, Germany) and a digital tablet camera (VisiCam ® TC10, VWR International B.V, Amsterdam, The Netherlands). ImageJ for Windows 1.48 software (National Institutes of Health, USA) was used for image analysis, taking the pixel-to-aspect ratio into account.

Cardiomyocyte cross-sectional area

Hematoxylin & eosin (HE)-stained cardiac cryosections (5 μ m) were used to determine left ventricular (LV) and RV cardiomyocyte cross-sectional area (CSA). Cardiomyocyte size for each ventricle was expressed as the average CSA of minimally twenty transversally cut cardiomyocytes at the level of the nucleus, randomly distributed over the ventricles.

Cardiac fibrosis

Picrosirius red staining (5 μ m cryosections) was used for analysis of cardiac fibrosis. LV and RV fibrosis were expressed as the percentage tissue area positive for collagen, measured over minimally five randomly areas per ventricle.

Relative wall thickness of pulmonary arterioles

Lung cryosections (5 μ m) were stained with Elastica van Giesson for morphometric analysis of vascular dimensions. Minimally fifty transversally pulmonary arterioles cut, with an outer diameter between 25 and 100 μ m, randomly distributed over the lungs, were measured. Media and intima wall thickness were measured in duplicate as described previously.⁸

RV and lung immunofluorescence

Cryosections of RV apex (5µm) were blocked with 1% bovine serum albumin (BSA) in phosphate-buffered saline (PBS), and incubated for 60 min or overnight with primary CD31/CD45 (1:35; sc-1506-R, sc-53045, Santa Cruz Biotechnology, Dallas, TX), alpha-7 nicotinic acetylcholine receptor (α-7nAChR; 1:50; ANC-007; Alomone, Jerusalem, Israel) and muscarinic acetylcholine type 2 receptor (m2AChR; 1:50; M9558, Sigma-Aldrich, St. Louis, MO), followed by appropriate secondary antibody (Invitrogen, MA) for 1 hour. Sections were also incubated with WGA (glycocalyx), α-actinin (1:1000; A7732 Sigma-Aldrich, St. Louis, MO) and DAPI (nuclei) counterstaining.

Lung cryosections (5µm) were also blocked with 1% BSA in PBS and incubated overnight with the same α-7nAChR and m2AChR-antibodies followed by appropriated secondary antibody. Lung sections were also incubated with anti α-smooth muscle actin- Cy3 antibody (1:100; Sigma-Aldrich, St. Louis, MO), von willebrand factor (1:200; AB8822; Abcam; Cambridge, UK) and DAPI (nuclei) counterstaining.

Immunofluorescence quantification

Image acquisition was performed on a Marianas digital imaging microscopy workstation (Intelligent Imaging Innovations (3i), Denver, CO). SlideBook imaging analysis software (SlideBook 6, 3i) was used to semi-automatically quantify the images. Capillary density and leukocyte infiltration was expressed as the number of capillaries and of positive CD45-nuclei per area, measured over three randomly areas per ventricle. Lung α-7nAChR and m2AChR mean relative fluorescence intensity was semi-automatically quantified and measured over fifteen vessels.

ELISA measurements

Cytokine levels in rat plasma were measured by ELISA for IL-6 and MCP-1 (Ready-SET-Go!, eBioscience) according to the manufacturers' instructions. In addition, acetylcholinesterase activity was measured in plasma, MVECs, RV, lung and pulmonary artery homogenates from PAH-patients, PH-rats and controls by ELISA (ThermoFisher Scientific, A12217) according to the manufacturers' instructions.

Protein expression by Western Blot in Lung Homogenates

To evaluate the downstream signalling of the α-7nAChR in lung homogenates from experimental-PH, the expression of the phosphorylated form of-ERK (p-ERK; 1:2000; CS9106; Cell Signaling), total protein expression of ERK (tERK; 1:1000; CS9102; Cell Signaling) and NF-κB-p65 (phospho-Ser311; 1:1000; 11260; Sabbiotech) were evaluated by western blot analysis.

Human engineered heart tissue generation, treatment, contraction measurements

Human engineered heart tissue (EHT) was prepared as previously described, with small modifications.^{9, 10} Briefly, iCell® cardiomyocytes² (Cellular Dynamics International), which are human induced pluripotent stem cell (HiPSC)-derived cardiomyocytes, were thawed according to manufacture instructions. HiPSC-EHT reconstitution mix was prepared with 3.5×10^5 cardiomyocytes per 70 μ l HiPSC-EHT. EHT was generated in agarose molds with solid silicone racks as previously described.^{11, 12} Cells were mixed with 100 μ l/ml Matrigel™ (Corning, 354234), 5 mg/ml bovine fibrinogen (Sigma, F8630; 200 mg/ml in 0.9% NaCl plus 0.5 μ g/mg aprotinin; Sigma, A1153), 2×DMEM (matching the volume of fibrinogen and thrombin for isotonicisation) and EHTs were generated with 70 μ l per EHT (3.5×10^5 cells), and 3 U/ml thrombin (100 U/ml; Sigma, T7513). The cell mix was pipetted into the agarose casting molds around the silicone posts. After fibrin polymerization (37°C, 2h) the silicone racks were transferred to a new 24-wells plate filled with culture medium, consisting of Dulbecco's modified Eagle's medium (DMEM; Biochrom, F0415), 1% penicillin/streptomycin, 10% horse serum (Gibco, 26050), 10 μ g/ml insulin (Sigma, I9278) and 33 μ g/ml of aprotinin, and maintained in the incubator (37°C, 21% O₂, 7% CO₂). Culture medium was changed 3 times a week. After 10-14 days, human EHTs displayed spontaneous coherent contractions. Contractile analysis was performed on 20-35-day-old EHTs in serum-free culture medium, supplemented with 10 mM HEPES for pH-steadiness, pre-incubated at 37°C, 21% O₂, 7% CO₂ for 2 h. EHTs were treated with 10 μ M acetylcholine (Sigma Aldrich, A2661) or 10 mM pyridostigmine (Sigma Aldrich, P9797). Contractility measurements were performed at baseline, 15 minutes and 60 minutes after the respective treatment. Force was measured based on automated video-optical recording and EHT contour recognition as described (EHT Technologies, A0001).⁴ Values for beating frequency (heart rate), maximal force, contraction velocity (dF/dt max) and relaxation velocity (dF/dt min) were calculated with a specific custom-made algorithm.^{12, 13}

SUPPLEMENTAL TABLES AND FIGURES

Table S1 - Cardiovascular autonomic function after PYR-treatment

	PH	PH-PYR	p-value
	(n=6)	(n=6)	PH vs. PYR
Δ HRV_var (ms ²)	28±18	175±5	0.18
Δ Peak LF (Hz)	-0.4±5.2	-8.6±8.1	0.48
Δ LF (ms ²)	-36±19	149±104	0.18
Δ LF (nu)	9.5±15	19±18	0.59
Δ Peak HF (Hz)	-7.0±8.8	-12±5.8	0.94
Δ HF (ms ²)	-27±18	87±35	0.03
Δ HF (nu)	0.6±3.2	0.5±3.9	0.82
Δ LF/HF index	24±18	11±20	0.79
Δ SAP_var (mmHg ²)	36±17	6.6±24	0.33
Δ VLF (mmHg ²)	69±20	-20±19	0.004
Δ LF (mmHg ²)	53±27	-45±11	0.009
Δ HF (mmHg ²)	26±14	62±26	0.48
Δ α -index (ms/mmHg)	-23±14	212±98	0.02

All data are presented as mean \pm SEM. Delta (Δ) percentage (%) between PH and PH-PYR; Mann-Whitney test. Abbreviations: PYR= pyridostigmine; HR= heart rate; HRV_var= heart rate variability; LF= low frequency; HF= high frequency; SAP_var= systolic arterial pressure variability; VLF= very low frequency.

Table S2 - Baseline echocardiography characteristics

	Control (n=7)	PH (n=12)	PH-PYR (n=12)	p-value	
				Control vs. PH	PH vs. PYR
Cardiac output (mL/min)	77±6.1	67±6.0	69±6.3	0.33	0.75
Stroke volume (mL)	0.26±0.02	0.23±0.02	0.24±0.02	0.36	0.65
Heart rate (bpm)	299±7.8	292±7.7	283±6.9	0.49	0.39
TAPSE (mm)	3.3±0.07	1.9±0.08	1.9±0.11	<0.001	0.74
RV wall thickness (mm)	0.56±0.06	1.2±0.05	1.2±0.04	<0.001	0.29
RVEDD (mm)	3.8±0.14	6.5±0.31	6.5±0.29	<0.001	0.97
PAAT/cl (*100)	10.0±0.24	4.2±0.2	4.2±0.3	<0.001	0.83
eRVSP (mmHg)	47.3±1.3	89.2±1.7	90.2±2.7	<0.001	0.76
PVR (mmHg/ml/min)	0.42±0.04	0.90±0.09	0.95±0.15	0.02	0.75

All data are presented as mean ± SEM; One-way ANOVA followed by Bonferroni correction; Abbreviations: PYR= pyridostigmine; TAPSE= tricuspid annular plane systolic excursion; RVEDD= right ventricular end-diastolic diameter; PAAT/cl= pulmonary acceleration time divided by cycle length; eRVSP= estimated right ventricular systolic pressure; PVR= pulmonary vascular resistance.

Table S3 - Echocardiographic characteristics at the end of the study

	Control (n=7)	PH (n=9)	PH-PYR (n=12)	p-value	
				Control vs. PH	PH vs. PYR
Cardiac output (mL/min)	90±4.0	57±5.9	73±5.7	<0.001	0.05
Stroke volume (mL)	0.30±0.02	0.19±0.02	0.25±0.01	<0.001	0.04
Heart rate (bpm)	300±5.6	293±6.7	289±10.9	>0.999	>0.999
TAPSE (mm)	3.5±0.09	1.6±0.10	2.1±0.15	<0.001	0.03
RV wall thickness (mm)	0.56±0.04	1.5±0.08	1.1±0.03	<0.001	<0.001
RVEDD (mm)	3.9±0.19	7.1±0.35	6.1±0.28	<0.001	0.05
PAAT/cl (*100)	10.2±0.26	3.8±0.36	5.1±0.22	<0.001	0.003
eRVSP (mmHg)	46.5±1.4	94.5±4.0	81.2±1.9	<0.001	0.003
PVR (mmHg/ml/min)	0.36±0.02	1.17±0.18	0.77±0.08	<0.001	0.04

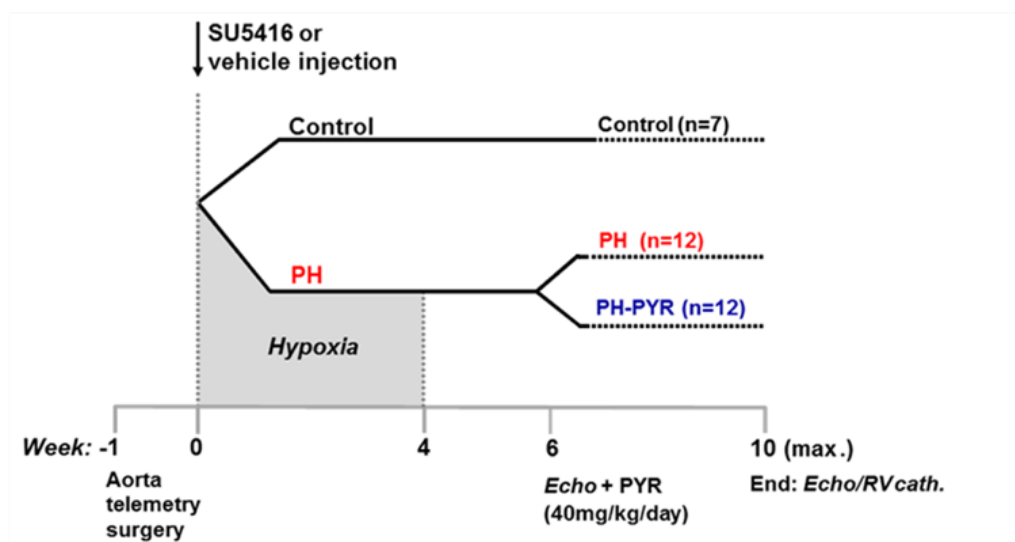
All data are presented as mean ± SEM; One-way ANOVA followed by Bonferroni correction; Abbreviations: PYR= pyridostigmine; TAPSE= tricuspid annular plane systolic excursion; RVEDD= right ventricular end-diastolic diameter; PAAT/cl= pulmonary acceleration time divided by cycle length; eRVSP= estimated right ventricular systolic pressure; PVR= pulmonary vascular resistance.

Table S4 - Autopsy and hemodynamic data

	Control (n=7)	PH (n=9)	PH-PYR (n=12)	p-value	
				Control vs. PH	PH vs. PYR
Body mass (g)	515±36	478±27	458±12	0.31	0.52
Tibia length (mm)	40.9±0.7	39.3±0.7	41.8±1.8	0.47	0.21
Lungs/tl (g/mm*1000)	41.4±1.3	55.3±2.8	56.8±3.3	<0.01	0.71
RV mass/tl (g/mm*1000)	5.4±0.4	14.2±0.7	12.7±1.0	<0.001	0.21
LV + S mass/tl (g/mm*1000)	15.9±1.8	22.9±1.5	22.5±1.6	<0.01	0.83
RV/(LV+S)	0.35±0.02	0.63±0.04	0.56±0.03	<0.001	0.15
LV CD45+ cells (CD45+/ mm ²)	14.4±2.0	24.3±2.2	25.8±2.1	0.01	0.61
RVESP (mmHg)	23.6±0.9	58.1±1.6	53.4±4.7	<0.001	0.41
RVEDP (mmHg)	3.5±0.6	5.2±0.8	4.9±0.8	0.16	0.80
Liver/tl (g/mm*1000)	397±38	402±18	347±10	0.86	0.06
Left Kidney/tl (g/mm*1000)	35.2±2.5	35.8±1.8	33.5±1.4	0.82	0.34
Right kidney/tl (g/mm*1000)	36.5±2.6	36.4±1.6	34.0±1.3	0.99	0.31

All data are presented as mean ± SEM. One-way ANOVA followed by Bonferroni correction; Abbreviations: PYR= pyridostigmine; tl= tibia length; RV=right ventricle; LV + S=left ventricle (including septum); RV/(LV+S)= RV over LV (including septum) mass ratio; RVESP= right ventricular end-systolic pressure; RVEDP= right ventricular end-diastolic pressure.

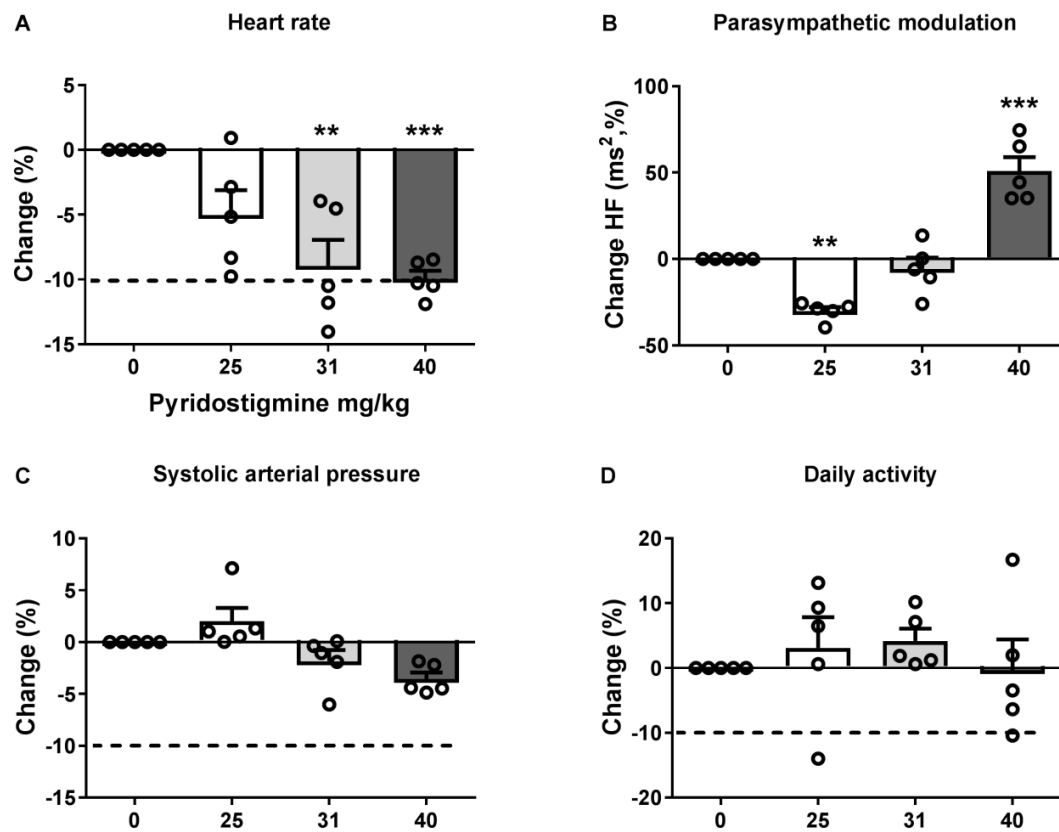
Figure S1 – Study design



SU5416 combined with chronic hypoxia: Study design of SU5416 combined with chronic hypoxia, as PH-experimental model. Control: n=7, PH: n=12, PH-PYR: n=12; Week 0: SU5416 (25 mg/kg, s.c.) or 0.5% carboxymethylcellulose (CMC) injection and placed in hypoxia (10% oxygen) for 4 weeks. At week

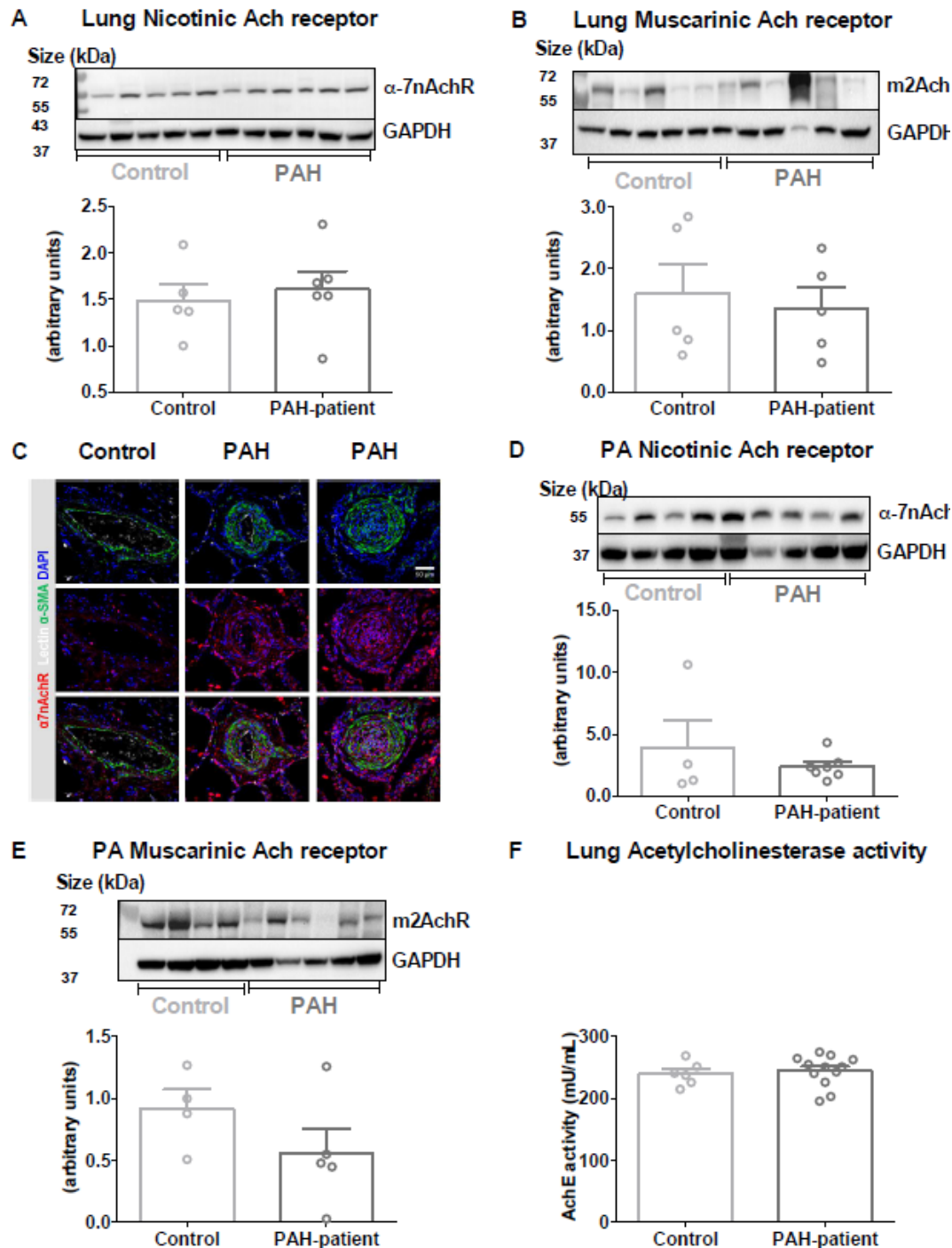
6 (normoxia), echocardiogram (Echo) followed by PYR-treatment (40mg/kg). At the end of study, at week 10 or when animals develop signs of heart failure, echocardiogram and right ventricle (RV) catheterization (cath.) were performed

Figure S2 – Pyridostigmine pilot dose finding



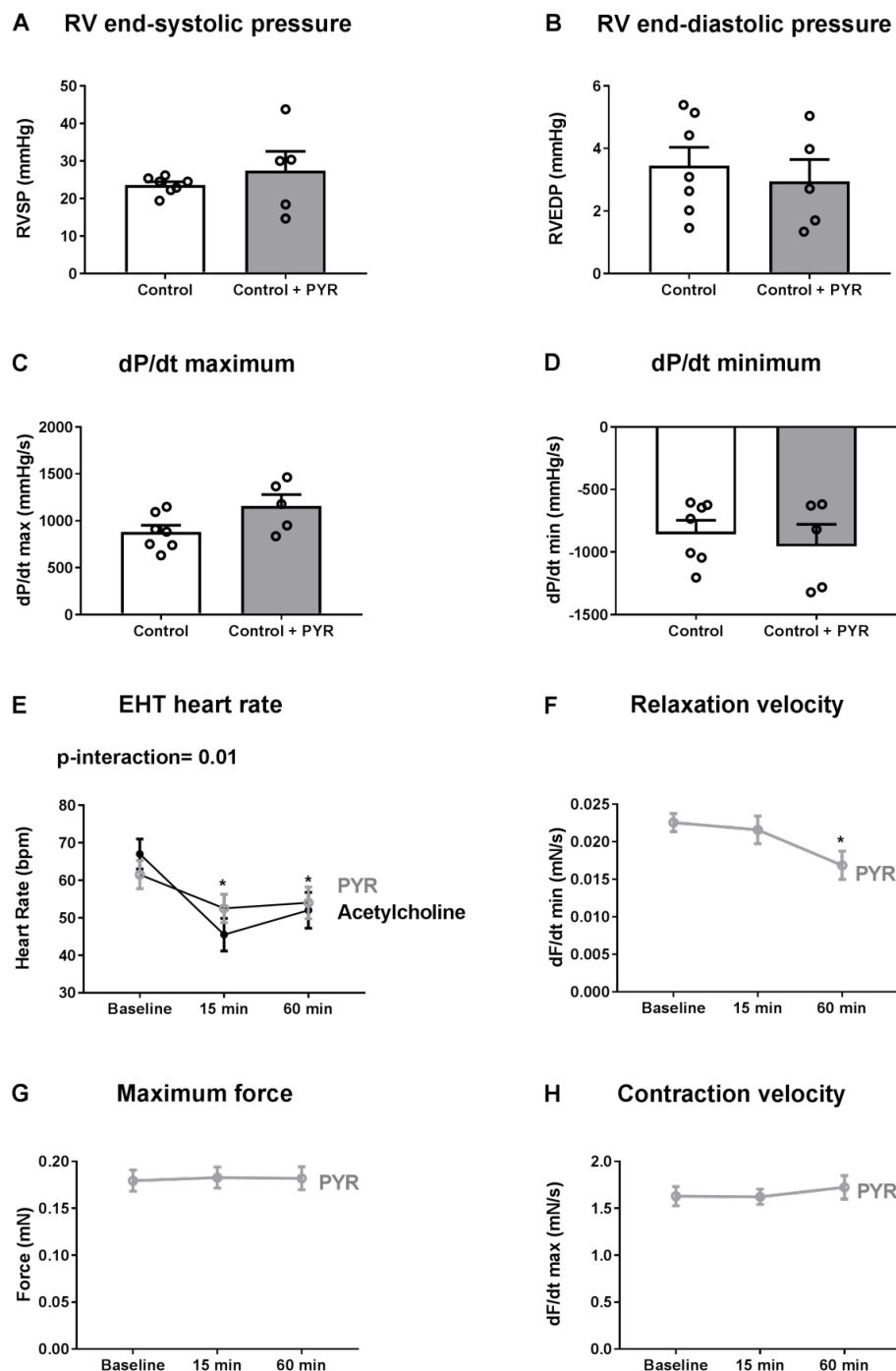
Telemetry results from previous pilot study using 5 male Sprague Dawley rats. The same animals were treated with pyridostigmine at different doses for five days (with a washout in between). The 40mg/kg dose significantly reduced heart rate by 10% (A) and significantly increase the parasympathetic modulation (B) without relevant effect in systolic arterial pressure (C) or in daily activity (D). One-way ANOVA for repeated measurement followed by Bonferroni corrected post-hoc analysis. ** $p < 0.01$, *** $p < 0.001$ versus 0 (no-pyridostigmine).

Figure S3 – Cholinergic signaling in pulmonary vasculature and lung homogenates from PAH-patients



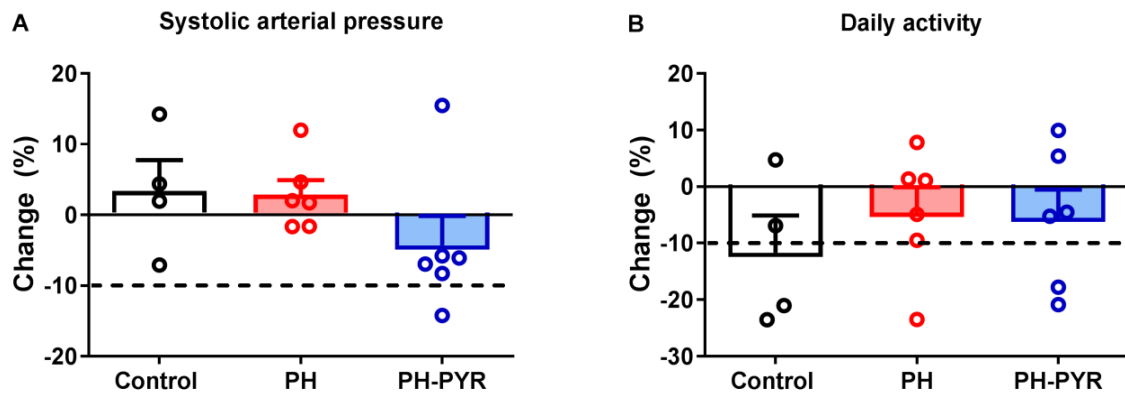
Representative western blot analyses from alpha-7 nicotinic acetylcholine (Ach) receptor (α -7nAchR; A) and muscarinic acetylcholine type 2-receptor (m2AchR; B) expression in lung homogenates from controls and PAH-patients. Representative immunofluorescence staining for α -7nAchR (C) for control and PAH-patients; α -7nAchR (red), α -smooth muscle actin (green), lectin (white) and nuclei (DAPI, blue). Western blot analyses from α -7nAchR (D) and m2AchR (E) expression in pulmonary artery (PA) homogenates for control and PAH-patients. Acetylcholinesterase (AchE) activity in whole lung homogenates from PAH-patients and controls. (F) Unpaired t-test, no significant differences were observed between PAH-patients versus controls.

Figure S4 – Effects of PYR in control animals and in human 3D engineered heart tissue



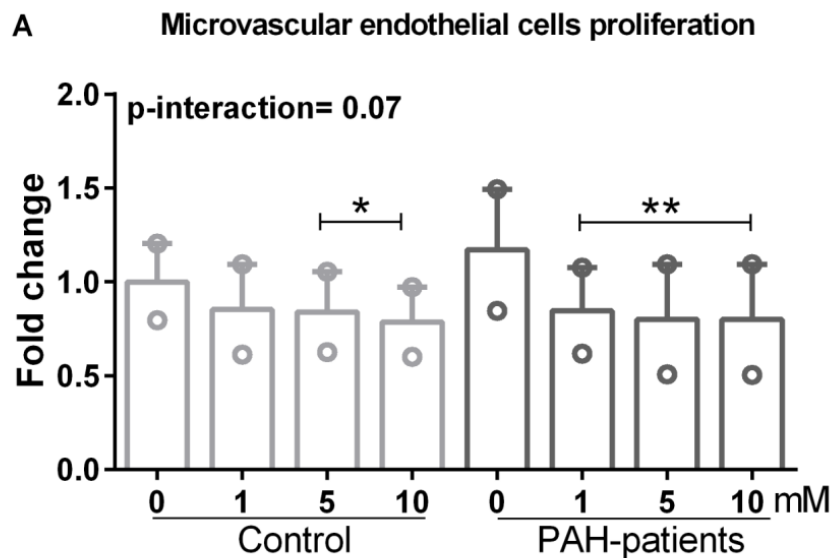
Effect of PYR in control rats in RV function. (**A**) RV end-systolic pressure, (**B**) RV end-diastolic pressures, (**C**) RV contractility and (**D**) RV relaxation. From E-H: effect of PYR in healthy human 3D engineered heart tissue (EHT). (**E**) Effect of acetylcholine (Ach) and PYR on heart rate; 2-way ANOVA for repeated measurements followed by Bonferroni corrected post-hoc analysis. (**F**) Relaxation velocity corrected by heart rate after 15 and 60 min of PYR treatment. (**G**) Maximum force after 15 and 60 min of PYR treatment. (**H**) Contraction velocity after 15 and 60 min of PYR treatment. **G-H**: One-way ANOVA for repeated measurement followed by Bonferroni corrected post-hoc analysis. * $p < 0.05$ vs. baseline measurement. bpm: beats per minute; mN: milinewton; mN/s: milinewton per second.

Figure S5 – Effects of chronic pyridostigmine treatment on systolic arterial pressure and daily activity



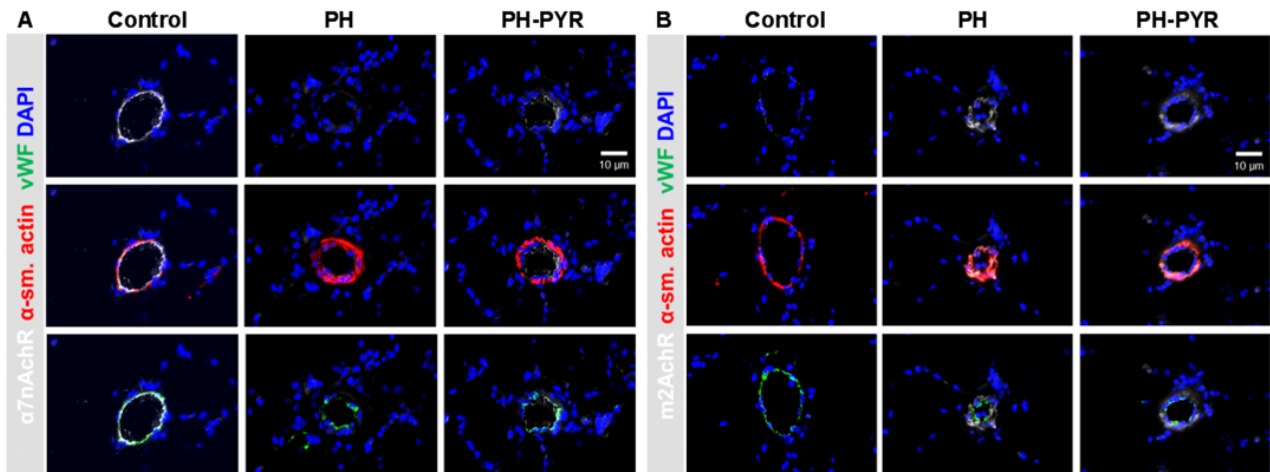
Telemetry results from chronic pyridostigmine treatment. (A) No significant effects on systolic arterial pressure or daily activity (B) were observed by PYR treatment. One-way ANOVA for repeated measurement followed by Bonferroni corrected post-hoc analysis.

Figure S6 – Pyridostigmine reduced microvascular endothelial cells proliferation in vitro



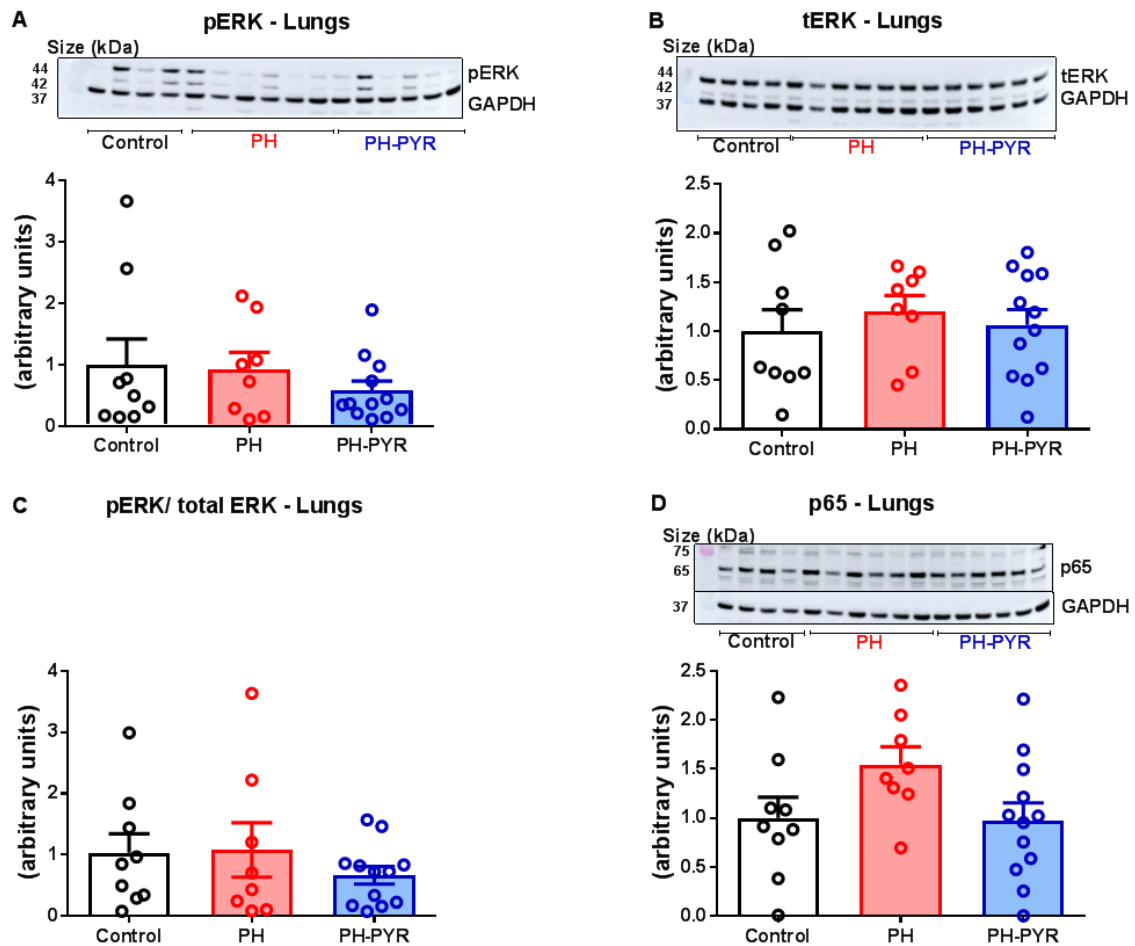
Different concentrations of pyridostigmine (PYR) reduced human microvascular endothelial cells (MVECs) proliferation in vitro from pulmonary arterial hypertension (PAH) cells. analysis; * $p < 0.05$, ** $p < 0.01$ comparison between 0 mM dose. $n = 2$ in each condition. 2-way ANOVA for repeated measurements followed by Bonferroni corrected post-hoc.

Figure S7 - Representative immunofluorescence staining for cholinergic receptors in the pulmonary vasculature from experimental-PH



Representative immunofluorescence staining for alpha-7 nicotinic acetylcholine receptor ($\alpha 7$ -nAChR; **A**) and muscarinic acetylcholine type 2-receptor (m2AChR; **B**) for control, PH and PH-PYR groups. $\alpha 7$ -nAChR and m2AChR (white), α -smooth muscle actin (red), von willebrand factor (green) and nuclei (DAPI).

Figure S8 – Downstream signaling of alpha-7 nicotinic acetylcholine receptor in lung homogenates from experimental PH



Representative example of protein expression of alpha-7 nicotinic acetylcholine receptor downstream targets on whole lung homogenates. No significant differences were observed in phosphorylated-ERK (**A**), total-ERK (**B**) and on NF- κ B-p65 (**D**) after PYR-treatment.

SUPPLEMENTAL REFERENCES

1. Handoko ML, de Man FS, Happe CM, SchaliJ I, Musters RJ, Westerhof N, Postmus PE, Paulus WJ, van der Laarse WJ and Vonk-Noordegraaf A. Opposite effects of training in rats with stable and progressive pulmonary hypertension. *Circulation*. 2009;120:42-9.
2. Handoko ML, SchaliJ I, Kramer K, SebkhI A, Postmus PE, van der Laarse WJ, Paulus WJ and Vonk-Noordegraaf A. A refined radio-telemetry technique to monitor right ventricle or pulmonary artery pressures in rats: a useful tool in pulmonary hypertension research. *Pflugers Arch*. 2008;455:951-9.
3. Chemla D, Castelain V, Humbert M, Hebert JL, Simonneau G, Lecarpentier Y and Herve P. New formula for predicting mean pulmonary artery pressure using systolic pulmonary artery pressure. *Chest*. 2004;126:1313-7.
4. Selimovic N, Rundqvist B, Bergh CH, Andersson B, Petersson S, Johansson L and Bech-Hanssen O. Assessment of pulmonary vascular resistance by Doppler echocardiography in patients with pulmonary arterial hypertension. *J Heart Lung Transplant*. 2007;26:927-34.
5. de Man FS, Handoko ML, van Ballegoij JJ, SchaliJ I, Bogaards SJ, Postmus PE, van der Velden J, Westerhof N, Paulus WJ and Vonk-Noordegraaf A. Bisoprolol delays progression towards right heart failure in experimental pulmonary hypertension. *Circ Heart Fail*. 2012;5:97-105.
6. Brimiouille S, Wauthy P, Ewalenko P, Rondelet B, Vermeulen F, Kerbaul F and Naeije R. Single-beat estimation of right ventricular end-systolic pressure-volume relationship. *Am J Physiol Heart Circ Physiol*. 2003;284:H1625-30.
7. Suga H, Sagawa K and Shoukas AA. Load independence of the instantaneous pressure-volume ratio of the canine left ventricle and effects of epinephrine and heart rate on the ratio. *Circ Res*. 1973;32:314-22.
8. de Raaf MA, SchaliJ I, Gomez-Arroyo J, Rol N, Happe C, de Man FS, Vonk-Noordegraaf A, Westerhof N, Voelkel NF and Bogaard HJ. SuHx rat model: partly reversible pulmonary hypertension and progressive intima obstruction. *Eur Respir J*. 2014;44:160-
9. Mannhardt I, Breckwoldt K, Letuffe-Breniere D, Schaaf S, Schulz H, Neuber C, Benzin A, Werner T, Eder A, Schulze T, Klampe B, Christ T, Hirt MN, Huebner N, Moretti A, Eschenhagen T and Hansen A. Human Engineered Heart Tissue: Analysis of Contractile Force. *Stem Cell Reports*. 2016;7:29-42.
10. Mannhardt I, Eder A, Dumotier B, Prondzynski M, Kramer E, Traevert M, Sohren KD, Flenner F, Stathopoulou K, Lemoine MD, Carrier L, Christ T, Eschenhagen T and Hansen A. Blinded contractility analysis in hiPSC-cardiomyocytes in engineered heart tissue format: Comparison with human atrial trabeculae. *Toxicol Sci*. 2017.
11. Schaaf S, Eder A, Vollert I, Stohr A, Hansen A and Eschenhagen T. Generation of strip-format fibrin-based engineered heart tissue (EHT). *Methods Mol Biol*.
12. Hansen A, Eder A, Bonstrup M, Flato M, Mewe M, Schaaf S, Aksehirlioglu B, Schwoerer AP, Uebeler J and Eschenhagen T. Development of a drug screening platform based on engineered heart tissue. *Circ Res*. 2010;107:35-44.
13. Wijnker PJ, Friedrich FW, Dutsch A, Reischmann S, Eder A, Mannhardt I, Mearini G, Eschenhagen T, van der Velden J and Carrier L. Comparison of the effects of a truncating and a missense MYBPC3 mutation on contractile parameters of engineered heart tissue. *J Mol Cell Cardiol*. 2016;97:82-92.

4

INTERPLAY OF SEX HORMONES AND LONG-TERM RIGHT VENTRICULAR ADAPTATION IN A DUTCH PULMONARY ARTERIAL HYPERTENSION COHORT

J van Wezenbeek* & JA Groeneveldt* & A Llucà-Valldeperas*, CE van der Bruggen, SMA Jansen, AJ Smits, R Smal, JW van Leeuwen, C dos Remedios, A Keogh, M Humbert, P Dorfmueller, O Mercier, C Guignabert, HWM Niessen, ML Handoko, JT Marcus, LJ Meijboom, FPT Oosterveer, BE Westerhof, AC Heijboer, HJ Bogaard, A Vonk Noordegraaf, MJ Goumans, FS de Man

**Authors contributed equally*

Submitted

ABSTRACT

Aim: To investigate the association between altered sex hormone expression and long-term right ventricular (RV) adaptation and progression of right heart failure in a Dutch cohort of Pulmonary Arterial Hypertension (PAH)-patients across a wide range of ages.

Methods: In this study we included 306 PAH-patients, of which 196 females and 110 males. From 55 patients and 15 controls we collected plasma samples for sex hormone analysis. In 280 patients, right heart catheterization (RHC) and/or cardiac magnetic resonance (CMR) imaging was performed at baseline. For longitudinal data analysis we selected patients that underwent a RHC and/or CMR maximally 1,5 years prior to an event (death or transplantation, N=49).

Results: Dehydroepiandrosterone-sulfate (DHEA-S) levels were reduced in both male and female PAH-patients compared to controls, whereas androstenedione and testosterone were only reduced in female patients. Interestingly, low DHEA-S and high testosterone levels were correlated to worse RV function in male patients. Subsequently, we analyzed prognosis and RV adaptation in females stratified by age. Females ≤ 45 years had best prognosis in comparison to females ≥ 55 years and males. No differences in RV function at baseline were observed, except higher pressure-overload in females ≤ 45 years. Longitudinal data demonstrated a clear distinction in RV adaptation over time. Although females ≤ 45 years had an event at a later time point, RV function was more impaired at end-stage disease.

Conclusions: RV dysfunction in male PAH-patients was associated with altered androgen expression. Females PAH-patients had lower expression of androgens. Females ≤ 45 years could persevere pressure-overload for a longer time, but had a more severe RV phenotype at end-stage disease.

INTRODUCTION

Pulmonary arterial hypertension (PAH) is a progressive disease characterized by narrowing of pulmonary arterioles and right heart failure[1-3]. Although females are more prone to develop PAH (female: male prevalence ~2:1), their survival is significantly better than male patients[4-8]. Previous studies showed that this survival benefit in females may be explained by a different RV response to treatment[4, 9].

Sex differences are common in cardiovascular physiology and disease. The multi-ethnic study of atherosclerosis (MESA) in 4000 healthy community-based participants revealed that RV mass and volume are smaller in females, while RV ejection fraction (RVEF) is higher compared to age-matched males[10]. To a great extent, this distinction was explained by differences in sex hormone levels, especially estrogens[11]. Higher RVEF and lower RV end-systolic volume were associated with higher estrogen serum levels in healthy postmenopausal women using hormone replacement therapy (HRT)[11].

Different expression levels of sex hormones have also been observed in PAH[12-17]. Especially high estradiol and reduced dehydroepiandrosterone-sulfate (DHEA-S) have been associated to PAH-severity in male and postmenopausal females. In addition, several animal studies have been performed to investigate the effect of sex hormones on pulmonary vascular remodeling and right heart failure[12]. However, due to conflicting data between patients and animal models, and due to limited data in younger females of productive age, the exact association between sex hormones and RV adaptation remains elusive. In addition, most data on sex hormones has been obtained in US centers. With the known differences in demographic characteristics and use of hormone replacement therapy between US and European patients, it is of importance to investigate sex hormones in a non-US PAH-cohort as well[18]. Finally, the majority of data is cross-sectional or at one time-point during the disease course, whereas longitudinal data of RV function during progression towards right heart failure is pivotal to understand differential RV adaptation patterns between male and female patients. Therefore, in this study we aimed to investigate the association between altered sex hormone expression levels and RV adaptation and to assess progression of right heart failure over time in a Dutch cohort of patients with a wide range of ages. We performed a translational study in which we combined cross-sectional analyses of sex hormones with longitudinal analyses of RV adaptation and histopathological analyses of RV tissue from female and male PAH-patients.

METHODS

More detailed information can be found in the supplementary material.

Study design and patients for RV function assessment

We included PAH-patients diagnosed according to European Respiratory Society (ERS) and European Society of Cardiology (ESC) guidelines at Amsterdam UMC (location VUmc) between March 1996 and September 2019 (N=306). From 55 patients and 15 controls we had collected plasma samples on which we performed sex hormone analysis (Medical Ethics Approval Numbers 2015.220-Liquid Biopsy and 2017.318-DOLPHIN). We retrospectively assessed patient charts for contraceptive and/or hormone replacement therapy use. In 280 patients, right heart catheterization (RHC) and/or cardiac magnetic resonance (CMR) imaging was performed within a maximum interval of one month at baseline prior to receiving PAH-specific therapy. In addition, of 49 patients that had an event (death or transplantation), a last RHC and/or CMR measurement was available with a maximum of 1.5 years before the event. From these patients we also collected RHC/CMR data at earlier time points during the disease. Lastly, in explanted and post-mortem RV tissue of male and female patients (N=8) and controls (N=5), we assessed histopathological differences. The Medical Ethics Review Committee of Amsterdam UMC did not consider the current study to fall within the scope of the Medical Research Involving Human Subjects (WMO), therefore informed consent was not required (approval number 2012288). Approval from the Sydney Heart Bank was received for use of RV samples (HREC #2814; HREC #7326). The use of human RV autopsy samples was approved by and performed according to guidelines of the ethics committee of Amsterdam UMC, location VUmc, and conformed to the Declaration of Helsinki principles.

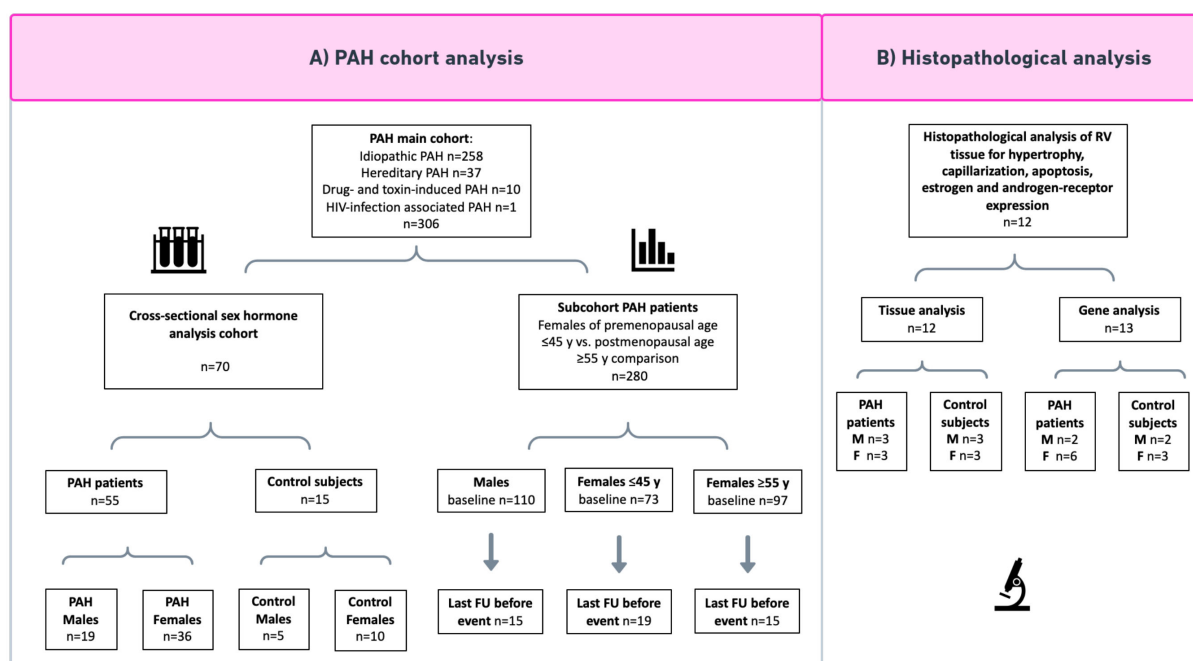
Table 4.1 – Characteristics of the subgroup of patients and controls in the sex hormone analysis

Characteristic	Control F	PAH F	Control M	PAH M	P-value
Number	10	36	5	19	
Age at visit, years	48 (20)	51 (16)	46 (19)	50 (14)	NS
BSA, m ²	1.7 (0.1)	1.8 (0.2) #	2.0 (0.2)	2.0 (0.2)	<0.001
BMI, kg/m ²	24 (3)	26 (5)	26 (5)	25 (4)	NS
NYHA FC					
Class I, n (%)		3 (8)		1 (5)	
Class II, n (%)		25 (69)		14 (74)	
Class III, n (%)		8 (22)		4 (21)	NS
NTproBNP, ng/L		202 [111 - 399]		172 [105 - 953]	NS
RHC					
mPAP, mmHg		48 (14)		48 (13)	NS
mRAP, mmHg		7 [6 - 9]		7 [5 - 10]	NS
PAWP, mmHg		12 (3)		11 (2)	NS
PVR index, WU*m ²		4 [2 - 6]		3 [2 - 4]	NS
Cardiac index, L/m ²		2.9 (0.7)		3.0 (0.9)	NS
CMR					
Heart rate, bpm	72 (9)	72 (12)	59 (10)	72 (13)	NS
RVEDV index, ml/m ²	66 (17)	89 (27) ‡	77 (23)	99 (20)	<0.01
RVESV index, ml/m ²	30 (14)	48 (22)	29 (12)	61 (24) *	<0.01
SV index, ml/m ²	40 (6)	40 (11)	53 (11)	40 (11)	NS
RVEF, %	59 (6)	48 (11) #	63 (6)	40 (14)	<0.001

RV mass index, g/m ²	25 (2)	43 (14) [‡]	18 (4)	52 (15) [*]	<0.001
Therapy					
Monotherapy, n (%)		11 (31)		8 (42)	
Dual therapy, n (%)		19 (53)		8 (42)	
Triple Therapy, n (%)		6 (17)		3 (16)	NS
Medication type					
ERA, n (%)		25 (69)		17 (90)	NS
PDE5, n (%)		29 (81)		11 (58)	NS
Prostacyclin, n (%)		12 (33)		4 (21)	NS
Hormonal treatment					
Contraceptive use, n (%)	1 (10)	6 (17)			
Hormone replacement therapy, n (%)	0 (0)	1 (3)			

Data is presented as mean (SD) or as median [IQR] or as n (%). # Male vs. female PAH patients ‡Female PAH patients vs. Female controls * Male PAH patients vs. Female control.

Figure 4.1 – Flow chart



Schematic overview of study populations used for each analysis. PAH = Pulmonary Arterial Hypertension; HIV = Human Immunodeficiency Virus; F≤45 = Females ≤45 years; F≥55 = Females ≥55 years; RV = Right Ventricular; M = Male; F = Female.

Sex Hormone Analysis

All samples were analyzed at the Endocrine Laboratory of Amsterdam UMC. DHEA-S, testosterone and androstenedione were measured in plasma using isotope diluted liquid chromatography mass spectrometry (ID-LC-MS/MS)[19, 20]. Sex hormone-binding globulin (SHBG) was measured using an automated immunoassay (Architect, Abbott Diagnostics). Free testosterone levels were calculated according to the Vermeulen formula[21].

Right heart catheterization

Hemodynamic assessment was performed using a balloon-tipped, flow-directed 7.5-F triple lumen Swan-Ganz catheter (Edwards Lifesciences LLC, Irvine, CA, USA), as previously described[22].

Cardiac Magnetic Resonance Imaging

Measures of RV function and volumes were taken using CMR imaging. Scans were obtained using a Siemens 1.5-T Sonata or Avanto scanner (Siemens Medical Solutions, Erlangen, Germany). Acquisition of images and post-processing was carried out as reported[23].

Immunohistofluorescence

RV paraffin-embedded tissue of PAH-patients (N=3 females, N=3 males) and controls (N=3 females, N=3 males) were sectioned and stained for CD31, rhodamine Ulex europaeus agglutinin I (Ulex), and wheat germ agglutinin (WGA). Tissue apoptosis was assessed by Terminal deoxynucleotidyl transferase dUTP Nick-End Labeling (TUNEL) assay. Images were captured under a laser confocal microscope (Nikon A1R). Quantitative histological measurements were assessed through ImageJ (NIH) with at least 10 random fields/patient.

Statistical analysis

Data are presented as mean (standard deviation) or median [interquartile range]. Transplant-free differences in survival were assessed using Kaplan-Meier curves and log-rank test with Bonferroni-corrected pairwise comparison. For normally distributed continuous variables, group differences were assessed using one-way ANOVA and post-hoc unpaired t-tests with Bonferroni correction. For non-normally distributed data, logarithmic transformation was applied prior to testing or Kruskal-Wallis test and post-hoc testing with pairwise Mann-Whitney U-tests was performed. For categorical variables, group differences were assessed with Pearson's χ^2 test or Fisher's exact test. Univariate and multivariate linear regression was used to assess the relation between two or more continuous variables. Confounding by age and Body Mass Index (BMI) were checked and corrected for when necessary. A p-value of <0.05 was considered statistically significant. Statistical analyses were performed in R (version 3.5.2).

RESULTS

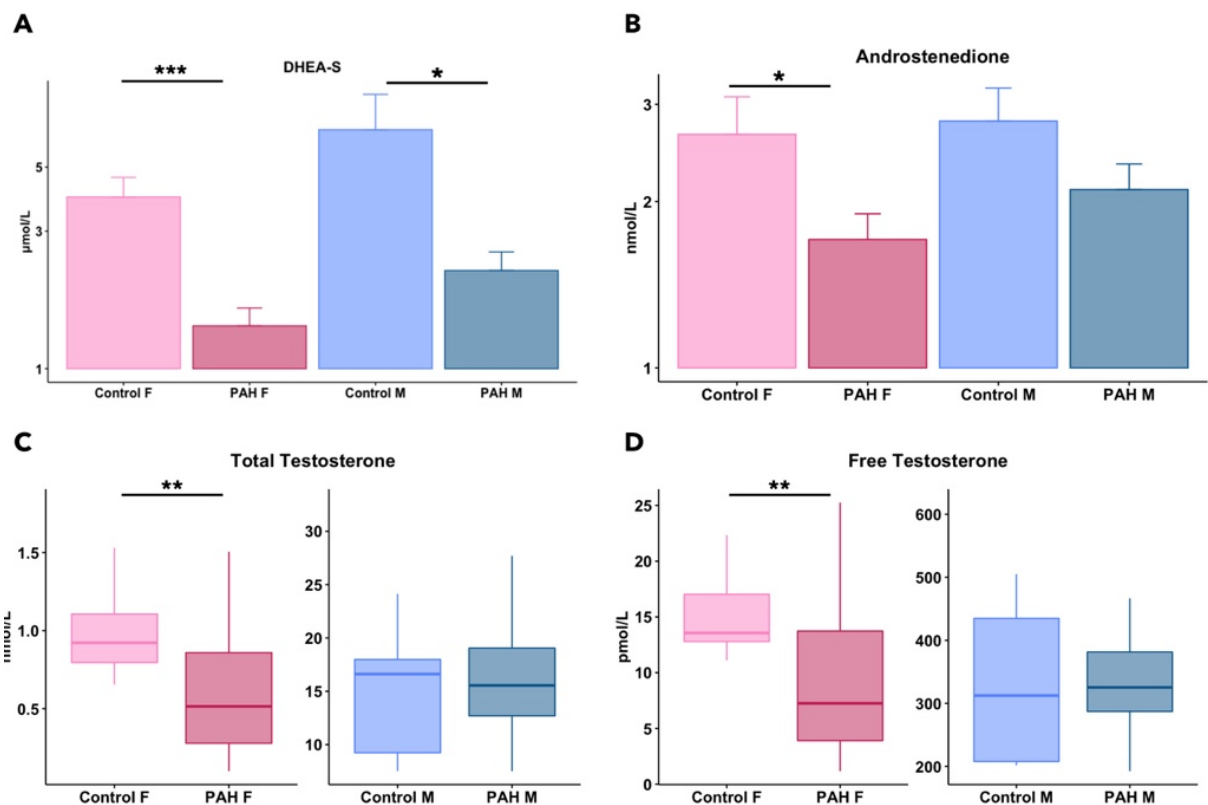
PAH-induced sex differences in survival, RV function and adaptation

We included 258 idiopathic PAH, 37 hereditary PAH, 10 drug- and toxin-induced PAH and 1 PAH patient associated with HIV-infection, resulting in 110 male and 196 female patients in total (Figure 4.1).

Low DHEA-S and high testosterone levels associated with worse RV function in male PAH

To investigate the association of RV adaptation and sex hormones, we quantified plasma levels of sex hormones in a subgroup of patients. We cross-sectionally determined levels of precursors to estrogens and androgens (Figure 4.1 Supplementary) in 19 male and 36 female PAH-patients, and 5 male and 10 female healthy controls. Characteristics of the cross-sectional cohort are presented in Table 4.1 and compared to the main cohort in Supplementary Table 4.1. No differences were observed in therapy or medication type at time of blood sampling.

Figure 4.2 – Lower DHEA-S and lower testosterone in PAH-patients compared to controls

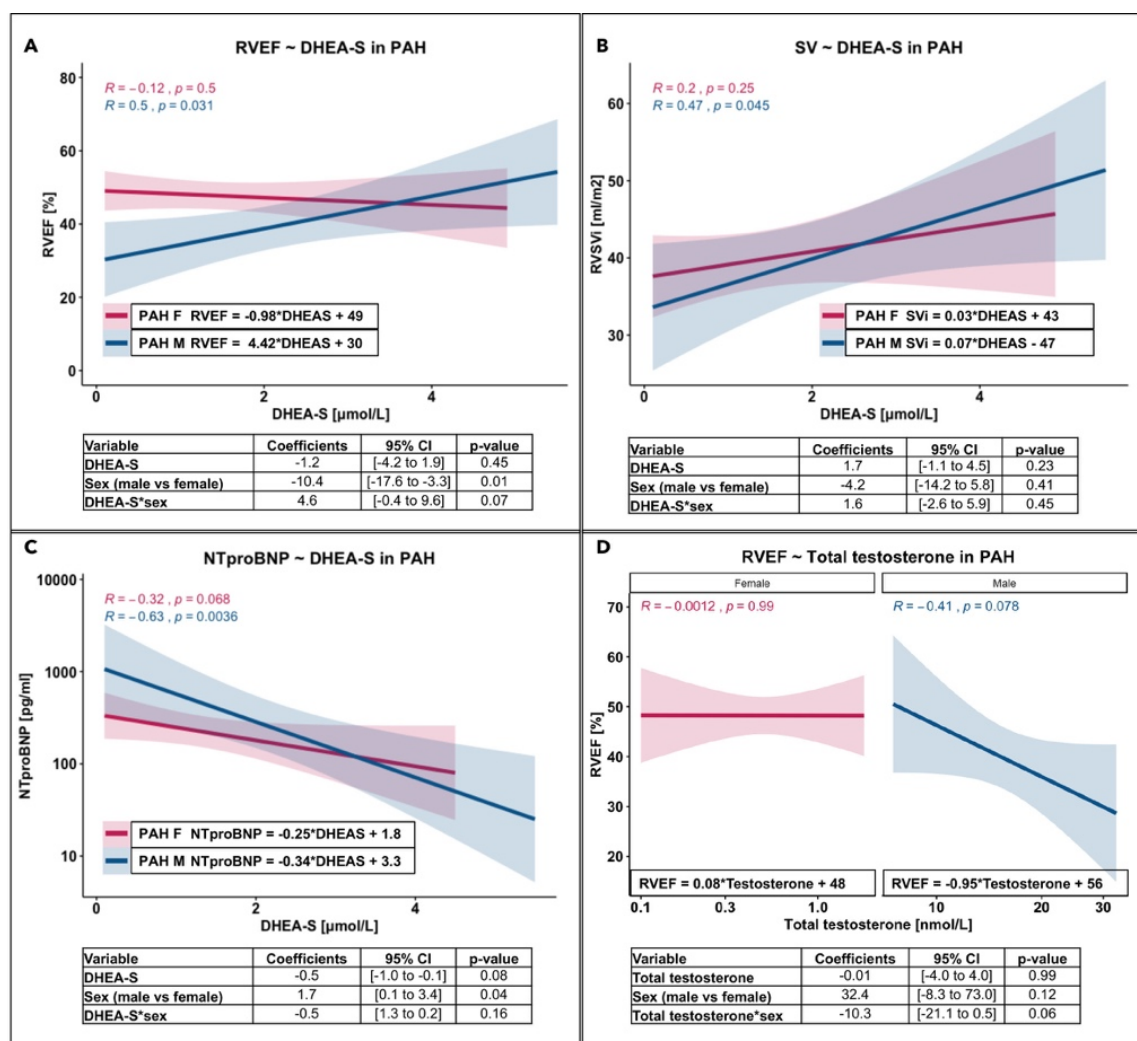


Cross-sectional hormone analysis of male and female PAH-patients and controls for DHEA-S (A), Androstenedione (B), Total testosterone (C) and Calculated free testosterone (D) levels. * $P < 0.05$; ** $P < 0.01$; *** $P < 0.001$. DHEA-S = Dehydroepiandrosterone-sulfate; F = Females; PAH = Pulmonary Arterial Hypertension; M = Males.

Levels of DHEA-S were reduced in both female and male PAH-patients compared to controls (Figure 4.2A). Intriguingly, androstenedione levels, as well as total and free testosterone levels, were significantly lower in female patients compared to controls, but did not differ between male patients and controls (Figure 4.2B-D). In addition, we investigated the association between sex hormone levels and RV functional parameters. Interestingly, the relationship between DHEA-S or total testosterone with RV function was different for male and female patients: lower DHEA-S and higher testosterone levels were correlated to worse RV function in males, whereas no correlations were observed in females (Figure 4.3A, B, D).

In both male and female patients, lower levels of DHEA-S were related to higher levels of NTproBNP (Figure 4.3C). These data indicate that the association between DHEA-S and testosterone with RV function is different in male and female patients.

Figure 4.3 - Sex hormones are differently related to RV function in PAH males and females



Relationship between levels of DHEA-S and RVEF in (A), DHEA-S and SV in (B), DHEA-S and NTproBNP in (C), and between total testosterone and RVEF (D), in both male and female PAH-patients. DHEA-S = Dehydroepiandrosterone-sulfate; RVEF = Right Ventricular Ejection Fraction; SV = Stroke Volume; PAH = Pulmonary Arterial Hypertension; F = Females; M = Males.

Table 4.2 - Baseline characteristics of PAH patients with females divided on age.

Characteristic	Females ≤45 y	Females ≥55 y	Males	P-value
Number	73	97	110	
Age at Diagnosis, y	34 (8)	68 (8)	61 (17)	<0.001
BSA, m ²	1.9 (0.3)	1.9 (0.2) *	2.0 (0.2)	<0.01
BMI, kg/m ²	28 (7)	28 (5) *	26 (4)	<0.01
sABP, mmHg	125 (16)	134 (25)	127 (20)	<0.05
dABP, mmHg	76 (12)	75 (15)	76 (14)	NS
NYHA FC				
Class I, n (%)	5 (8)	1 (1)	3 (4)	
Class II, n (%)	17 (29)	21 (28)	27 (34)	
Class III, n (%)	29 (49)	42 (57)	39 (49)	
Class IV, n (%)	8 (14)	10 (14)	11 (14)	NS
6MWD, m	448 [335-497] ^{##}	314 [218-415]	330 [186-456]	<0.001
NTproBNP, ng/L	813 [355-1932]	1269 [369-2945]	1090 [299-2870]	NS
HPAH BMPR2, n (%)	15 (21) [#]	6 (6)	10 (9)	<0.05
Low DLCO, n (%)	0 (0) [‡]	14 (14) *	35 (32)	<0.001
Comorbidities				
Smoking, n (%)	25 (36) ^{##}	46 (54)	64 (65)	<0.01
Coronary Artery Disease, n (%)	0 (0) [#]	13 (15) *	25 (25)	<0.001
Hypertension, n (%)	8 (12) [#]	37 (44)	30 (30)	<0.001
Diabetes, n (%)	3 (4) [#]	25 (29)	18 (18)	<0.001
RHC				
sPAP, mmHg	88 (23) ^{##}	80 (19)	78 (19)	<0.001
dPAP, mmHg	38 (13) ^{##}	31 (10)	32 (10)	<0.001
mPAP, mmHg	57 (15) ^{##}	49 (12)	49 (12)	<0.001
mRAP, mmHg	9 [5 - 11]	8 [6 - 11]	7 [5 - 11]	NS
PAWP, mmHg	9 (3)	11 (3) *	9 (3)	0.001
PVR index, WU*m2	5.8 [3.4 - 7.6] [‡]	4.8 [3.1 - 7.7]	4.3 [3.1 - 5.9]	0.04
Cardiac index, L/m ²	2.5 (0.8)	2.5 (0.9)	2.4 (0.8)	NS
CMR				
Heart rate, bpm	82 (14)	78 (10)	77 (15)	NS
RVEDV index, ml/m ²	83 (21)	79 (30)	87 (23)	NS
RVESV index, ml/m ²	56 (19)	51 (28)	61 (24)	NS
SV index, ml/m ²	27 (8)	28 (8)	28 (8)	NS
RVEF, %	33 (11)	37 (13)	33 (12)	NS

RV mass index, g/m ²	53 (14)	47 (13)	56 (15)	<0.05
Therapy				
Monotherapy, n (%)	45 (63)	60 (62)	70 (64)	
Dual therapy, n (%)	23 (32)	33 (34)	32 (29)	
Triple therapy, n (%)	2 (3)	1 (1)	1 (1)	NS
Medication type				
ERA, n (%)	42 (58)	63 (65)	59 (54)	NS
PDE5, n (%)	28 (39)	56 (58)	59 (54)	<0.05
Prostacyclin, n (%)	21 (30) #	6 (6)	15 (14)	<0.05

Data is presented as mean (SD) or as median [IQR] or as n (%) #Females ≤45 vs. females ≥55 ‡Females ≤45 vs. males * Females≥55 vs. males.

Superior RV adaptation in females of reproductive age

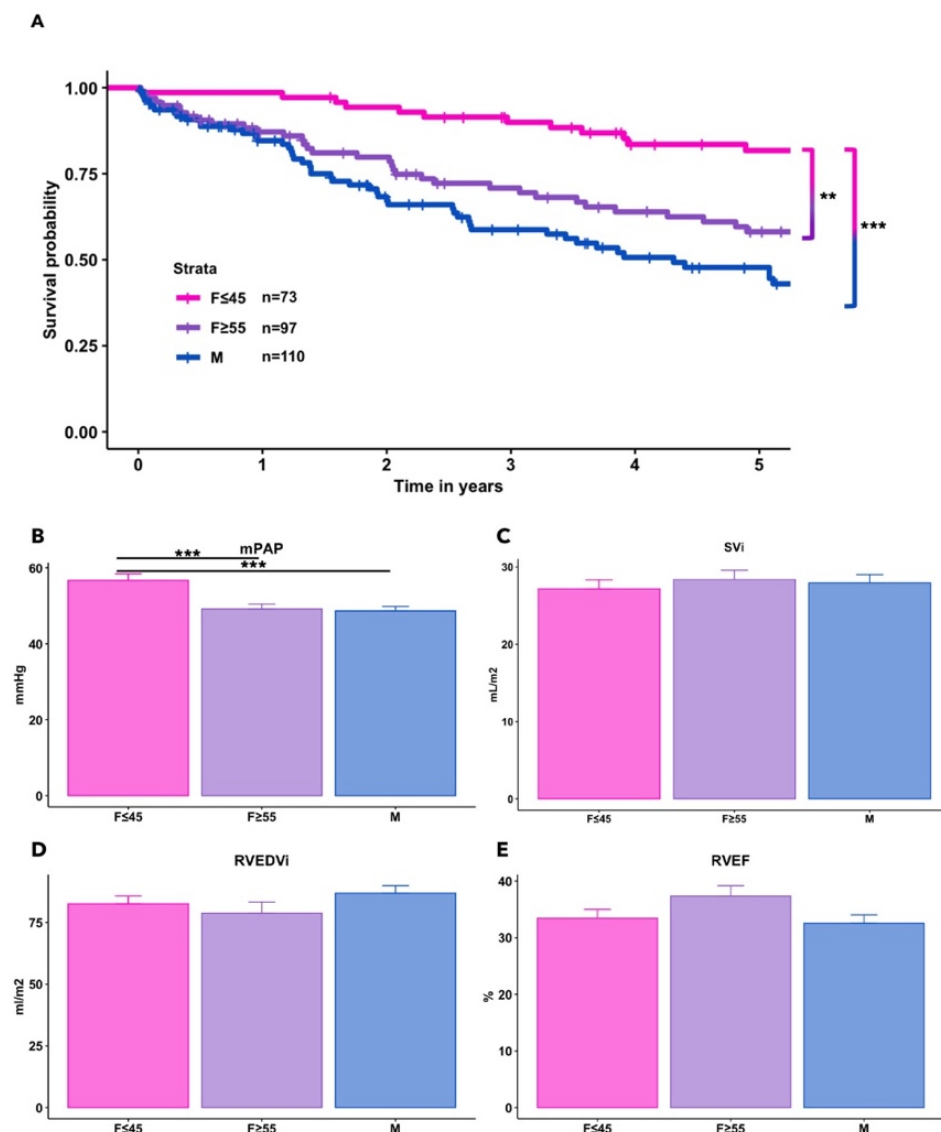
Several indications in literature point to the direction of estrogen as a main regulator of RV adaptation in PAH. However, since estrogen levels are variable throughout the menstrual cycle, it is challenging to interpret estrogen plasma levels in females[17], and as estrogen levels are known to drop around the age of 50 years[24]. Therefore, to get a general idea on the contribution of estrogens to RV adaptation, we stratified the female cohort on age: females of reproductive age (N=73, ≤45 years), and females of postmenopausal age (N=97, ≥55 years old). The male cohort was included as a reference group and was not stratified on age. Baseline characteristics are presented in Table 4.2. Females≤45years had a higher BMI and *BMPR2* mutations were more prevalent. A low diffusing capacity of the lung for carbon monoxide (DLCO) (≤45%) and comorbidities were more prevalent in male PAH-patients. The frequency distribution of mono-, duo- and triple therapy was comparable between the groups, although PDE5 inhibitors were more frequently provided to male PAH and females≥55years and prostacyclin therapy was more frequent in females≤45years.

At baseline, no differences were observed in hemodynamic or RV imaging data, besides a significantly higher mean pulmonary artery pressure and pulmonary vascular resistance in females≤45years in comparison to females≥55years and males. As can be appreciated in Figure 4.4A, females≤45years had the best prognosis, whereas males had the worse prognosis.

To investigate the difference in RV adaptation over time towards end-stage disease in more detail, we subsequently performed longitudinal analyses on RHC and CMR data. For this purpose, we selected patients that underwent a RHC and/or CMR maximally 1,5 years prior to an event (death or transplantation). Subsequently, we analyzed CMR and/or RHC data at three earlier time-points during the disease including a baseline scan. Median time from last follow-up to event was similar for all patients (females≤45years: 0.47 vs females≥55years: 0.77 vs males: 0.52 years, P=0.42), whereas median time from baseline to last follow-up was

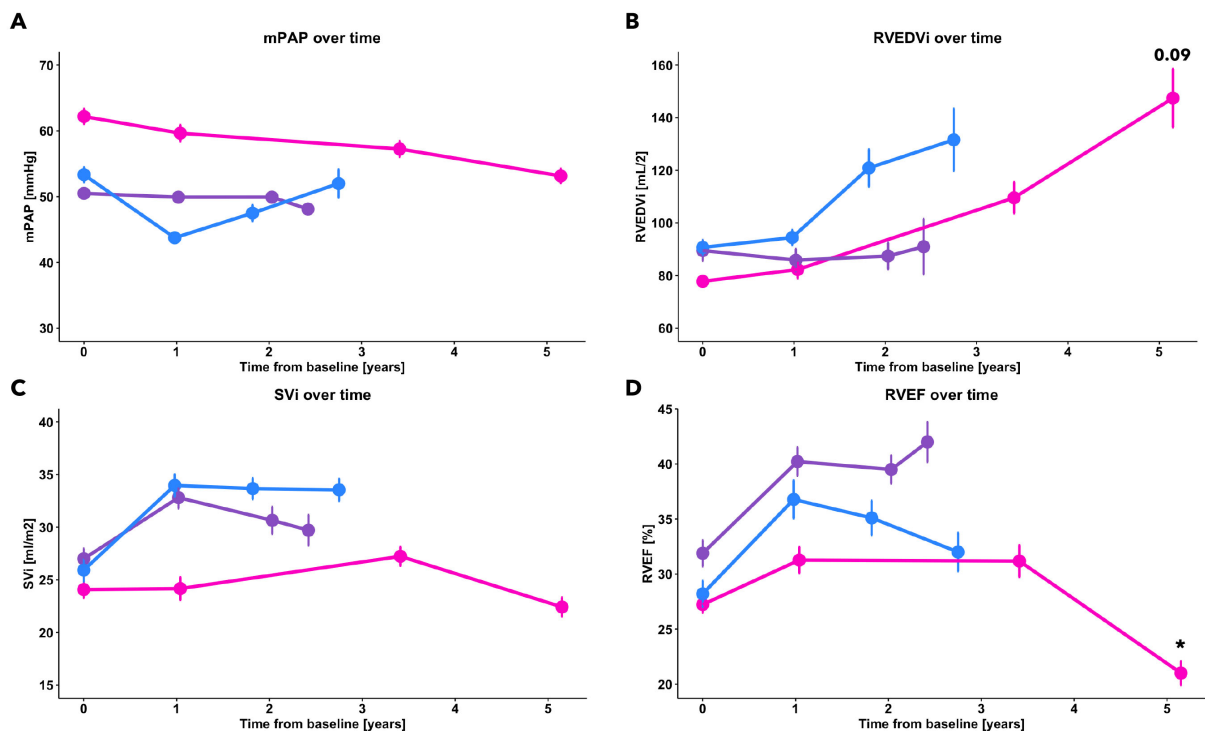
different, as expected from the survival curve (females ≤ 45 years: 5.2 vs females ≥ 55 years: 2.0 vs males: 1.8 years, respectively, $P < 0.05$). Figure 4.5 shows the longitudinal data of RHC and CMR of PAH-patients with an event. Intriguingly, although females ≤ 45 years have an event at a later time-point than male and females ≥ 55 years, RV function has significantly deteriorated over time in comparison to baseline values. In contrast, in males and females ≥ 55 years no drop in RV function in comparison to baseline was observed. These data suggest that females of reproductive age can persevere pressure-overload for a longer time, but have a worse RV phenotype at end-stage disease.

Figure 4.4 - Five-year survival of PAH patients and hemodynamics and RV phenotype at baseline



Females are stratified on age into females of reproductive age (≤ 45 years) and females of postmenopausal age (≥ 55 years). Sex and age differences in the 5-year transplant-free survival probability in male and female PAH patients in (A). Baseline measurements of mPAP in (B), SVi (C), RVEDVi (D) and RVEF (E) in PAH females ≤ 45 years compared to females ≥ 55 years and males. ** $P < 0.01$; *** $P < 0.001$. F ≤ 45 = Females ≤ 45 years; F ≥ 55 = Females ≥ 55 years; M = Males; mPAP = mean Pulmonary Arterial Pressure; RVEDVi = Right Ventricular End-Diastolic Volume index; SVi = Stroke Volume index; RVEF = Right Ventricular Ejection Fraction.

Figure 4.5 – Change in hemodynamics, RV morphology and function over time from baseline to last follow-up before an event

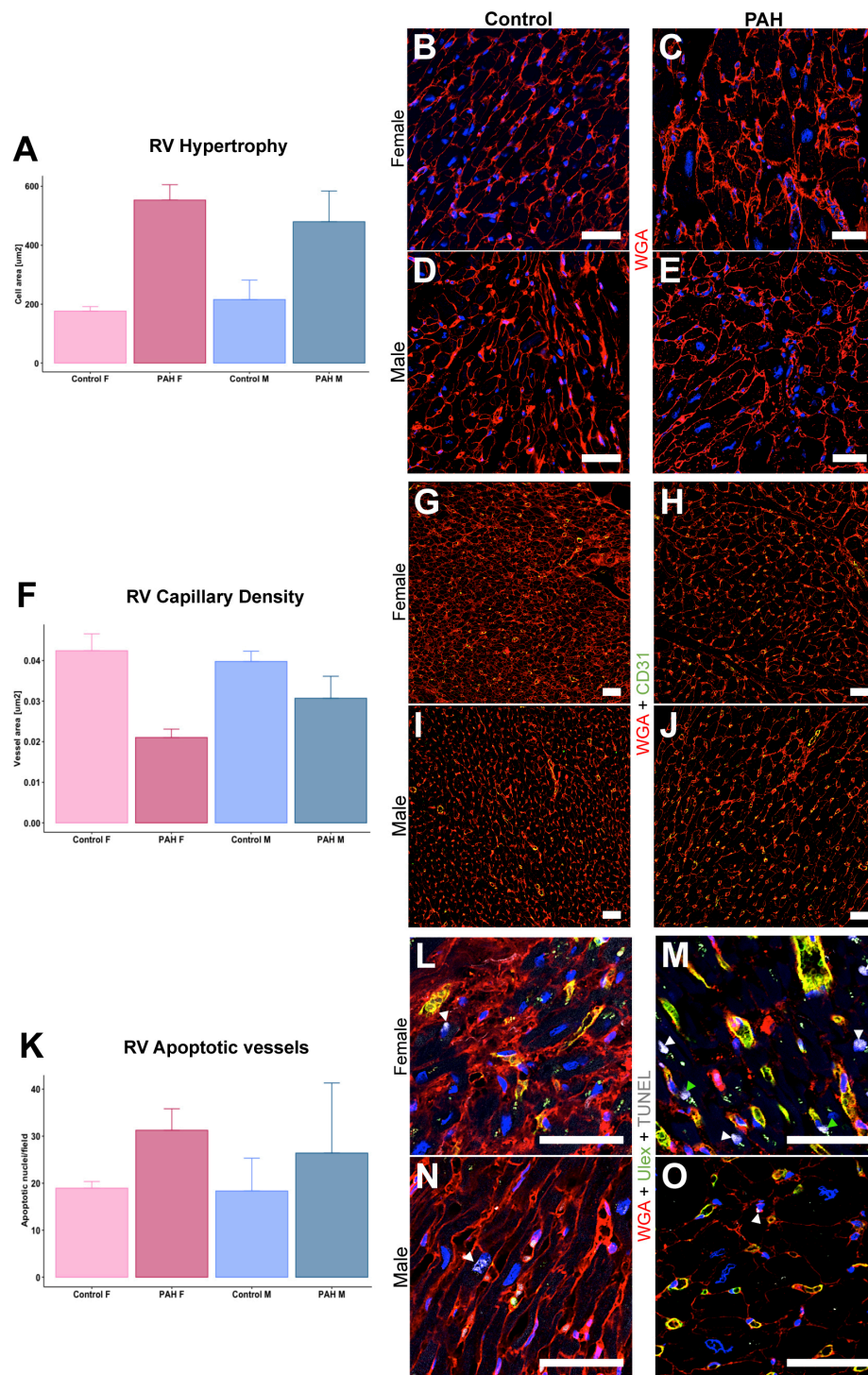


Change in measurements from baseline over time of mPAP (A), RVEDVi (B), SVi (C) and RVEF (D) to last follow-up with a maximum of 1.5 years before an event in PAH females of reproductive age (≤ 45 years) compared to females of postmenopausal age (≥ 55 years) and to males. * $P < 0.05$ at last follow-up vs baseline. $F_{\leq 45}$ = Females ≤ 45 years; $F_{\geq 55}$ = Females ≥ 55 years; M = Males; mPAP = mean Pulmonary Arterial Pressure; RVEDVi = Right Ventricular End-Diastolic Volume index; SVi = Stroke Volume index; RVEF = Right Ventricular Ejection Fraction.

Sex differences in end-stage RV tissue

Lastly, we investigated sex differences in end-stage RV tissue of PAH-patients. Post-mortem and transplanted RV tissue was used to investigate RV hypertrophy, capillary density and apoptosis (Figure 4.6), in male and female end-stage PAH-patients and controls. All female tissue was obtained of patients with an age < 55 years old. Although no statistical analyses could be performed due to the limited number of tissue samples per group, representative images and quantification suggest a more pronounced capillary rarefaction and endothelial cell apoptosis in female RV tissue in comparison to males also indicating a more severe RV phenotype in females in comparison to male PAH-patients.

Figure 4.6 – Histopathological analyses in RV tissue of PAH-patients and controls



RV cardiomyocyte cross-sectional area quantification (Hypertrophy, A) and representative pictures for cell membrane counterstaining (WGA; B-E). Vascular density quantification (F) and illustrative overviews (CD31, green; G-I). Vascular apoptosis quantification (K) and characteristic stainings (L-O) against apoptotic nuclei (TUNEL, grey) and vessels (Ulex, green). White arrowheads indicate apoptotic cardiomyocytes, while green arrowheads indicate apoptotic vessels. Nuclei were counterstained with Hoechst 33342 (blue, B-E and L-O) and WGA (red). N=3 subjects/group and ≥ 10 fields/subject. Scale bars= 50 μm . RV = Right Ventricular; PAH = Pulmonary Arterial Hypertension; CD31= cluster of differentiation 31; WGA= wheat germ agglutinin; Ulex = Ulex europaeus agglutinin.

DISCUSSION

Using a comprehensive set of hormone analyses combined with longitudinal imaging and hemodynamic data, we were able to demonstrate that:

1. For the first time, we show a link between androgen levels and worse RV function in male PAH-patients.
2. DHEA-S plasma levels are reduced in male and female PAH-patients across a wide range of ages, whereas reduced testosterone and androstenedione levels are observed in female patients only.
3. Females of reproductive age may tolerate RV pressure-overload for a longer period of time resulting in a more severe RV phenotype at end-stage disease.

Beneficial effect of DHEA-S on RV adaptation to pressure-overload

In contrast to the controversial findings on estrogens in animal and human studies, DHEA-S has consistently shown to be beneficial in RV adaptation [25-27]. First, DHEA-S levels of healthy subjects were associated to larger RV volumes and mass in females, with a trend in males [10]. Second, DHEA-S levels were reduced in both postmenopausal female and older male PAH-patients, and throughout the menstrual cycle in a small study of reproductive PAH females [15-17]. Furthermore, DHEA-S levels were associated with disease severity, progression and survival. Third, DHEA-S treatment in experimental PAH improved both systolic and diastolic RV function, and reduced RV maladaptive remodeling [25, 27]. In our study, we could confirm the reduced expression of DHEA-s in a Dutch cohort of male and female PAH-patients across a wide range of ages. This further supports the rationale of a phase two clinical trial currently being conducted to study the effects of DHEA supplementation on RV functional parameters (EDIPHY trial: NCT03648385). Interestingly, in our cohort the relation of DHEA-S with RV dysfunction was more pronounced in male PAH-patients. Therefore, sex-specific analyses of treatment effects of DHEA-S supplementation would be of interest.

Possible detrimental relation between androgens and RV adaptation

Androgens may also be involved in RV adaptation to pressure-overload. Elevated levels of androgens are associated with higher RV mass and volumes in males[11]. Interestingly, we show for the first time that plasma testosterone is differentially associated to RV dysfunction in males and female PAH-patients. Similar to previous studies in PAH, we only detect lower plasma levels of testosterone in PAH females[15]. Nevertheless, testosterone levels were associated to RV dysfunction in male PAH-patients, suggesting that testosterone levels may negatively affect RV adaptation in males. This is in line with experimental data in which testosterone was associated with dysfunctional RV hypertrophy and excessive RV fibrosis in male mice with pulmonary artery banding [28], suggesting that androgens may have a detrimental effect on RV adaptation to pressure-overload, predisposing to an earlier onset of

RV failure and possibly resulting in worse survival in males. Therefore, a lack of testosterone may be protective in females.

Worse end-stage disease phenotype in PAH females

Female PAH-patients have a better prognosis and, at the same time, the worst RV phenotype at end-stage disease, which can be appreciated by more RV dilation and worse RV function shortly before death or transplantation. Our histopathologic results evidenced more hypertrophy, decreased capillary density and increased apoptosis in the PAH RV tissue. Unfortunately, it is difficult to draw definite conclusions with limited number of human end-stage RV samples; thus, novel translational tools, like cardiac tissue engineered models, are highly necessary. Hence, increased estrogen or reduced testosterone levels may protect the female heart and allow better endurance to increased afterload, subsequently resulting in a worse stage of RV failure at a later point in time. The remaining question is whether the younger female heart is intrinsically better to adapt to these pressures and maintain cardiac function, or whether older female and male patients die at an earlier stage due to other causes than RV failure. The latter may be plausible, as older patients from our cohort more frequently had comorbidities, such as smoking, previously associated with worse survival in PAH [29]. Nevertheless, as we were unable to retrieve cause of death in all patients, no definite conclusions can be drawn.

Limitations and strengths

One of the limitations of this study is the relatively small sample size of male patients compared to female patients. Nonetheless, the smaller representation of males is reflective of the PAH patient population. Furthermore, we were unable to measure estrogen levels of patients in our cohort, hence, we could not study direct associations of estrogen and RV adaptation. Lastly, as availability of human end-stage disease RV tissue samples is limited, numbers were small, and we could not match patient samples on age, the histopathological analyses suggest more capillary rarefaction in females, providing a hypothesis for future studies. Although our clinical cohort mostly consisted of idiopathic and hereditary PAH-patients, CHD RV tissue samples were useful to study pressure-overloaded RV failure. Again, new approaches are necessary to overcome limited RV tissue availability, but also to investigate the direct effect of sex hormones on the right ventricle throughout *in vitro* cardiac models to study the cardiomyocyte/endothelial cell interaction in females in more detail. However, even with limited numbers, we have provided insight into the underlying pathophysiological mechanisms of RV failure in end-stage disease of PAH-patients. The strength of our study is the combination of RHC and CMR longitudinal functional data with cross-sectional sex hormone data and histopathological analyses of end-stage disease RV tissue. Importantly, we show that previous findings on sex hormone alterations in PAH can be extrapolated to a European cohort of PAH-patients across a wide range of ages. In addition, we used ID-LC-MS/MS for quantification of sex hormone levels, which has shown to be more

reliable and accurate compared to immunoassays[30]. Finally, although follow-up is performed on a regular basis in our clinic, additional follow-up may have been indicated only in patients with clinical deterioration, which could have led to a bias in the follow-up population.

CONCLUSIONS

In a large Dutch cohort of PAH-patients across a wide range of ages, we show for the first time a link between androgens and worse RV function in male PAH-patients. While DHEA-S levels were decreased in both male and female patients, reduced androstenedione and testosterone levels were observed in females only. Our longitudinal data suggest that females of reproductive age may persevere pressure-overload for a longer time period resulting in a worse RV phenotype at end-stage disease.

REFERENCES

1. Vonk Noordegraaf A, Westerhof BE, Westerhof N. The Relationship Between the Right Ventricle and its Load in Pulmonary Hypertension. *Journal of the American College of Cardiology* 2017; 69(2): 236-243.
2. Humbert M, Guignabert C, Bonnet S, Dorfmueller P, Klinger JR, Nicolls MR, Olschewski AJ, Pullamsetti SS, Schermuly RT, Stenmark KR, Rabinovitch M. Pathology and pathobiology of pulmonary hypertension: state of the art and research perspectives. *The European respiratory journal* 2019; 53(1).
3. Simonneau G, Montani D, Celermajer DS, Denton CP, Gatzoulis MA, Krowka M, Williams PG, Souza R. Haemodynamic definitions and updated clinical classification of pulmonary hypertension. *The European respiratory journal* 2019; 53(1).
4. Jacobs W, van de Veerdonk MC, Trip P, de Man F, Heymans MW, Marcus JT, Kawut SM, Bogaard HJ, Boonstra A, Vonk Noordegraaf A. The right ventricle explains sex differences in survival in idiopathic pulmonary arterial hypertension. *Chest* 2014; 145(6): 1230-1236.
5. Humbert M, Sitbon O, Chaouat A, Bertocchi M, Habib G, Gressin V, Yaïci A, Weitzenblum E, Cordier JF, Chabot F, Dromer C, Pison C, Reynaud-Gaubert M, Haloun A, Laurent M, Hachulla E, Cottin V, Degano B, Jaïs X, Montani D, Souza R, Simonneau G. Survival in patients with idiopathic, familial, and anorexigen-associated pulmonary arterial hypertension in the modern management era. *Circulation* 2010; 122(2): 156-163.
6. Humbert M, Sitbon O, Yaïci A, Montani D, O'Callaghan DS, Jaïs X, Parent F, Savale L, Natali D, Günther S, Chaouat A, Chabot F, Cordier JF, Habib G, Gressin V, Jing ZC, Souza R, Simonneau G. Survival in incident and prevalent cohorts of patients with pulmonary arterial hypertension. *The European respiratory journal* 2010; 36(3): 549-555.
7. Benza RL, Miller DP, Gomberg-Maitland M, Frantz RP, Foreman AJ, Coffey CS, Frost A, Barst RJ, Badesch DB, Elliott CG, Liou TG, McGoon MD. Predicting survival in pulmonary arterial hypertension: insights from the Registry to Evaluate Early and Long-Term Pulmonary Arterial Hypertension Disease Management (REVEAL). *Circulation* 2010; 122(2): 164-172.
8. Shapiro S, Traiger GL, Turner M, McGoon MD, Wason P, Barst RJ. Sex differences in the diagnosis, treatment, and outcome of patients with pulmonary arterial hypertension enrolled in the registry to evaluate early and long-term pulmonary arterial hypertension disease management. *Chest* 2012; 141(2): 363-373.
9. Tello K, Richter MJ, Yogeswaran A, Ghofrani HA, Naeije R, Vanderpool R, Gall H, Tedford RJ, Seeger W, Lahm T. Sex Differences in Right Ventricular-Pulmonary Arterial Coupling in Pulmonary Arterial Hypertension. *American journal of respiratory and critical care medicine* 2020; 202(7): 1042-1046.
10. Kawut SM, Lima JA, Barr RG, Chahal H, Jain A, Tandri H, Praestgaard A, Bagiella E, Kizer JR, Johnson WC, Kronmal RA, Bluemke DA. Sex and race differences in right ventricular structure and function: the multi-ethnic study of atherosclerosis-right ventricle study. *Circulation* 2011; 123(22): 2542-2551.
11. Ventetuolo CE, Ouyang P, Bluemke DA, Tandri H, Barr RG, Bagiella E, Cappola AR, Bristow MR, Johnson C, Kronmal RA, Kizer JR, Lima JA, Kawut SM. Sex hormones are associated with right ventricular structure and function: The MESA-right ventricle study. *American journal of respiratory and critical care medicine* 2011; 183(5): 659-667.
12. Frump AL, Goss KN, Vayl A, Albrecht M, Fisher A, Tursunova R, Fierst J, Whitson J, Cucci AR, Brown MB, Lahm T. Estradiol improves right ventricular function in rats with severe angioproliferative pulmonary hypertension: effects of endogenous and exogenous sex hormones. *American journal of physiology Lung cellular and molecular physiology* 2015; 308(9): L873-890.
13. Lahm T, Tuder RM, Petrache I. Progress in solving the sex hormone paradox in pulmonary hypertension. *American journal of physiology Lung cellular and molecular physiology* 2014; 307(1): L7-26.
14. Liu A, Schreier D, Tian L, Eickhoff JC, Wang Z, Hacker TA, Chesler NC. Direct and indirect protection of right ventricular function by estrogen in an experimental model of pulmonary arterial hypertension. *American journal of physiology Heart and circulatory physiology* 2014; 307(3): H273-283.
15. Baird GL, Archer-Chicko C, Barr RG, Bluemke DA, Foderaro AE, Fritz JS, Hill NS, Kawut SM, Klinger JR, Lima JAC, Mullin CJ, Ouyang P, Palevsky HI, Palmisicano AJ, Pinder D, Preston IR, Roberts KE, Smith KA, Walsh T, Whittenhall M, Ventetuolo CE. Lower DHEA-S levels predict disease and worse outcomes in post-menopausal women with idiopathic, connective tissue disease- and congenital heart disease-associated pulmonary arterial hypertension. *The European respiratory journal* 2018; 51(6).
16. Ventetuolo CE, Baird GL, Barr RG, Bluemke DA, Fritz JS, Hill NS, Klinger JR, Lima JA, Ouyang P, Palevsky HI, Palmisicano AJ, Krishnan I, Pinder D, Preston IR, Roberts KE, Kawut SM. Higher Estradiol and Lower Dehydroepiandrosterone-Sulfate Levels Are Associated with Pulmonary Arterial Hypertension in Men. *American journal of respiratory and critical care medicine* 2016; 193(10): 1168-1175.
17. Baird GL, Walsh T, Aliotta J, Allahua M, Andrew R, Bourjeily G, Brodsky AS, Denver N, Dooner M, Harrington EO, Klinger JR, MacLean MR, Mullin CJ, Pereira M, Poppas A, Whittenhall M, Ventetuolo CE. Insights from the Menstrual Cycle in Pulmonary Arterial Hypertension. *Annals of the American Thoracic Society* 2020.

18. de Jong-van den Berg LT, Faber A, van den Berg PB. HRT use in 2001 and 2004 in The Netherlands--a world of difference. *Maturitas* 2006; 54(2): 193-197.
19. Büttler RM, Struys EA, Addie R, Blankenstein MA, Heijboer AC. Measurement of dehydroepiandrosterone sulfate (DHEAS) in serum and cerebrospinal fluid by isotope-dilution liquid chromatography tandem mass spectrometry. *Clinica chimica acta; international journal of clinical chemistry* 2012; 414: 246-247.
20. Büttler RM, Martens F, Ackermans MT, Davison AS, van Herwaarden AE, Kortz L, Krabbe JG, Lentjes EG, Syme C, Webster R, Blankenstein MA, Heijboer AC. Comparison of eight routine unpublished LC-MS/MS methods for the simultaneous measurement of testosterone and androstenedione in serum. *Clinica chimica acta; international journal of clinical chemistry* 2016; 454: 112-118.
21. Vermeulen A, Verdonck L, Kaufman JM. A critical evaluation of simple methods for the estimation of free testosterone in serum. *The Journal of clinical endocrinology and metabolism* 1999; 84(10): 3666-3672.
22. Trip P, Kind T, van de Veerdonk MC, Marcus JT, de Man FS, Westerhof N, Vonk-Noordegraaf A. Accurate assessment of load-independent right ventricular systolic function in patients with pulmonary hypertension. *The Journal of heart and lung transplantation : the official publication of the International Society for Heart Transplantation* 2013; 32(1): 50-55.
23. van de Veerdonk MC, Kind T, Marcus JT, Mauritz GJ, Heymans MW, Bogaard HJ, Boonstra A, Marques KM, Westerhof N, Vonk-Noordegraaf A. Progressive right ventricular dysfunction in patients with pulmonary arterial hypertension responding to therapy. *Journal of the American College of Cardiology* 2011; 58(24): 2511-2519.
24. Ober C, Loisel DA, Gilad Y. Sex-specific genetic architecture of human disease. *Nature reviews Genetics* 2008; 9(12): 911-922.
25. Alzoubi A, Toba M, Abe K, O'Neill KD, Rocic P, Fagan KA, McMurtry IF, Oka M. Dehydroepiandrosterone restores right ventricular structure and function in rats with severe pulmonary arterial hypertension. *American journal of physiology Heart and circulatory physiology* 2013; 304(12): H1708-1718.
26. Hampl V, Bíbová J, Povýsilová V, Herget J. Dehydroepiandrosterone sulphate reduces chronic hypoxic pulmonary hypertension in rats. *The European respiratory journal* 2003; 21(5): 862-865.
27. Dumas de La Roque E, Bellance N, Rossignol R, Begueret H, Billaud M, dos Santos P, Ducret T, Marthan R, Dahan D, Ramos-Barbón D, Amor-Carro Ó, Savineau JP, Fayon M. Dehydroepiandrosterone reverses chronic hypoxia/reoxygenation-induced right ventricular dysfunction in rats. *The European respiratory journal* 2012; 40(6): 1420-1429.
28. Hemnes AR, Maynard KB, Champion HC, Gleaves L, Penner N, West J, Newman JH. Testosterone negatively regulates right ventricular load stress responses in mice. *Pulmonary circulation* 2012; 2(3): 352-358.
29. Trip P, Nossent EJ, de Man FS, van den Berk IA, Boonstra A, Groepenhoff H, Leter EM, Westerhof N, Grünberg K, Bogaard HJ, Vonk-Noordegraaf A. Severely reduced diffusion capacity in idiopathic pulmonary arterial hypertension: patient characteristics and treatment responses. *The European respiratory journal* 2013; 42(6): 1575-1585.
30. Herold DA, Fitzgerald RL. Immunoassays for testosterone in women: better than a guess? *Clinical chemistry* 2003; 49(8): 1250-1251.

4

INTERPLAY OF SEX HORMONES AND LONG-TERM RIGHT VENTRICULAR ADAPTATION IN A DUTCH PULMONARY ARTERIAL HYPERTENSION COHORT

Supplemental material

SUPPLEMENTAL METHODS

Right heart catheterization

Hemodynamic assessment was performed using a balloon-tipped, flow-directed 7.5-F triple lumen Swan-Ganz catheter (Edwards Lifesciences LLC, Irvine, CA, USA), as previously described [1]. Measurements of mPAP, right atrial pressure (RAP), pulmonary artery wedge pressure (PAWP) and cardiac output (CO) were taken at baseline and follow-up visits. CO measurements were obtained using the thermodilution or the direct Fick method. PVR was determined using the formula: $(\text{mean PAP} - \text{PAWP}) / \text{CO}$.

Cardiac Magnetic Resonance Imaging

Measures of RV function and volumes were taken using CMR imaging. Scans were obtained using a Siemens 1.5-T Sonata or Avanto scanner (Siemens Medical Solutions, Erlangen, Germany). Acquisition of images and post-processing was carried out as previously reported [2]. RV end-diastolic and end-systolic endocardial and epicardial contours were manually drawn using Mass Analysis software (MEDIS Medical Imaging Systems, Leiden, the Netherlands). End-diastole was determined using the onset of the R-wave in the ECG. Volumes and mass were indexed to body surface area (BSA) using the Mosteller formula. Stroke volume (SV) was determined according to left ventricular volumes (left ventricular end-diastolic volume (LVEDV) - left ventricular end-systolic volume (LVESV)).

Sex Hormone Analysis

All samples were analyzed at the Endocrine Laboratory of the Amsterdam UMC. DHEAS, testosterone and androstenedione were measured in plasma using isotope diluted liquid chromatography mass spectrometry (ID-LC-MS/MS), as described earlier [3, 4]. DHEAS was measured using Isotope-Dilution Liquid Chromatography Tandem Mass Spectrometry (ID-LC-MS/MS), slightly adapted from before [4]. In short, a deuterated internal standard ([2H₆] DHEAS) (Sigma-Aldrich) was added to the serum sample and a protein precipitation step took place using acetonitrile. The supernatants were analyzed on a LC-MS/MS (Acquity, Waters Corp., Milford, MA). The lower limit of quantitation was 0.1 µmol/L. The intra-assay variation was 4% to concentrations of 4.2 and 8 µmol/L. The inter-assay variation was <6% over the whole concentration range.

Testosterone and androstenedione were also measured using ID-LC-MS/MS, as published before (method C) [3]. In short, a deuterated internal standard [d₃-testosterone and d₇-androstenedione) (both CDN isotopes) were added to the serum sample and later protein precipitation using acetonitrile. Samples were extracted using Porvair Sciences P3 filtration plates. Samples were analyzed on a LC-MS/MS (Xevo TQS, Waters Corp., Milford, MA). The lower limit of quantitation was 0.1 nmol/L for testosterone and 0.1 nmol/L for androstenedione. For testosterone the intra-assay variation was 6.5% in the female

concentration range and 4.1% in the male concentration range. For androstenedione the intra-assay variation was 4.3%. The inter-assay variation was <7.6% over the whole concentration range for both testosterone and androstenedione. SHBG was measured using an automated immunoassay (Architect, Abbott Diagnostics, Chicago, IL, USA). The lower limit of quantitation was 2 nmol/L. The intra-assay CV was 6.3% and 4.9% at concentrations of 34 and 134 nmol/L respectively. Free testosterone levels were calculated according to the Vermeulen formula using the total testosterone and SHBG measurement and using a fixed albumin concentration of 43 g/dl [5]. A fixed albumin concentration was used as it was not measured in all patients. However, in the patients where albumin measurements were available, the mean concentration was 39 g/dl.

RV paraffin-embedded tissue of PAH-patients (N=3 females, N=3 males) and controls (N=3 females, N=3 males) were sectioned and stained for CD31, rhodamine Ulex europaeus agglutinin I (Ulex), and wheat germ agglutinin (WGA). Tissue apoptosis was assessed by Terminal deoxynucleotidyl transferase dUTP Nick-End Labeling (TUNEL) assay. Images were captured under a laser confocal microscope (Nikon A1R). Quantitative histological measurements were assessed through ImageJ (NIH) with at least 10 random fields/patient.

Immunohistofluorescence

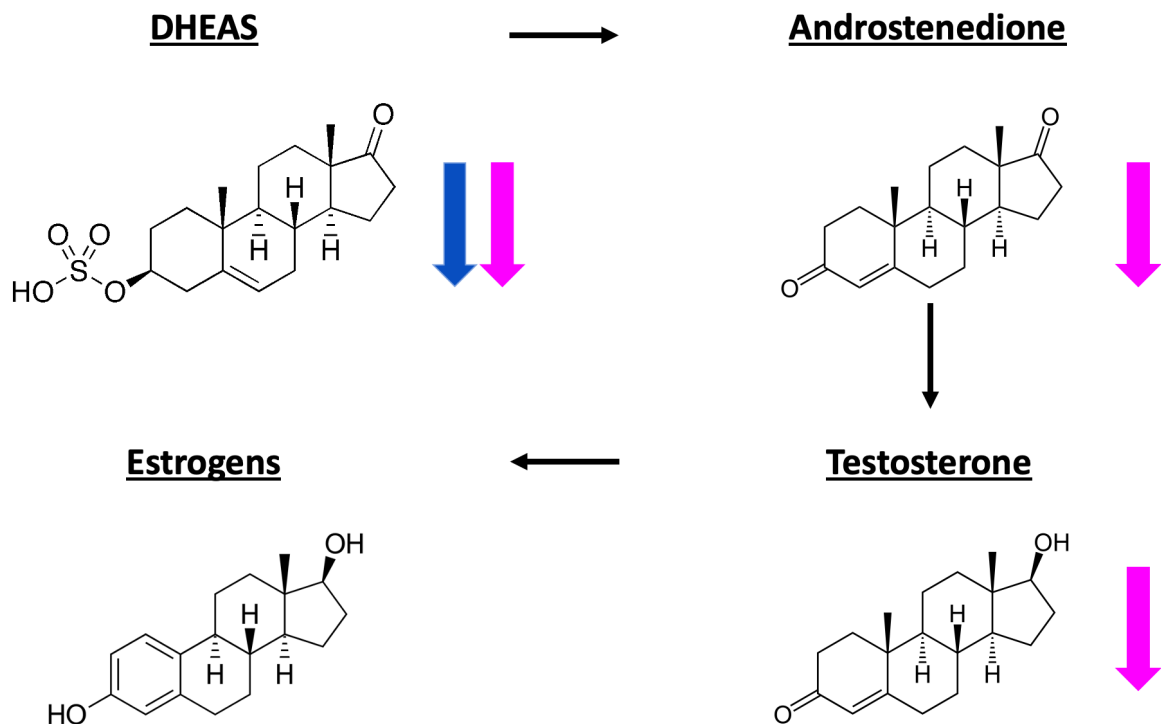
Right ventricle tissue from deceased healthy subjects (N=3 females, N=3 males) and both deceased or transplanted PAH patients (N=3 females, N=3 males) were fixed in 4% paraformaldehyde in phosphate-buffered saline (PBS, pH 7.4) for 24 h, and embedded into paraffin. Afterwards, the paraffin block was cut into 5- μ m sections and mounted into the slide with 3-aminopropyl-triethoxysilane (APES).

Tissue sections were dewaxed with two 3-min xylene washes, one 3-min xylene:ethanol, 3-min graded ethanol washes of 100% (twice), 95%, 70%, and 50% followed by running cold tap water. Next, sections were steamed in antigen retrieval EDTA-based pH=9 solution 4 times 5 minutes. The sections were permeabilized, blocked and incubated at 4°C overnight with the primary antibody. Sections were stained for cluster of differentiation 31 (also known as *Platelet endothelial cell adhesion molecule* (PECAM-1)) (CD31, diluted 1:50; Santa Cruz Biotechnologies). Samples were then incubated for 1 h at room temperature with anti-mouse secondary antibody conjugated with Alexa-488 (diluted 1:500; Abcam). The sections were counterstained with Hoechst 33342 nuclear dye (diluted 1:500; Santa Cruz Biotechnology), rhodamine Ulex europaeus agglutinin I (Ulex, diluted 1:200; Vectorlabs), and Alexa-647 conjugated wheat germ agglutinin (WGA, diluted 1:300; Thermo Fisher Scientific). Finally, samples were coverslipped with ProLong™ Gold Antifade Mountant (Thermofisher Scientific). Cell apoptosis was assessed by Terminal deoxynucleotidyl transferase (TdT) dUTP Nick-End Labeling (TUNEL) assay using the *In situ cell death detection kit fluorescein* (Roche) following manufacturer's protocol. Images were captured at 20x, 40x and 60x magnifications under a laser confocal microscope (Nikon A1R). Whole-slide image acquisition was performed on

Vectra Polaris (Akoya) at 10x and 20x magnifications. Quantitative histological measurements (cardiomyocyte cross-sectional area, vessel density and apoptotic nuclei) were assessed through ImageJ analysis software (NIH) with at least 10 random fields averaged per patient.

SUPPLEMENTAL TABLES AND FIGURES

Figure S1 – Overview sex-hormone pathway in PAH



Overview of sex hormone pathway and findings in our PAH cohort of reduced DHEAS levels in both male (blue arrow) and female patients (pink arrow), and reduced androstenedione and testosterone levels in female patients.

Table S1 - Characteristics general cohort compared to cross-sectional sex hormones cohort

	PAH F general	PAH F hormones	P-value F	PAH M general	PAH M hormones	P-value M
n	196	36		110	19	
Age at visit, y	53 (17)	51 (16)	NS	61 (17)	50 (14)	<0.05
BSA, m ²	1.9 (0.3)	1.8 (0.2)	NS	2.0 (0.2)	2.0 (0.2)	NS
BMI, kg/m ²	28 (7)	26 (5)	NS	26 (4)	25 (4)	NS
NT/HA FC						
Class I, n (%)	7 (5)	3 (8)		3 (4)	1 (5)	
Class II, n (%)	46 (30)	25 (69)		27 (34)	14 (74)	
Class III, n (%)	80 (52)	8 (22)		39 (49)	4 (21)	
Class IV, n (%)	21 (14)	0 (0)	<0.001	11 (13.8)	0 (0)	<0.05
NTproBNP, ng/L	985 [253 - 2839]	202 [111 - 399]	NS	1090 [299 - 2870]	172 [105 - 953]	<0.05
RHC						
mPAP, mmHg	53 (14)	48 (14)	NS	49 (12)	48 (13)	NS
mrAP, mmHg	8 [6 - 11]	7 [6 - 9]	NS	7 [5 - 11]	7 [5 - 10]	NS
PAMP, mmHg	10 (3)	12 (3)	NS	9 (3)	11 (2)	NS
PVRI, WU*m2	5 [3 - 8]	4 [2 - 6]	NS	4 [3 - 6]	3 [2 - 4]	NS
Cardiac index, L/m ²	2.5 (0.9)	2.9 (0.7)	NS	2.5 (0.8)	3.0 (0.9)	NS
CMR						
Heart rate, bpm	80 (13)	72 (12)	NS	77 (15)	72 (13)	NS
RVEDV index, ml/m ²	80 (25)	89 (27)	NS	87 (23)	99 (20)	NS
RVESV index, ml/m ²	52 (22)	48 (22)	NS	61 (24)	61 (24)	NS
SV index, ml/m ²	28 (8)	40 (11)	<0.001	28 (8)	41 (11)	<0.001
RVEF, %	36 (12)	48 (11)	<0.001	33 (12)	40 (14)	NS
RV mass index, g/m ²	49 (13)	43 (14)	NS	56 (15)	52 (15)	NS
Therapy						
Monotherapy, n (%)	123 (63)	11 (31)		70 (64)	8 (42)	
Dual therapy, n (%)	63 (32)	19 (53)		32 (29)	8 (42)	
Triple Therapy, n (%)	4 (2)	6 (17)	<0.01	1 (1)	3 (16)	<0.01
Medication type						
ERA, n (%)	119 (61)	25 (69)	<0.01	59 (54)	17 (90)	NS
PDES, n (%)	97 (50)	29 (81)	NS	59 (54)	11 (58)	<0.05
Prostaeyclin, n (%)	35 (18)	12 (33)	NS	15 (14)	4 (21)	NS

HRT = Hormone replacement therapy. Data is presented as mean (SD) or as median [IQR] or as n (%).

REFERENCES

1. Trip P, Kind T, van de Veerdonk MC, Marcus JT, de Man FS, Westerhof N, Vonk-Noordegraaf A. Accurate assessment of load-independent right ventricular systolic function in patients with pulmonary hypertension. *The Journal of heart and lung transplantation : the official publication of the International Society for Heart Transplantation* 2013; 32(1): 50-55.
2. van de Veerdonk MC, Kind T, Marcus JT, Mauritz GJ, Heymans MW, Bogaard HJ, Boonstra A, Marques KM, Westerhof N, Vonk-Noordegraaf A. Progressive right ventricular dysfunction in patients with pulmonary arterial hypertension responding to therapy. *Journal of the American College of Cardiology* 2011; 58(24): 2511-2519.
3. Büttler RM, Martens F, Ackermans MT, Davison AS, van Herwaarden AE, Kortz L, Krabbe JG, Lentjes EG, Syme C, Webster R, Blankenstein MA, Heijboer AC. Comparison of eight routine unpublished LC-MS/MS methods for the simultaneous measurement of testosterone and androstenedione in serum. *Clinica chimica acta; international journal of clinical chemistry* 2016; 454: 112-118.
4. Büttler RM, Struys EA, Addie R, Blankenstein MA, Heijboer AC. Measurement of dehydroepiandrosterone sulfate (DHEAS) in serum and cerebrospinal fluid by isotope-dilution liquid chromatography tandem mass spectrometry. *Clinica chimica acta; international journal of clinical chemistry* 2012; 414: 246-247.
5. Vermeulen A, Verdonck L, Kaufman JM. A critical evaluation of simple methods for the estimation of free testosterone in serum. *The Journal of clinical endocrinology and metabolism* 1999; 84(10): 3666-3672.

5

RIGHT VENTRICULAR PRESSURE OVERLOAD: FROM HYPERTROPHY TO FAILURE

CE van der Bruggen, RJ Tedford, ML Handoko, J van der Velden, FS de Man

Cardiovascular research, 2017

ABSTRACT

In pulmonary arterial hypertension (PAH), right ventricular (RV) adaptation is essential to overcome the chronic increases in RV pressure overload. Ultimately, RV compensatory mechanisms are not sufficient and patients succumb to RV failure. The processes underlying the transition of RV adaptation to RV failure are not well understood. In this review, we propose that important insights in RV adaptation processes can be obtained by comparing different etiologies of PAH, namely patients with PAH secondary to Eisenmenger syndrome, patients with PAH secondary to systemic sclerosis and patients where no cause is identified: idiopathic PAH. Although the amount of RV afterload does not differ between these patient groups, their prognosis is distinctly different. We will show that an adaptive RV phenotype, as is observed in Eisenmenger patients, coincides with RV hypertrophy, increased RV contractility, low RV fibrosis and low RV diastolic stiffness. Whereas a phenotype of RV failure, as is observed in patients with PAH-secondary to systemic sclerosis, is characterized by impaired contractile reserve, RV fibrosis and RV diastolic stiffness.

INTRODUCTION

The first systematic explanation of the cardiopulmonary circulation was provided by the Roman scientist and philosopher Galen in the second century AD. He claimed that the liver-produced blood would flow into the right ventricle, where it would move directly to the left ventricle (LV) via invisible holes in the interventricular septum. After that, the blood would flow to the local tissue in need, where it would disappear.^{1,2} Despite the discovery of Ibn al-Nafis in the 13th century that blood from the right ventricle passes through the lungs before returning to the LV, Galen's theory dominated and influenced Western medical science for 15 centuries.³ In 1628, William Harvey published his '*Exercitatio Anatomica de Motu Cordis et Sanguinis in Animalibus*', where he was the first to describe the importance of right ventricular (RV) function by arguing; 'If Nature does nothing in vain, she would not have added the right ventricle for the sole purpose of nourishing the lungs, but to propel blood through the lungs into the cavity of the LV'.² Ever since, significant progress has been made in understanding the right ventricle, both in physiological and pathophysiological circumstances. In recent years, it has become clear that RV function is a significant determinant of prognosis and symptomatology in many cardiovascular diseases such as left-sided heart failure, congenital heart disease or pulmonary arterial hypertension (PAH).^{4,5} Therefore, understanding the right ventricle has become increasingly relevant to researchers and clinicians alike.

In PAH, RV afterload increases due to progressive remodeling and proliferation of the pulmonary vasculature. Even though RV adaptation mechanisms initially suffice, the progressive increases in pressure-overload leads almost inevitably to RV failure and death.⁶ Except for lung transplantation, no curative treatment is available. Currently available vasodilators can only achieve a partial afterload reduction, but typically not enough to prevent RV failure, leading to an unsatisfactory median survival of 7 years.⁷ Interestingly, there is a wide heterogeneity in the time between RV adaptation to RV failure, which is independent of the pressure-overload.⁸ This observation suggests that the *response* of the RV rather than the *amount* of pressure-overload defines the fate of the RV in PAH. In aortic stenosis (AS), the LV equivalent of a chronic pressure overloaded ventricle, mechanisms underlying the conversion of LV adaptation towards LV failure have been more robustly studied.⁹⁻¹⁵ However, despite the apparent resemblances between chronic RV and LV pressure overload, it is important to remember the relative increase in pressure overload is roughly two times higher in PAH than in AS. Additionally, while in both situations the ventricles adapt by increasing their mass, only the LV succeeds in normalizing the wall stress.¹⁶⁻¹⁸ For these reasons and others, processes known to play a role in the transition from LV adaptation to LV failure can not necessarily be extrapolated to the RV. In this review, we will provide a perspective on the mechanisms of RV adaptation in PAH and discuss which mechanisms play a role in the transition from RV adaptation to right heart failure.

Possible mechanisms underlying transition of RV adaptation to RV failure

To preserve cardiac output and thus systolic function in PAH, the RV initially adapts by increasing its contractility via the enhancement of intrinsic contractile properties and via muscular hypertrophy.^{19,20} However, as the load progressively increases, the hypertrophic response will be hampered and a vicious cycle of RV dilatation, RV systolic and diastolic dysfunction ensues.^{16,20-22} Although it is unknown what triggers the transition from an adaptive to maladaptive state, several mechanisms that could play a role have been proposed including 1) genetic factors, 2) neurohormonal overactivation and 3) RV ischemia.^{16,23-25} (Figure 5.1)

Genetics

The BMPR2-mutation

The most common genetic cause of PAH are loss-of-function mutations in the Bone Morphogenetic Protein Receptor type 2 (*BMPR2*) gene.^{26,27} The *BMPR2* receptor is a member of the transforming growth factor β (TGF- β) superfamily, and mutations have been shown to result in a disturbed TGF- β /BMP balance. Also less common genetic causes of PAH have their origin in the TGF- β superfamily (mutations in the activin receptor-like kinase 1 (*ALK1*), *BMPR1B*, *caveolin-1*, and *SMAD9*).²⁸⁻³⁰ In the pulmonary vasculature, the over-activity of the TGF- β signaling leads to intimal hyperplasia, smooth muscle cell proliferation and apoptosis resistance.³¹⁻³⁴ From a clinical perspective, it is known that patients with a *BMPR2* mutation present at a younger age, with more severe hemodynamic derangements.³⁵

Most importantly, *BMPR2* mutation carriers carry a worse prognosis – either dying at a younger age or requiring earlier lung transplantation, as elegantly shown in a recent meta-analysis by Evans and coworkers.³⁶ In addition, the authors conclude more severe RV dysfunction in *BMPR2* mutated patients is responsible for the disparate outcomes. Other clinical studies have also revealed advanced RV dysfunction (as measured by stroke work index, stroke volume and cardiac index) at time of diagnosis in *BMPR2* mutation carriers.^{35,37,38} Most convincingly, a recent study found that *BMPR2* mutation carriers have a reduced RV ejection fraction compared to patients without a *BMPR2* mutation, both at baseline and after PAH-specific therapy, despite similar RV afterload.³⁹ This points towards an important role of the TGF- β /BMP balance in RV adaptation during a chronic pressure-overload.

In the heart, the *BMPR2* receptor is expressed by cardiomyocytes and the ventricular endocardium.⁴⁰⁻⁴² Signalling is activated to modulate angiogenic activity, cell growth, cell behaviour and survival.⁴¹⁻⁴⁴ However, the cause of *BMPR2* mutation-induced maladaptive RV-remodeling is still unknown. From left heart failure, it is known that TGF- β overactivation in pressure-overloaded hearts directly lead to maladaptive hypertrophy, fibrosis and hypertrophy.⁴⁵⁻⁴⁸ Although LV and RV pressure-overload are distinctly different as discussed above, Megalou et al. demonstrated in a monocrotaline-induced PAH-rat model that TGF- β blockage indeed attenuated PAH by both lowering RV afterload and improving RV function.⁴⁹ Moreover, Hemnes et al. has shown in multiple experimental models that the *BMPR2* mutation

can result in a disturbed hypertrophic response.⁵⁰ These data suggest that the complex cardiac metabolic program of fatty acid oxidation and glycolysis is impaired in PAH, evident from lipid accumulation and RV lipotoxicity.⁵⁰⁻⁵² By comparing human RV tissue of healthy controls and PAH patients with and without *BMPR2* mutation, our group observed increased mRNA levels of both the glycolysis and fatty acid oxidation pathway in PAH-patients without *BMPR2* mutation. This might suggest that an impaired metabolic compensatory mechanism plays a role in the maladaptive hypertrophic response in the *BMPR2*. In addition, we were able to demonstrate that PAH-patients, independent of their *BMPR2* mutation status, both show signs of cardiac fibrosis, inflammation and angiogenic alterations in terms of capillary density. No differences were seen between *BMPR2* mutation carriers and non-carriers.³⁹

Neurohormonal activation

As a response to the chronic pressure-overload in PAH neurohormonal systems are activated, in particular the sympathetic and renin-angiotensin-aldosterone-system (RAAS).⁵³⁻⁵⁵ Although important for maintaining cardiac output via the enhancement of contractility and hypertrophy in the short term, autonomic dysregulation might be a key player in transition of RV adaptation to RV failure in PAH.⁵⁶

Sympathetic nervous system

Although it still has to be clarified when in the course of PAH sympathetic overstimulation in the RV begins, it has been shown that increased sympathetic activity is associated with a reduced chronotropic response to exercise, a delayed heart rate recovery and an increased mortality.^{57,58} In 1986, Bristow et al. showed reduced β_1 -adrenoreceptor density in the PAH-patients.⁵³ Later, this finding was confirmed in an experimental study of Piao et al., where the authors demonstrate a downregulation of mRNA and protein expression of the adrenergic receptors in a sugen-hypoxia and pulmonary artery banding model.⁵⁹ As a consequence, less protein kinase A (PKA) will be activated through the binding of norepinephrine to the β_1 -adrenoreceptor, resulting in less PKA-mediated phosphorylation of key proteins involved in calcium handling and myofilament function.⁶⁰ As a result, increased diastolic stiffness in the RV of PAH-patients is observed due to interstitial and perivascular fibrosis as well as stiffening of the RV cardiomyocyte caused by hypophosphorylation of titin.²¹

In experimental studies a (partial) restoration of the sympathetic overdrive by beta-blocker therapy led to a survival benefit as well as improved systolic and diastolic RV function, by restoring PKA-signaling.^{61,62} Despite the common use in left heart failure treatment, the PAH field has been reluctant to study the therapeutic potential of β -blocker therapy in patients because of the potential negative inotropic effects and further impairment of exercise capacity.^{63,64} In recent years, several retrospective studies reported no detrimental effects of β -blockage in terms of hemodynamics, clinical and functional outcomes, paving the way for a prospective randomized controlled trials assessing the safety and efficacy of β -blockers in PAH.^{65,66} Explorative studies enrolling relatively small numbers of PAH-patients show trends

towards better cardiac function yet mixed results in terms of exercise tolerance and hemodynamic improvements.^{67,68}

Parasympathetic activity

Sympathetic nerve system activity is closely related to parasympathetic activity, in such a way that increased activity in one will result in reduced activity in the other. Little data exist about the contribution of parasympathetic activity in PAH-induced right heart failure.

In PAH-patients reduced heart rate recovery, a marker of parasympathetic activity, is a strong predictor of prognosis and is associated with reduced exercise capacity.^{69,70} Although not well studied in PAH, targeting impaired parasympathetic signaling in left heart failure is beneficial, with previous studies showing improvement in LV function and survival after applying electric vagal stimulation and acetylcholinesterase inhibitors.⁷¹⁻⁷³ In addition, preliminary data of our own group demonstrate potential therapeutic effects of enhancing parasympathetic activity in an animal model of PAH (da Silva Gonçalves Bos, D et al. *Am J Resp Crit Care Med* 2016;193:A3878, abstract). Future experimental studies should reveal whether restoring the sympatho-vagal balance via parasympathetic stimulation is a new potential treatment target in PAH.

RAAS-system

Increases in RV wall stress and RV dysfunction lead to the release of renin secondary to chronically reductions in kidney perfusion. Consequently, the RAAS-system is constitutively activated in PAH and its degree of activation has been associated with disease progression and worse prognosis.⁷⁴ There is even some data to suggest that the pulmonary effects of RAAS-activation are even greater than the cardiac effects, and it has been demonstrated that several RAAS-inhibiting agents affect RV adaptation.⁷⁵ For example, chronic angiotensin II type 1 (AT1)-receptor blocker treatment restores RV-arterial coupling, RV dilatation and RV diastolic stiffness in a monocrotaline PAH-model.⁷⁴ In addition, renal denervation (affecting both the sympathetic and RAAS system) not only demonstrated improvement in hemodynamics, but also a significant reduction in RV fibrosis and diastolic stiffness.⁷⁶ Aldosterone inhibitors, which are currently a mainstay of therapy for symptomatic left ventricular failure, have shown promise in RV failure due to PAH.⁷⁷ In retrospective cohort study combining an aldosterone-inhibitor with an endothelin-receptor antagonist lead to more significant improvements in functional status and cardiac function compared to endothelin-receptor antagonists alone.⁷⁸ The results of a large randomized controlled trial assessing the effects of aldosterone-inhibitor spironolactone treatment in PAH-patients are to be expected soon (Clinicaltrials.gov NCT01468571).

Ischaemia

A hallmark in the transition of RV adaptation to RV failure is the occurrence of capillary rarefaction.⁷⁹⁻⁸¹ In the pressure-overloaded RV, oxygen demand increases due to higher RV

wall stress. To preserve the oxygen consumption/oxygen supply balance, the RV has to increase its myocardial efficiency and blood supply. Initially, these mechanisms are effective, as is proven by the fact that RV hypertrophy alone is not associated with worse survival.⁸² However, at a certain point capillary density and myocardial efficiency decrease and the RV begins to fail.^{81,83} Ruiter et al. demonstrated that despite similar capillaries per myocyte in PAH versus controls, capillary density is actually less given the hypertrophied RV cardiomyocytes.⁸¹ Preserved capillary density is associated with HIF-1 α and PGC-1 α encoding for VEGF expression and therefore angiogenesis. As a consequence, HIF-1 α - and PGC-1 α -related capillary angiogenesis are reduced in RV failure, but not in well adapted RV.⁸⁴ The loss of myocardial capillaries and loss of integrity in the remaining capillaries lead to microvascular RV dysfunction, apoptosis and inflammation. A recent experimental study underlines the importance of the reduced capillary density in a maladapted pig model, where a mismatch between capillary density and workload was associated with increased myocardial fibrosis and worse RV failure.⁸⁵ An additional factor hampering myocardial blood supply in PAH patients may be reduced flow in the right coronary artery, a consequence of low systemic pressures, high RV pressures and myocardial systolic compression.⁸⁶ Reduced flow is correlated to RV mass and RV systolic pressures, indicating more ischemia as pressure afterload further increases. Although Brooks et al. showed a strong correlation between occlusion of the right coronary artery and RV contractility, the functional consequences in a chronic pressure-overload RV are still to be investigated.⁸⁷⁻⁹⁰

Taken this together, a reduced myocardial efficiency, reduced right coronary artery flow and capillary rarefaction occur during the transition from RV adaptation to RV failure.

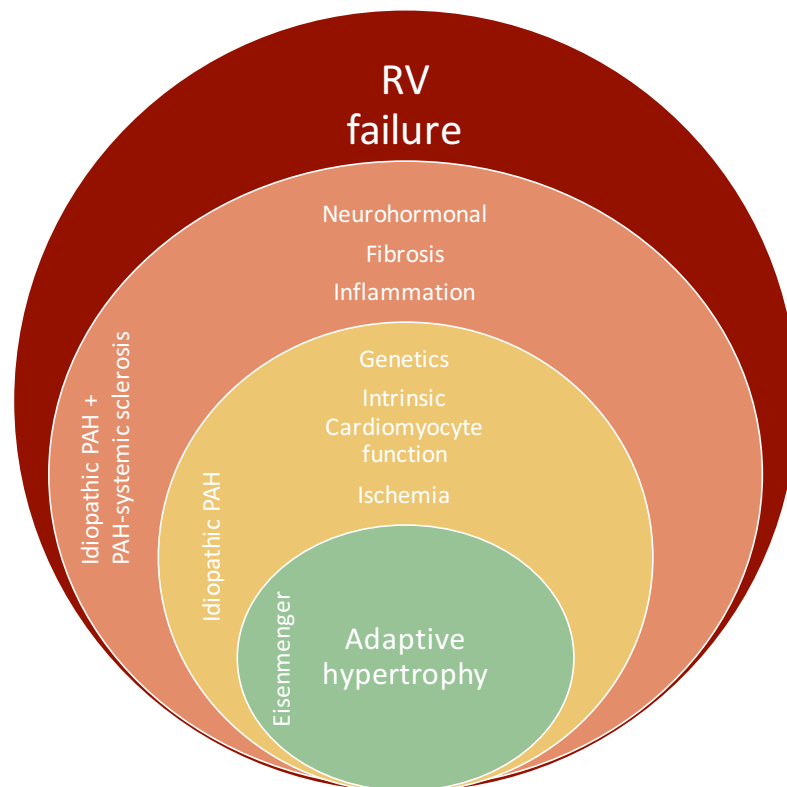
WHAT CAN WE LEARN FROM THE COMPARISON OF DIFFERENT ETIOLOGIES OF RV PRESSURE OVERLOAD?

Determining the relevance and causality of the above described pathophysiological mechanisms is difficult. Although there are several animal models available which allow one to study the pathophysiological mechanisms in more detail, there are significant differences between the human and rodent heart and the difference in disease progression (human: years, rats: weeks) making it difficult to translate the results to the human applications.⁹¹ In addition, mice are resistant to the development of severe PH and RV pressure overload, limiting the use of genetic mice models. In future, cardiac specific gene therapy in rats may provide a solution.⁹²

Ideally, a comparison of protein changes in RV biopsies at different stages of the disease would define the key pathomechanisms. However, due to the high trabeculation and the thickness of the RV free wall, the technical complexity in addition to the non-negligible risk of a ruptured RV free wall makes the procedure too challenging.⁹³ An alternative could be to obtain a biopsy of the interventricular septum at the side of the RV, assuming that wall tension is similar around the RV cavity. The wall tension of the right ventricular free wall may differ from the tension in the interventricular septum, because of the structure of the right ventricle.

Therefore, cardiomyocytes from the interventricular septum may or may not be comparable to cardiomyocytes from the right ventricular free wall.

Figure 5.1 – The pressure overloaded right ventricle



Summary of the proposed pathophysiological mechanisms contributing to the transition of RV adaptation to RV failure. Right ventricular adaptation to the increased pressure overload occurs in patients with Eisenmenger Syndrome by adaptive right ventricular hypertrophy.¹⁰³ In patients with idiopathic pulmonary arterial hypertension, RV hypertrophy is not sufficient to cope with the increased pressure overload, and ischemia⁷⁹⁻⁸¹ and intrinsic cardiomyocyte dysfunction^{19,21,109-112} have been described. In addition, RV adaptation can further be hampered due to genetic mutation in the bone morphogenetic protein receptor 2 (BMPR2).^{26,27,39} RV maladaptation in patients with systemic sclerosis is characterized by excessive RV fibrosis^{115,120,121}, inflammation¹²⁵ and disturbed contractile reserve⁵³⁻⁵⁵ which is more pronounced than in patients with idiopathic pulmonary arterial hypertension. Abbreviations: PAH, pulmonary arterial hypertension; RV, right ventricular.

At least one study suggests that the gene expression of alpha-myosin heavy chain is expressed in all ventricular regions in nonfailing human ventricular myocardium, signifying that biopsies of the interventricular septum could be used as a surrogate for the RV free wall.⁹⁴ However, a recent study in PAH-rats showed that important pathophysiological characteristics such as fibrosis, hypertrophy and capillary rarefaction may not be comparable between the RV free wall and RV septum.⁹⁵ Therefore, current tissue analysis is limited to the comparison of end-stage disease. Nevertheless, important insights may be obtained when different etiologies of PAH are compared to each other, for example PAH where no cause is identified

(idiopathic PAH), PAH secondary to systemic sclerosis and PAH secondary to Eisenmenger syndrome. Epidemiological studies show that these 3 etiologies of PAH differ significantly in prognosis. As is shown in Figure 5.2, patients with PAH secondary to Eisenmenger syndrome have the best outcome with a 3-years survival of 85%, whereas this is only 63% in patients with idiopathic PAH and even worse in PAH-secondary to systemic sclerosis in which 3-years survival is only 52%.⁹⁶ Furthermore, data suggest that these survival differences cannot be described to the severity of the pulmonary vascular remodelling, but is most likely ascribed to differences in the RV response to pressure overload.^{97,98} The magnitude of RV pressure overload is similar among the groups, or even lower in the PAH-patients with systemic sclerosis, but the adaptation of the right ventricle differs significantly. Therefore, these three PAH etiologies could be divided into 3 phenotypes of RV adaptation to increased pressure overload: 1. Eisenmenger patients represents a phenotype with RV adaptation; 2. Patients with PAH-secondary to systemic sclerosis represents a phenotype of RV failure; 3. idiopathic PAH-patients have a mixed phenotype of RV adaptation and RV failure.

Idiopathic pulmonary arterial hypertension

When during clinical assessment no cause of pulmonary hypertension is found (such as left heart failure, pulmonary embolism, chronic obstructive pulmonary disease, etcetera), the diagnoses of idiopathic PAH is made.⁹⁹ The disease is further characterized by the relative young age of patients (average 49 years) and the female predominance (~80%).¹⁰⁰ PAH is caused by excessive remodelling of the pulmonary vasculature, due to increased proliferation of the endothelial and smooth muscle cells of the small pulmonary arterioles. As a consequence of the pulmonary vascular remodelling, resistance in the pulmonary vasculature is increased resulting in elevated pulmonary artery pressure and pressure overload.

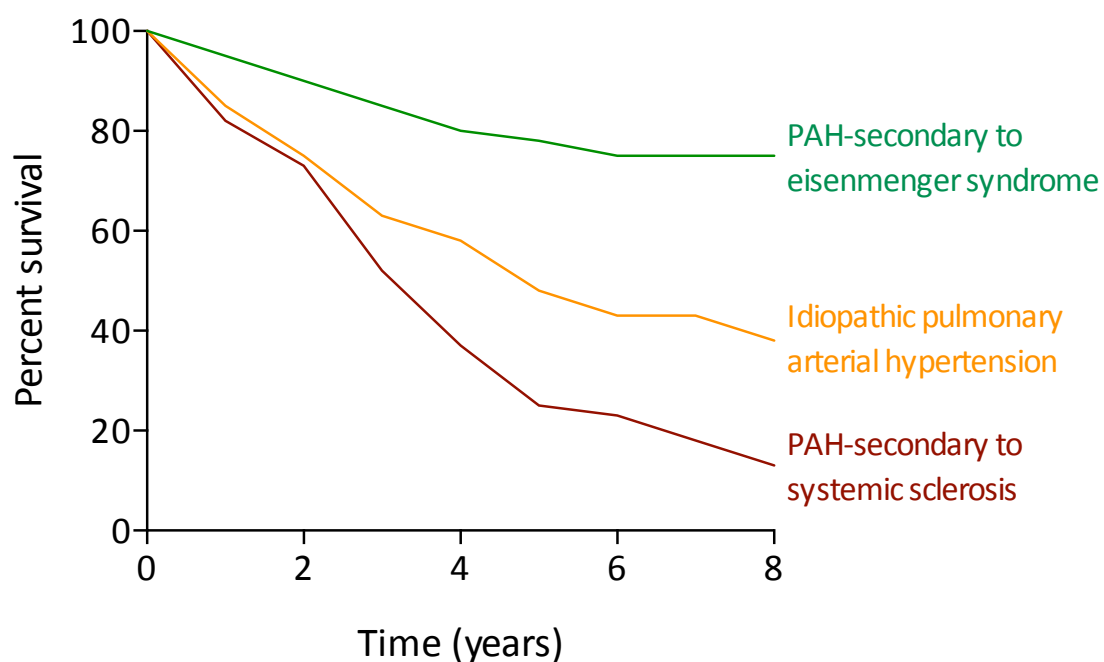
PAH secondary to systemic sclerosis

Systemic sclerosis is an autoimmune disorder which is characterized by increased inflammation and fibrosis formation in skin and visceral organs. Two forms of systemic sclerosis have been described: 1. Limited systemic sclerosis, in which the disease mainly affects the skin of the face, hands and feet, and; 2. Diffuse systemic sclerosis, in which the disease also affects the visceral organs such as kidneys, heart, lungs and gastrointestinal tract. The prevalence of PAH in systemic sclerosis patients is estimated around 12%, and is more common in patients with limited systemic sclerosis than in patients with diffuse systemic sclerosis.¹⁰¹ The development of PAH in systemic sclerosis has been ascribed to severe fibrotic and hypertrophic remodelling of the pulmonary arterioles. In addition, PAH is a principle cause of death in patients with systemic sclerosis.

PAH secondary to Eisenmenger syndrome

Eisenmenger syndrome occurs in patients with a congenital heart defect, and is characterized by severe PAH with dilatation of the central pulmonary arterial, and reversal of a previous left-to-right shunt at the atrial and ventricular or aorta-pulmonary level.¹⁰² Eisenmenger syndrome is mostly prevalent in patients with a shunt or defect distal to the tricuspid valve. Defects located proximal to the tricuspid valve include all atrial septum defects, sinus venosus defects and common atria, whereas post-tricuspid defects include all ventricular septum defects, single ventricles and aortapulmonary communications.¹⁰³ Eisenmenger syndrome only occurs in patients with a large defect which is hemodynamically unrestrictive, indicating that there is no pressure difference from one side of the defect to the other.¹⁰⁴ The systemic level pulmonary artery pressure and increased pulmonary artery flow causes muscular hypertrophy of the small pulmonary arteries resulting in excessive pulmonary vascular remodelling.

Figure 5.2 – Survival in different PH-etologies



Survival analyses of the three etiologies of pulmonary hypertension discussed in this review. Patients with PAH secondary to Eisenmenger syndrome have the best outcome with a 3-years survival of 85%, whereas this is only 63% in patients with idiopathic PAH and even worse in PAH-secondary to systemic sclerosis in which 3-years survival is only 52%.⁹⁶ Data suggest that these survival differences cannot be described to the severity of the pulmonary vascular remodelling, but is most likely ascribed to differences in the RV response to pressure overload. The magnitude of RV pressure overload is similar among the groups, or even lower in the PAH-patients with systemic sclerosis, but the adaptation of the right ventricle differs significantly. Abbreviations: PAH, pulmonary arterial hypertension.

Right ventricular hypertrophy

Right ventricular adaptation

As discussed above, one of the mechanisms of adaptation to an increased pressure overload of the right ventricle is the induction of hypertrophy. Although it has been suggested in several previous review papers that the right ventricle in PAH-patients first adapt with concentric hypertrophy and eventually evolves into eccentric hypertrophy, this transition is difficult to prove due to the limitations of tissue collection. Indeed there is relatively little known about the *kind* of RV hypertrophy that is induced by increased pressure overload.

The *amount* of RV hypertrophy has been compared between iPAH-patients, patients with PAH-secondary to systemic sclerosis and Eisenmenger patients by different imaging techniques. Interestingly, these analyses have revealed that the amount of hypertrophy between idiopathic PAH and PAH secondary to systemic sclerosis does not differ significantly.^{105,106} In contrast, in Eisenmenger patients RV hypertrophy is more pronounced,⁹⁸ despite similar pulmonary vascular remodelling and RV afterload in all three groups. This suggest that the adaptation of the right ventricle to increased RV afterload is best in Eisenmenger patients in comparison to iPAH and PAH-secondary to systemic sclerosis (Figure 5.3).

The heart of Eisenmenger patients (NB: post-tricuspid defects) is more comparable to a fetal heart than an adult heart.¹⁰³ Like in the fetal circulation in which pulmonary and systemic arterial pressures are equal because of the fetal ductus arteriosus, the heart of Eisenmenger patients has similar RV and LV free wall thickness and a flattened interventricular septum. In addition, whereas patients with other forms of PAH undergo regression of RV wall thickness during infancy, this does not occur in patients with Eisenmenger syndrome. Therefore, it has been hypothesized that the RV cardiomyocytes of Eisenmenger patients are “primed” to endure the increased pressure overload. It is of utmost importance to unravel the molecular changes that are associated with the priming of the RV cardiomyocytes to endure prolonged RV pressure overload to enable the generation of therapeutic targets to induce a compensatory RV phenotype in other forms of PAH-induced right heart failure.

Right ventricular recovery

Right ventricular hypertrophy in patients with pulmonary hypertension is reversible. Studies before and after lung transplantation demonstrated that normalization of RV afterload results in normalization of RV mass. Whether intrinsic RV function is also restored remains to be established, though data from patients with chronic thromboembolic disease after effective pulmonary endarterectomy suggest the RV still may be impaired.^{129,130} Recent advancements with balloon pulmonary angioplasty in patients with chronic thrombo-embolic pulmonary hypertension allows to study the process of RV recovery following a decrease in RV afterload in the absence of interfering drugs in large number of patients.¹⁰⁷

Intrinsic cardiomyocyte dysfunction

In addition to the size of the RV cardiomyocytes, intrinsic cardiomyocyte function is essential for the adaptation of the right ventricle to increased pressure overload. RV pressure-volume analyses can give an indication on the load-independent alterations of RV function in PAH-patients. Because the original pressure-volume approach of obtaining multiple pressure volume loops by temporary vena cava occlusions are not without risks in PAH-patients, alternative approaches have been developed during past years. Translating from work performed on the LV, Brimiouille et al. described a single beat method to determine load-independent RV systolic function,¹⁰⁸ which has been implemented in several clinical studies.^{19,21,109-112} A Valsalva manoeuvre to decrease preload, and more recently, external inferior vena cava pressure, have recently been used to generate multiple pressure-volume loops and assess load-independent systolic function in PAH-patients^{97,105}. It should be noted that the studies that we will discuss in the following paragraph, may differ on the techniques that were used to generate the information on load-independent RV systolic function.

In patients with idiopathic PAH, an increase in RV contractility is observed in all patients independent of disease severity.¹⁹ This is also confirmed on tissue level, in which we have determined force generation of RV cardiomyocyte from PAH-patients (both idiopathic PAH and Eisenmenger) in comparison to donors. RV cardiomyocytes of PAH-patients generated over the whole spectrum of calcium concentrations, more force than RV cardiomyocytes of donor hearts also after correction for differences in RV cardiomyocyte size.²¹ Also a subgroup analyses was performed to compare idiopathic PAH and Eisenmenger patients, but no difference was observed, although it should be noted that the study was not powered for such an analyses.

These measurements do not indicate whether the increase in RV contractility is sufficient to cope with the increase in RV pressure overload as is seen in PAH-patients. When RV contractility is corrected for the increase in RV afterload (RV-arterial coupling), we observed that the RV contractility increase is indeed insufficient to cope with the RV afterload in end-stage PAH-patients.

Interestingly, recent studies suggest that in patients with PAH secondary to systemic sclerosis the increase in RV contractility is absent (Figure 5.3). Overbeek et al. demonstrated that RV pump function was more affected in PAH-patients with systemic sclerosis in comparison to idiopathic PAH.¹¹³ In addition, also with pressure-volume analyses it was shown that RV contractility was reduced in PAH-patients with systemic sclerosis in comparison to idiopathic PAH, resulting in an abnormal RV-arterial coupling.⁹⁷ More recently, preliminary data by Hsu and colleagues have extended this observation with RV cardiomyocyte measurements in which they confirmed the increased force generation of RV cardiomyocytes of idiopathic PAH-patients, which was absent in RV cardiomyocytes of patients with PAH-secondary to systemic sclerosis (Hsu S, et al. *J Heart Lung Transplant* 2017, abstract).

There are several possible explanations for this discrepancy between idiopathic PAH and PAH secondary to systemic sclerosis including impaired calcium handling¹⁰⁵ or dysfunctional contractile machinery. Additionally, differences in beta-adrenergic receptor signalling may

also play a role. Although it has been demonstrated that beta-adrenergic receptor signalling is also disturbed in idiopathic PAH patients,⁶⁰ this could be more pronounced in PAH secondary to systemic sclerosis. Increased inflammation could lead to increased expression of prostaglandin E₂, which can inhibit intracellular beta-adrenergic receptor signalling by preventing cAMP diffusion to the sarcoplasmic reticulum thereby blocking the beta-adrenergic induced contractile response of cardiomyocytes.¹¹⁴ This hypothesis is supported by the recent finding of Hsu et al, that the contractile reserve upon exercise in patients with PAH secondary to systemic sclerosis is more impaired than in patients with idiopathic PAH.^{105,110} Future studies should further investigate the contribution of inflammation on the disturbed contractile reserve in patients with systemic sclerosis.

RV fibrosis and RV inflammation

RV fibrosis

There are various techniques available to quantify right ventricular fibrosis in vivo as well as ex vivo. Most often used techniques in PAH-patients is delayed gadolinium enhancement and T1 mapping by magnetic resonance imaging (in vivo)¹¹⁵⁻¹¹⁹ or histomorphometric analyses in cardiac tissue (ex vivo).^{21,120,121} All studies have reported increased levels of RV fibrosis in PAH-patients. However, with imaging techniques the observed RV fibrosis is often limited to the hinge-points of the right ventricle connected to the interventricular septum, whereas histomorphometric analyses also illustrates increased RV fibrosis in the RV free wall. This discrepancy may be explained by the observation that the RV fibrosis in PAH-patients is not replacement fibrosis but interstitial fibrosis. The latter being more difficult to detect by imaging techniques such as magnetic resonance imaging due to the limited resolution.

The functional relevance of the observed increase in RV fibrosis remained elusive until recently. Although the differences between control and PAH RV fibrosis are modest,²¹ it is sufficient to explain the impaired RV diastolic stiffness observed in end-stage right heart failure.¹²² Besides the *amount* of RV fibrosis, also the *type* of RV fibrosis may be relevant. However, currently no data is available on the type of collagen deposition and cross-linking in the right ventricle of PAH-patients with different etiologies.

The amount of RV fibrosis has been compared between idiopathic PAH patients and patients with PAH secondary to systemic sclerosis or Eisenmenger. Intriguingly, no difference in RV fibrosis has been observed in idiopathic PAH patients and patients with PAH-secondary to systemic sclerosis, both with in vivo analyses as well as with histomorphometric analyses on RV tissue.^{115,120} This observation was unexpected based on the fact that systemic sclerosis is an auto-immune disease characterized by increased collagen deposition in visceral organs. In line with the similar amount of RV fibrosis between idiopathic PAH-patients and patients with PAH-secondary to systemic sclerosis, also no difference in RV diastolic stiffness has been observed,⁹⁷ indicating that the effect of RV pressure overload on RV diastolic function is similar between the two patient groups.

A recent post-mortem morphometric analyses by Gomez-Arroyo et al. comparing cardiac tissue of patients with idiopathic PAH, Eisenmenger and control subjects, revealed increased RV fibrosis in both PAH-patient groups.¹²¹ However Eisenmenger patients appeared to have less RV fibrosis than idiopathic PAH-patients, suggesting that RV diastolic function is more preserved in Eisenmenger patients. This hypothesis is further supported by the observation that right atrial pressures are normal in Eisenmenger patients, whereas this is increased in idiopathic PAH and PAH secondary to systemic sclerosis (Figure 3).

From current literature, we can conclude that an adaptive RV phenotype, as is observed in Eisenmenger patients, coincides with less RV fibrosis and RV diastolic impairment. Future therapeutic studies should reveal whether targeting RV fibrosis could be a strategy to prevent the development of right heart failure.

RV inflammation

Little is known about the contribution of RV inflammation on RV adaptation in PAH. From in vitro studies in left heart failure, increased wall stress due to pressure overload results in the secretion of pro-inflammatory cytokines such as tumor necrosis factor alpha by cardiomyocytes.^{123,124} In addition, increased RV inflammatory cell infiltration has been described in an animal model of PAH.⁸³ We could therefore speculate that impaired adaptation of the right ventricle to the increased load would lead to increased RV wall stress, thereby stimulating RV cardiomyocytes to secrete pro-inflammatory cytokines and attract inflammatory cells. Interestingly, more inflammatory cell infiltration is indeed observed in patients with PAH secondary to systemic sclerosis than in idiopathic PAH-patients, though it is unknown if this is a result of the systemic disease or response to pressure overload.^{120,125} Novel developed tracers for positron emission tomography imaging may enable us to better study these hypotheses, for example inflammation can be visualized by a macrophage cell membrane tracer (18F-FMCH),¹²⁶ fibrosis may be visualized by RGD based PET tracers,¹²⁷ neurohormonal activity may be visualized by a beta-adrenergic receptor tracer (11C-CGP12177).¹²⁸ Overall, future studies should reveal whether RV inflammation is a contributor to the transition towards right heart failure.

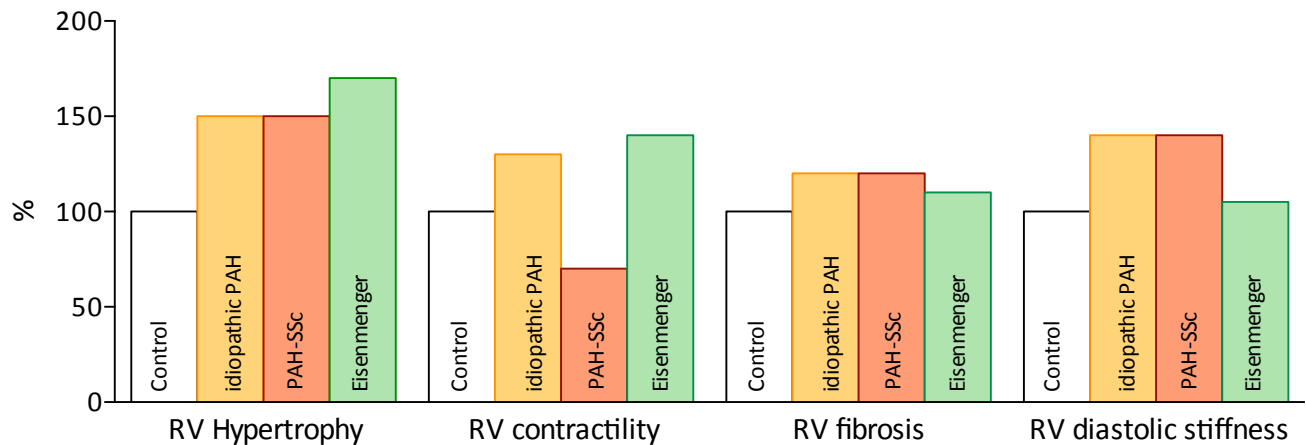
CONCLUSION

By comparing different PAH etiologies, we could identify 3 phenotypes of RV adaptation: 1. RV adaptation, as is observed in Eisenmenger patients, which is coincided with RV hypertrophy, RV contractility and low levels of RV fibrosis and RV diastolic stiffness; 2. RV failure, as is observed in PAH-patients secondary to systemic sclerosis, which is characterized by impaired contractile reserve, increased RV fibrosis and RV diastolic stiffness; 3. A mixed phenotype, as is observed in patients with idiopathic PAH.

Further in depth comparison of RV hypertrophy development, neurohormonal regulation and RV function between patients with idiopathic PAH, PAH secondary to systemic sclerosis and

Eisenmenger patients will gain our understanding of the different RV adaptation profiles. In addition, progress in new models such as cell culture models or nuclear imaging techniques is of utmost importance to extend our analyses from end-stage heart failure to longitudinal analyses of heart failure development.

Figure 5.3 – Right ventricular adaptation



Right ventricular adaptation in patients with idiopathic pulmonary arterial hypertension, patients with PAH secondary to systemic sclerosis and patients with PAH secondary to Eisenmenger syndrome. RV adaptation in patients with idiopathic PAH is characterized by increased RV hypertrophy, enhanced RV contractility, excessive RV fibrosis and RV diastolic stiffness.²¹ RV adaptation in patients with PAH secondary to systemic sclerosis is comparable to idiopathic PAH except that patients with systemic sclerosis suffer from impaired RV contractility.¹⁰⁵ RV adaptation in patients with Eisenmenger syndrome is more beneficial indicated by the lower amount of RV fibrosis and RV diastolic stiffness in comparison to patients with idiopathic PAH and PAH secondary to systemic sclerosis.¹²¹

REFERENCES

- Schultz SG. William Harvey and the circulation of the blood: the birth of a scientific revolution and modern physiology. *News Physiol Sci* 2002;**17**:175–180.
- AIRD WC. Discovery of the cardiovascular system: from Galen to William Harvey. *J Thromb Haemost* 2011;**9**:118–129.
- West JB. Ibn al-Nafis, the pulmonary circulation, and the Islamic Golden Age. *J Appl Physiol* 2008;**105**:1877–1880.
- Haddad F, Doyle R, Murphy DJ, Hunt SA. Right ventricular function in cardiovascular disease, part II: pathophysiology, clinical importance, and management of right ventricular failure. *Circulation* 2008;**117**:1717–1731.
- van de Veerdonk MC, Kind T, Marcus JT, Mauritz G-J, Heymans MW, Bogaard H-J, Boonstra A, Marques KMJ, Westerhof N, Vonk-Noordegraaf A. Progressive right ventricular dysfunction in patients with pulmonary arterial hypertension responding to therapy. *J Am Coll Cardiol* 2011;**58**:2511–2519.
- Galie N, Humbert M, Vachiery J-L, Gibbs S, Lang I, Torbicki A, Simonneau G, Peacock A, Vonk-Noordegraaf A, Beghetti M, Ghofrani A, Gomez Sanchez MA, Hansmann G, Klepetko W, Lancellotti P, Matucci M, McDonagh T, Pierard LA, Trindade PT, Zompatori M, Hoeper M, Aboyans V, Vaz Carneiro A, Achenbach S, Agewall S, Allanore Y, Asteggiano R, Paolo Badano L, Albert Barbera J, Bouvaist H, et al. 2015 ESC/ERS Guidelines for the diagnosis and treatment of pulmonary hypertension: The Joint Task Force for the Diagnosis and Treatment of Pulmonary Hypertension of the European Society of Cardiology (ESC) and the European Respiratory Society (ERS): Endorsed by: Association for European Paediatric and Congenital Cardiology (AEPC), International Society for Heart and Lung Transplantation (ISHLT). *Eur Heart J* 2016;**37**:67–119.
- Benza RL, Miller DP, Barst RJ, Badesch DB, Frost AE, McGoon MD. An evaluation of long-term survival from time of diagnosis in pulmonary arterial hypertension from the REVEAL Registry. *Chest* 2012;**142**:448–456.
- Vonk-Noordegraaf A, Galie N. The role of the right ventricle in pulmonary arterial hypertension. *Eur Resp Rev* 2011;**20**:243–253.
- Hein S, Arnon E, Kostin S, Schönburg M, Elsässer A, Polyakova V, Bauer EP, Klövekorn W-P, Schaper J. Progression From Compensated Hypertrophy to Failure in the Pressure-Overloaded Human Heart. *Circulation* 2003;**107**:984–991.
- Hess OM, Villari B, Krayenbuehl HP. Diastolic dysfunction in aortic stenosis. *Circulation* 1993;**87**:IV73–IV76.
- Kupari M. Left ventricular hypertrophy in aortic valve stenosis: preventive or promotive of systolic dysfunction and heart failure? *Eur Heart J* 2005;**26**:1790–1796.
- Călin A, Roșca M, Beladan CC, Enache R, Mateescu AD, Gînghină C, Popescu BA. The left ventricle in aortic stenosis – imaging assessment and clinical implications. *Cardiovasc Ultrasound* 2015;**13**:1231.
- Lips DJ, deWindt LJ, van Kraaij DJW, Doevendans PA. Molecular determinants of myocardial hypertrophy and failure: alternative pathways for beneficial and maladaptive hypertrophy. *Eur Heart J* 2003;**24**:883–896.
- Hill BG, Benavides GA, Lancaster JR, Ballinger S, Dell'Italia L, Zhang J, Darley-Usmar VM. Integration of cellular bioenergetics with mitochondrial quality control and autophagy. *Biol Chem* 2012;**393**:1485–1512.
- Popescu AC, Antonini-Canterin F, Enache R, Nicolosi GL, Piazza R, Faggiano P, Cassin M, Dimulescu D, Gînghină C, Popescu BA. Impact of Associated Significant Aortic Regurgitation on Left Ventricular Remodeling and Hemodynamic Impairment in Severe Aortic Valve Stenosis. *Cardiology* 2013;**124**:174–181.
- Rain S, Handoko ML, Vonk-Noordegraaf A, Bogaard HJ, van der Velden J, de Man FS. Pressure-overload-induced right heart failure. *Pflügers Archiv* 2014;**466**:1055–1063.
- Gan CT-J, Lankhaar J-W, Marcus JT, Westerhof N, Marques KM, Bronzwaer JGF, Boonstra A, Postmus PE, Vonk-Noordegraaf A. Impaired left ventricular filling due to right-to-left ventricular interaction in patients with pulmonary arterial hypertension. *Am J Physiol Heart Circ Physiol* 2006;**290**:H1528–H1533.
- Grossman W, Jones D, McLaurin LP. Wall stress and patterns of hypertrophy in the human left ventricle. *J Clin Invest* 1975;**56**:56–64.

19. Trip P, Rain S, Handoko ML, van der Bruggen CE, Bogaard HJ, Marcus JT, Boonstra A, Westerhof N, Vonk-Noordegraaf A, de Man FS. Clinical relevance of right ventricular diastolic stiffness in pulmonary hypertension. *Eur Resp J* 2015;**45**:1603-1612.
20. Vonk-Noordegraaf A, Westerhof BE, Westerhof N. The Relationship Between the Right Ventricle and its Load in Pulmonary Hypertension. *J Am Coll Cardiol* 2017;**69**:236-243.
21. Rain S, Handoko ML, Trip P, Gan CT-J, Westerhof N, Stienen GJ, Paulus WJ, Ottenheijm CAC, Marcus JT, Dorfmueller P, Guignabert C, Humbert M, Macdonald P, Remedios Dos C, Postmus PE, Saripalli C, Hidalgo CG, Granzier HL, Vonk-Noordegraaf A, van der Velden J, de Man FS. Right ventricular diastolic impairment in patients with pulmonary arterial hypertension. *Circulation* 2013;**128**:2016-2025.
22. van Wolferen SA, Marcus JT, Boonstra A, Marques KMJ, Bronzwaer JGF, Spreeuwenberg MD, Postmus PE, Vonk-Noordegraaf A. Prognostic value of right ventricular mass, volume, and function in idiopathic pulmonary arterial hypertension. *Eur Heart J* 2007;**28**:1250-1257.
23. Vonk-Noordegraaf A, Haddad F, Chin KM, Forfia PR, Kawut SM, Lumens J, Naeije R, Newman J, Oudiz RJ, Provencher S, Torbicki A, Voelkel NF, Hassoun PM. Right heart adaptation to pulmonary arterial hypertension: physiology and pathobiology. *J Am Coll Cardiol* 2013;**62**:D22-D33.
24. Voelkel NF, Gomez-Arroyo J, Abbate A, Bogaard HJ, Nicolls MR. Pathobiology of pulmonary arterial hypertension and right ventricular failure. *Eur Resp J* 2012;**40**:1555-1565.
25. Ryan JJ, Archer SL. The right ventricle in pulmonary arterial hypertension: disorders of metabolism, angiogenesis and adrenergic signaling in right ventricular failure. *Circ Res* 2014;**115**:176-188.
26. Deng Z, Morse JH, Slager SL, Cuervo N, Moore KJ, Venetos G, Kalachikov S, Cayanis E, Fischer SG, Barst RJ, Hodge SE, Knowles JA. Familial Primary Pulmonary Hypertension (Gene PPH1) Is Caused by Mutations in the Bone Morphogenetic Protein Receptor-II Gene. *Am J Hum Genet* 2000;**67**:737-744.
27. International PPH Consortium, Lane KB, Machado RD, Pauciulo MW, Thomson JR, Phillips JA, Loyd JE, Nichols WC, Trembath RC. Heterozygous germline mutations in BMPR2, encoding a TGF-beta receptor, cause familial primary pulmonary hypertension. *Nat Genet* 2000;**26**:81-84.
28. Cogan JD, Pauciulo MW, Batchman AP, Prince MA, Robbins IM, Hedges LK, Stanton KC, Wheeler LA, Phillips JA III, Loyd JE, Nichols WC. High Frequency of BMPR2 Exonic Deletions/Duplications in Familial Pulmonary Arterial Hypertension. *Am J Resp Crit Care Med* 2006;**174**:590-598.
29. Machado RD, Eickelberg O, Elliott CG, Geraci MW, Hanaoka M, Loyd JE, Newman JH, Phillips JA III, Soubrier F, Trembath RC, Chung WK. Genetics and Genomics of Pulmonary Arterial Hypertension. *J Am Coll Cardiol* 2009;**54**:S32-S42.
30. Soubrier F, Chung WK, Machado R, Grunig E, Aldred M, Geraci M, Loyd JE, Elliott CG, Trembath RC, Newman JH, Humbert M. Genetics and genomics of pulmonary arterial hypertension. *J Am Coll Cardio* 2013;**62**:D13-D21.
31. Morrell NW. Pulmonary hypertension due to BMPR2 mutation: a new paradigm for tissue remodeling? *Proc Am Thorac Soc* 2006;**3**:680-686.
32. Rudrarakanchana N, Flanagan JA, Chen H, Upton PD, Machado RD, Patel D, Trembath RC, Morrell NW. Functional analysis of bone morphogenetic protein type II receptor mutations underlying primary pulmonary hypertension. *Hum Mol Genet* 2002;**11**:1517-1525.
33. Zhang S, Fantozzi I, Tigno DD, Yi ES, Platoshyn O, Thistlethwaite PA, Kriett JM, Yung G, Rubin LJ, Yuan JXJ. Bone morphogenetic proteins induce apoptosis in human pulmonary vascular smooth muscle cells. *Am J Physiol Lung Cell Mol Physiol* 2003;**285**:L740-L754.
34. Lagna G, Nguyen PH, Ni W, Hata A. BMP-dependent activation of caspase-9 and caspase-8 mediates apoptosis in pulmonary artery smooth muscle cells. *Am J Physiol Lung Cell Mol Physiol* 2006;**291**:L1059-L1067.
35. Sztrymf B, Coulet F, Girerd B, Yaïci A, Jais X, Sitbon O, Montani D, Souza R, Simonneau G, Soubrier F, Humbert M. Clinical Outcomes of Pulmonary Arterial Hypertension in Carriers of BMPR2 Mutation. *Am J Resp Crit Care Med* 2008;**177**:1377-1383.
36. Evans JDW, Girerd B, Montani D, Wang X-J, Galie N, Austin ED, Elliott G, Asano K, Grunig E, Yan Y, Jing Z-C, Manes A, Palazzini M, Wheeler LA, Nakayama I, Satoh T, Eichstaedt C, Hinderhofer K, Wolf M, Rosenzweig EB, Chung WK, Soubrier F, Simonneau G, Sitbon O, Gräf S, Kaptoge S, Di Angelantonio E, Humbert M, Morrell NW. BMPR2 mutations and survival in pulmonary arterial hypertension: an individual participant data meta-analysis. *Lancet Respir Med*

37. Rosenzweig EB, Morse JH, Knowles JA, Chada KK, Khan AM, Roberts KE, McElroy JJ, Juskiw NK, Mallory NC, Rich S, Diamond B, Barst RJ. Clinical implications of determining BMPR2 mutation status in a large cohort of children and adults with pulmonary arterial hypertension. *J Heart Lung Transplant* 2008;**27**:668–674.
38. Brittain EL, Pugh ME, Wheeler LA, Robbins IM, Loyd JE, Newman JH, Larkin EK, Austin ED, Hemnes AR. Shorter survival in familial versus idiopathic pulmonary arterial hypertension is associated with hemodynamic markers of impaired right ventricular function. *Pulm Circ* 2013;**3**:589–598.
39. van der Bruggen CE, Happe CM, Dorfmueller P, Trip P, Spruijt OA, Rol N, Hoevenaars FP, Houweling AC, Girerd B, Marcus JT, Mercier O, Humbert M, Handoko ML, van der Velden J, Vonk-Noordegraaf A, Bogaard H-J, Goumans M-J, de Man FS. Bone Morphogenetic Protein Receptor Type 2 Mutation in Pulmonary Arterial Hypertension: A View on the Right Ventricle. *Circulation* 2016;**133**:1747–1760.
40. Morrell NW, Bloch DB, Dijke ten P, Goumans M-JTH, Hata A, Smith J, Yu PB, Bloch KD. Targeting BMP signalling in cardiovascular disease and anaemia. *Nat Rev Cardiol* 2016;**13**:106–120.
41. Yoshimatsu Y, Lee YG, Akatsu Y, Taguchi L, Suzuki HI, Cunha SI, Maruyama K, Suzuki Y, Yamazaki T, Katsura A, Oh SP, Zimmers TA, Lee SJ, Pietras K, Koh GY, Miyazono K, Watabe T. Bone morphogenetic protein-9 inhibits lymphatic vessel formation via activin receptor-like kinase 1 during development and cancer progression. *Proc Natl Acad Sci U S A* 2013;**110**:18940–18945.
42. Wu X, Sagave J, Rutkovskiy A, Haugen F, Baysa A, Nygard SL, Czibik G, Dahl CP, Gullestad L, Vaage J, Valen G. Expression of bone morphogenetic protein 4 and its receptors in the remodeling heart. *Life Sci* 2014;**97**:145–154.
43. Pachori AS, Custer L, Hansen D, Clapp S, Kempa E, Klingensmith J. Bone morphogenetic protein 4 mediates myocardial ischemic injury through JNK-dependent signaling pathway. *J Mol Cell Cardiol* 2010;**48**:1255–1265.
44. Chan MC, Nguyen PH, Davis BN, Ohoka N, Hayashi H, Du K, Lagna G, Hata A. A Novel Regulatory Mechanism of the Bone Morphogenetic Protein (BMP) Signaling Pathway Involving the Carboxyl-Terminal Tail Domain of BMP Type II Receptor. *Mol Cell Biol* 2007;**27**:5776–5789.
45. Koitabashi N, Danner T, Zaiman AL, Pinto YM, Rowell J, Mankowski J, Zhang D, Nakamura T, Takimoto E, Kass DA. Pivotal role of cardiomyocyte TGF- β signaling in the murine pathological response to sustained pressure overload. *J Clin Invest* 2011;**121**:2301–2312.
46. Dobaczewski M, Chen W, Frangogiannis NG. Transforming growth factor (TGF)- β signaling in cardiac remodeling. *J Mol Cell Cardiol* 2011;**51**:600–606.
47. ROSENKRANZ S. TGF-beta1 and angiotensin networking in cardiac remodeling. *Cardiovasc Res* 2004;**63**:423–432.
48. Akhurst RJ. TGF β signaling in health and disease. *Nat Genet* 2004;**36**:790–792.
49. Megalou AJ, Glava C, Oikonomidis DL, Vilaeti A, Agelaki MG, Baltogiannis GG, Papalois A, Vlahos AP, Kolettis TM. Transforming growth factor- β inhibition attenuates pulmonary arterial hypertension in rats. *Int J Clin Exp Med* 2010;**3**:332–340.
50. Hemnes AR, Brittain EL, Trammell AW, Fessel JP, Austin ED, Penner N, Maynard KB, Gleaves L, Talati M, Absi T, Disalvo T, West J. Evidence for right ventricular lipotoxicity in heritable pulmonary arterial hypertension. *Am J Resp Crit Care Med* 2014;**189**:325–334.
51. Talati MH, Brittain EL, Fessel JP, Penner N, Atkinson J, Funke M, Grueter C, Jerome WG, Freeman M, Newman JH, West J, Hemnes AR. Mechanisms of Lipid Accumulation in the Bone Morphogenetic Protein Receptor 2 Mutant Right Ventricle. *Am J Resp Crit Care Med* 2016;**194**:719–728.
52. Brittain EL, Talati M, Fessel JP, Zhu H, Penner N, Calcutt MW, West JD, Funke M, Lewis GD, Gerszten RE, Hamid R, Pugh ME, Austin ED, Newman JH, Hemnes AR. Fatty Acid Metabolic Defects and Right Ventricular Lipotoxicity in Human Pulmonary Arterial Hypertension Clinical Perspective. *Circulation* 2016;**133**:1936–1944.
53. Bristow MR, Ginsburg R, Umans V, Fowler M, Minobe W, Rasmussen R, Zera P, Menlove R, Shah P, Jamieson S. Beta 1- and beta 2-adrenergic-receptor subpopulations in nonfailing and failing human ventricular myocardium: coupling of both receptor subtypes to muscle contraction and selective beta 1-receptor down-regulation in heart failure. *Circ Res* 1986;**59**:297–309.
54. Mak S, Witte KK, Al-Hesayen A, Granton JJ, Parker JD. Cardiac sympathetic activation in patients with pulmonary arterial hypertension. *Am J Physiol Regul Integr Comp Physiol* 2012;**302**:R1153–R1157.
55. Velez-Roa S, Ciarka A, Najem B, Vachieri J-L, Naeije R, van de Borne P. Increased sympathetic nerve

- activity in pulmonary artery hypertension. *Circulation* 2004;**110**:1308–1312.
56. de Man FS, Handoko ML, Guignabert C, Bogaard HJ, Vonk-Noordegraaf A. Neurohormonal axis in patients with pulmonary arterial hypertension: friend or foe? *Am J Resp Crit Care Med* 2013;**187**:14–19.
 57. Ciarka A, Doan V, Velez-Roa S, Naeije R, van de Borne P. Prognostic significance of sympathetic nervous system activation in pulmonary arterial hypertension. *Am J Resp Crit Care Med* 2010;**181**:1269–1275.
 58. Dimopoulos S, Anastasiou-Nana M, Katsaros F, Papazachou O, Tzanis G, Gerovasili V, Pozios H, Roussos C, Nanas J, Nanas S. Impairment of autonomic nervous system activity in patients with pulmonary arterial hypertension: a case control study. *J Card Fail* 2009;**15**:882–889.
 59. Piao L, Fang Y-H, Parikh KS, Ryan JJ, D'Souza KM, Theccanat T, Toth PT, Pogoriler J, Paul J, Blaxall BC, Akhter SA, Archer SL. GRK2-mediated inhibition of adrenergic and dopaminergic signaling in right ventricular hypertrophy: therapeutic implications in pulmonary hypertension. *Circulation* 2012;**126**:2859–2869.
 60. Rain S, Bos DDSG, Handoko ML, Westerhof N, Stienen G, Ottenheijm C, Goebel M, Dorfmueller P, Guignabert C, Humbert M, Bogaard H-J, Remedios CD, Saripalli C, Hidalgo CG, Granzier HL, Vonk-Noordegraaf A, van der Velden J, de Man FS. Protein changes contributing to right ventricular cardiomyocyte diastolic dysfunction in pulmonary arterial hypertension. *Journal of the American Heart Association* 2014;**3**:e000716–e000716.
 61. de Man FS, Handoko ML, van Ballegoij JJM, Schalij I, Bogaards SJP, Postmus PE, van der Velden J, Westerhof N, Paulus WJ, Vonk-Noordegraaf A. Bisoprolol delays progression towards right heart failure in experimental pulmonary hypertension. *Circ Heart Fail* 2012;**5**:97–105.
 62. Bogaard HJ, Natarajan R, Mizuno S, Abbate A, Chang PJ, Chau VQ, Hoke NN, Kraskauskas D, Kasper M, Salloum FN, Voelkel NF. Adrenergic receptor blockade reverses right heart remodeling and dysfunction in pulmonary hypertensive rats. *Am J Resp Crit Care Med* 2010;**182**:652–660.
 63. Provencher S, Herve P, Jais X, Lebrec D, Humbert M, Simonneau G, Sitbon O. Deleterious effects of beta-blockers on exercise capacity and hemodynamics in patients with portopulmonary hypertension. *Gastroenterology* 2006;**130**:120–126.
 64. Peacock A, Ross K. Pulmonary hypertension: a contraindication to the use of beta-adrenoceptor blocking agents. *Thorax* 2010;**65**:454–455.
 65. So PP-S, Davies RA, Chandy G, Stewart D, Beanlands RSB, Haddad H, Pugliese C, Mielniczuk LM. Usefulness of beta-blocker therapy and outcomes in patients with pulmonary arterial hypertension. *Am J Cardiol* 2012;**109**:1504–1509.
 66. Bandyopadhyay D, Bajaj NS, Zein J, Minai OA, Dweik RA. Outcomes of β -blocker use in pulmonary arterial hypertension: a propensity-matched analysis. *Eur Resp J* 2015;**46**:750–760.
 67. van Campen JSJA, de Boer K, van de Veerdonk MC, van der Bruggen CEE, Allaart CP, Raijmakers PG, Heymans MW, Marcus JT, Harms HJ, Handoko ML, de Man FS, Vonk-Noordegraaf A, Bogaard H-J. Bisoprolol in idiopathic pulmonary arterial hypertension: an explorative study. *Eur Resp J* 2016;**48**:787–796.
 68. Grinnan D, Bogaard H-J, Grizzard J, Van Tassell B, Abbate A, DeWilde C, Priday A, Voelkel NF. Treatment of group I pulmonary arterial hypertension with carvedilol is safe. *Am J Resp Crit Care Med* 2014;**189**:1562–1564.
 69. Minai OA, Gudavalli R, Mummadi S, Liu X, McCarthy K, Dweik RA. Heart Rate Recovery Predicts Clinical Worsening in Patients with Pulmonary Arterial Hypertension. *Am J Resp Crit Care Med* 2012;**185**:400–408.
 70. Ramos RP, Arakaki JSO, Barbosa P, Treptow E, Valois FM, Ferreira EVM, Nery LE, Neder JA. Heart rate recovery in pulmonary arterial hypertension: relationship with exercise capacity and prognosis. *Am Heart J* 2012;**163**:580–588.
 71. Durand MT, Becari C, Oliveira M de, do Carmo JM, Aguiar Silva CA, Prado CM, Fazan R, Salgado HC. Pyridostigmine restores cardiac autonomic balance after small myocardial infarction in mice. Gonzalez GE, ed. *PloS one* 2014;**9**:e104476.
 72. Li M. Vagal Nerve Stimulation Markedly Improves Long-Term Survival After Chronic Heart Failure in Rats. *Circulation* 2003;**109**:120–124.
 73. Lатарo RM, Silva CAA, Fazan R, Rossi MA, Prado CM, Godinho RO, Salgado HC. Increase in parasympathetic tone by pyridostigmine prevents ventricular dysfunction during the onset of heart failure. *Am J Physiol Regul, Integr and Comp Physiol* 2013;**305**:R908–R916.
 74. de Man FS, Tu L, Handoko ML, Rain S, Ruiter G,

- François C, Schalij I, Dorfmueller P, Simonneau G, Fadel E, Perros F, Boonstra A, Postmus PE, van der Velden J, Vonk-Noordegraaf A, Humbert M, Eddahibi S, Guignabert C. Dysregulated renin-angiotensin-aldosterone system contributes to pulmonary arterial hypertension. *Am J Resp Crit Care Med* 2012;**186**:780–789.
75. Maron BA, Leopold JA. The role of the renin-angiotensin-aldosterone system in the pathobiology of pulmonary arterial hypertension (2013 Grover Conference series). *Pulm Circ* 2014;**4**:200–210.
 76. da Silva Gonçalves Bós D, Happe C, Schalij I, Pijacka W, Paton JFR, Guignabert C, Tu L, Thuillet R, Bogaard H-J, van Rossum AC, Vonk-Noordegraaf A, de Man FS, Handoko ML. Renal Denervation Reduces Pulmonary Vascular Remodeling and Right Ventricular Diastolic Stiffness in Experimental Pulmonary Hypertension. *JACC: Basic to Translational Science* 2017;**2**:22–35.
 77. McMurray JJV, Adamopoulos S, Anker SD, Auricchio A, Böhm M, Dickstein K, Falk V, Filippatos G, Fonseca C, Gomez Sanchez MA, Jaarsma T, Køber L, Lip GYH, Maggioni AP, Parkhomenko A, Pieske BM, Popescu BA, Rønnevik PK, Rutten FH, Schwitter J, Seferovic P, Stepinska J, Trindade PT, Voors AA, Zannad F, Zeiher A, ESC Committee for Practice Guidelines. ESC Guidelines for the diagnosis and treatment of acute and chronic heart failure 2012: The Task Force for the Diagnosis and Treatment of Acute and Chronic Heart Failure 2012 of the European Society of Cardiology. Developed in collaboration with the Heart Failure Association (HFA) of the ESC. *Eur Heart J* 2012;**33**:1787–1847.
 78. Maron BA, Waxman AB, Opatowsky AR, Gillies H, Blair C, Aghamohammadzadeh R, Loscalzo J, Leopold JA. Effectiveness of spironolactone plus ambrisentan for treatment of pulmonary arterial hypertension (from the [ARIES] study 1 and 2 trials). *Am J Cardiol* 2013;**112**:720–725.
 79. Bogaard HJ, Natarajan R, Henderson SC, Long CS, Kraskauskas D, Smithson L, Ockaili R, McCord JM, Voelkel NF. Chronic pulmonary artery pressure elevation is insufficient to explain right heart failure. *Circulation* 2009;**120**:1951–1960.
 80. Drake JI, Bogaard HJ, Mizuno S, Clifton B, Xie B, Gao Y, Dumur CI, Fawcett P, Voelkel NF, Natarajan R. Molecular signature of a right heart failure program in chronic severe pulmonary hypertension. *Am J Resp Cell Mol Biol* 2011;**45**:1239–1247.
 81. Ruiter G, Ying Wong Y, de Man FS, Louis Handoko M, Jaspers RT, Postmus PE, Westerhof N, Niessen HWM, van der Laarse WJ, Vonk-Noordegraaf A. Right ventricular oxygen supply parameters are decreased in human and experimental pulmonary hypertension. *J Heart Lung Transplant* 2013;**32**:231–240.
 82. van Wolferen SA, van de Veerdonk MC, Mauritz G-J, Jacobs W, Marcus JT, Marques KMJ, Bronzwaer JGF, Heymans MW, Boonstra A, Postmus PE, Westerhof N, Vonk-Noordegraaf A. Clinically Significant Change in Stroke Volume in Pulmonary Hypertension. *Chest* 2011;**139**:1003–1009.
 83. Handoko ML, de Man FS, Happé CM, Schalij I, Musters RJP, Westerhof N, Postmus PE, Paulus WJ, van der Laarse WJ, Vonk-Noordegraaf A. Opposite effects of training in rats with stable and progressive pulmonary hypertension. *Circulation* 2009;**120**:42–49.
 84. Gomez-Arroyo J, Mizuno S, Szczepanek K, Van Tassell B, Natarajan R, Remedios Dos CG, Drake JI, Farkas L, Kraskauskas D, Wijesinghe DS, Chalfant CE, Bigbee J, Abbate A, Lesnefsky EJ, Bogaard HJ, Voelkel NF. Metabolic gene remodeling and mitochondrial dysfunction in failing right ventricular hypertrophy secondary to pulmonary arterial hypertension. *Circ Heart Fail* 2013;**6**:136–144.
 85. Noly P-E, Haddad F, Ataam JA, Langer N, Dorfmueller P, Loisel F, Guilhaire J, Decante B, Lamrani L, Fadel E, Mercier O. The importance of Capillary Density/Stroke Work Mismatch for Right Ventricular adaptation to Chronic Pressure Overload. *J Thoracic Cardiovasc Surg* 2017: in press.
 86. van Wolferen SA, Marcus JT, Westerhof N, Spreeuwenberg MD, Marques KMJ, Bronzwaer JGF, Henkens IR, Gan CTJ, Boonstra A, Postmus PE, Vonk-Noordegraaf A. Right coronary artery flow impairment in patients with pulmonary hypertension. *Eur Heart J* 2007;**29**:120–127.
 87. Brooks H, Kirk ES, Vokonas PS, Urschel CW, Sonnenblick EH. Performance of the right ventricle under stress: relation to right coronary flow. *J Clin Invest* 1971;**50**:2176–2183.
 88. Murray PA, Baig H, Fishbein MC, Vatner SF. Effects of experimental right ventricular hypertrophy on myocardial blood flow in conscious dogs. *J Clin Invest* 1979;**64**:421–427.
 89. Huo Y, Linares CO, Kassab GS. Capillary Perfusion and Wall Shear Stress Are Restored in the Coronary Circulation of Hypertrophic Right Ventricle. *Circ Res* 2007;**100**:273–283.
 90. Olivetti G, Lagrasta C, Ricci R, Sonnenblick EH, Capasso

- JM, Anversa P. Long-term pressure-induced cardiac hypertrophy: capillary and mast cell proliferation. *Am J Physiol* 1989;**257**:H1766–H1772.
91. Stenmark KR, Meyrick B, Galie N, Mooi WJ, McMurtry IF. Animal models of pulmonary arterial hypertension: the hope for etiological discovery and pharmacological cure. *Am J Physiol Lung Cell Mol Physiol* 2009;**297**:L1013–L1032.
 92. Tilemann L, Ishikawa K, Weber T, Hajjar RJ. Gene therapy for heart failure. *Circ Res* 2012;**110**:777–793.
 93. Brooksby IAB, Coltart DJ, Jenkins BS, Webb-Peploe MM, Davies MJ. LEFT-VENTRICULAR ENDOMYOCARDIAL BIOPSY. *Lancet* 1974;**304**:1222–1225.
 94. Lowes BD, Minobe W, Abraham WT, Rizeq MN, Bohlmeier TJ, Quaife RA, Roden RL, Dutcher DL, Robertson AD, Voelkel NF, Badesch DB, Groves BM, Gilbert EM, Bristow MR. Changes in gene expression in the intact human heart. Downregulation of alpha-myosin heavy chain in hypertrophied, failing ventricular myocardium. *J Clin Invest* 1997;**100**:2315–2324.
 95. Ruiter G, van de Veerdonk MC, Bogaard H-J, Wong YY, Marcus JT, Lammertsma AA, Westerhof N, van der Laarse WJ, de Man FS, Vonk-Noordegraaf A. The interventricular septum in pulmonary hypertension does not show features of right ventricular failure. *Int J Cardiol* 2014;**173**:509–512.
 96. Hurdman J, Condliffe R, Elliot CA, Davies C, Hill C, Wild JM, Capener D, Sephton P, Hamilton N, Armstrong IJ, Billings C, Lawrie A, Sabroe I, Akil M, O'Toole L, Kiely DG. ASPIRE registry: assessing the Spectrum of Pulmonary hypertension Identified at a REferral centre. *Eur Resp J* 2012;**39**:945–955.
 97. Tedford RJ, Mudd JO, Girgis RE, Mathai SC, Zaiman AL, Houston-Harris T, Boyce D, Kelemen BW, Bacher AC, Shah AA, Hummers LK, Wigley FM, Russell SD, Saggat R, Saggat R, Maughan WL, Hassoun PM, Kass DA. Right Ventricular Dysfunction in Systemic Sclerosis–Associated Pulmonary Arterial Hypertension Clinical Perspective. *Circ Heart Fail* 2013;**6**:953–963.
 98. Giusca S, Popa E, Amzulescu MS, Ghiorgiu I, Coman IM, Popescu BA, Delcroix M, Voigt J-U, Ginhina C, Jurcut R. Is Right Ventricular Remodeling in Pulmonary Hypertension Dependent on Etiology? An Echocardiographic Study. *Echocardiography* 2016;**33**:546–554.
 99. Task Force for Diagnosis, ESC TOPHOESOC, European Respiratory Society (ERS), International Society of Heart, ISHLT LT, Galie N, Hoeper MM, Humbert M, Torbicki A, Vachiery JL, Barbera JA, Beghetti M, Corris P, Gaine S, Gibbs JS, Gomez-Sanchez MA, Jondeau G, Klepetko W, Opitz C, Peacock A, Rubin L, Zellweger M, Simonneau G. Guidelines for the diagnosis and treatment of pulmonary hypertension. *Eur Resp J* 2009;**34**:1219–1263.
 100. Humbert M, Sitbon O, Chaouat A, Bertocchi M, Habib G, Gressin V, Yaïci A, Weitzenblum E, Cordier J-F, Chabot F, Dromer C, Pison C, Reynaud-Gaubert M, Haloun A, Laurent M, Hachulla E, Cottin V, Degano B, Jais X, Montani D, Souza R, Simonneau G. Survival in patients with idiopathic, familial, and anorexigen-associated pulmonary arterial hypertension in the modern management era. *Circulation* 2010;**122**:156–163.
 101. Maron BA. Independence Day. *Circulation* 2016;**133**:2345–2347.
 102. Hopkins WE. Severe pulmonary hypertension in congenital heart disease: a review of Eisenmenger syndrome. *Curr Opin Cardiol* 1995;**10**:517–523.
 103. Hopkins WE. The remarkable right ventricle of patients with Eisenmenger syndrome. *Coronary artery disease* 2005;**16**:19–25.
 104. Hopkins WE, Waggoner AD. Severe pulmonary hypertension without right ventricular failure: the unique hearts of patients with Eisenmenger syndrome. *Am J Cardiol* 2002;**89**:34–38.
 105. Hsu S, Houston BA, Tampakakis E, Bacher AC, Rhodes PS, Mathai SC, Damico RL, Kolb TM, Hummers LK, Shah AA, McMahan Z, Corona-Villalobos CP, Zimmerman SL, Wigley FM, Hassoun PM, Kass DA, Tedford RJ. Right Ventricular Functional Reserve in Pulmonary Arterial Hypertension. *Circulation* 2016;**133**:2413–2422.
 106. Ramjug S, Hussain N, Hurdman J, Billings C, Charamopoulos A, Elliot CA, Kiely DG, Sabroe I, Rajaram S, Swift AJ, Condliffe R. Idiopathic and Systemic Sclerosis associated Pulmonary Arterial Hypertension: A Comparison of Demographic, Haemodynamic and Magnetic Resonance Imaging Characteristics and Outcomes. *Chest* 2017:in press.
 107. Olsson KM, Wiedenroth CB, Kamp J-C, Breithecker A, Fuge J, Krombach GA, Haas M, Hamm C, Kramm T, Guth S, Ghofrani H-A, Hinrichs JB, Cebotari S, Meyer K, Hoeper MM, Mayer E, Liebetrau C, Meyer BC. Balloon pulmonary angioplasty for inoperable patients with chronic thromboembolic pulmonary hypertension: the initial German experience. *Eur Resp J* 2017;**49**:in press.

108. Brimioulle S, Wauthy P, Ewalenko P, Rondelet B, Vermeulen F, Kerbaul F, Naeije R. Single-beat estimation of right ventricular end-systolic pressure-volume relationship. *Am J Physiol Heart Circ Physiol* 2003;**284**:H1625–H1630.
109. Trip P, Kind T, van de Veerdonk MC, Marcus JT, de Man FS, Westerhof N, Vonk-Noordegraaf A. Accurate assessment of load-independent right ventricular systolic function in patients with pulmonary hypertension. *J Heart Lung Transplant* 2013;**32**:50–55.
110. Spruijt OA, de Man FS, Groepenhoff H, Oosterveer F, Westerhof N, Vonk-Noordegraaf A, Bogaard H-J. The effects of exercise on right ventricular contractility and right ventricular-arterial coupling in pulmonary hypertension. *Am J Resp Crit Care Med* 2015;**191**:1050–1057.
111. Vanderpool RR, Pinsky MR, Naeije R, Deible C, Kosaraju V, Bunner C, Mathier MA, Lacomis J, Champion HC, Simon MA. RV-pulmonary arterial coupling predicts outcome in patients referred for pulmonary hypertension. *Heart* 2014;**101**:37–43.
112. Gerges M, Gerges C, Pistrutto A-M, Lang MB, Trip P, Jakowitsch J, Binder T, Lang IM. Pulmonary Hypertension in Heart Failure. Epidemiology, Right Ventricular Function, and Survival. *Am J Resp Crit Care Med* 2015;**192**:1234–1246.
113. Overbeek MJ, Lankhaar J-W, Westerhof N, Voskuyl AE, Boonstra A, Bronzwaer JGF, Marques KMJ, Smit EF, Dijkmans BAC, Vonk-Noordegraaf A. Right ventricular contractility in systemic sclerosis-associated and idiopathic pulmonary arterial hypertension. *Eur Resp J* 2008;**31**:1160–1166.
114. Liu S, Li Y, Kim S, Fu Q, Parikh D, Sridhar B, Shi Q, Zhang X, Guan Y, Chen X, Xiang YK. Phosphodiesterases coordinate cAMP propagation induced by two stimulatory G protein-coupled receptors in hearts. *Proc Natl Acad Sci U S A* 2012;**109**:6578–6583.
115. Spruijt OA, Vissers L, Bogaard H-J, Hofman MBM, Vonk-Noordegraaf A, Marcus JT. Increased native T1-values at the interventricular insertion regions in precapillary pulmonary hypertension. *Int J Cardiovasc Imaging* 2016;**32**:451–459.
116. Blyth KG, Groenning BA, Martin TN, Foster JE, Mark PB, Dargie HJ, Peacock AJ. Contrast enhanced-cardiovascular magnetic resonance imaging in patients with pulmonary hypertension. *Eur Heart J* 2005;**26**:1993–1999.
117. McCann GP. Delayed contrast-enhanced magnetic resonance imaging in pulmonary arterial hypertension. *Circulation* 2005;**112**:e268–e268.
118. McCann GP, Gan CT, Beek AM, Niessen HWM, Noordegraaf AV, van Rossum AC. Extent of MRI Delayed Enhancement of Myocardial Mass Is Related to Right Ventricular Dysfunction in Pulmonary Artery Hypertension. *Am J Roentgenology* 2007;**188**:349–355.
119. Sanz J, Dellegrottaglie S, Kariisa M, Sulica R, Poon M, O'Donnell TP, Mehta D, Fuster V, Rajagopalan S. Prevalence and correlates of septal delayed contrast enhancement in patients with pulmonary hypertension. *Am J Cardiol* 2007;**100**:731–735.
120. Overbeek MJ, Mouchaers KTB, Niessen HM, Hadi AM, Kupreishvili K, Boonstra A, Voskuyl AE, Belien JAM, Smit EF, Dijkmans BC, Vonk-Noordegraaf A, Grunberg K. Characteristics of interstitial fibrosis and inflammatory cell infiltration in right ventricles of systemic sclerosis-associated pulmonary arterial hypertension. *Int J Rheumatol* 2010;**2010**:1–10.
121. Gomez-Arroyo J, Santos-Martinez LE, Aranda A, Pulido T, Beltran M, Muñoz-Castellanos L, Dominguez-Cano E, Sonnino C, Voelkel NF, Sandoval J. Differences in Right Ventricular Remodeling Secondary to Pressure Overload in Patients with Pulmonary Hypertension. *Am J Resp Crit Care Med* 2014;**189**:603–606.
122. Rain S, Andersen S, Najafi A, Gammelgaard Schultz J, da Silva Gonçalves Bós D, Handoko ML, Bogaard H-J, Vonk-Noordegraaf A, Andersen A, van der Velden J, Ottenheim CAC, de Man FS. Right Ventricular Myocardial Stiffness in Experimental Pulmonary Arterial Hypertension: Relative Contribution of Fibrosis and Myofibril Stiffness. *Circ Heart Fail* 2016;**9**:e002636.
123. Kapadia SR, Oral H, Lee J, Nakano M, Taffet GE, Mann DL. Hemodynamic Regulation of Tumor Necrosis Factor- α Gene and Protein Expression in Adult Feline Myocardium. *Circ Res* 1997;**81**:187–195.
124. Sun M, Chen M, Dawood F, Zurawska U, Li JY, Parker T, Kassiri Z, Kirshenbaum LA, Arnold M, Khokha R, Liu PP. Tumor necrosis factor-alpha mediates cardiac remodeling and ventricular dysfunction after pressure overload state. *Circulation* 2007;**115**:1398–1407.
125. Bissell L-A, Md Yusof MY, Buch MH. Primary myocardial disease in scleroderma—a comprehensive review of the literature to inform the UK Systemic Sclerosis Study Group cardiac working group. *Rheumatology* 2016;**kew364**.
126. Joseph P, Tawakol A. Imaging atherosclerosis with positron emission tomography. *Eur Heart J* 2016;**37**:2974–2980.

127. de Haas HJ, Arbustini E, Fuster V, Kramer CM, Narula J. Molecular imaging of the cardiac extracellular matrix. *Circ Res* 2014;**114**:903–915.
128. Merlet P, Delforge J, Syrota A, Angevin E, Mazière B, Crouzel C, Valette H, Loisançe D, Castaigne A, Randé JL. Positron emission tomography with ¹¹C CGP-12177 to assess beta-adrenergic receptor concentration in idiopathic dilated cardiomyopathy. *Circulation* 1993;**87**:1169–1178.
129. Houston BA, Tedford RJ. Putting 'at rest' evaluations of the right ventricle to rest: Insights Gained from evaluation of the Right Ventricle During Exercise in CTPEH patients with and without pulmonary endarterectomy. *J Am Heart Assoc*; 2015;**4**:e001895
130. Claessen G, La Gerche A, Dymarkowski S, Claus P, Delcroix M, Heidbuchel H. Pulmonary vascular and right ventricular reserve in patients with normalized resting hemodynamics after pulmonary endarterectomy. *J Am Heart Assoc*; 2015;**4**:e001602

PART II

NOVEL INSIGHTS IN (ASSESSING) TREATMENT
RESPONSE IN PULMONARY ARTERIAL
HYPERTENSION

6

THE VALUE OF HEMODYNAMIC MEASUREMENTS OR CARDIAC MAGNETIC RESONANCE IMAGING IN THE FOLLOW-UP OF PATIENTS WITH PULMONARY ARTERIAL HYPERTENSION

CE van der Bruggen, ML Handoko, HJ Bogaard, JT Marcus, FPT Oosterveer, LJ
Meijboom, BE Westerhof, A Vonk Noordegraaf,
FS de Man

CHEST, 2020

ABSTRACT

Background: Management of Pulmonary Arterial Hypertension (PAH) patients is conventionally based on functional plus invasive measurements obtained during right heart catheterization (RHC). Whether risk-assessment during repeated measurements could also be performed using imaging parameters is unclear, as a direct comparison of strategies is lacking.

Research question: How do the predictive value of non-invasive parameters compare with invasive hemodynamic measurements at 1 year after the diagnosis of iPAH?

Study Design & Methods: 118 iPAH-patients who underwent RHC and cardiac magnetic resonance imaging (CMR) were included in this study (median time between baseline evaluation and first parameter measures: 1.0[0.8-1.2] years). 44 patients died or received a lung transplantation. Forward cox-regression analyses were used to determine the best predictive functional, hemodynamic and/or imaging model. Patients were classified as high-risk if the event occurred <5 years after diagnosis (n=24), whereas patients without event were classified as low-risk.

Results: A prognostic model that was based on age, sex and absolute values at follow-up of functional parameters (6-minute walk distance) performed well (Akaike information criterion (AIC): 279, concordance: 0.67). Predictive models with only hemodynamic (right atrial pressure, mixed venous oxygen saturation; AIC: 322, concordance: 0.68) or imaging parameters (right ventricular ejection fraction; AIC: 331, concordance: 0.63) at 1 year of follow up performed similar. The predictive value improved when functional data was combined with either hemodynamic data (AIC: 268, concordance: 0.69) or imaging data (AIC: 273, concordance 0.70). A model comprised of functional, hemodynamic and imaging data performed only marginally better (AIC: 266, concordance: 0.69). Finally, changes between baseline and 1 year follow up were observed for multiple hemodynamic and CMR-parameters, only a change in CMR-parameters was of prognostic predictive value.

Interpretation: Risk-assessment at 1-year of follow-up based on CMR is at least equal to risk-assessment based on RHC. In this study, only changes in CMR- but not hemodynamic parameters are of prognostic predictive value during the first-year of follow-up.

INTRODUCTION

Pulmonary arterial hypertension (PAH) is a progressive condition, characterized by extensive pulmonary vascular remodeling, resulting in an ongoing rise in right ventricular (RV) pressure overload.¹ To secure RV systolic function and thus oxygen supply to all organs, the right ventricle adapts via several compensatory mechanisms. However, ultimately these are insufficient and progression to RV dysfunction and failure remains inevitable, with a grim prognosis as a result.²

According to the guidelines, a right heart catheterization (RHC) is recommended to support the diagnosis of PAH. In addition, RHC should be considered to guide treatment decisions including adjustments in treatment regimen and/or referral to a transplantation center (IIa recommendation).³ However, whether hemodynamic assessment during follow-up is preferred above non-invasive monitoring is currently unclear.

A risk-stratification algorithm has been published in the ERS/ESC guidelines and has been validated by several groups.⁴⁻⁶ In addition, recent studies of Weatherald et al.⁷ and Chin et al.⁸ have demonstrated that after 4-months of follow-up, right atrial pressure (RAP), stroke volume index (RHC-SVi) and serum levels of N-terminal pro brain natriuretic peptide (NT-proBNP) are independently associated with death or lung-transplantation and are therefore important parameters to determine treatment response in PAH-patients.

Notwithstanding the unquestionable predictive value of invasive hemodynamic assessment, several studies have shown that non-invasive imaging by cardiac magnetic resonance imaging (CMR) has also great predictive value at baseline.^{7, 9-13} The non-invasive character of CMR may enable easier routine follow-up of PAH-patients, as it is more patient-friendly and carries minimal patient risks. As in our institute functional, hemodynamic and imaging assessment is routinely combined during follow-up, we have a unique cohort to compare the predictive value of the different modalities of monitoring of idiopathic PAH-patients. Therefore, the aim of this study was to compare the predictive value of CMR parameters with invasive hemodynamic measurements at 1-year follow-up.

METHODS

Study objects

We retrospectively evaluated all idiopathic and hereditary PAH (iPAH)-patients seen between March 2000 and September 2018 at the Amsterdam University Medical Center, location VU University Medical Center, The Netherlands (a tertiary referral center for PAH). A diagnosis of idiopathic or hereditary PAH was made by a multidisciplinary pulmonary hypertension team after extensive clinical evaluation according to the ERS/ESC guidelines in the relevant time-period.³ Since the repeated functional, hemodynamic and imaging measurements were performed for clinical purposes, this study did not fall within the scope of the Medical

Research Involving Human Subjects Act (confirmed by the Medical Ethics Review Committee of the VU University Medical Center, 2012.288).

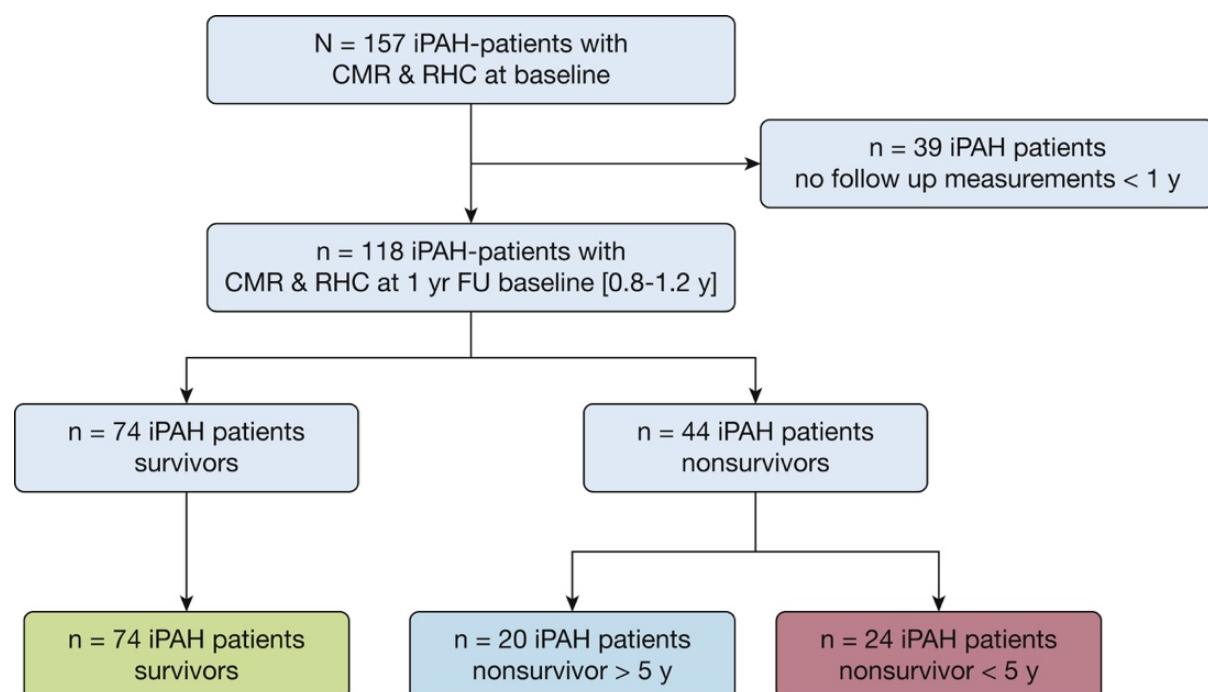
Functional assessment

Functional assessment of the patients was performed by 6-minute walk distance (6MWD), New York Heart Association (NYHA) classification and NT-proBNP.

Hemodynamic assessment by right heart catheterization

RHC was performed using a balloon-tipped, flow directed 7.5F triple lumen Swan-Ganz catheter (Edwards Lifesciences LLC, Irvine, CA, USA). Cardiac output (CO) was measured by either the Fick method or thermodilution (23% direct Fick, 4% indirect Fick and 73% thermodilution). Pulmonary vascular resistance (PVR) was calculated as: $PVR = (mPAP - PAWP) / CO$, where mPAP is mean pulmonary arterial pressure and PAWP is pulmonary arterial wedge pressure.

Figure 6.1 – Flow chart of patient selection



In total 157 iPAH-patients were identified that had CMR and RHC assessment at baseline. In 39 patients, no follow-up analyses including both CMR and RHC were available. Median follow-up time was 1 year with an interquartile range between 0.8-1.2 years. Of the 118 patients with follow-up measurements, 2 patients were excluded because from 1 patient no baseline data was available and 1 patient was misclassified as iPAH. In total, 44 patients died or had a lung transplantation (24 patients had an event within 5 years after diagnosis, 20 patients had an event later than 5 years after diagnoses). Patients without events were defined as survivors.

Imaging by cardiac magnetic resonance imaging

CMR was performed on a 1.5T Avanto or Sonata scanner equipped with a 6-element phased array coil (Siemens Medical Solutions, Erlangen, Germany). Image acquisition and post-processing were performed as described previously.^{14, 15} RV ejection fraction (RVEF) was calculated according to the following formula: $RVEF = (RVEDV - RVESV) / RVEDV * 100\%$, where RVESV is RV end-systolic volume, and RVEDV is RV end-diastolic volume. In line with Mauritz et al., stroke volume was calculated by using left ventricular volumes (left ventricular end-diastolic volume (LVEDV) minus left ventricular end-systolic volume (LVESV)).¹⁶

Statistical analysis

Data are presented as mean \pm standard deviation or median [interquartile range] depending on distribution. Categorical variables are presented as absolute numbers and relative frequencies (percentage). No further analyses were computed on the missing data, neither data imputation was executed.

Average and median values of general characteristics of patients at baseline were calculated with R package tableone (<https://CRAN.R-project.org/package=tableone>). Individual baseline and follow-up graphs were constructed using R package ggpubr (<https://CRAN.R-project.org/package=ggpubr>). Differences between baseline and follow-up were tested by paired t-test for continuous variables and McNemar's test for categorical variables, with correction for multiple comparisons by Bonferroni.

The predictive value of functional, hemodynamic and imaging parameters was tested by univariate and multivariate cox regression analyses using R package survival (<https://CRAN.R-project.org/package=survival>). Forward cox-regression modeling was used to determine the best predictive functional, hemodynamic or imaging model using a $p < 0.1$ as cut-off to be included to the final model. To compare the predictive value of the different models, the concordance (c-statistics) and Akaike information criteria (AIC) are provided. The Akaike information criterion provides a relative measure of the quality of the model and estimates the information lost by the number of parameters in the models and the strength of the predictive value. A low number means less information lost and could be interpreted as a better model. The concordance or C-statistics provides measure of goodness-of-fit in survival models. A higher concordance value means that the model gives a better prediction for survival. Pairwise comparisons were performed and corrected for multiple comparison with Bonferroni correction. All graphs were generated with ggplot2.

All tests were two-sided and a $p < 0.05$ was considered significant. Statistical analyses were performed using R studio (Version 1.1.463 – © 2009-2018 RStudio, Inc., Boston, MA).

RESULTS

Baseline characteristics

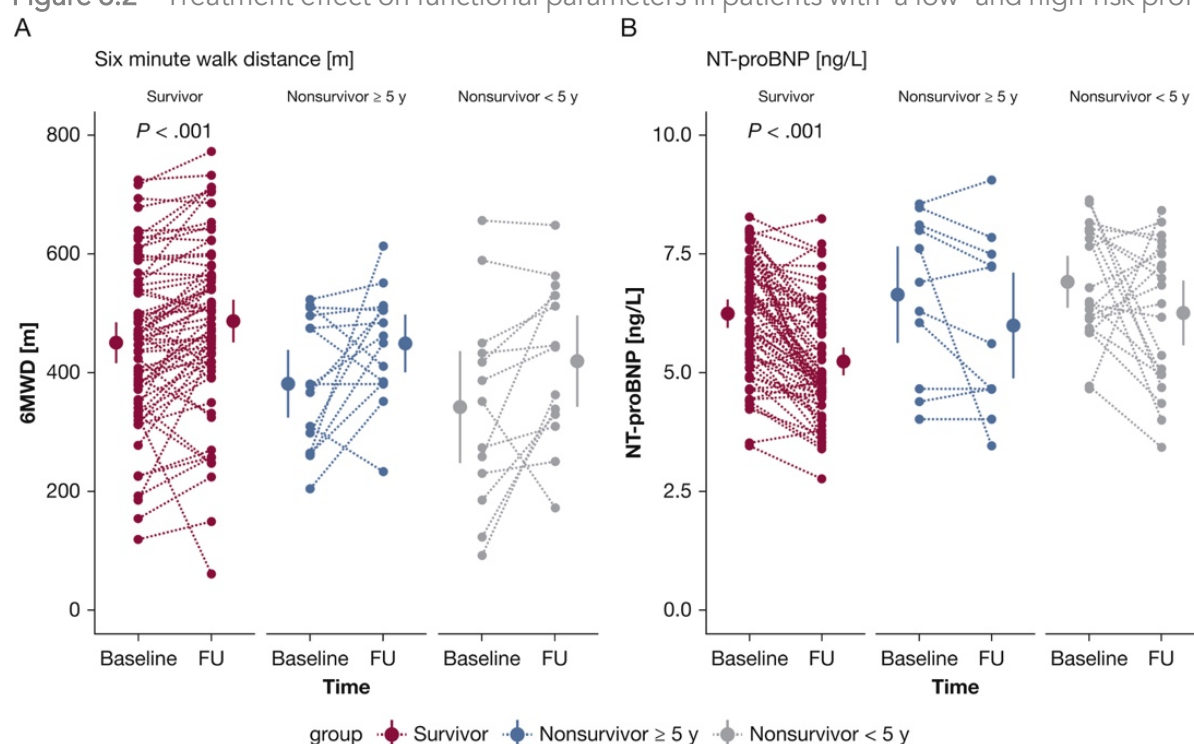
In total 118 patients with As can be observed in Figure 1, baseline CMR and RHC data was available for 157 iPAH-patients (Figure 1). In 39 iPAH-patients, no complete follow-up with CMR and RHC was available and we therefore excluded these patients. In total, 118 patients with functional, hemodynamic and imaging assessment at baseline and follow-up were included in this study with a median time between the baseline measurement and the following complete CMR+RHC measurement of 1.0 year and interquartile range of 0.8-1.2 years.

Sixty-three percent of the patients classified as survivor, whereas in 37% an event (death or lung transplantation) had occurred. In 24 patients this event occurred <5 years after diagnosis. These patients were classified as high-risk patients, whereas patients classified as survivors were considered as low-risk patients (Figure 6.1).

General characteristics of the patients are presented in Table 6.1. The study population was 49 ± 17 years old and consisted predominantly of females (69%). Most patients were in NYHA functional class II and III. In 52 out of 118 patients (44%) monotherapy was the initial treatment strategy of choice. Combination therapy or triple therapy was initiated in respectively 51% and 5% of the study population.

Patients presented with a mPAP of 54 ± 14 mmHg, mixed venous oxygen saturation (SvO₂) of 64 ± 8 %, mRAP of 8 ± 5 mmHg, NT-proBNP of 657[246-1999] ng/L and a RVEF of 36 ± 12 %. The first follow-up was performed after a median time of 1.0 [0.8-1.2] years.

Figure 6.2 – Treatment effect on functional parameters in patients with a low- and high-risk profile



A significant improvement in 6-minute walk distance (A) and NT-proBNP (B) is only observed in patients with a low risk (survivors). Non-survivor patients with short survival time (<5 years) are classified as high-risk patients, whereas survivor patients with follow-up data > 5 years after diagnosis were classified as low-risk patients. All p-values are corrected for multiple comparison by Bonferroni. Abbreviations: 6MWD, 6-minute walk distance; FU, follow-up.

The predictive value of functional, hemodynamic and imaging parameters

In order to determine the individual predictive value of functional, hemodynamic and imaging parameters in our cohort, univariate Cox-regression was performed. At follow-up, all variables except age were associated with the risk of death or lung transplantation (Table 6.2).

A multivariate Cox-regression analysis was performed to compare the additional value of CMR parameters. First, we determined the best functional model, by using Cox-regression analyses with age, sex, 6MWD, NYHA functional class and NT-proBNP. A model only with age, sex and 6MWD reached statistical significance with an AIC of 279 and a concordance index of 0.67 (Table 6.3, Supplemental Figure 6.2).

Subsequently, we determined the predictive value of hemodynamic prognostic model using forward cox-regression analyses with all hemodynamic parameters in addition to age and sex. Although the parameters individually all reached a significant predictive value, the forward cox-regression model resulted in a model containing age, sex, SvO₂ and mRAP.

In a similar analysis for the CMR-derived right ventricular parameters, the forward cox-regression analyses resulted in a model containing age, sex and RVEF.

The predictive value of the models with only hemodynamic or CMR parameters was comparable. (Table 6.3). The combination of hemodynamic or CMR parameters with functional measurements provided the best predictive value. Combining all three modalities did result in a trivial improvement in quality of the prognostication (Supplemental figure 6.1). These analyses suggest that during follow-up, functional assessment in combination with either hemodynamic or imaging provides the best prognostic information.

Change in CMR parameters discriminate between high- and low-risk patients

To determine whether a *change* between baseline measurements and measurements after 1 year would provide further information on the clinical status of the patients, we assessed the discriminative value of the change in functional, hemodynamic and imaging parameters to identify low- and high-risk patients (Table 6.4). High-risk patients were defined as patients having an event within 5 years after diagnosis. Low-risk patients had no event during >5 years of follow-up. Treatment and comorbidities in the distinctive groups can be observed in the supplemental material (Table S6.1 and S6.2).

Table 6.1 – Patient characteristics at baseline

Variable	Patients
<i>General characteristics</i>	
Number of patients	118
Age (years)	49 ± 17
Female sex, n (%)	81 (69)
Body mass index	26 ± 4.9
follow-up time (years)	5.5 [3-8]
<i>NYHA (N=106), n(%)</i>	
I	8 (7)
II	40 (35)
III	58 (51)
IV	7 (6)
<i>Treatments during follow-up</i>	
Mono, n (%)	52 (44)
Duo, n (%)	60 (51)
Triple, n (%)	6 (5)
Calcium antagonists, n (%)	10 (8)
Endothelin antagonists, n (%)	84 (71)
PDE5 inhibitors, n (%)	76 (64)
Prostacyclin analogue, n (%)	18 (15)
<i>Events</i>	
No event > 5 years, n(%)	42 (36)
No event < 5 years, n (%)	32 (27)
Event > 5 years, n (%)	20 (17)
Event < 5 years, n (%)	24 (20)

Data presented as mean ± SD or median [IQR] when data is not normally distributed. Abbreviations: NYHA, New York Heart Association; PDE5, phosphodiesterase 5.

Because of the arbitrary nature of the 5-year cut-off, analyses were repeated with a cut-off of an event within 3- and 7-years after diagnosis, as can be observed in the supplemental material (Table S6.3 and S6.4). Hemodynamic parameters showed improvements in all groups at follow-up independent of high or low-risk patients (Figure 6.3). In contrast, 6MWD, NT-proBNP (Figure 6.2) and RV function (Figure 6.4, Supplemental Figure I) only improved in low-risk patients. To further corroborate this finding, we determined the prognostic value of a change in functional, hemodynamic and imaging parameters. Only a change of RVEF was significant associated with survival after correction for possible confounding by sex and age

(HR: 0.96, 95%CI: 0.92-0.99, p=0.005). This suggests that although a patient improves hemodynamically, this does not necessarily translate into improved prognosis.

Table 6.2 – Univariate cox-regression analyses of the functional, hemodynamic and imaging parameters

TABLE 2] Univariate Cox Regression Analyses of Functional, Hemodynamic, and Imaging Parameters

Parameter	Hazard Ratio	95% CI	P Value
Functional			
Age, y	1.02	1.00-1.04	.099
Sex, female vs male	0.41	0.22-0.76	< .001
6-min walk distance (per 10 m)	0.96	0.94-0.99	.002
NT-proBNP, pg/mL	1.20	1.04-1.39	.012
New York Heart Association (class I vs class II)	1.52	0.45-5.11	.500
New York Heart Association (class I vs class III)	5.38	1.55-18.74	.008
Hemodynamic			
RHC: Mean pulmonary artery pressure, mm Hg	1.02	1.00-1.04	.017
RHC: Stroke volume index, mL/m ²	0.96	0.94-0.99	.003
RHC: Right atrial pressure, mm Hg	1.10	1.04-1.17	.002
RHC: Cardiac index, mL/m ²	0.66	0.47-0.94	.020
RHC: Pulmonary vascular resistance index, dyn × s/cm ⁵	1.69	1.10-2.60	.017
RHC: Mixed venous oxygen saturation, %	0.94	0.90-0.97	< .001
RHC: Heart rate, beats/min	1.02	0.99-1.04	.174
Imaging			
CMR: Stroke volume index, mL/m ²	0.95	0.92-0.99	.008
CMR: RV ejection fraction, %	0.96	0.94-0.98	< .001
CMR: RV end-systolic volume index, mL/m ²	1.02	1.01-1.03	< .001
CMR: RV end-diastolic volume index, mL/m ²	1.02	1.00-1.03	.017

For sex, male patients are used as reference. CMR = cardiac MRI; NT-proBNP = N-terminal pro-brain natriuretic peptide; RHC = right heart catheterization.

For sex; males are used as reference. Abbreviations: NT-proBNP, N-terminal pro brain natriuretic peptide; RHC, right heart catheterization; CMR Cardiac Magnetic Resonance.

Table 6.3 – Multivariate cox-regression analyses of function, hemodynamic and imaging parameters

Part I – Functional, hemodynamic and imaging models

	Parameters	Hazards Ratio	95% CI	P-value	AIC	Concordance
Model 1: Functional	Age	1.00	0.98-1.02	0.681	279	0.67
	Sex	0.44	0.22-0.89	0.023		
	6MWD	1.00	0.99-1.00	0.003		
Model 2: Hemodynamic	Age	1.02	1.00-1.04	0.062	322	0.66
	Sex	0.46	0.24-0.89	0.021		
	RHC-RAP	1.08	1.01-1.15	0.024		
	RHC-SvO ₂	0.94	0.90-0.98	0.005		
Model 3: Imaging	Age	1.03	1.01-1.05	0.009	331	0.63
	Sex	0.52	0.27-0.99	0.045		
	CMR-RVEF	0.96	0.93-0.98	<0.001		

Part II – Functional, hemodynamic and imaging models combined

Model 1+2 : Functional + Hemodynamic	Age	1.01	0.98-1.01	0.539	268	0.69
	Sex	0.43	0.21-0.89	0.022		
	6MWD	1.00	0.99-1.00	0.220		
	RHC-RAP	1.05	0.98-1.13	0.180		
	RHC-SvO ₂	0.95	0.90-1.00	0.064		
Model 1+3: Functional + Imaging	Age	1.01	0.99-1.04	0.298	273	0.70
	Sex	0.51	0.25-1.05	0.069		
	6MWD	1.00	0.99-1.00	0.045		
	CMR-RVEF	0.96	0.94-0.99	0.004		
Model 2+3: Hemodynamic + Imaging	Age	1.03	1.01-1.05	0.012	320	0.71
	Sex	0.49	0.26-0.95	0.036		
	RHC-RAP	1.05	0.98-1.12	0.180		
	RHC-SvO ₂	0.96	0.92-1.01	0.102		
	CMR-RVEF	0.97	0.94-1.00	0.040		
Model 1+2+3: Functional + Hemodynamic + Imaging	Age	1.02	0.99-1.04	0.227	266	0.69
	Sex	0.47	0.23-0.98	0.044		
	6MWD	1.00	0.99-1.00	0.220		
	RHC-RAP	1.02	0.95-1.10	0.577		
	RHC-SvO ₂	0.98	0.92-1.04	0.451		
	CMR-RVEF	0.97	0.94-1.00	0.052		

Abbreviations: 6MWD, six minute walk distance; NT-proBNP, N-terminal pro brain natriuretic peptide; NYHA, New York Heart Association; RHC, right heart catheterization; SVi, stroke volume index; RAP, right atrial pressure; CI, cardiac index; PVRi, pulmonary vascular resistance indexed; SVO₂, mixed venous oxygen saturation; HR, heart rate; RVEF, right ventricular ejection fraction; RVESVi, right ventricular end-systolic volume indexed; RVEDVi, right ventricular end-diastolic volume indexed; AIC, Akaike information criterion. Sex: male is used as reference, NYHA: NYHA class I is used as reference.

DISCUSSION

In the present study, we compared the predictive value of functional, hemodynamic and imaging parameters one year after the diagnosis of iPAH. We were able to demonstrate that:

- 1) Both invasive RHC and CMR parameters have prognostic value at follow-up.
- 2) The predictive value of follow-up with RHC (RHC-SvO₂ and mRAP) and CMR (RVEF) alone was similar
- 3) The predictive value of a model combining functional parameters with hemodynamic or imaging parameters provided the best predictive model. Combining all three modalities did not provide further prognostic information. The additional value of hemodynamics or imaging parameters to functional parameters was similar.
- 4) With repeated measurements after 1-year follow-up, hemodynamic parameters improved even in non-survivors, whereas RV imaging and functional parameters only improved in survivors. Only a change in RVEF was shown to be of predictive value.

Taking these findings together, we can conclude that follow-up by CMR is at least equal to invasive hemodynamic measurements to discriminate between high- and low-risk PAH-patients, and that combining functional with either hemodynamic or imaging measurements is of additional value during follow-up of PAH-patients.

Predictive value of non-invasive follow-up using CMR

RHC is recommended in the ERS/ESC guidelines at time of diagnosis. In addition, there is a IIa recommendation to perform a RHC to assess of treatment response and in case of clinical deterioration.³ However, as is known from multiple registry studies, not all PAH-institutes perform routine hemodynamic assessment at follow-up. It can be argued that an invasive follow-up strategy is not superior to a non-invasive strategy, as a direct comparison is currently lacking. In this unique study we were able to compare 3 follow-up strategies: 1. Functional: with 6MWD, NT-proBNP NYHA functional class; 2. Hemodynamic: with RHC-obtained data, and 3. Imaging: with CMR-derived data. The best predictive model was obtained by combining functional assessment with imaging and hemodynamic analyses. However, the differences between the models containing functional assessment with imaging or hemodynamics were minimal. This indicates that routine follow-up of iPAH-patients may be performed non-invasively using CMR.

Recent advances with artificial intelligence in cardiovascular imaging may open new opportunities to combine multiple clinical modalities and CMR in the future.¹⁷ Future prospective cohort studies should reveal whether such an approach is beneficial and should be incorporated in the treatment algorithm of PAH.

Table 6.4 – Patients hemodynamics, functional and right ventricular characteristics at baseline and 1 year follow-up stratified on survival time

		Survivor		Non-survivor			
		N=74		≥ 5 years N=20		< 5 years N=24	
		Baseline	FU	Baseline	FU	Baseline	FU
Functional	Age (years)	48 ± 17		47 ± 14		54 ± 20	
	Sex (% female) - *	86		70		54	
	6 MWD (m)	450 ± 17	493 ± 18***	382 ± 28	449 ± 24	345 ± 44	418 ± 36
	NT-proBNP [ng/L]	586 [215-1292]	138 [94-442]****	997 [266-3136]	274 [106-1597]	775 [439-2950]	785 [143-1881]
Hemodynamic	NYHA I/II/III/IV (%)	8/44/46/3	26/67/8/0*	5/35/55/5	10/75/15/0	5/15/70/10	5/35/60/0
	RHC-SVi (ml/m ²)	35 ± 2	47 ± 2****	29 ± 2	31 ± 2	29 ± 2	38 ± 3***
	RAP (mmHg)	7 ± 0.4	5 ± 0.4*	10 ± 1.4	9 ± 1.1	10 ± 1.2	8 ± 1.2
	RHC-CI (L/min/m ²)	2.7 ± 0.1	3.4 ± 0.1****	2.2 ± 0.1	2.5 ± 0.2	2.5 ± 0.2	3.2 ± 0.3**
	RHC-PVRI (WU*m ²)	4.9 ± 0.3	2.7 ± 0.2****	5.7 ± 1.4	3.6 ± 1.0*	6.7 ± 0.8	4.1 ± 0.7***
	RHC-SVO ₂ (%)	67 ± 1	71 ± 1****	61 ± 2	63 ± 2	59 ± 2	65 ± 2*
	RHC-HR (beats/min)	79 ± 2	75 ± 1*	79 ± 4	83 ± 3	89 ± 4	80 ± 3*
Imaging	CMR-SVi (ml/m ²)	30 ± 1	37 ± 1****	26 ± 2	29 ± 2	26 ± 2	30 ± 2
	CMR-RVEF (%)	38 ± 1	49 ± 1****	32 ± 2	33 ± 3	32 ± 2	37 ± 3
	CMR-RVESVi (ml/m ²)	49 ± 2	40 ± 2****	59 ± 5	58 ± 5	55 ± 4	55 ± 5
	CMR-RVEDVi (ml/m ²)	77 ± 2	76 ± 2	85 ± 5	84 ± 5	80 ± 4	84 ± 5

Abbreviations: 6MWD, six minute walk distance; NT-proBNP, N-terminal pro brain natriuretic peptide; NYHA, New York Heart Association; RHC, right heart catheterization; SVi, stroke volume index; RAP, right atrial pressure; CI, cardiac index; PVRI, pulmonary vascular resistance indexed; SVO₂, mixed venous oxygen saturation; HR, heart rate; RVEF, right ventricular ejection fraction;

Changes in invasive and non-invasive assessments after 1-year of follow-up

Non-invasive imaging was performed by CMR, because previous studies have shown that CMR is more sensitive to detect changes in RV function over time than echocardiography.¹⁸ After 1-year of follow-up, no change in RAP and RVEDVi was observed, whereas only patients with a low-risk of mortality (and not in high-risk) showed significant improvements in 6MWD, NTproBNP, CMR-SVi, RVEF and RVESVi. In contrast, improvement in hemodynamic parameters were observed in low-and high-risk patients (non-survivors <5 years). This indicates that patients can still be at high-risk for mortality although their hemodynamic parameters improved.

Right ventricle as a treatment target

The results of this study highlight again the importance of RV adaptation on prognosis of iPAH-patients. All identified predictive markers are closely related to reduced RV function. Unfortunately, to date no specific RV therapies exist.² Current pharmaceutical strategies are not sufficient to normalize RV function.¹⁵ This is confirmed in our study where no improvements in RV volume or RAP could be observed after 1-year of treatment. Recent studies have suggested that when PVR is reduced by >40%, reverse remodeling of the right ventricle may occur.^{19, 20} Future treatment strategies with (upfront) double or triple therapy^{21, 22} may prove to induce early reverse remodeling of the right ventricle and ultimately may improve prognosis of this serious condition. Another possible way to improve prognosis of PAH-patients is identification of novel therapeutic compounds directed to the right ventricle. However, it is difficult to identify proper treatment targets when tissue is only available in end-stage right heart failure or from animal models with important differences in RV physiology when compared to humans.²³

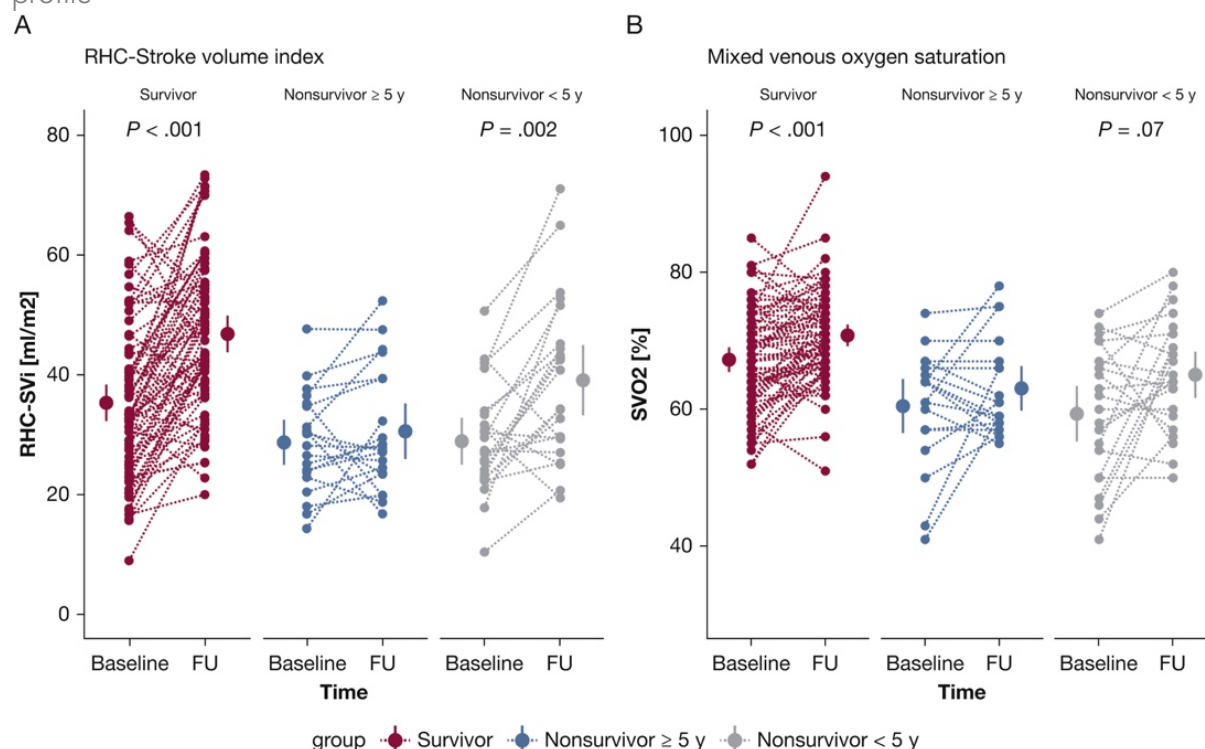
Study limitations

The sample size of this study is relatively small in comparison to earlier studies due to the strict selection criteria. This limited the possibilities to perform multivariate regression analyses including general prognostic markers of PAH. In addition, the relatively small sample size might have led to an overfit of the developed models and are not validated in additional populations.

More importantly, this is the first study in which paired analyses of function, hemodynamic and imaging are performed in a sample size of 118 iPAH-patients with a meaningful follow-up of more than 5 years.

Because prognostic importance was determined after 1-year of follow-up, there may have been a selection bias by not selecting patients that died or received a lung transplantation in the first year after diagnosis. In addition, due to the retrospective nature of this study, we had missing values in hemodynamic and functional parameters.

Figure 6.3 – Treatment effect on hemodynamic parameters in patients with a low- and high-risk profile



Improvements in hemodynamic parameters are observed in both patients with low as well as in patients with high risk of mortality (Table 4). Individual data of stroke volume index (A) and mixed venous oxygen saturation (B) are demonstrated at baseline and after 1 year of follow-up. All *p*-values are corrected for multiple comparison by Bonferroni. Abbreviations: RHC, right heart catheterization; SVi, stroke volume index; SVO₂, mixed venous oxygen saturation

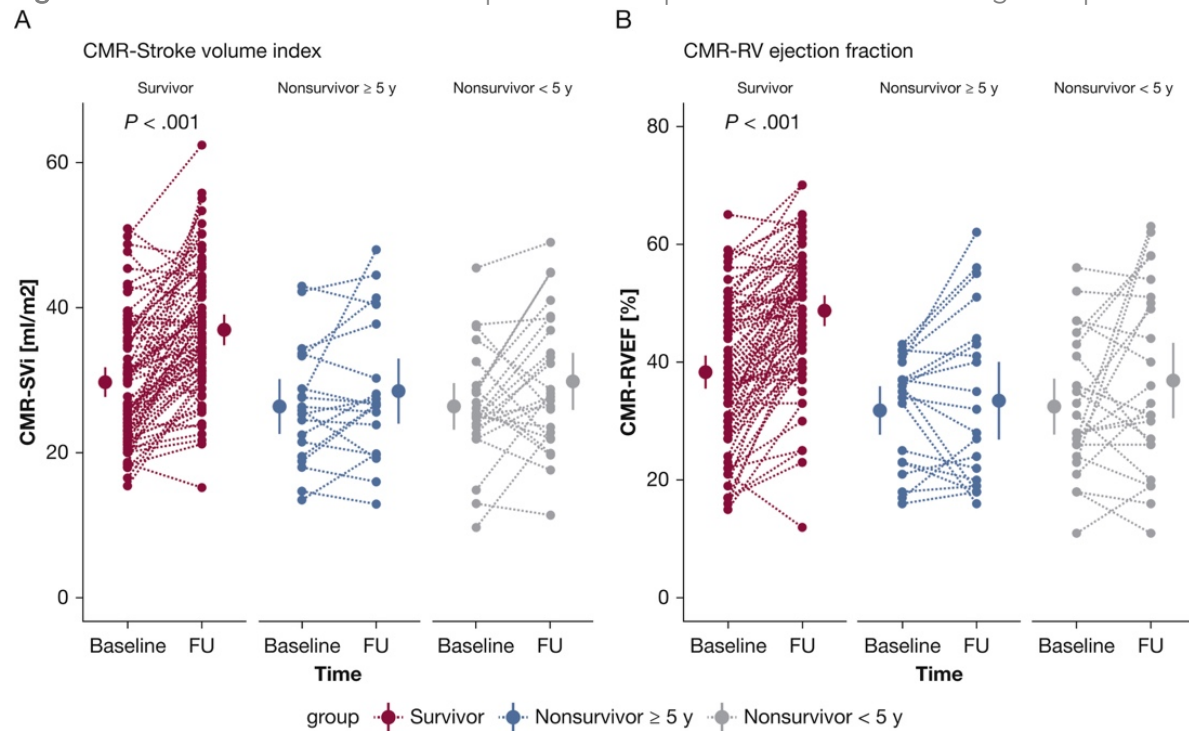
This study was performed in a single center. Although the overall hemodynamic and general characteristics of our iPAH population was comparable with previous published studies by Weatherald et al, our 5 years survival was higher. This may be explained by the difference in mean age between both studies (average age our study: 49 years, average age Weatherald et al.: 64 years). Age has been shown to be a key prognostic indicator in PAH before.⁵ The age difference between the studies can further be explained by the high prevalence of hereditary PAH included in this study (20%), who are on average diagnosed at an earlier age than iPAH-patients.²⁴

The definition of high vs. low risk at 5 years of follow-up is arbitrary. Similar results were obtained when repeating the analyses with a cut-off of 3 and 7 years (Tables S1, S2), which demonstrates the robustness of our analysis.

Interpretation

Risk-assessment based on CMR measurements is at least equal to risk-assessment based on invasive hemodynamic measurements during repeated measurements 1-year after diagnosis.

Figure 6.4 – Treatment effect of CMR parameters in patients with a low- and high-risk profile



Significant improvements in RV function and morphology were only observed in patients with a low risk-profile. Individual data of A. Stroke volume index measured by CMR and B. RV ejection fraction are demonstrated.

REFERENCES

1. Vonk Noordegraaf A, Westerhof BE and Westerhof N. The Relationship Between the Right Ventricle and its Load in Pulmonary Hypertension. *J Am Coll Cardiol*. 2017;69:236-243.
2. van der Bruggen CEE, Tedford RJ, Handoko ML, van der Velden J and de Man FS. RV pressure overload: from hypertrophy to failure. *Cardiovasc Res*. 2017;113:1423-1432.
3. Galie N, Humbert M, Vachiery JL, Gibbs S, Lang I, Torbicki A, Simonneau G, Peacock A, Vonk Noordegraaf A, Beghetti M, Ghofrani A, Gomez Sanchez MA, Hansmann G, Klepetko W, Lancellotti P, Matucci M, McDonagh T, Pierard LA, Trindade PT, Zompatori M, Hoeper M, Aboyans V, Vaz Carneiro A, Achenbach S, Agewall S, Allanore Y, Asteggiano R, Paolo Badano L, Albert Barbera J, Bouvaist H, Bueno H, Byrne RA, Carerj S, Castro G, Erol C, Falk V, Funck-Brentano C, Gorenflo M, Granton J, lung B, Kiely DG, Kirchhof P, Kjellstrom B, Landmesser U, Lekakis J, Lionis C, Lip GY, Orfanos SE, Park MH, Piepoli MF, Ponikowski P, Revel MP, Rigau D, Rosenkranz S, Voller H and Luis Zamorano J. 2015 ESC/ERS Guidelines for the diagnosis and treatment of pulmonary hypertension: The Joint Task Force for the Diagnosis and Treatment of Pulmonary Hypertension of the European Society of Cardiology (ESC) and the European Respiratory Society (ERS): Endorsed by: Association for European Paediatric and Congenital Cardiology (AEPC), International Society for Heart and Lung Transplantation (ISHLT). *Eur Heart J*. 2016;37:67-119.
4. Boucly A, Weatherald J, Savale L, Jais X, Cottin V, Prevot G, Picard F, de Groote P, Jevnikar M, Bergot E, Chaouat A, Chabanne C, Bourdin A, Parent F, Montani D, Simonneau G, Humbert M and Sitbon O. Risk assessment, prognosis and guideline implementation in pulmonary arterial hypertension. *Eur Respir J*. 2017;50.
5. Hoeper MM, Kramer T, Pan Z, Eichstaedt CA, Spiesshoefer J, Benjamin N, Olsson KM, Meyer K, Vizza CD, Vonk-Noordegraaf A, Distler O, Opitz C, Gibbs JSR, Delcroix M, Ghofrani HA, Huscher D, Pittrow D, Rosenkranz S and Grunig E. Mortality in pulmonary arterial hypertension: prediction by the 2015 European pulmonary hypertension guidelines risk stratification model. *Eur Respir J*. 2017;50.
6. Kylhammar D, Kjellstrom B, Hjalmarsson C, Jansson K, Nisell M, Soderberg S, Wikstrom G and Radegran G. A comprehensive risk stratification at early follow-up determines prognosis in pulmonary arterial hypertension. *Eur Heart J*. 2018;39:4175-4181.
7. Weatherald J, Boucly A, Chemla D, Savale L, Peng M, Jevnikar M, Jais X, Taniguchi Y, O'Connell C, Parent F, Sattler C, Herve P, Simonneau G, Montani D, Humbert M, Adir Y and Sitbon O. Prognostic Value of Follow-Up Hemodynamic Variables After Initial Management in Pulmonary Arterial Hypertension. *Circulation*. 2018;137:693-704.
8. Chin KM, Rubin LJ, Channick R, Di Scala L, Gaine S, Galie N, Ghofrani HA, Hoeper MM, Lang IM, McLaughlin VV, Preiss R, Simonneau G, Sitbon O and Tapson VF. Association of N-Terminal Pro Brain Natriuretic Peptide and Long-Term Outcome in Patients With Pulmonary Arterial Hypertension. *Circulation*. 2019;139:2440-2450.
9. D'Alonzo GE, Barst RJ, Ayres SM, Bergofsky EH, Brundage BH, Detre KM, Fishman AP, Goldring RM, Groves BM, Kernis JT and et al. Survival in patients with primary pulmonary hypertension. Results from a national prospective registry. *Ann Intern Med*. 1991;115:343-9.
10. van Wolferen SA, Marcus JT, Boonstra A, Marques KM, Bronzwaer JG, Spreeuwenberg MD, Postmus PE and Vonk-Noordegraaf A. Prognostic value of right ventricular mass, volume, and function in idiopathic pulmonary arterial hypertension. *Eur Heart J*. 2007;28:1250-7.
11. Swift AJ, Capener D, Johns C, Hamilton N, Rothman A, Elliot C, Condliffe R, Charalampopoulos A, Rajaram S, Lawrie A, Campbell MJ, Wild JM and Kiely DG. Magnetic Resonance Imaging in the Prognostic Evaluation of Patients with Pulmonary Arterial Hypertension. *Am J Respir Crit Care Med*. 2017;196:228-239.
12. Courand PY, Pina Jomir G, Khouatra C, Scheiber C, Turquier S, Glerant JC, Mastroianni B, Gentil B, Blanchet-Legens AS, Dib A, Derumeaux G, Humbert M, Mornex JF, Cordier JF and Cottin V. Prognostic value of right ventricular ejection fraction in pulmonary arterial hypertension. *Eur Respir J*. 2015;45:139-49.
13. Swift AJ, Rajaram S, Campbell MJ, Hurdman J, Thomas S, Capener D, Elliot C, Condliffe R, Wild JM and Kiely DG. Prognostic value of cardiovascular magnetic resonance imaging measurements corrected for age and sex in idiopathic pulmonary arterial hypertension. *Circ Cardiovasc Imaging*. 2014;7:100-6.
14. van der Bruggen CE, Happe CM, Dorfmueller P, Trip P, Spruijt OA, Rol N, Hoevenaars FP, Houweling AC, Gierd B, Marcus JT, Mercier O, Humbert M, Handoko ML, van der Velden J, Vonk Noordegraaf A, Bogaard HJ, Goumans MJ and de Man FS. Bone Morphogenetic Protein Receptor Type 2 Mutation in Pulmonary Arterial Hypertension: A View on the Right Ventricle. *Circulation*. 2016;133:1747-60.
15. van de Veerdonk MC, Kind T, Marcus JT, Mauritz GJ, Heymans MW, Bogaard HJ, Boonstra A, Marques KM, Westerhof N and Vonk-Noordegraaf A. Progressive right ventricular dysfunction in patients with pulmonary arterial hypertension responding to therapy. *J Am Coll Cardiol*. 2011;58:2511-9.

16. Mauritz GJ, Marcus JT, Boonstra A, Postmus PE, Westerhof N and Vonk-Noordegraaf A. Non-invasive stroke volume assessment in patients with pulmonary arterial hypertension: left-sided data mandatory. *J Cardiovasc Magn Reson*. 2008;10:51.
17. Swift AJ, Lu H, Uthoff J, Garg P, Coglianò M, Taylor J, Metherall P, Zhou S, Johns CS, Alabed S, Condliffe RA, Lawrie A, Wild JM and Kiely DG. A machine learning cardiac magnetic resonance approach to extract disease features and automate pulmonary arterial hypertension diagnosis. *Eur Heart J Cardiovasc Imaging*. 2020.
18. Spruijt OA, Di Pasqua MC, Bogaard HJ, van der Bruggen CE, Oosterveer F, Marcus JT, Vonk-Noordegraaf A and Handoko ML. Serial assessment of right ventricular systolic function in patients with precapillary pulmonary hypertension using simple echocardiographic parameters: A comparison with cardiac magnetic resonance imaging. *J Cardiol*. 2017;69:182-188.
19. van de Veerdonk MC, Huis in t Veld AE, Marcus JT, Westerhof N, Heymans MW, Bogaard H-J and Vonk-Noordegraaf A. Upfront combination therapy reduces right ventricular volumes in pulmonary arterial hypertension. *European Respiratory Journal*. 2017;In press.
20. Badagliacca R, Poscia R, Pezzuto B, Papa S, Reali M, Pesce F, Manzi G, Gianfrilli D, Ciciarello F, Sciomer S, Biondi-Zoccai G, Torre R, Fedele F and Vizza CD. Prognostic relevance of right heart reverse remodeling in idiopathic pulmonary arterial hypertension. *J Heart Lung Transplant*. 2017.
21. Sitbon O, Jais X, Savale L, Cottin V, Bergot E, Macari EA, Bouvaist H, Dauphin C, Picard F, Bulifon S, Montani D, Humbert M and Simonneau G. Upfront triple combination therapy in pulmonary arterial hypertension: a pilot study. *Eur Respir J*. 2014;43:1691-7.
22. Sitbon O and Gaine S. Beyond a single pathway: combination therapy in pulmonary arterial hypertension. *Eur Respir Rev*. 2016;25:408-417.
23. Lahm T, Douglas IS, Archer SL, Bogaard HJ, Chesler NC, Haddad F, Hemnes AR, Kawut SM, Kline JA, Kolb TM, Mathai SC, Mercier O, Michelakis ED, Naeije R, Tudor RM, Ventetuolo CE, Vieillard-Baron A, Voelkel NF, Vonk-Noordegraaf A, Hassoun PM and American Thoracic Society Assembly on Pulmonary C. Assessment of Right Ventricular Function in the Research Setting: Knowledge Gaps and Pathways Forward. An Official American Thoracic Society Research Statement. *Am J Respir Crit Care Med*. 2018;198:e15-e43.
24. Sztrymf B, Coulet F, Girerd B, Yaici A, Jais X, Sitbon O, Montani D, Souza R, Simonneau G, Soubrier F and Humbert M. Clinical outcomes of pulmonary arterial hypertension in carriers of BMPR2 mutation. *Am J Respir Crit Care Med*. 2008;177:1377-83.

6

THE VALUE OF HEMODYNAMIC MEASUREMENTS OR
CARDIAC MAGNETIC RESONANCE IMAGING IN THE
FOLLOW-UP OF PATIENTS WITH PULMONARY
ARTERIAL HYPERTENSION

SUPPLEMENTAL MATERIAL

Table S1 – Treatment, stratified on event time of 5 year

	Survivor	Non-Survivor		
	n=74	≥5 year (n=20)	<5 year (n=24)	P-value
Monotherapy	26 (35%)	13 (65%)	13 (54%)	0.01
Duotherapy	45 (61%)	6 (30%)	8 (33%)	
Triple therapy	2 (3%)	0 (0%)	3 (13%)	
Calcium-antagonist	6 (8%)	3 (15%)	1 (4%)	ns
Endothelin receptor antagonist	58 (78%)	13 (65%)	13 (54%)	0.04
PDE-5 inhibitor	52 (70%)	5 (25%)	19 (79%)	<0.001
Prostacyclin analogue	6 (8%)	7 (35%)	5 (21%)	<0.01

Table S2 – Comorbidities, stratified on event time of 5 years

	Survivor	Non-Survivor		
	n=74	≥5 year (n=20)	<5 year (n=24)	P-value
Coronary disease	3 (4%)	0 (0%)	3 (12.5%)	0.157
Hypertension	12 (16%)	1 (5%)	5 (20.8%)	0.380
Diabetes Mellitus	3 (4%)	2 (10%)	3 (12.5%)	0.197
Thyroid disease	7 (9%)	0 (0%)	1 (4.2%)	0.440
Pulmonary disease				
COPD Gold I-II	1 (1%)	1 (5%)	3 (12.5%)	0.041
OSAS	3 (4%)	1 (5%)	1 (4.2%)	1.000
Asthma	7 (9%)	1 (5%)	2 (8.4%)	1.000
Malignancy	7 (9%)	1 (5%)	1 (4.2%)	0.637

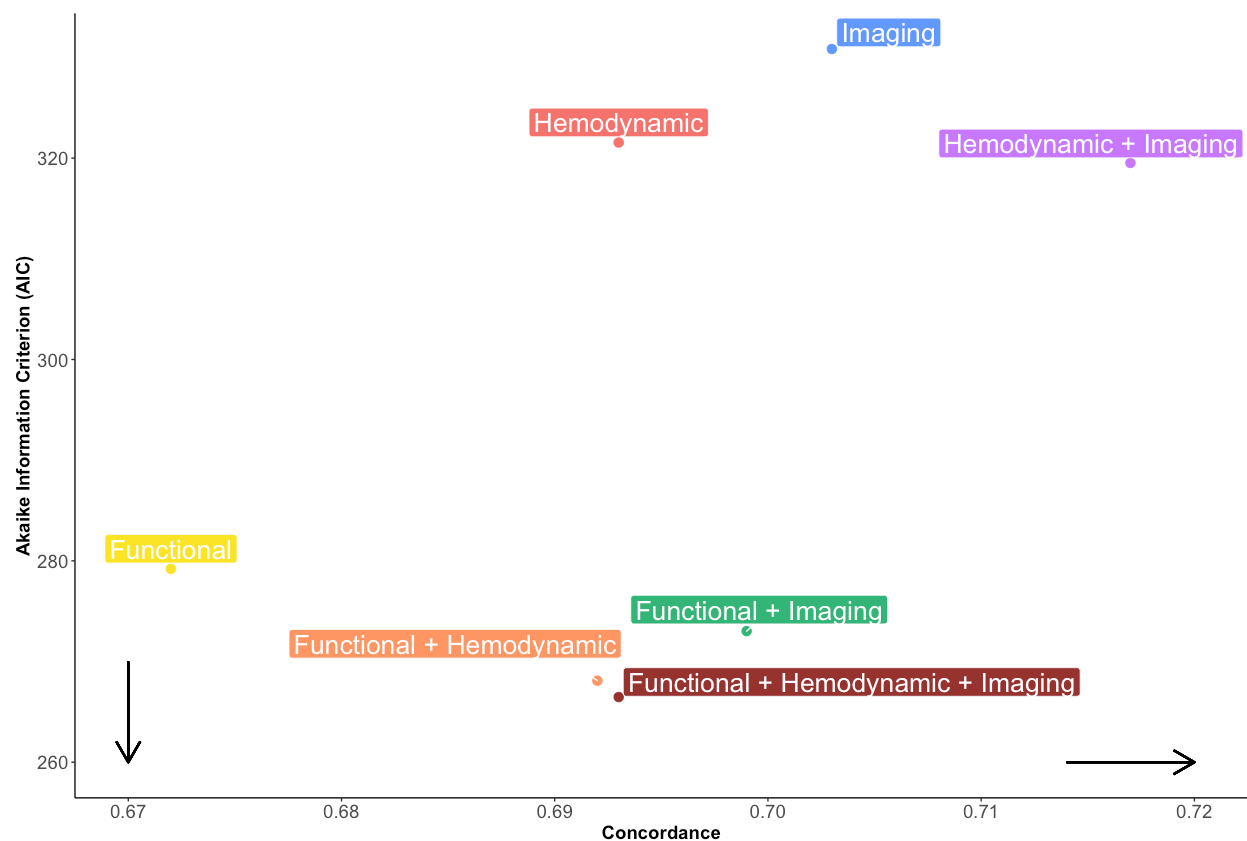
Table S3 – Patients hemodynamics and imaging characteristics at baseline and 1-year follow-up stratified on event time of 3 years

		Survivor		Non-survivor			
		N=74		≥ 3 years N=39		< 3 years N=15	
		Baseline	FU	Baseline	FU	Baseline	FU
Functional	Age (years)	48 ± 17		50 ± 18		52 ± 19	
	Sex (% female)	86		66		53	
	6 MWD (m)	450 ± 17	493 ± 18***	379 ± 28	441 ± 22	330 ± 58	423 ± 51
	NTproBNP (ng/L)	586 [215-1292]	138 [94-442] ****	563 [350-2679]	634 [106-1613]	2518 [619-3155]	575[143-1946]
	NYHA I/II/III/IV (%)	8/44/46/3	26/67/8/0*	7/29/61/4	7/71/21/0	0/17/67/17	8/17/75/0
Hemodynamic	RHC-SVi (ml/m²)	35 ± 2	47 ± 2****	29 ± 1	32 ± 2	28 ± 3	41 ± 4**
	RAP (mmHg)	7 ± 0.4	5 ± 0.4*	9 ± 1	8 ± 1	11 ± 2	8 ± 2
	RHC-CI (L/min/m²)	2.7 ± 0.1	3.4 ± 0.1****	2.3 ± 0.1	2.6 ± 0.2	2.4 ± 0.2	3.3 ± 0.4
	RHC-PVRI (WU*m²)	4.9 ± 0.3	2.7 ± 0.2****	6.1 ± 1.1	4.2 ± 0.9	6.6 ± 0.7	3.8 ± 0.7**
	RHC-SVO₂ (%)	67 ± 1	71 ± 1****	62 ± 2	63 ± 1	57 ± 3	65 ± 2
	RHC-HR (beats/min)	79 ± 2	75 ± 1*	81 ± 3	81 ± 3	87 ± 5	81 ± 4
Imaging	CMR-SVi (ml/m²)	30 ± 1	37 ± 1****	27 ± 1	28 ± 2	26 ± 2	31 ± 3
	CMR-RVEF (%)	38 ± 1	49 ± 1****	32 ± 2	35 ± 3	32 ± 3	37 ± 4
	CMR-RVESVi (ml/m²)	49 ± 2	40 ± 2****	57 ± 4	55 ± 4	56 ± 6	58 ± 7
	CMR-RVEDVi (ml/m²)	77 ± 2	76 ± 2	83 ± 4	81 ± 4	81 ± 6	90 ± 6

Table S3 – Patients hemodynamics and imaging characteristics at baseline and 1-year follow-up stratified on event time of 7 years

		Survivor		Non-survivor			
		N=74		≥ 7 years N=14		< 7 years N=30	
		Baseline	FU	Baseline	FU	Baseline	FU
Functional	Age (years)	48 ± 17		44 ± 14		54 ± 19	
	Sex (% female) - *	86		71		57	
	6 MWD (m)	450 ± 17	493 ± 18***	383 ± 39	419 ± 32	354 ± 35	443 ± 29*
	NTproBNP (ng/L)	586 [215-1292]	138 [94-442] ****	769 [455-1766]	190 [105-1097]	887 [380-3044]	936 [143-1807]
	NYHA I/II/III/IV (%)	8/44/46/3	26/67/8/0*	7/43/43/7	0/79/21/0	4/15/73/8	12/42/46/0
Hemodynamic	RHC-SVi (ml/m²)	35 ± 2	47 ± 2****	29 ± 2	29 ± 2	29 ± 2	38 ± 3***
	RAP (mmHg)	7 ± 0.4	5 ± 0.4*	11 ± 2	9 ± 1	10 ± 1	8 ± 1
	RHC-CI (L/min/m²)	2.7 ± 0.1	3.4 ± 0.1****	2.1 ± 0.1	2.3 ± 0.2	2.4 ± 0.1	3.1 ± 0.2*
	RHC-PVRI (WU*m²)	4.9 ± 0.3	2.7 ± 0.2****	6.7 ± 2.7	3.8 ± 1.7	6.3 ± 0.7	4.0 ± 0.6**
	RHC-SVO₂ (%)	67 ± 1	71 ± 1****	63 ± 2	64 ± 2	59 ± 2	64 ± 1*
	RHC-HR (beats/min)	79 ± 2	75 ± 1*	74 ± 4	81 ± 4	88 ± 3	81 ± 3
Imaging	CMR-SVi (ml/m²)	30 ± 1	37 ± 1****	26 ± 2	28 ± 3	27 ± 1	30 ± 2
	CMR-RVEF (%)	38 ± 1	49 ± 1****	32 ± 2	34 ± 4	32 ± 2	36 ± 3
	CMR-RVESVi (ml/m²)	49 ± 2	40 ± 2****	56 ± 6	53 ± 6	57 ± 4	58 ± 5
	CMR-RVEDVi (ml/m²)	77 ± 2	76 ± 2	82 ± 6	79 ± 6	82 ± 4	87 ± 4

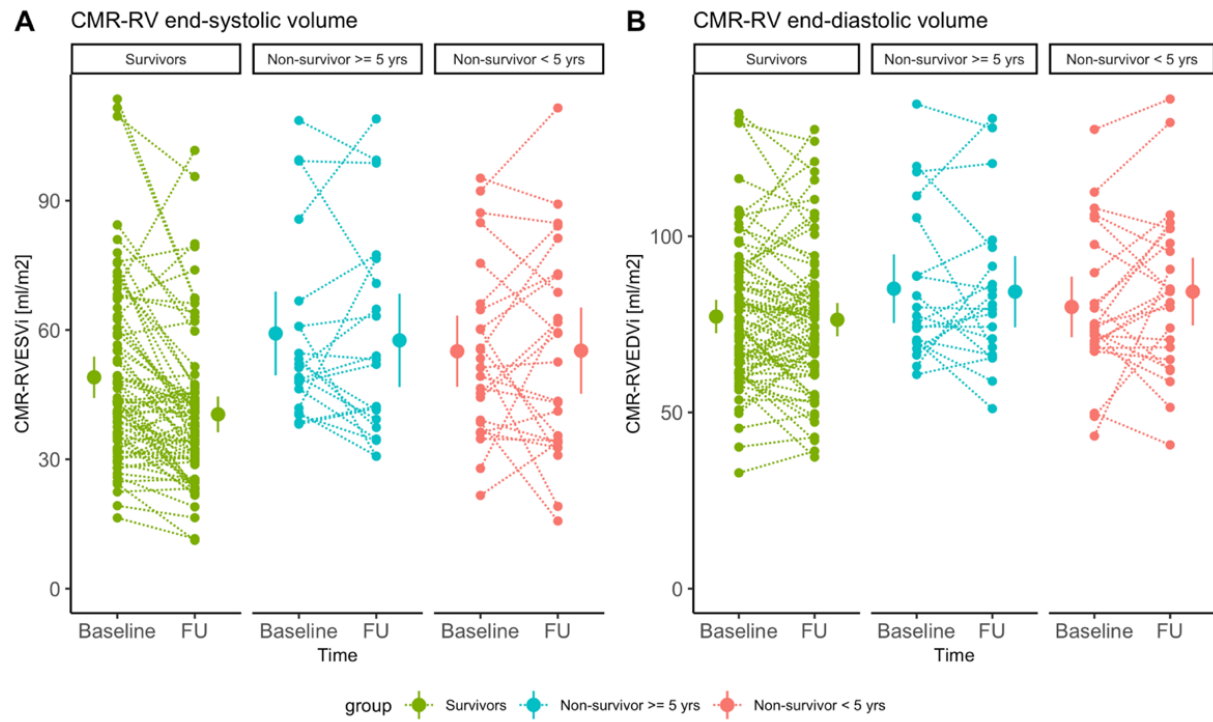
Figure S1 – Akaike information criterion and concordance index of the predictive models



The Akaike information criterion provides a relative measure of the quality of the model and estimates the information lost by the number of parameters in the models and the strength of the predictive value. A low number means less information lost and could be interpreted as a better model. The concordance or C-statistics provides measure of goodness-of-fit in survival models. A higher concordance value means that the model gives a better prediction for survival. All models constructed by forward cox regression analyses are presented: Model 1 – Functional: Age + Sex + 6MWD; Model 2 – Hemodynamic: Age + Sex + RHC-mRAP + RHC-SvO₂; Model 3 – Imaging: Age + Sex + RVEF; Model 1+2: Age + Sex + 6MWD + RHC-mRAP + SvO₂; Model 1+3: Age + Sex + 6MWD + CMR-RVEF; Model 2+3: Age + Sex + RHC- mRAP + RHC-SvO₂ + RVEF; Model 1+2+3: Age + Sex + 6MWD + RHC- mRAP + RHC-SvO₂ + CMR-RVEF. The combination of functional with either hemodynamic and/or imaging parameters yielded highest predictive value.

Abbreviations: NYHA, New York Heart Association class; 6MWD, 6-minute walk distance; RHC, right heart catheterization; SVi, stroke volume index; RAP, right atrial pressure; SvO₂, mixed venous oxygen saturation; CI, cardiac index; CMR, cardiac magnetic resonance imaging, RVEDVi, RV end-diastolic volume index.

Figure S2 – Treatment effects on imaging parameters in patients with low- and high-risk profiles



7

TREATMENT RESPONSE IN PATIENTS WITH IDIOPATHIC PULMONARY ARTERIAL HYPERTENSION AND A SEVERELY REDUCED DIFFUSION CAPACITY

CE van der Bruggen & OA Spruijt, EJ Nossent, P Trip, JT Marcus, FS de Man, HJ Bogaard, A Vonk Noordegraaf

Pulmonary Circulation, 2017

ABSTRACT

Introduction: Patients with idiopathic pulmonary arterial hypertension (IPAH) and a reduced diffusion capacity of the lung for carbon monoxide (DLCO) have a worse survival compared to IPAH patients with a preserved DLCO. Whether this poor survival can be explained by unresponsiveness to pulmonary hypertension (PH)-specific vasodilatory therapy is unknown. Therefore, the aim of this study was to evaluate the hemodynamic and cardiac response to PH-specific vasodilatory therapy in patients with IPAH and a reduced DLCO.

Methods: Retrospectively, we studied treatment naïve hereditary and IPAH patients diagnosed between January 1990 and May 2015 at the VU University Medical Center. After exclusion of participants without available baseline DLCO measurement or right heart catheterization data and participants carrying a BMPR2 mutation, 166 participants could be included in this study. Subsequently, hemodynamics, cardiac function, exercise capacity, and oxygenation at baseline and after PH-specific vasodilatory therapy were compared between IPAH patients with a preserved DLCO (DLCO >62%), IPAH patients with a moderately reduced DLCO (DLCO 43–62%), and IPAH patients with a severely reduced DLCO (DLCO <43%).

Results: Baseline hemodynamics and right ventricular function were not different between groups. Baseline oxygenation was worse in patients with IPAH and a severely reduced DLCO. Hemodynamics and cardiac function improved in all groups after PH-specific vasodilatory therapy without worsening of oxygenation at rest or during exercise.

Conclusion: Patients with IPAH and a severely reduced DLCO show a similar response to PH-specific vasodilatory therapy in terms of hemodynamics, cardiac function, and exercise capacity as patients with IPAH and a moderately reduced or preserved DLCO.

INTRODUCTION

Patients with pulmonary hypertension tend to have a mildly reduced pulmonary diffusion capacity for carbon monoxide (DLCO) compared to healthy subjects (1). A severely reduced DLCO is most often seen in pulmonary hypertension related to connective tissue disease, lung parenchymal disease or in pulmonary veno-occlusive disease, but also in a subset of patients with idiopathic pulmonary arterial hypertension (IPAH) without signs of these underlying conditions (2-5). Recent studies revealed that IPAH patients with a low DLCO have a worse survival (6). Although it is yet unknown what causes this difference in survival, it has been argued that compared to other IPAH patients, IPAH patients with a severely reduced DLCO may have a distinct type of pulmonary vasculopathy that is less responsive to PAH-specific therapy (7, 8).

Therefore, the aim of this study was to compare the response to pulmonary arterial hypertension specific vasodilatory therapy in terms of hemodynamics, cardiac function, exercise capacity and oxygenation between IPAH patients with different degrees of DLCO impairment.

METHODS

Patient selection

We studied retrospectively treatment naïve hereditary- and IPAH patients who were diagnosed between January 1990 and May 2015 at the VU University Medical Center. Part of this cohort was described in the study of Trip et al. (5). A diagnosis of hereditary- and IPAH was established by a multidisciplinary PH team, after rigorous clinical evaluation according to the ERS/ESC guideline (9).

Subjects without available baseline DLCO measurement, with severe emphysema or pulmonary fibrosis on HRCT (5) were excluded from this study. Furthermore, to avoid clouding of the results, patients carrying a BMPR2 mutation were excluded from this study as recent studies showed the reduced life-expectancy but preserved DLCO status in these subjects (4, 10). In total 166 patients were included in this study (Figure 7.1).

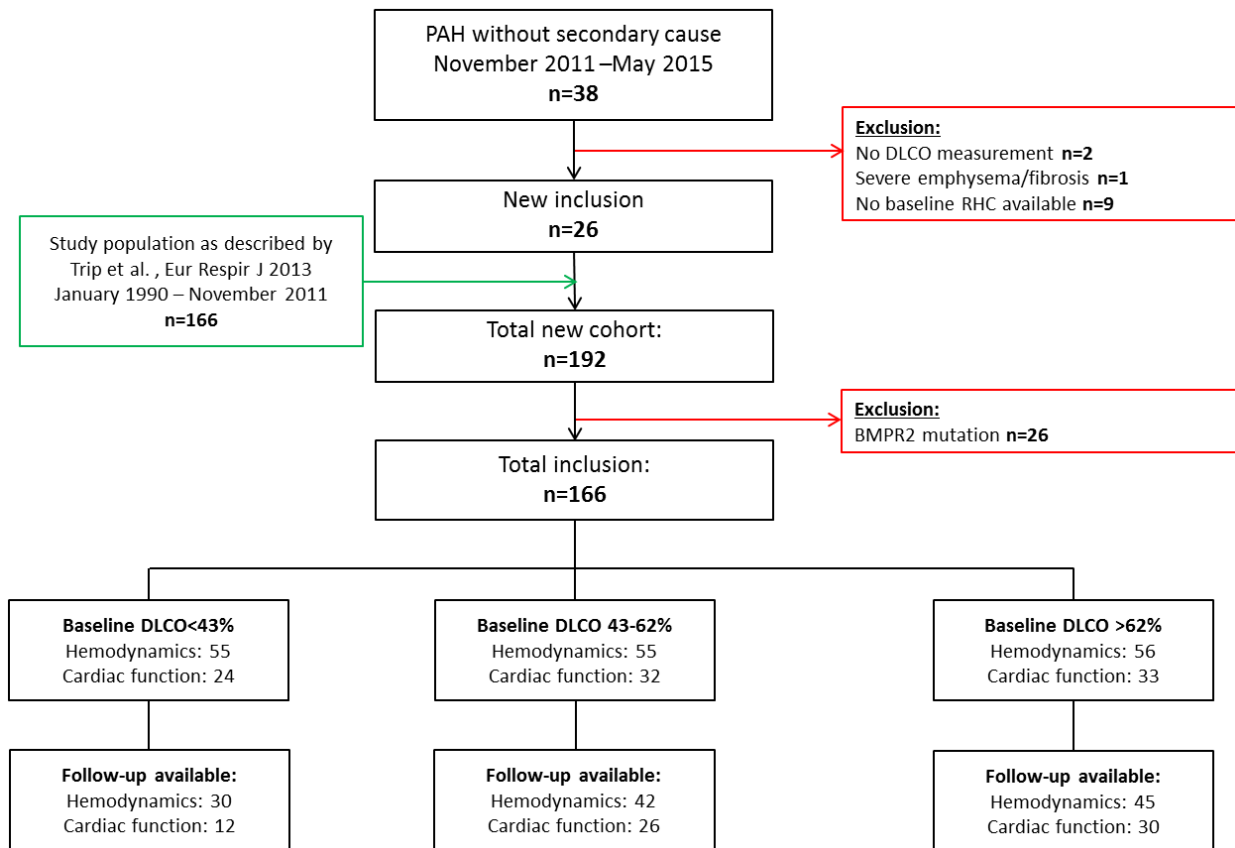
The cohort was divided into three groups using tertiles, leading to one group with a severely reduced DLCO (<43%), one group with a moderately reduced DLCO (43%-62%) and one group with a preserved DLCO (>62%) .

Right heart catheterization

Hemodynamics and RV pressure curve recordings were assessed with a balloon-tipped, flow directed 7.5F triple lumen Swan-Ganz catheter (Edwards Lifesciences LLC, Irvine, CA, USA).

Cardiac output measurements were performed using thermodilution or the direct Fick method.

Figure 7.1 – Flow chart



PAH = pulmonary arterial hypertension; RHC = right heart catheterization

Cardiac function and volumes

RV function and volumes were assessed using cardiac magnetic resonance imaging (CMRI). All scans were performed on a Siemens 1.5T Sonata or Avanto scanner (Siemens Medical Solutions, Erlangen, Germany). Image acquisition and post-processing was done as described previously (11). Left and RV volumes were indexed to body surface area (BSA). Stroke volume (SV) and ejection fraction (EF) were calculated according to the following formulas, in which EDV = end-diastolic volume and ESV = end-systolic volume: $SV = EDV - ESV$ and $EF = (EDV - ESV) / EDV$.

Six-minute walking test (6 MWT):

6MWTs were performed according to the ATS guidelines (12, 13). The distance walked (in meters) and the arterial oxygen saturation at rest and during exercise were measured at baseline and during follow-up.

Treatment response:

Treatment responses were assessed by the baseline-to-follow-up responses in hemodynamics, cardiac function and 6MWD. Time between baseline and follow-up was 1.9 ± 1.6 years in the DLCO<43% group, 1.6 ± 1.2 years in the DLCO 43-62% group and 2.1 ± 2.2 years in the DLCO>62% group ($p=0.860$).

Statistical analysis:

Data are presented as mean \pm standard deviation (SD) unless stated otherwise. Comparisons of baseline hemodynamics, cardiac function and the change in hemodynamic and cardiac function after PAH-specific therapies between the DLCO<43%, DLCO 43-62% and the DLCO>62% group were performed using one-way ANOVA with Bonferroni post-hoc corrections and Kruskal-Wallis tests with Dunn's multiple comparisons post-hoc test as appropriate.

Kaplan-Meier analyses were performed to test for survival differences between the DLCO<43%, DLCO 43-62% and the DLCO>62% groups in the entire cohort and the cohort in which a MRI at follow-up was present. Kaplan-meier analysis was also performed to test for survival differences between the subjects with and without a CMRI at follow-up in the DLCO<43% group. Subsequently, multivariable cox regression analyses were performed to correct the association between DLCO and survival for age differences.

Statistical analyses were performed using SPSS for Windows version 20 (IBM Corp., Armonk, NY, USA) and GraphPad Prism for Windows version 6 (GraphPad Software, Inc., San Diego, CA, USA). P-values <0.05 were considered statistically significant.

RESULTS

Characteristics of the DLCO<43%, DLCO 43-62% and DLCO>62% patients are summarized in Table 7.1. A detailed characterization of the majority of patients was already given in our previous study (5).

Baseline measurements

SvO₂, LVEDVI and LVESVI were significantly lower in the DLCO<42% group compared to the DLCO>62% group. Except from these, baseline hemodynamics and cardiac function were not different between groups.

Exercise capacity, assessed by the 6MWT, was significantly lower in the DLCO<42% group compared to the moderately reduced and preserved DLCO group, as well as the arterial oxygen tension and saturation at rest. Furthermore, the DLCO<42% group showed a larger drop in arterial oxygen saturation during exercise (Table 7.1).

Treatment response

As can be appreciated from Table 2, the DLCO<42% group received more double-therapy, more prostacyclin monotherapy and less endothelin receptor antagonist or phosphodiesterase type 5 inhibitor monotherapy. Interestingly, a significantly higher percentage of patients switched from monotherapy to combination therapy in the severely reduced DLCO group. (Table 7.3)

All groups showed a decrease in mPAP and pulmonary vascular resistance (PVR), an increase in cardiac index (CI) and no change in pulmonary arterial wedge pressure (PAWP) and heart rate (HR) from baseline to follow-up (Figure 7.2).

Cardiac responses are depicted in Figure 7.3. Both groups showed no change in left ventricular end-systolic volume index (LVESVI). Delta left ventricular end-diastolic volume index (LVEDVI) and delta left ventricular ejection fraction (LVEF) did not differ between the three groups. Delta RVEDVI, RVESVI and RVEF were similar between severely reduced DLCO group, the moderately reduced group and the group with a preserved DLCO.

6MWD increased in all three groups after PH specific vasodilatory therapy. Arterial oxygen saturation did not change from baseline to follow-up, while the moderately reduced DLCO group had a lower arterial oxygen saturation after exercise compared to the severely reduced DLCO and preserved DLCO group (Figure 7.4).

Survival analyses

LVEDVI and LVESVI proved to be confounders to the survival analysis. LVEDVI and age-corrected survival was worse for patients with a DLCO<43% (Figure 7.5A). These survival differences between DLCO<43% and DLCO 43-62% and DLCO>62% were also present in the selected cohort with a CMRI available at follow-up (figure 7.5B). No difference in survival was seen between patients with and without a CMRI at follow-up in the DLCO<43% group (figure 7.5C).

Table 7.1 – Baseline characteristics

	DLCO <43%	DLCO 43–62%	DLCO >62%	P value
<i>General characteristics</i>				
Age at diagnosis (years)	65 ± 13	53 ± 18*	48 ± 14 [†]	<0.0001
Male (%)	58	18	27	<0.0001
<i>6MWT</i>				
6MWD (m)	286 ± 136	366 ± 119*	416 ± 134 [†]	<0.0001
6MWD (% predicted)	56 ± 23	70 ± 19*	71 ± 23 [†]	<0.01
SaO ₂ -rest (%)	91 ± 4	94 ± 3*	95 ± 2 [†]	<0.0001
SaO ₂ -exercise (%)	79 ± 7	89 ± 6*	89 ± 6 [†]	<0.0001
ΔSaO ₂ (%)	–11 (–16 – 6)	–4 (–8 – 2)*	–5 (–10 – 2) [†]	<0.0001
<i>Laboratory tests</i>				
NT-proBNP (ng·L)	1004 (304–2487)	802 (194–2888)	555 (156–1887)	0.45
PCO ₂ (mmHg)	30 ± 6	33 ± 7	33 ± 6	0.19
PO ₂ (mmHg)	61 ± 15	68 ± 11	72 ± 13 [†]	<0.05
SaO ₂ (%)	91 ± 5	94 ± 3*	94 ± 3 [†]	<0.01
<i>Baseline hemodynamics</i>				
HR (beats/min)	80 ± 17	78 ± 15	80 ± 13	0.84
mPAP (mmHg)	48 ± 12	51 ± 14	52 ± 15	0.33
mRAP (mmHg)	7 (4–9)	7 (4–11)	8 (5–11)	0.67
PAWP (mmHg)	10 ± 3	9 ± 4	8 ± 4	0.27
PVR (dynes·s·cm ^{–5})	706 (540–1000)	858 (476–1041)	569 (441–961)	0.56
CI (L/min/m ²)	2.3 ± 0.7	2.5 ± 1.0	2.7 ± 0.9	0.18
SvO ₂ (%)	61 ± 9	63 ± 9	67 ± 9 [†]	<0.01
<i>Baseline cardiac function and volumes</i>				
LV EDVI (mL/m ²)	40 ± 10	41 ± 11	48 ± 13 [†]	<0.05
LV ESVI (mL/m ²)	15 ± 6	14 ± 6	18 ± 7 [‡]	<0.05
LV EF (%)	63 ± 10	66 ± 10	62 ± 10	0.21
RV EDVI (mL/m ²)	76 ± 27	76 ± 17	88 ± 21	0.06
RV ESVI (mL/m ²)	54 ± 26	50 ± 18	59 ± 23	0.31
RV EF (%)	33 ± 12	36 ± 12	35 ± 12	0.67

6MWD = six minute walking distance; SaO₂ = arterial oxygen saturation; HR = heart rate; mPAP = mean pulmonary arterial pressure; mRAP = mean right atrial pressure; PAWP = pulmonary arterial wedge pressure; PVR = pulmonary vascular resistance; CI = cardiac index; SvO₂ = mixed venous oxygen saturation; LVEDVI = left ventricular end-diastolic volume index; LVESVI = left ventricular end-systolic volume index; LVEF = left ventricular ejection fraction; RVEDVI = right ventricular end-diastolic volume index; RVESVI = right ventricular end-systolic volume index; RVEF = right ventricular ejection fraction. *DLCO<43% significantly different compared to DLCO 43-62%, †DLCO<43% significantly different compared to DLCO>62%, ‡DLCO 43-62% significantly different compared to DLCO>62%

Table 7.2 – PAH-specific medication during follow-up

	DLCO <43%	DLCO 43–62%	DLCO >62%	P value
Mono ERA/PDE5i (%)	26.7	41.9	52.8	<0.001
Mono PGI ₂ (%)	26.7	7.0	11.1	<0.001
Double: ERA+PDE5i (%)	40.0	37.2	22.2	<0.05
Double: PGI ₂ +ERA/PDE5i (%)	5.7	2.3	0	<0.05
Triple (%)	0	2.3	8.3	<0.01
Calcium antagonist (%)	0	9.3	5.6	<0.01

ERA = endothelin receptor antagonist; PGI₂ = prostacyclin; PDE5i = phosphodiesterase type 5 inhibitor.

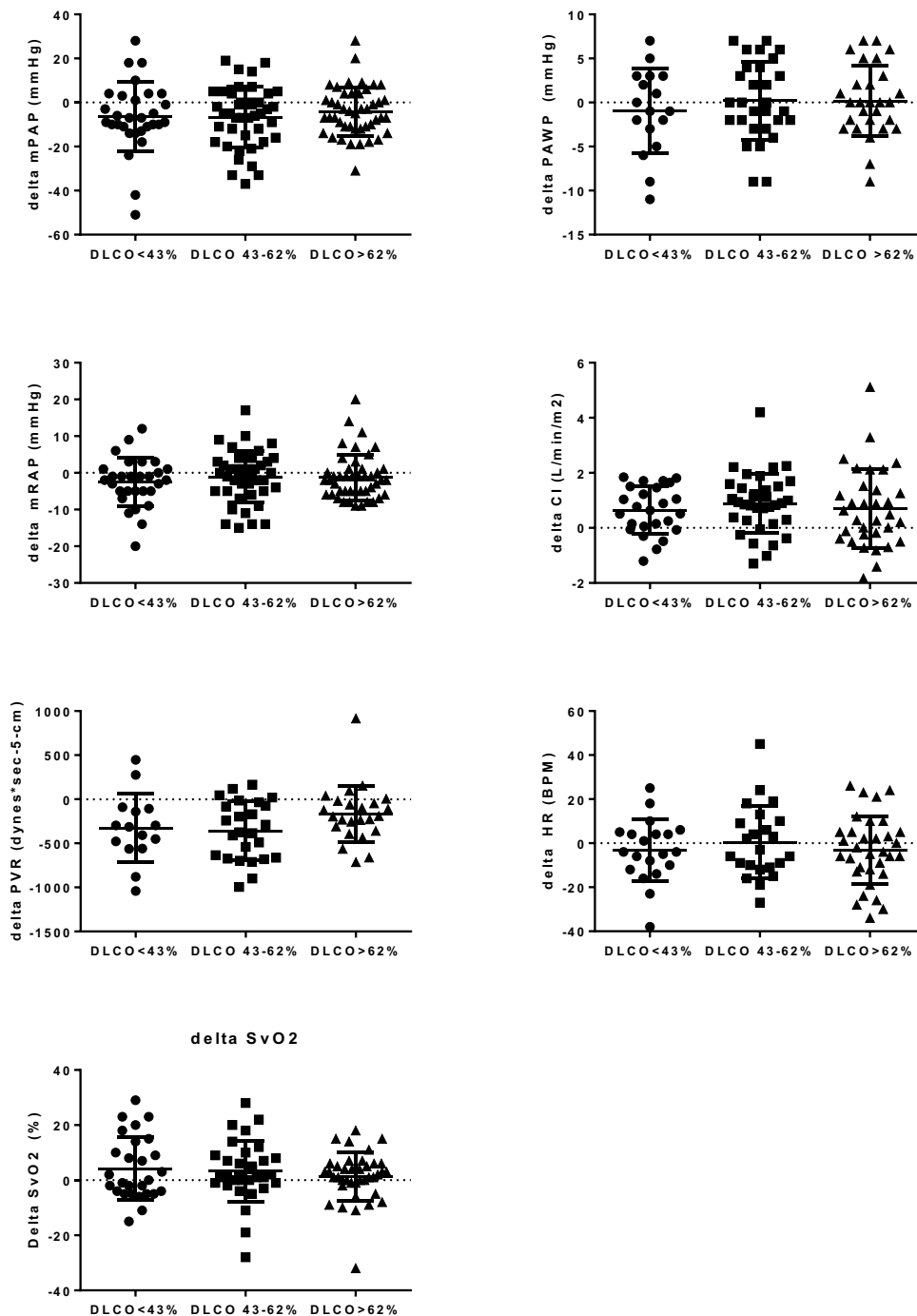
Table 7.3 – Treatment changes during follow-up (changes after an unsatisfactory response to previous treatment, hemodynamic or clinical worsening)

	DLCO <43%	DLCO 43–62%	DLCO >62%	P value
Monotherapy to combination therapy (%)	32.0	20.0	11.1	<0.01
Monotherapy to triple therapy (%)	0	0	2.8	0.05
Combination therapy to triple therapy (%)	0	2.5	2.8	0.22

DISCUSSION

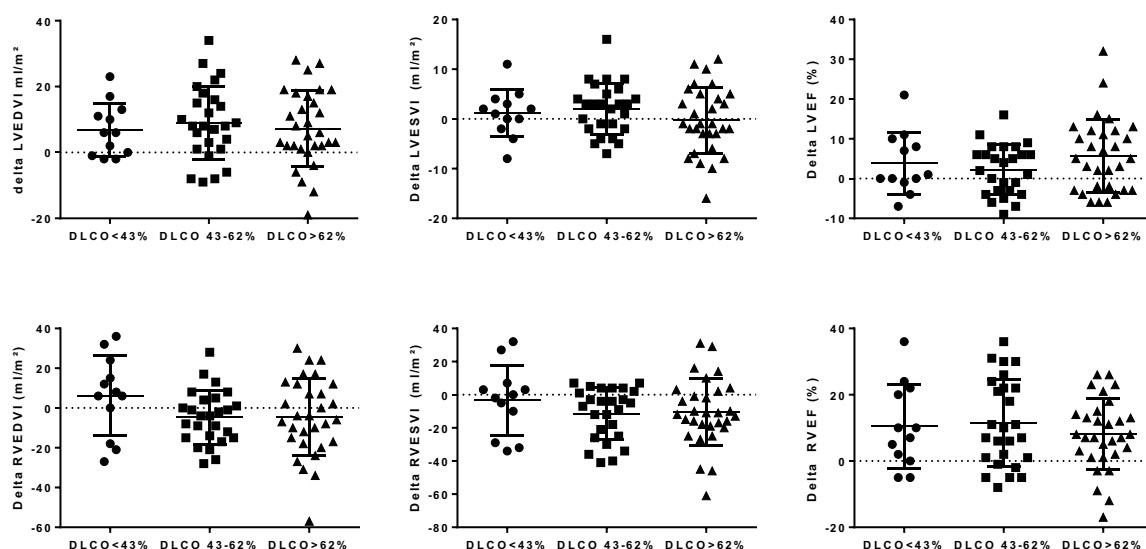
In the present study we evaluated the effects of pulmonary hypertension specific vasodilatory therapy in IPAH patients with a severely reduced DLCO. It is known that IPAH patients with a low DLCO have a worse survival compared to IPAH patients with a preserved DLCO (6). In addition, it has been shown that IPAH patients with a low DLCO have more coronary artery disease, a higher tobacco exposure, a higher body mass index, are older, have worse pulmonary function tests and show more mild abnormalities on HRCTs compared to IPAH patients with a preserved DLCO (5). Although it seems that the IPAH patients with a low DLCO share some risk factors with group 2 and group 3 PH, normal PAWP pressures, spirometry and HRCT excluded left heart conditions and lung disease as a cause of PH. In addition, HRCTs of the IPAH patients with a low DLCO showed no signs of PVOD (14, 15). The question rises whether the low DLCO group has a different pulmonary vasculopathy compared to IPAH patients with a preserved DLCO (7, 8). The answer to this question remains elusive and requires further investigation. As a first step, we analyzed the treatment response in this patient cohort.

Figure 7.2 – Hemodynamic treatment response



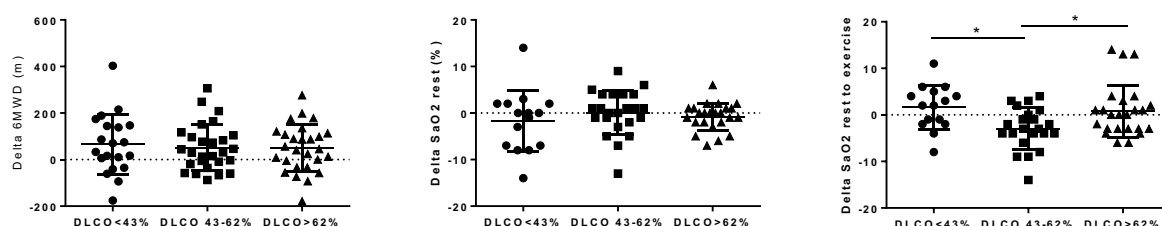
Hemodynamic treatment response. mPAP = mean pulmonary artery pressure; PAWP = pulmonary arterial wedge pressure; mRAP = mean right atrial pressure; PVR = pulmonary vascular resistance; CI = cardiac index; HR = heart rate. ns = non-significant. Data is presented as mean \pm SEM.

Figure 7.3 – Cardiac response to treatment



LVEDV = left ventricular end-diastolic volume index; LVESVI = left ventricular end-systolic volume index; LVEF = left ventricular ejection fraction; RVEDVI = right ventricular end-diastolic volume index; RVESVI = right ventricular end-systolic volume index; RVEF = right ventricular ejection fraction. Data is presented as mean \pm SEM.

Figure 7.4 – Treatment response in oxygenation and 6MWD



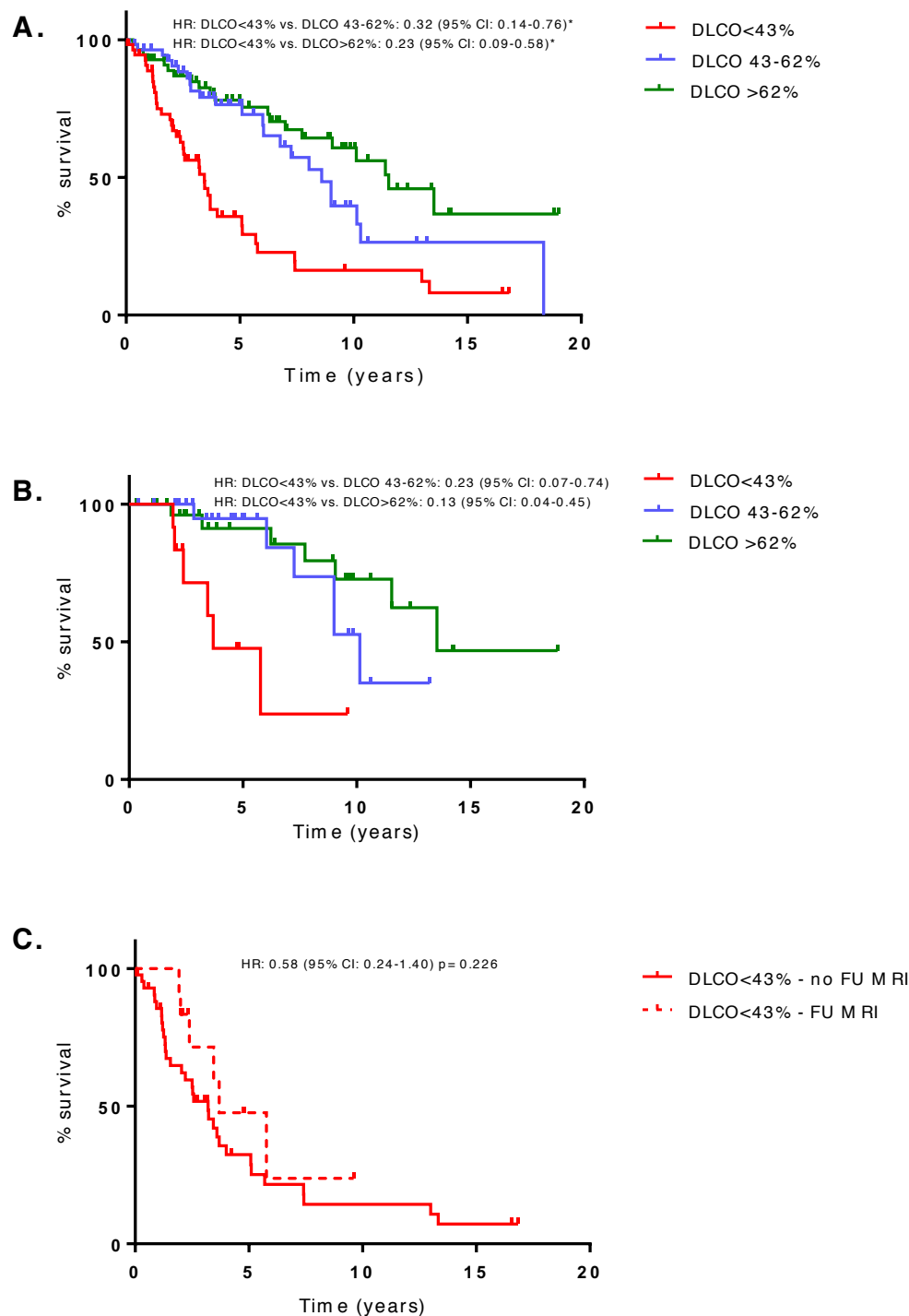
6MWD = 6 minute walking distance; SaO2 rest = arterial oxygen saturation in rest; SaO2 rest-ex = change in arterial oxygen saturation during exercise. * = $p < 0.05$. Data is presented as mean \pm SEM.

Remarkably, we observed a significant improvement in hemodynamics, right ventricular function and exercise capacity upon pulmonary hypertension specific vasodilatory therapy without an impact on oxygen saturation in this cohort as in comparison to the IPAH patients with an moderately reduced or preserved DLCO.

Less follow-up data was available in the DLCO<43% group compared to the DLCO 43-62% and DLCO>62% group which could have led to a selection bias and subsequent overestimation of the treatment effect in the DLCO<43% group. However, no survival difference existed in the DLCO<43% group between the subjects with and without available follow-up data. This to some extent suggests that the subjects in the DLCO<43% group with follow-up data are representative for the total DLCO<43% group. Furthermore, survival

differences between the DLCO<43% and the moderately reduced and preserved DLCO groups continued to exist when only the subjects with follow-up data were entered in the survival analysis further arguing against the presence of an important selection bias. At follow-up, the DLCO<43% group received more combination therapy compared to the DLCO≥43% groups. This may have confounded our results.

Figure 7.5 – Survival analyses



*A: Difference in survival between the DLCO<42%, DLCO 43-62% and DLCO≥63% groups in the total cohort (n=166). The DLCO<42% group showed a worse survival than the moderately reduced DLCO and preserved DLCO groups. B: Difference in survival between the severely reduced DLCO group, the moderately reduced DLCO and preserved DLCO group in the cohort in which a CMRI at follow-up was available (n=68). Also in this selected cohort the DLCO<42% group showed a worse survival compared to other two groups. C: Difference in survival between the group with and without a CMRI at follow up in the DLCO<42% group (n=42). No difference in survival was found between the group with and without a CMRI at follow-up in the DLCO<42% group. * adjusted for age and left ventricular end diastolic volume index.*

Based on the pulmonary vascular response on treatment there is no reason to withhold pulmonary arterial hypertension specific treatment from patients with IPAH and a severely reduced DLCO. The similarities in hemodynamic and cardiac treatment responses between IPAH patients with a severely reduced DLCO and IPAH patients with a preserved DLCO suggests that the poor survival in the low DLCO group is not explained by unresponsiveness of the pulmonary vasculature to current pulmonary arterial hypertension specific medications. Survival differences may be partially explained by the fact that the DLCO<42% group was older (16). Cox proportional hazard analyses showed that age was a confounder for the differences in survival between groups, however, survival differences remained after adjusting for age. As such, the question remains why survival in this subgroup of patients with IPAH and a severely reduced DLCO is so poor (6).

CONCLUSIONS

Patients with IPAH and a severely reduced DLCO show a similar response to PH specific vasodilatory therapy as patients with IPAH and a moderately or preserved DLCO in terms of hemodynamics, right ventricular function, exercise capacity and oxygenation.

REFERENCES

1. Sun XG, Hansen JE, Oudiz RJ, Wasserman K. Pulmonary function in primary pulmonary hypertension. *Journal of the American College of Cardiology*. 2003;41(6):1028-35.
2. Allanore Y, Borderie D, Avouac J, Zerkak D, Meune C, Hachulla E, et al. High N-terminal pro-brain natriuretic peptide levels and low diffusing capacity for carbon monoxide as independent predictors of the occurrence of precapillary pulmonary arterial hypertension in patients with systemic sclerosis. *Arthritis and rheumatism*. 2008;58(1):284-91.
3. Montani D, Achouh L, Dorfmueller P, Le Pavec J, Sztrymf B, Tcherakian C, et al. Pulmonary veno-occlusive disease: clinical, functional, radiologic, and hemodynamic characteristics and outcome of 24 cases confirmed by histology. *Medicine*. 2008;87(4):220-33.
4. Trip P, Girerd B, Bogaard HJ, de Man FS, Boonstra A, Garcia G, et al. Diffusion capacity and BMPR2 mutations in pulmonary arterial hypertension. *The European respiratory journal*. 2014;43(4):1195-8.
5. Trip P, Nossent EJ, de Man FS, van den Berk IA, Boonstra A, Groepenhoff H, et al. Severely reduced diffusion capacity in idiopathic pulmonary arterial hypertension: patient characteristics and treatment responses. *The European respiratory journal*. 2013;42(6):1575-85.
6. Chandra S, Shah SJ, Thenappan T, Archer SL, Rich S, Gomberg-Maitland M. Carbon monoxide diffusing capacity and mortality in pulmonary arterial hypertension. *J Heart Lung Transplant*. 2010;29(2):181-7.
7. Hoeper MM, Simon RGJ. The changing landscape of pulmonary arterial hypertension and implications for patient care. *Eur Respir Rev*. 2014;23(134):450-7.
8. Souza R, Fernandes CJ, Hoeper MM. Carbon monoxide diffusing capacity and the complexity of diagnosis in pulmonary arterial hypertension. *The European respiratory journal*. 2014;43(4):963-5.
9. Galie N, Humbert M, Vachiery JL, Gibbs S, Lang I, Torbicki A, et al. 2015 ESC/ERS Guidelines for the diagnosis and treatment of pulmonary hypertension: The Joint Task Force for the Diagnosis and Treatment of Pulmonary Hypertension of the European Society of Cardiology (ESC) and the European Respiratory Society (ERS): Endorsed by: Association for European Paediatric and Congenital Cardiology (AEPC), International Society for Heart and Lung Transplantation (ISHLT). *The European respiratory journal*. 2015;46(4):903-75.
10. Evans JD, Girerd B, Montani D, Wang XJ, Galie N, Austin ED, et al. BMPR2 mutations and survival in pulmonary arterial hypertension: an individual participant data meta-analysis. *Lancet Respir Med*. 2016;4(2):129-37.
11. van de Veerdonk MC, Kind T, Marcus JT, Mauritz GJ, Heymans MW, Bogaard HJ, et al. Progressive right ventricular dysfunction in patients with pulmonary arterial hypertension responding to therapy. *Journal of the American College of Cardiology*. 2011;58(24):2511-9.
12. ATS statement: guidelines for the six-minute walk test. *American journal of respiratory and critical care medicine*. 2002;166(1):111-7.
13. Erratum: ATS Statement: Guidelines for the Six-Minute Walk Test. *American journal of respiratory and critical care medicine*. 2016;193(10):1185.
14. Resten A, Maitre S, Capron F, Simonneau G, Musset D. [Pulmonary hypertension: CT findings in pulmonary veno-occlusive disease]. *Journal de radiologie*. 2003;84(11 Pt 1):1739-45.
15. Resten A, Maitre S, Humbert M, Rabiller A, Sitbon O, Capron F, et al. Pulmonary hypertension: CT of the chest in pulmonary venoocclusive disease. *Ajr*. 2004;183(1):65-70.
16. Hoeper MM, Huscher D, Ghofrani HA, Delcroix M, Distler O, Schweiger C, et al. Elderly patients diagnosed with idiopathic pulmonary arterial hypertension: results from the COMPERA registry. *International journal of cardiology*. 2013;168(2):871-80.

8

IMAGING IN PULMONARY HYPERTENSION

CE van der Bruggen, OA Spruijt, LJ Meijboom, A Vonk Noordegraaf

European Respiratory Society Monograph, 2017

SUMMARY

Pulmonary hypertension (PH) is a hemodynamic condition leading to a progressive increase in pulmonary vascular resistance (PVR) and mean pulmonary artery pressure (mPAP). Irrespective of its cause, the main cause of death in PH patients is right ventricular failure. Noninvasive imaging techniques play an essential role in the diagnostic process, differential diagnosis and in monitoring disease progression. This chapter will give an overview of the most important noninvasive imaging tools for assessing pulmonary pressures, RV function and RV monitoring.

INTRODUCTION

Pulmonary hypertension is rapidly progressive and lethal disease and is defined as a hemodynamic condition with a mean pulmonary arterial pressure (mPAP) > 25 mmHg at rest, measured invasively by right heart catheterization (RHC).(1) Although primarily a lung disease, prognosis of PH patients is closely related to right ventricular (RV) function.(2–6) Initially, the RV adapts to it increased afterload by several compensatory mechanisms but in the end these are not sufficient to prevent progression to RV dysfunction and failure.

Table 8.1 – Clinical classification of pulmonary hypertension

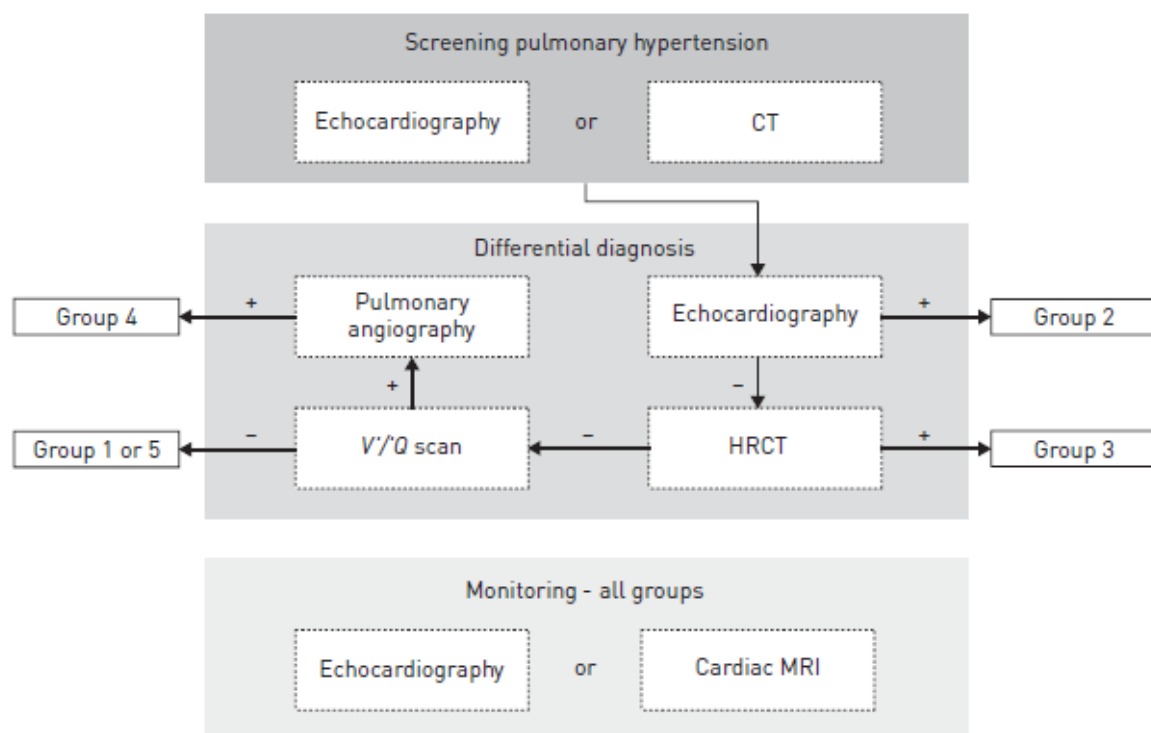
1. Pulmonary Arterial Hypertension
1.1 Idiopathic PAH
1.2 Heritable PAH
1.3 Drugs and toxins induced
1.4 Associated PAH (connective tissue disease, HIV infection, portal hypertension, congenital heart disease, schistosomiasis, chronic haemolytic anaemia)
1'. Pulmonary veno-occlusive disease and/or pulmonary capillary haemangiomatosis
1". Persistent pulmonary hypertension of the newborn (PPHN)
2. Pulmonary Hypertension due to left heart disease
2.1 Systolic dysfunction
2.2 Diastolic dysfunction
2.3 Valvular disease
2.4 Congenital/acquired left heart inflow /outflow tract obstruction and congenital cardiomyopathies
3. Pulmonary hypertension due to lung diseases and/or hypoxia
3.1 Chronic obstructive pulmonary disease
3.2 Interstitial lung disease
3.3 Other pulmonary diseases with mixed restrictive and obstructive pattern
3.4 Sleep-disordered breathing
3.5 Alveolar hypoventilation disorders
3.6 Chronic exposure to high altitude
3.7 Developmental abnormalities
4. Chronic thromboembolic pulmonary hypertension
5. PH with unclear and/or multifactorial mechanisms
5.1 Haematological disorders
5.2 Systemic disorders
5.3 Metabolic disorders
5.4 Others

Despite the fact that the five PH entities as described in the updated clinical classification of Nice 2013 (Table 8.1) are characterized by an increased pulmonary vascular resistance (PVR) and mPAP, underlying mechanisms, prognosis and treatment strategies vary significantly. (1) A critical distinction is the division in pre- and post-capillary pulmonary hypertension, as post-capillary pulmonary hypertension patients do not respond to pulmonary arterial hypertension

(PAH) specific treatment. Therefore, it is of utmost importance to determine a right diagnosis, assessed by a complete evaluation of both hemodynamics and RV function.

Multiple noninvasive imaging techniques are applicable and essential in addition to RHC measurements to assess the correct diagnosis. Furthermore, given the increased knowledge of disease progression and the importance of timely referral for lung transplantation, the role of noninvasive imaging techniques is indispensable. In this chapter, we provide an overview of imaging techniques in the diagnostic process as well as the monitoring of PH patients over time, as summarized in Figure 8.1.

Figure 8.1 – Screening, diagnosing and monitoring pulmonary hypertension



HRCT: high resolution computed tomography, V/Q scan: ventilation/perfusion scanning, cMRI: cardiac magnetic resonance imaging.

The diagnostic process

Most PH patients are diagnosed when the disease is already in an advanced stage, due to the non-specific and subtle onset of symptoms at presentation (exercise-induced dyspnea, syncope, unexplained fatigue).(7–9) Early detection and thereby early initiation of treatment can improve clinical outcome. Often, noninvasive imaging techniques as computed tomography (CT) and cardiac echocardiography are performed during the diagnostic work-up of patients presenting with shortness of breath. Both techniques provide the opportunity to assess highly sensitive and specific parameters either pointing towards or ruling out PH.

Computed Tomography

Routinely performed CT's from patients presenting with shortness of breath may provide important clues about the presence of PH. The most extensively studied parameter to predict PH on CT pulmonary angiography (CTPA) is a diameter ratio > 1 of the pulmonary artery (PA) to ascending aorta (AA), measured at the level of the bifurcation of the pulmonary trunk. (10–13) In 2014, a meta-analysis showed a relatively high sensitivity of 74% and a specificity of 81%. (14) In 2014, Spruijt et al. showed an increased predictive value and sensitivity of CTPA when adding ventricular measurements to the PA/AA ratio. (15) Other important parameters are the PA diameter versus bronchus diameter and right ventricular hypertrophy. Hence, isolated CTPA measurements are not suitable to rule out or confirm PAH, and as a next diagnostic step echocardiography is recommended.

Echocardiography

Echocardiography is a noninvasive, inexpensive and widely available technique and therefore attractive as a screening tool to estimate pulmonary pressure and to assess RV function. Yock et al. were the first to find a strong correlation between echo Doppler (DE)-derived estimated pulmonary pressures and RHC derived RV pressures, using the simplified Bernoulli to calculate the pressure gradient between the right ventricle and right atrium. (16) More recent studies showed a tendency of both under- and overestimation using this method, particularly at higher pressures. (17–19) Thus, despite the initial impressive associations, DE derived pressures cannot be used as a substitute for invasive pressure measurements during a RHC. Nevertheless, this method remains a reliable and adequate screening tool for PH. An apical 4-chamber view may give further indications for the diagnosis PH, by showing RV hypertrophy, dilatation or RA dilation.

Assessing the correct diagnosis

When PH is likely based on the results of echocardiography or CT scan, or confirmed by means of RHC, multiple underlying causes should be considered. Noninvasive imaging modalities play an important role in assessing the correct diagnosis. In the following paragraph, the added value of imaging techniques in the diagnostic process will be discussed in the order of the current ERS diagnostic guidelines, depicted in figure 8.1.

1. *Excluding the most common causes of PH: PH due to left heart disease and PH due to hypoxia/lung diseases.*

PH due to left heart disease (PH-LHD), classified as group 2 PH, is the most common cause of PH and is defined as a mPAP > 25 mmHg at rest, accompanied with a pulmonary arterial wedge pressure (PAWP) > 15 mmHg. (20) The presence of PH in combination with predominantly HF with preserved or reduced EF, results in more severe symptoms, worse exercise tolerance and is associated with high morbidity and mortality in comparison to heart failure patients without PH. (21–23) Diagnosing PH-LHD correctly is crucial in the diagnostic

process, given the potential detrimental effects of pre-capillary drugs in patients suffering PH-LHD.

Echocardiography plays a crucial role in diagnosing PH-LHD, in particular by making a distinction between diastolic and systolic heart failure or by showing a combination of both conditions. (25,26) Although the diagnosis of systolic heart failure is straightforward, diagnosing diastolic heart failure remains a challenge. One of the most sensitive echocardiographic parameters to diagnose diastolic heart failure might be left atrial dilatation.(27,28) High resolution chest computed tomography (HRCT) plays a minor role in the diagnostic process of PH-LHD, although mosaic perfusion patterns and ground-glass opacities might be indicative for this type of disease.

The prevalence of PH due to hypoxia/lung diseases varies from 5-36% in chronic obstructive pulmonary disease (COPD) to around 12% in idiopathic pulmonary fibrosis patients (IPF) and an estimated 40% in patients with combined pulmonary fibrosis and emphysema (CPFE).(29–33) Although the sensation of dyspnea and the decreased exercise tolerance in this patient group is usually not primarily due to circulatory limitations, PH is a strong predictor of mortality and therefore important to acknowledge. (34)

Estimating pulmonary pressures may be challenging in group 3 PH patients. Several factors affected by pulmonary diseases, such as hyperinflation of the lungs and alterations in heart position, may influence the accuracy to assess the velocity of the TR jet. In previous studies pulmonary pressures could be estimated in 44-87%, depending of disease severity. (35–38) Moreover, as sensitivity and specificity are lower compared to other PH groups and poor positive predictive value is poor (87%), reliance on echocardiography can lead to overestimation of the prevalence of PH. (37,39,40) Using RV characteristics, PH can reliably be excluded by the absence of RV abnormalities (RV hypertrophy, dilation or systolic dysfunction). (39)

Notably, as COPD and other lung diseases have a high prevalence, the presence of PH may be coincidental. To differentiate between group 1 and group 3, noninvasive imaging may play an important role in combination with pulmonary function test and exercise testing. HRCT plays a crucial role in the assessment of an underlying lung disease as a possible cause of PH (group 3).

2. Chronic Thromboembolic Pulmonary Hypertension (CTEPH)

If PH-LHD and PH due to hypoxia/lung disease are excluded as the underlying cause of PH, the following diagnostic step is to study the probability of CTEPH.

The first description of CTEPH dates back to the 1920s, when Barnes et al. recognized nonresolving thromboemboli as a possible cause of RV failure. (41) Nearly a century later, even though knowledge has increased drastically, pathogenesis is still not fully understood. The main contributors of disease development and progression are persistent vascular obstruction, small vessel arteriopathy and vasoconstriction. (42) Even though it is suggested that 1-4% of patients with acute pulmonary emboli (APE) develop CTEPH, a large subgroup

of CTEPH patients (25-63%) does not have a prehistory of APE or deep venous thrombi, making it challenging to assess true incidence and prevalence. (43–45)

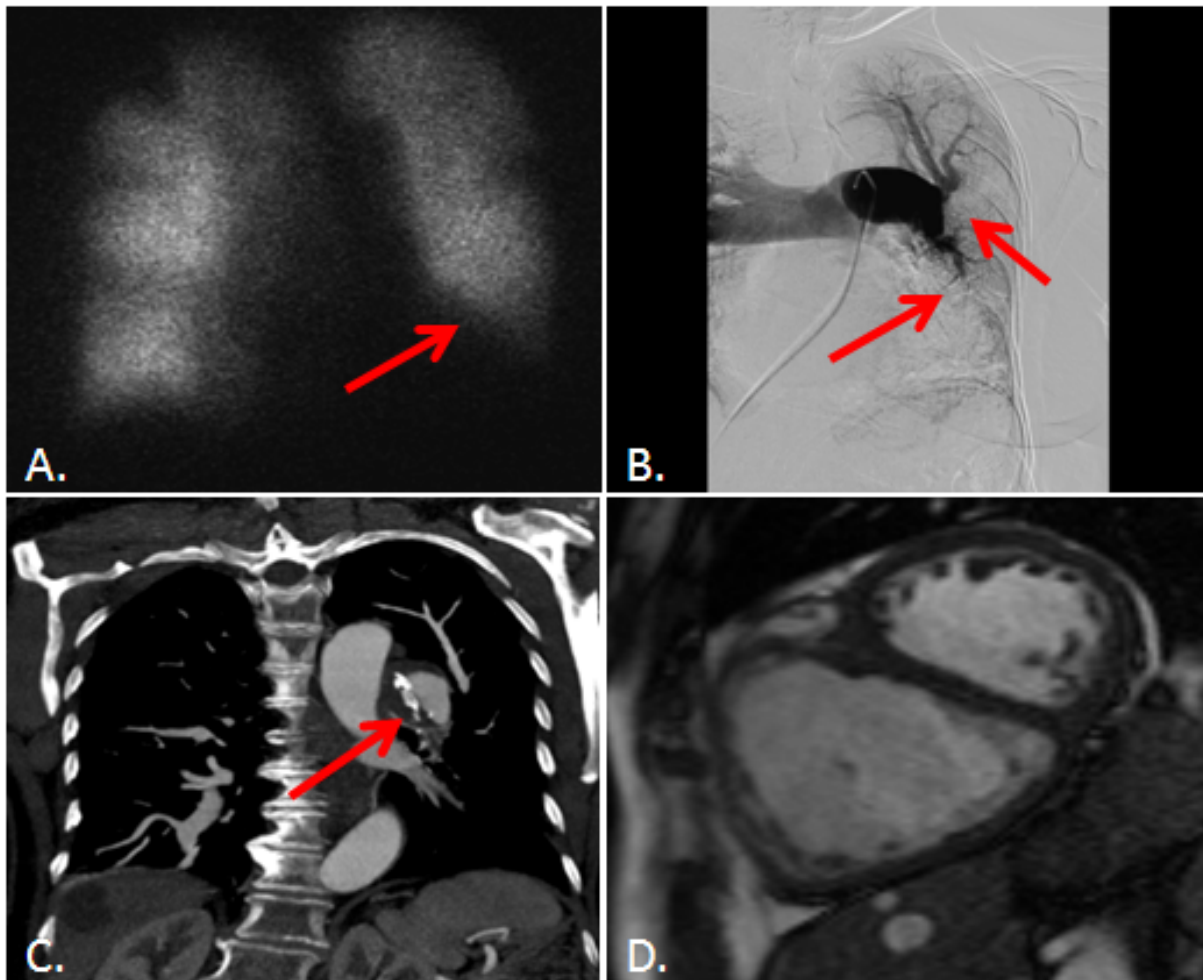
For 60-80% of patients, a potentially curative treatment is available: pulmonary endarterectomy (PEA). This surgical procedure involves the eradication of obstructive tissue from the pulmonary arteries during circulatory arrest. However invasive and considerable mortality rates, long-term outcomes after PEA regarding functional status, quality of life and hemodynamics are very positive. (46–48) Therefore it is of utmost importance to diagnose CTEPH early, and furthermore to recognize patients eligible for PEA.

Diagnosis is based on two criteria: 1) PH ascertained by RHC, 2) at least one larger defect as shown by planar radionuclide ventilation-perfusion scanning (V/Q) after at least three months of adequate anticoagulation therapy.(20,49,50) In recent years, computed tomography angiography (CTA) largely replaced V/Q scanning. However earlier studies suggest a superior sensitivity of V/Q scanning, novel publications show a comparable or non-inferior accuracy of CTA in diagnosing CTEPH. (51–53) A recent study of Rajaram et al. showed a similar sensitivity (94%) using 3D contrast-enhanced lung perfusion MRI, with the advantage of a better assessment of regional perfusion abnormalities without using ionizing radiation. (54)

If V/Q is suggestive for CTEPH, further diagnostic steps are required to assess if patients are suitable for PEA. CTA and pulmonary angiography play an important role in this process. Whereas CTA might be superior in the assessment of more central lesions, pulmonary angiography has superior qualities in imaging more peripheral lesions. Vascular abnormalities which can be observed in CTEPH consist of completely obstructed vessels due to organized thrombi (sudden loss of contrast filled vessels) and partly obstructed vessels (narrowed vasculature, bands, webs). (55) A typical example of CTEPH imaging is depicted in Figure 8.2.

Parenchymal signs visible on CTA may include a mosaic perfusion pattern, bronchial anomalies and focal ground-glass opacities. Moreover, bronchial circulation can a thirty fold increase in CTEPH patients, leading to bronchial hypervascularisation which is visible as dilatation and tortuosity at CTA. (56–58) Recent developments of dual-energy CT (DECT) suggest future possibilities for better detection of peripheral thromboembolic disease. (59,60) The use of MRI in diagnosing CTEPH is upcoming, particularly because of the large benefits considering combined perfusion measurements, MR-angiography and the possibility to assess RV function (54,61)

Figure 8.2 – CTEPH



Images of a 59-year-old chronic thromboembolic pulmonary hypertension (CTEPH) patient. **(A)** ventilation-perfusion scanning (V/Q), **(B)** pulmonary angiography, **(C)** CT angiography and **(D)** cardiac MRI. Arrows indicate perfusion defects **(A and B)** and calcified intraluminal thrombi organisation **(C)**. cMRI shows typical features of a pressure-overloaded right ventricle; RV hypertrophy, dilatation and intraventricular septal flattening (D-shape of the left ventricle).

The less common causes; Pulmonary Arterial Hypertension (PAH) or PH with unclear and/or multifactorial mechanisms

Pulmonary arterial hypertension is primarily a disease of the pulmonary vasculature, characterized by progressive vascular remodeling and narrowing of the precapillary pulmonary arteries. It may be idiopathic (IPAH) or associated with an underlying condition, like congenital heart disease, a genetic mutation (mostly the bone morphogenetic protein receptor 2 mutations (*BMPR2*)) connective tissue disease or HIV/Aids. Despite the different origins, the different groups share a similar clinical presentation and pathological changes of the lung microvasculature.⁽²⁰⁾ As PAH is a rare disease, population-based estimates of incidence and prevalence are not available. However, large registries from France, the United Kingdom and the United States of America report an incidence of 2-8 cases per million

population per year. (9,62–66) Diagnosis is primarily based on absence of other causes of pre-capillary disease, mostly PH due to lung diseases and chronic thromboembolic PH.

Besides clinical history, physical and laboratory analysis and prehistory, noninvasive imaging techniques may give important clues to differentiate within group 1 PAH.

PAH is a common complication in patients born with a congenital heart defect, as a response to a chronic volume overload of the pulmonary circulation, as caused by a left-to-right shunt. Important diagnostic tools to diagnose systemic-to-pulmonary shunts, Eisenmenger's syndrome or small defects are cardiac MRI and transthoracic and/or transesophageal echocardiography. Furthermore, a recent study found that PA calcifications and mural thrombi as found at CT strongly indicate PAH-CHD, as well as centrilobular ground glass opacities. (67)

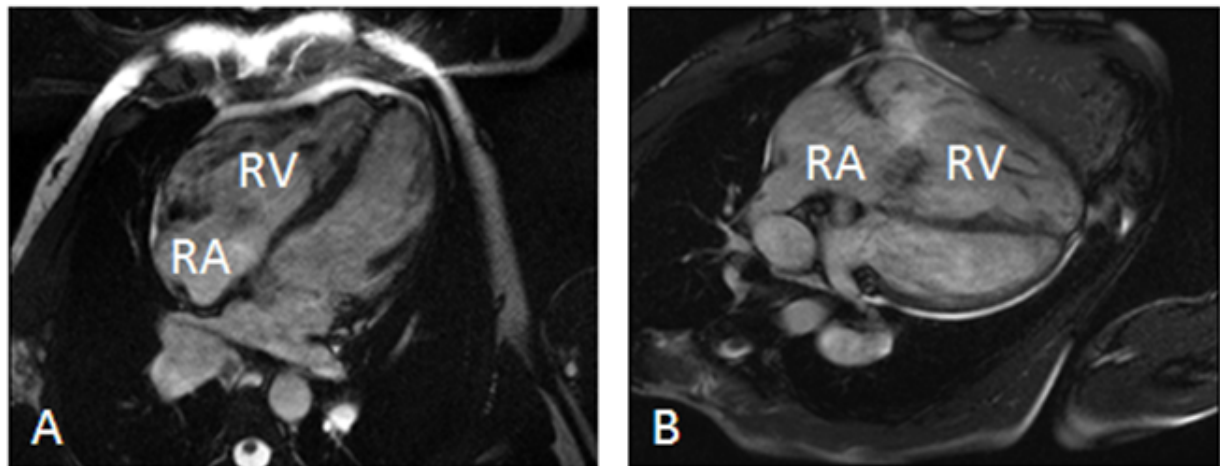
An abdominal ultrasound may be very helpful where there is a clinical suspicion of portal hypertension. To improve diagnostic accuracy, a colour-Doppler examinations may be added. Pulmonary veno-occlusive disease (PVOD) is a very rare cause of pulmonary hypertension and is often misdiagnosed as idiopathic PAH (IPAH). A definite diagnosis can only be assessed via a surgical biopsy, but as this is contraindicated in PH patients, a noninvasive diagnostic approach is needed. Hallmarks at HRCT are typical bilateral thickening of the interlobular septae, ground-glass opacities and interstitial edema. (68–70)

Group 5, PH with unclear and/or multifactorial mechanisms is a very heterogeneous group with different pathogenesis and etiologies, varying from systemic disorders to hematological diseases. Diagnosis is primarily based on physical analysis and laboratory testing.

Disease severity & monitoring

Currently available therapies target the pulmonary vasculature, predominantly by vasodilation. Despite a wide range of therapeutic options, only partial reductions in PVR are achieved. These are not sufficient to achieve normal PVR values in the majority of patients, and therefore insufficient to prevent progression to right heart failure in PAH patients. (71) Furthermore, there is a very heterogeneous response to an increased afterload, independent of the amount of pressure itself, as is illustrated in Figure 8.3. As RV function is closely related to prognosis, measures for systolic (RV ejection fraction (RVEF), tricuspid annular systolic excursion (TAPSE) and RV fractional area change (FAC)) and diastolic function (RV end diastolic volume (EDV) and isovolumic relaxation (IVRT)) are the most important focus of monitoring PH-patients. The practicality as a monitoring tool for CT is limited due to its relatively high radiation use and lack of clinical applicable parameters which have proven to be reflective of changes in pressures or function. Meanwhile, a broad range of cardiac MRI and echocardiography parameters have proven to be reproducible, prognostic and sensitive to treatment. (4,6,72–74)

Figure 8.3 – Cardiac adaptation is independent of pressure overload



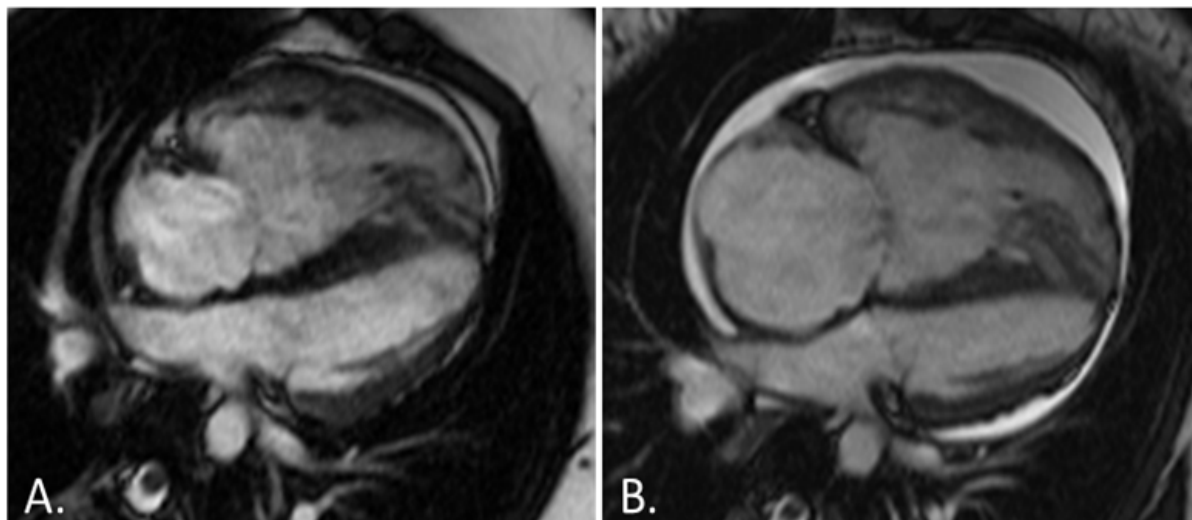
Cardiac adaptation is independent of pressure-overload. Four-chamber cardiac MRI obtained for two patients with a different cardiac response to a similar pressure overload. A) The adapted right ventricle (RV) of patient A shows a hypertrophied RV accompanied by a small right atrium (RA). B) The failing RV of patient B shows RV dilatation together with a dilated RA, despite an even lower pressure overload (mean pulmonary artery pressure of 45 mmHg (patient B) compared to 55 mmHg (patient A)).

Echocardiography

Echocardiography is a widely used monitoring tool in PAH, supported by an excellent cost-effectiveness, widespread availability and safety. Despite difficulties assessing the complex anatomy of the highly trabeculated RV using two-dimensional imaging, transthoracic echocardiography and Doppler imaging can provide important information on chamber sizes and LV and RV function. (26,75) A major drawback in the evidence of using echocardiography in the follow-up of PH-patients is the lack of longitudinal studies assessing echocardiographic parameters over time.

A comprehensive summary of echocardiographic values of the right heart is offered by the American Society of Echocardiography guidelines.(26) The two most important parameters of RV systolic function are TAPSE and RV fractional area change (RV FAC). TAPSE is a measure assessing longitudinal shortening. In contrast to the LV, which contracts almost uniformly in both the transverse and longitudinal plane, the RV contracts predominantly along the longitudinal plane. (76) Baseline measurements of TAPSE have proven to be of great prognostic importance.(72) In end-stage disease, longitudinal shortening reaches a lower limit, where-after RV function deteriorates due to a loss of circumferential shortening. (77) The second parameter, RV FAC, combines longitudinal and transverse RV shortening. It has been shown that this parameter best reflects MRI-derived RVEF. (78,79) However, assessing RV-FAC might be challenging in severely dilated RVs.

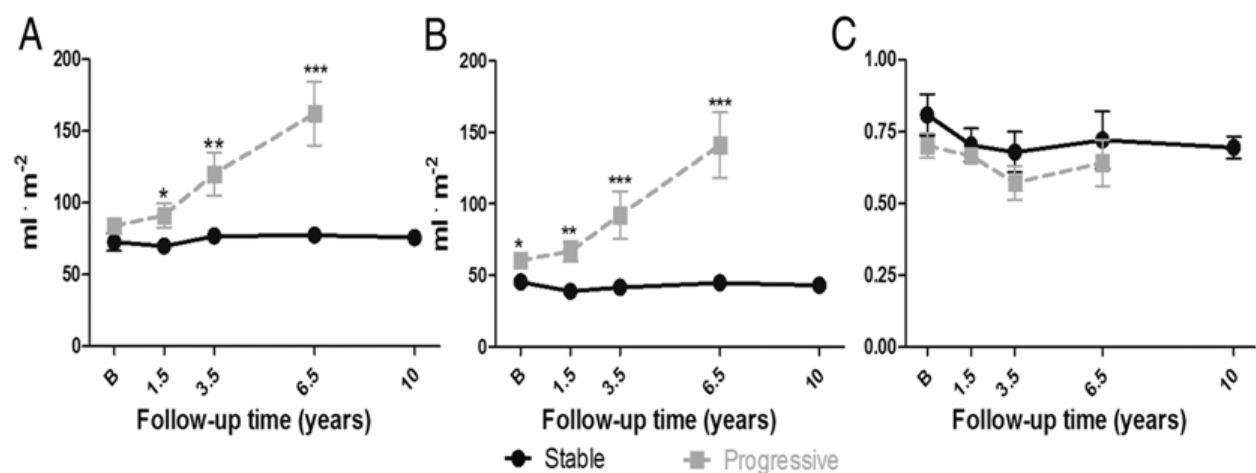
Figure 8.4 – Pulmonary hypertension over time



Scans of an idiopathic pulmonary arterial hypertension patient at a) baseline and b) after 3 years of follow-up. A) a compensated right heart is shown, consisting of a hypertrophied right ventricle (RV), relatively small right atrium (RA) and no pericardial effusion. B) a failing dilated RV is shown, together with a dilated RA and pericardial effusion.

Recent advances in echocardiography have led to the emerge of promising new 2D-techniques. RV strain is a measurement of myocardial deformation. The myocardium deforms via longitudinal and circumferential shortening as a result of sarcomere shortening. Using RV strain, global and regional assessment of RV function can be assessed. A worsening RV systolic strain is associated with increased pulmonary pressures and decreased functional class.(80,81) Furthermore, it has been shown that RV systolic strain predicts morbidity and mortality and is able to improve after PH therapy.(82) However, as no normative values are available yet, more research and experience is needed before applicable in clinical practice.

Figure 8.5 – The importance of right ventricular function



A) RV end-diastolic and B) RV end-systolic volume increased progressively in patients whose disease was progressing, but remained unchanged in stable patients (interaction p -value for both <0.01). C) RV relative wall thickness was comparable in both groups at follow-up. Data are shown as mean \pm SEM. B:

*Baseline. * $p < 0.05$ between groups; ** $p < 0.01$ between groups; ***: $p < 0.001$ between groups. Reproduced and modified from [81] with permission of the publisher.*

MRI

Cardiac MRI (cMRI) provides high-resolution, 3D-, accurate quantitative information of ventricular volumes, mass, flows, structure and function without the use of ionizing radiation and toxic contrast agents. Furthermore, cMRI is the golden standard to assess cardiac volumes. Despite the higher costs, limited accessibility and a more time-consuming analysis, cMRI is regarded as the ideal monitoring tool of patients with PAH. Figure 8.4 illustrates cMRIs of a PH patient over time.

Stroke volume, RV volumes, RVEF and LV end-diastolic volume have shown to be strongly predictive of survival both at baseline and during follow-up. (6,71) Interestingly, the presence of a dilating RV and atrophying LV may be observed before clinical symptoms manifest, providing the opportunity to intervene in an early stage of RV failure, as depicted in Figure 8.5. (83) One of the key measurements of systolic RV function is RVEF, calculated by dividing stroke volume by end diastolic volume. Underscoring the importance of this measure, van de Veerdonk et al. showed that changes in RVEF and not in PVR predict outcome. (71)

More detailed information about the RV myocardium can be obtained using MRI tagging to assess myocardial deformation and delayed contrast enhancement imaging with gadolinium or by T1-mapping to assess regional fibrosis.(84–86) Delayed contrast enhancement was found at the interventricular insertion points, suggesting focal fibrosis.(15,87,88) No studies have been published so far to study the significance and usefulness of these measurements in the follow-up of PH patients.

Besides the cardiac developments in MRI, recent studies focus on the role of MRI in estimating pulmonary pressures. A reliable noninvasive measure for pulmonary hemodynamics is an interesting and popular research topic, as it could make the invasive RHC unnecessary. Promising results in studies of Reiter et al. and Kreitner et al. indicate that the use of MRI derived velocity parameters enable an accurate noninvasive assessment of pulmonary hemodynamics. (89–91) However, further research in multiple subgroups of PH-patients are needed before applicable in clinical practice.

CONCLUSION

Noninvasive imaging techniques have a clear and vital role in both diagnosis and follow-up of PH patients. The initial tools to recognize PH are echocardiography and CT, however RHC is still inevitable for a definitive diagnosis. Subsequently, various noninvasive imaging techniques can be performed, depending on clinical suspicion and prehistory. The most common forms of PH, group 2 and 3, can be excluded using respectively echocardiography and HRCT. A V/Q scan followed by an CTA or pulmonary angiography gives additional information about the presence of chronic pulmonary emboli, as seen in CTEPH. As a monitoring tool, CMRI is the most informative and accurate step, followed by

echocardiography. Future imaging techniques will focus on more insight into the RV myocardium, but it is still questionable whether these techniques will eventually be applicable in clinical practice.

REFERENCES

1. Simonneau G, Gatzoulis MA, Adatia I, Celermajer D, Denton C, Ghofrani A, et al. Updated clinical classification of pulmonary hypertension. *J Am Coll Cardiol*. 2013 Dec 24;62(25 Suppl):D34–41.
2. Van de Veerdonk MC, Kind T, Marcus JT, Mauritz G-J, Heymans MW, Bogaard H-J, et al. Progressive Right Ventricular Dysfunction in Patients With Pulmonary Arterial Hypertension Responding to Therapy. *J Am Coll Cardiol*. 2011 Dec 6;58(24):2511–9.
3. Forfia PR, Fisher MR, Mathai SC, Houston-Harris T, Hemnes AR, Borlaug BA, et al. Tricuspid annular displacement predicts survival in pulmonary hypertension. *Am J Respir Crit Care Med*. 2006 Nov 1;174(9):1034–41.
4. Ghio S, Pazzano AS, Klersy C, Scelsi L, Raineri C, Camporotondo R, et al. Clinical and prognostic relevance of echocardiographic evaluation of right ventricular geometry in patients with idiopathic pulmonary arterial hypertension. *Am J Cardiol*. 2011 Feb 15;107(4):628–32.
5. Benza RL, Miller DP, Gomberg-Maitland M, Frantz RP, Foreman AJ, Coffey CS, et al. Predicting survival in pulmonary arterial hypertension: insights from the Registry to Evaluate Early and Long-Term Pulmonary Arterial Hypertension Disease Management (REVEAL). *Circulation*. 2010 Jul 13;122(2):164–72.
6. Van Wolferen SA, Marcus JT, Boonstra A, Marques KMJ, Bronzwaer JGF, Spreeuwenberg MD, et al. Prognostic value of right ventricular mass, volume, and function in idiopathic pulmonary arterial hypertension. *Eur Heart J*. 2007 May;28(10):1250–7.
7. Badesch DB, Raskob GE, Elliott CG, Krichman AM, Farber HW, Frost AE, et al. Pulmonary arterial hypertension: baseline characteristics from the REVEAL Registry. *Chest*. 2010 Feb;137(2):376–87.
8. Strange G, Gabbay E, Kermeen F, Williams T, Carrington M, Stewart S, et al. Time from symptoms to definitive diagnosis of idiopathic pulmonary arterial hypertension: The delay study. *Pulm Circ*. 2013 Jan;3(1):89–94.
9. Ling Y, Johnson MK, Kiely DG, Condliffe R, Elliot CA, Gibbs JSR, et al. Changing demographics, epidemiology, and survival of incident pulmonary arterial hypertension: results from the pulmonary hypertension registry of the United Kingdom and Ireland. *Am J Respir Crit Care Med*. 2012 Oct 15;186(8):790–6.
10. Ng CS, Wells AU, Padley SP. A CT sign of chronic pulmonary arterial hypertension: the ratio of main pulmonary artery to aortic diameter. *J Thorac Imaging*. 1999 Oct;14(4):270–8.
11. Tan RT, Kuzo R, Goodman LR, Siegel R, Haasler GB, Presberg KW. Utility of CT scan evaluation for predicting pulmonary hypertension in patients with parenchymal lung disease. Medical College of Wisconsin Lung Transplant Group. *Chest*. 1998 May;113(5):1250–6.
12. Sanal S, Aronow WS, Ravipati G, Maguire GP, Belkin RN, Lehrman SG. Prediction of moderate or severe pulmonary hypertension by main pulmonary artery diameter and main pulmonary artery diameter/ascending aorta diameter in pulmonary embolism. *Cardiol Rev*. 2006 Oct;14(5):213–4.
13. Gan CT-J, Lankhaar J-W, Westerhof N, Marcus JT, Becker A, Twisk JWR, et al. Noninvasively assessed pulmonary artery stiffness predicts mortality in pulmonary arterial hypertension. *Chest*. 2007 Dec;132(6):1906–12.
14. Shen Y, Wan C, Tian P, Wu Y, Li X, Yang T, et al. CT-base pulmonary artery measurement in the detection of pulmonary hypertension: a meta-analysis and systematic review. *Medicine (Baltimore)*. 2014 Dec;93(27):e256.
15. Spruijt OA, Bogaard H-J, Heijmans MW, Lely RJ, van de Veerdonk MC, de Man FS, et al. Predicting pulmonary hypertension with standard computed tomography pulmonary angiography. *Int J Cardiovasc Imaging*. 2015 Apr;31(4):871–9.
16. Yock PG, Popp RL. Noninvasive estimation of right ventricular systolic pressure by Doppler ultrasound in patients with tricuspid regurgitation. *Circulation*. 1984 Oct;70(4):657–62.
17. Hinderliter AL, Willis PW, Barst RJ, Rich S, Rubin LJ, Badesch DB, et al. Effects of long-term infusion of prostacyclin (epoprostenol) on echocardiographic measures of right ventricular structure and function in

primary pulmonary hypertension. Primary Pulmonary Hypertension Study Group. *Circulation*. 1997 Mar 18;95(6):1479–86.

18. Fisher MR, Forfia PR, Chamera E, Houston-Harris T, Champion HC, Girgis RE, et al. Accuracy of Doppler echocardiography in the hemodynamic assessment of pulmonary hypertension. *Am J Respir Crit Care Med*. 2009 Apr 1;179(7):615–21.

19. Greiner S, Jud A, Aurich M, Hess A, Hilbel T, Hardt S, et al. Reliability of noninvasive assessment of systolic pulmonary artery pressure by Doppler echocardiography compared to right heart catheterization: analysis in a large patient population. *J Am Heart Assoc*. 2014 Aug;3(4).

20. Galiè N, Hoeper MM, Humbert M, Torbicki A, Vachiery J-L, Barbera JA, et al. Guidelines for the diagnosis and treatment of pulmonary hypertension: the Task Force for the Diagnosis and Treatment of Pulmonary Hypertension of the European Society of Cardiology (ESC) and the European Respiratory Society (ERS), endorsed by the International Society of Heart and Lung Transplantation (ISHLT). *Eur Heart J*. 2009 Oct;30(20):2493–537.

21. Guazzi M, Borlaug BA. Pulmonary hypertension due to left heart disease. *Circulation*. 2012 Aug 21;126(8):975–90.

22. Fang JC, DeMarco T, Givertz MM, Borlaug BA, Lewis GD, Rame JE, et al. World Health Organization Pulmonary Hypertension group 2: pulmonary hypertension due to left heart disease in the adult—a summary statement from the Pulmonary Hypertension Council of the International Society for Heart and Lung Transplantation. *J Heart Lung Transplant Off Publ Int Soc Heart Transplant*. 2012 Sep;31(9):913–33.

23. Ghio S, Gavazzi A, Campana C, Inerra C, Klersy C, Sebastiani R, et al. Independent and additive prognostic value of right ventricular systolic function and pulmonary artery pressure in patients with chronic heart failure. *J Am Coll Cardiol*. 2001 Jan;37(1):183–8.

24. Lundgren J, Rådegran G. Pathophysiology and potential treatments of pulmonary hypertension due to systolic left heart failure. *Acta Physiol Oxf Engl*. 2014 Jun;211(2):314–33.

25. Lang RM, Badano LP, Mor-Avi V, Afalalo J, Armstrong A, Ernande L, et al. Recommendations for cardiac chamber quantification by echocardiography in adults: an update from the American Society of Echocardiography and the European Association of Cardiovascular Imaging. *J Am Soc Echocardiogr Off Publ Am Soc Echocardiogr*. 2015 Jan;28(1):1–39.e14.

26. Rudski LG, Lai WW, Afalalo J, Hua L, Handschumacher MD, Chandrasekaran K, et al. Guidelines for the echocardiographic assessment of the right heart in adults: a report from the American Society of Echocardiography endorsed by the European Association of Echocardiography, a registered branch of the European Society of Cardiology, and the Canadian Society of Echocardiography. *J Am Soc Echocardiogr Off Publ Am Soc Echocardiogr*. 2010 Jul;23(7):685–713; quiz 786–8.

27. Kurt M, Wang J, Torre-Amione G, Nagueh SF. Left Atrial Function in Diastolic Heart Failure. *Circ Cardiovasc Imaging*. 2009 Jan 1;2(1):10–5.

28. Motoki H, Borowski AG, Shrestha K, Troughton RW, Martin MG, Tang WHW, et al. Impact of left ventricular diastolic function on left atrial mechanics in systolic heart failure. *Am J Cardiol*. 2013 Sep 15;112(6):821–6.

29. Andersen KH, Iversen M, Kjaergaard J, Mortensen J, Nielsen-Kudsk JE, Bendstrup E, et al. Prevalence, predictors, and survival in pulmonary hypertension related to end-stage chronic obstructive pulmonary disease. *J Heart Lung Transplant Off Publ Int Soc Heart Transplant*. 2012 Apr;31(4):373–80.

30. Hamada K, Nagai S, Tanaka S, Handa T, Shigematsu M, Nagao T, et al. Significance of pulmonary arterial pressure and diffusion capacity of the lung as prognosticator in patients with idiopathic pulmonary fibrosis. *Chest*. 2007 Mar;131(3):650–6.

31. Kimura M, Taniguchi H, Kondoh Y, Kimura T, Kataoka K, Nishiyama O, et al. Pulmonary hypertension as a prognostic indicator at the initial evaluation in idiopathic pulmonary fibrosis. *Respir Int Rev Thorac Dis*. 2013;85(6):456–63.

32. Cottin V, Le Pavec J, Prévot G, Mal H, Humbert M, Simonneau G, et al. Pulmonary hypertension in patients with combined pulmonary fibrosis and emphysema syndrome. *Eur Respir J*. 2010 Jan;35(1):105–11.

33. Chaouat A, Bugnet A-S, Kadaoui N, Schott R, Enache I, Ducoloné A, et al. Severe pulmonary hypertension and chronic obstructive pulmonary disease. *Am J Respir Crit Care Med*. 2005 Jul 15;172(2):189–94.

34. Oswald-Mammoser M, Weitzenblum E, Quoix E, Moser G, Chaouat A, Charpentier C, et al. Prognostic factors in COPD patients receiving long-term oxygen therapy. Importance of pulmonary artery pressure. *Chest*. 1995 May;107(5):1193–8.

35. Torbicki A, Skwarski K, Hawrylkiewicz I, Pasierski T, Miskiewicz Z, Zielinski J. Attempts at measuring pulmonary arterial pressure by means of Doppler

echocardiography in patients with chronic lung disease. *Eur Respir J*. 1989 Oct;2(9):856–60.

36. Homma A, Anzueto A, Peters JL, Susanto I, Sako E, Zabalgoitia M, et al. Pulmonary artery systolic pressures estimated by echocardiogram vs cardiac catheterization in patients awaiting lung transplantation. *J Heart Lung Transplant Off Publ Int Soc Heart Transplant*. 2001 Aug;20(8):833–9.

37. Tamarin R, Torbicki A, Marchandise B, Laaban JP, Morpurgo M. Doppler echocardiographic evaluation of pulmonary artery pressure in chronic obstructive pulmonary disease. A European multicentre study. Working Group on Noninvasive Evaluation of Pulmonary Artery Pressure. European Office of the World Health Organization, Copenhagen. *Eur Heart J*. 1991 Feb;12(2):103–11.

38. Bach DS, Curtis JL, Christensen PJ, Iannettoni MD, Whyte RI, Kazerooni EA, et al. Preoperative echocardiographic evaluation of patients referred for lung volume reduction surgery. *Chest*. 1998 Oct;114(4):972–80.

39. Arcasoy SM, Christie JD, Ferrari VA, Sutton MSJ, Zisman DA, Blumenthal NP, et al. Echocardiographic assessment of pulmonary hypertension in patients with advanced lung disease. *Am J Respir Crit Care Med*. 2003 Mar 1;167(5):735–40.

40. Laaban JP, Diebold B, Zelinski R, Lafay M, Raffoul H, Rochemaure J. Noninvasive estimation of systolic pulmonary artery pressure using Doppler echocardiography in patients with chronic obstructive pulmonary disease. *Chest*. 1989 Dec;96(6):1258–62.

41. Barnes AR, Yater WM. Failure of Right Ventricle Due to Ancient Thrombus. *M Clin North America*. 1929;(12):1610.

42. Piazza G, Goldhaber SZ. Chronic Thromboembolic Pulmonary Hypertension. *N Engl J Med*. 2011 Jan 27;364(4):351–60.

43. Becattini C, Agnelli G, Pesavento R, Silingardi M, Poggio R, Taliani MR, et al. Incidence of chronic thromboembolic pulmonary hypertension after a first episode of pulmonary embolism. *Chest*. 2006 Jul;130(1):172–5.

44. Pengo V, Lensing AWA, Prins MH, Marchiori A, Davidson BL, Tiozzo F, et al. Incidence of chronic thromboembolic pulmonary hypertension after pulmonary embolism. *N Engl J Med*. 2004 May 27;350(22):2257–64.

45. Riedel M, Stanek V, Widimsky J, Prerovsky I. Longterm follow-up of patients with pulmonary thromboembolism. Late prognosis and evolution of

hemodynamic and respiratory data. *Chest*. 1982 Feb;81(2):151–8.

46. Jenkins D. Pulmonary endarterectomy: the potentially curative treatment for patients with chronic thromboembolic pulmonary hypertension. *Eur Respir Rev*. 2015 Jun 1;24(136):263–71.

47. Ishida K, Masuda M, Tanabe N, Matsumiya G, Tatsumi K, Nakajima N. Long-term outcome after pulmonary endarterectomy for chronic thromboembolic pulmonary hypertension. *J Thorac Cardiovasc Surg*. 2012 Aug;144(2):321–6.

48. Mayer E, Klepetko W. Techniques and Outcomes of Pulmonary Endarterectomy for Chronic Thromboembolic Pulmonary Hypertension. *Proc Am Thorac Soc*. 2006 Sep 1;3(7):589–93.

49. Wilkens H, Lang I, Behr J, Berghaus T, Grohe C, Guth S, et al. Chronic thromboembolic pulmonary hypertension (CTEPH): updated Recommendations of the Cologne Consensus Conference 2011. *Int J Cardiol*. 2011 Dec;154 Suppl 1:S54–60.

50. Condliffe R, Kiely DG, Gibbs JSR, Corris PA, Peacock AJ, Jenkins DP, et al. Prognostic and aetiological factors in chronic thromboembolic pulmonary hypertension. *Eur Respir J*. 2009 Feb 1;33(2):332–8.

51. He J, Fang W, Lv B, He J-G, Xiong C-M, Liu Z-H, et al. Diagnosis of chronic thromboembolic pulmonary hypertension: comparison of ventilation/perfusion scanning and multidetector computed tomography pulmonary angiography with pulmonary angiography. *Nucl Med Commun*. 2012 May;33(5):459–63.

52. Sugiura T, Tanabe N, Matsuura Y, Shigeta A, Kawata N, Jujo T, et al. ROle of 320-slice ct imaging in the diagnostic workup of patients with chronic thromboembolic pulmonary hypertension. *Chest*. 2013 Apr 1;143(4):1070–7.

53. Tanabe N, Sugiura T, Tatsumi K. Recent progress in the diagnosis and management of chronic thromboembolic pulmonary hypertension. *Respir Investig*. 2013 Sep;51(3):134–46.

54. Rajaram S, Swift AJ, Telfer A, Hurdman J, Marshall H, Lorenz E, et al. 3D contrast-enhanced lung perfusion MRI is an effective screening tool for chronic thromboembolic pulmonary hypertension: results from the ASPIRE Registry. *Thorax*. 2013 Jul;68(7):677–8.

55. Ley S, Ley-Zaporozhan J, Pitton MB, Schneider J, Wirth GM, Mayer E, et al. Diagnostic performance of state-of-the-art imaging techniques for morphological

assessment of vascular abnormalities in patients with chronic thromboembolic pulmonary hypertension (CTEPH). *Eur Radiol*. 2011 Sep 27;22(3):607–16.

56. Endrys J, Hayat N, Cherian G. Comparison of bronchopulmonary collaterals and collateral blood flow in patients with chronic thromboembolic and primary pulmonary hypertension. *Heart Br Card Soc*. 1997 Aug;78(2):171–6.

57. Ley S, Kreitner K-F, Morgenstern I, Thelen M, Kauczor H-U. Bronchopulmonary shunts in patients with chronic thromboembolic pulmonary hypertension: evaluation with helical CT and MR imaging. *AJR Am J Roentgenol*. 2002 Nov;179(5):1209–15.

58. Shimizu H, Tanabe N, Terada J, Masuda M, Sakao S, Kasahara Y, et al. Dilatation of bronchial arteries correlates with extent of central disease in patients with chronic thromboembolic pulmonary hypertension. *Circ J Off J Jpn Circ Soc*. 2008 Jul;72(7):1136–41.

59. Ameli-Renani S, Rahman F, Nair A, Ramsay L, Bacon JL, Weller A, et al. Dual-energy CT for imaging of pulmonary hypertension: challenges and opportunities. *Radiogr Rev Publ Radiol Soc N Am Inc*. 2014 Dec;34(7):1769–90.

60. Dournes G, Verdier D, Montaudon M, Bullier E, Rivière A, Dromer C, et al. Dual-energy CT perfusion and angiography in chronic thromboembolic pulmonary hypertension: diagnostic accuracy and concordance with radionuclide scintigraphy. *Eur Radiol*. 2014 Jan;24(1):42–51.

61. Henzler T, Schmid-Bindert G, Schoenberg SO, Fink C. Diffusion and perfusion MRI of the lung and mediastinum. *Eur J Radiol*. 2010 Dec;76(3):329–36.

62. Peacock AJ, Murphy NF, McMurray JJV, Caballero L, Stewart S. An epidemiological study of pulmonary arterial hypertension. *Eur Respir J*. 2007 Jul;30(1):104–9.

63. Humbert M, Sitbon O, Chaouat A, Bertocchi M, Habib G, Gressin V, et al. Pulmonary arterial hypertension in France: results from a national registry. *Am J Respir Crit Care Med*. 2006 May 1;173(9):1023–30.

64. Tueller C, Stricker H, Soccal P, Tamm M, Aubert J-D, Maggiorini M, et al. Epidemiology of pulmonary hypertension: new data from the Swiss registry. *Swiss Med Wkly*. 2008 Jun 28;138(25-26):379–84.

65. Hurdman J, Condliffe R, Elliot CA, Davies C, Hill C, Wild JM, et al. ASPIRE registry: assessing the Spectrum

of Pulmonary hypertension Identified at a REferral centre. *Eur Respir J*. 2012 Apr;39(4):945–55.

66. Frost AE, Badesch DB, Barst RJ, Benza RL, Elliott CG, Farber HW, et al. The changing picture of patients with pulmonary arterial hypertension in the United States: how REVEAL differs from historic and non-US Contemporary Registries. *Chest*. 2011 Jan;139(1):128–37.

67. Rajaram S, Swift AJ, Condliffe R, Johns C, Elliot CA, Hill C, et al. CT features of pulmonary arterial hypertension and its major subtypes: a systematic CT evaluation of 292 patients from the ASPIRE Registry. *Thorax*. 2015 Apr;70(4):382–7.

68. Montani D, Achouh L, Dorfmueller P, Le Pavec J, Sztrymf B, Tchérakian C, et al. Pulmonary veno-occlusive disease: clinical, functional, radiologic, and hemodynamic characteristics and outcome of 24 cases confirmed by histology. *Medicine (Baltimore)*. 2008 Jul;87(4):220–33.

69. Montani D, Price LC, Dorfmueller P, Achouh L, Jaïs X, Yaïci A, et al. Pulmonary veno-occlusive disease. *Eur Respir J*. 2009 Jan 1;33(1):189–200.

70. Resten A, Maitre S, Humbert M, Rabiller A, Sitbon O, Capron F, et al. Pulmonary hypertension: CT of the chest in pulmonary venoocclusive disease. *AJR Am J Roentgenol*. 2004 Jul;183(1):65–70.

71. Van de Veerdonk MC, Kind T, Marcus JT, Mauritz G-J, Heymans MW, Bogaard H-J, et al. Progressive right ventricular dysfunction in patients with pulmonary arterial hypertension responding to therapy. *J Am Coll Cardiol*. 2011 Dec 6;58(24):2511–9.

72. Forfia PR, Fisher MR, Mathai SC, Houston-Harris T, Hemnes AR, Borlaug BA, et al. Tricuspid annular displacement predicts survival in pulmonary hypertension. *Am J Respir Crit Care Med*. 2006 Nov 1;174(9):1034–41.

73. Yeo TC, Dujardin KS, Tei C, Mahoney DW, McGoon MD, Seward JB. Value of a Doppler-derived index combining systolic and diastolic time intervals in predicting outcome in primary pulmonary hypertension. *Am J Cardiol*. 1998 May 1;81(9):1157–61.

74. Raymond RJ, Hinderliter AL, Willis I, Park W, Ralph D, Caldwell EJ, Williams W, et al. Echocardiographic predictors of adverse outcomes in primary pulmonary hypertension. *J Am Coll Cardiol*. 2002 Apr 3;39(7):1214–9.

75. McLaughlin VV, Archer SL, Badesch DB, Barst RJ, Farber HW, Lindner JR, et al. ACCF/AHA 2009 Expert Consensus Document on Pulmonary Hypertension: A Report of the American College of Cardiology Foundation Task Force on Expert Consensus Documents and the American

Heart Association Developed in Collaboration With the American College of Chest Physicians; American Thoracic Society, Inc.; and the Pulmonary Hypertension Association. *J Am Coll Cardiol*. 2009 Apr 28;53(17):1573–619.

76. Rushmer RF, Crystal DK, Wagner C. The Functional Anatomy of Ventricular Contraction. *Circ Res*. 1953 Mar 1;1(2):162–70.

77. Gert-Jan Mauritz TK. Progressive Changes in Right Ventricular Geometric Shortening and Long-term Survival in Pulmonary Arterial Hypertension. *Chest*. 2011;141(4):935–43.

78. Shiran H, Zamanian RT, McConnell MV, Liang DH, Dash R, Heidary S, et al. Relationship between echocardiographic and magnetic resonance derived measures of right ventricular size and function in patients with pulmonary hypertension. *J Am Soc Echocardiogr Off Publ Am Soc Echocardiogr*. 2014 Apr;27(4):405–12.

79. Kind T, Mauritz G-J, Marcus JT, van de Veerdonk M, Westerhof N, Vonk-Noordegraaf A. Right ventricular ejection fraction is better reflected by transverse rather than longitudinal wall motion in pulmonary hypertension. *J Cardiovasc Magn Reson*. 2010;12(1):35.

80. Haeck MLA, Scherptong RWC, Marsan NA, Holman ER, Schalij MJ, Bax JJ, et al. Prognostic Value of Right Ventricular Longitudinal Peak Systolic Strain in Patients With Pulmonary Hypertension. *Circ Cardiovasc Imaging*. 2012 Sep 1;5(5):628–36.

81. Li Y, Xie M, Wang X, Lu Q, Fu M. Right ventricular regional and global systolic function is diminished in patients with pulmonary arterial hypertension: a 2-dimensional ultrasound speckle tracking echocardiography study. *Int J Cardiovasc Imaging*. 2013 Mar;29(3):545–51.

82. Hardegree EL, Sachdev A, Villarraga HR, Frantz RP, McGoon MD, Kushwaha SS, et al. Role of serial quantitative assessment of right ventricular function by strain in pulmonary arterial hypertension. *Am J Cardiol*. 2013 Jan 1;111(1):143–8.

83. Van de Veerdonk MC, Marcus JT, Westerhof N, de Man FS, Boonstra A, Heymans MW, et al. Signs of right ventricular deterioration in clinically stable patients with pulmonary arterial hypertension. *Chest*. 2015 Apr 1;147(4):1063–71.

84. García-Álvarez A, García-Lunar I, Pereda D, Fernández-Jimenez R, Sánchez-González J, Mirelis JG, et al. Association of myocardial T1-mapping CMR with hemodynamics and RV performance in pulmonary hypertension. *JACC Cardiovasc Imaging*. 2015 Jan;8(1):76–82.

85. Shehata ML, Harouni AA, Skrok J, Basha TA, Boyce D, Lechtzin N, et al. Regional and global biventricular function in pulmonary arterial hypertension: a cardiac MR imaging study. *Radiology*. 2013 Jan;266(1):114–22.

86. Mewton N, Liu CY, Croisille P, Bluemke D, Lima JAC. Assessment of myocardial fibrosis with cardiovascular magnetic resonance. *J Am Coll Cardiol*. 2011 Feb 22;57(8):891–903.

87. Blyth KG, Groenning BA, Martin TN, Foster JE, Mark PB, Dargie HJ, et al. Contrast enhanced-cardiovascular magnetic resonance imaging in patients with pulmonary hypertension. *Eur Heart J*. 2005 Oct;26(19):1993–9.

88. McCann GP, Gan CT, Beek AM, Niessen HWM, Vonk Noordegraaf A, van Rossum AC. Extent of MRI delayed enhancement of myocardial mass is related to right ventricular dysfunction in pulmonary artery hypertension. *AJR Am J Roentgenol*. 2007 Feb;188(2):349–55.

89. Reiter G, Reiter U, Kovacs G, Kainz B, Schmidt K, Maier R, et al. Magnetic Resonance–Derived 3-Dimensional Blood Flow Patterns in the Main Pulmonary Artery as a Marker of Pulmonary Hypertension and a Measure of Elevated Mean Pulmonary Arterial Pressure. *Circ Cardiovasc Imaging*. 2008 Jul 1;1(1):23–30.

90. Reiter G, Reiter U, Kovacs G, Olschewski H, Fuchsjäger M. Blood flow vortices along the main pulmonary artery measured with MR imaging for diagnosis of pulmonary hypertension. *Radiology*. 2015 Apr;275(1):71–9.

91. Kreitner K-F, Wirth GM, Krummenauer F, Weber S, Pitton MB, Schneider J, et al. Noninvasive assessment of pulmonary hemodynamics in patients with chronic thromboembolic pulmonary hypertension by high temporal resolution phase-contrast MRI: correlation with simultaneous invasive pressure recordings. *Circ Cardiovasc Imaging*. 2013 Sep;6(5):722–9.

9

SUMMARY AND FUTURE PERSPECTIVES

Cathelijne E.E. van der Bruggen

SUMMARY

Pulmonary arterial hypertension (PAH) is a disease in which the lumen of small pulmonary arteries is narrowed because of vasoconstriction, hyperproliferation, inflammation and remodeling of smooth muscle cells and endothelial cells. This leads to an increase in resistance of the pulmonary vascular bed and an therefore an increase in pulmonary artery pressures. As a result the load on the right ventricle (RV) drastically increases, with a subsequent rise in RV wall stress. The RV will initially decrease this wall stress via increasing its wall thickness through hypertrophy and enhancing its contractility. Current PAH-medication decreases the pulmonary vascular resistance (PVR) and therefore reduce the RV afterload, but seldom normalizes it. As a result, the transition of RV adaptation towards RV failure, characterized by RV dilatation and decreased cardiac output, will be inevitable. To date, lung transplantation is the only cure for PAH-patients. To provide timely referral to a transplantation center, it is of utmost importance to identify 'adapted' PAH-patients who are prone to develop RV failure. To do so, key players in the transition from RV adaptation towards RV failure have to be identified. In this thesis, we aimed to further identify factors playing a role in RV adaptation and RV failure by comparing different phenotypes of PAH patients. Secondly, we evaluated the use of RV imaging during follow-up in PAH.

Part 1 – Right ventricular adaptation in Pulmonary Arterial Hypertension

In recent years, it has become clear that multiple factors influence RV adaptation during a state of chronic pressure overload. These factors are not only important to recognize because of timely treatment escalation, but also because of the emerging possibilities of the RV as treatment target.

A mutation in the Bone Morphogenetic Protein Receptor type 2 (BMPR2) gene is the most common mutation known to cause PAH. A loss-of-function of the BMPR2 mutation in the pulmonary vasculature leads to vasoconstriction and a pro-proliferative state of the endothelial cells and smooth muscle cells. (1) Previously, it has been shown that PAH-patients with a BMPR2 mutation had worse hemodynamics and a lower cardiac index than patients without a BMPR2 mutation.(2,3) In **chapter 2**, we investigated the effects of the BMPR2 mutation on the RV by combining in vivo measurements with molecular and histological analysis of human cardiac tissue. We found that RV function is more severely affected in PAH-patients with a BMPR2 mutation than without, despite a similar afterload. However, these differences could not be explained by a differential transforming growth factor- β (TGF- β), BMPR2 signaling or cardiac morphology.

The prognostic value of a sympathetic overdrive in PH is well-established. (5,6) In left heart failure the beneficial effects of stimulating its counterpart, the parasympathetic nervous system, are reported previously. (7–9) In **chapter 3** we reported that the systemic

parasympathetic nervous system is reduced in PAH, and associated with RV dysfunction. Furthermore, by enhancing parasympathetic activity through acetylcholinesterase inhibition by the oral drug pyridostigmine, we were able to improve survival, RV function and pulmonary vascular remodeling in a sugen/hypoxia rat model of PH.

Despite the fact that PAH predominantly affects females, male patients are known to have a worse survival. Our group has previously shown that this survival difference is explained by a differential RV treatment response in male and female patients. Despite a decrease in PVR in both groups, the right ventricular ejection fraction (RVEF) only increased in female patients and not in male patients. (4) This implicates a role for sex hormones in the pathophysiology of PAH.

Therefore, in **chapter 4**, we tested whether sex hormone expression levels are associated with RV adaptation. In our translational study we combined cross-sectional analyses of sex hormones with histopathological analyses of RV tissue and longitudinal analyses of RV adaptation in male and female PAH-patients. We were able to show that in female and not in male PAH patients androstenedione and testosterone levels were decreased, while DHEA-S levels were reduced in both male- and female patients. At end-stage, the female heart showed to be more severely affected in terms of capillary rarefaction, increased hypertrophy and apoptosis. This suggests, that the female RV is longer able to maintain an increased pressure-overload. Our longitudinal data strengthen this hypothesis, by revealing that females of reproductive age may persevere pressure-overload for a longer time period resulting in a worse RV phenotype at end-stage disease.

To further understand the processes underlying the transition from RV adaptation to RV failure, we summarized distinct RV phenotypes in **chapter 5**. Because even though RV afterload does not differ between PH secondary to Eisenmenger syndrome, PAH secondary to systemic sclerosis and idiopathic PAH, the prognosis is distinctly different. We showed that in an adaptive RV phenotype (as in Eisenmenger patients), is characterized by RV hypertrophy, an increased RV contractility, low RV fibrosis and a low diastolic stiffness. A RV failure phenotype (as in PAH-systemic sclerosis patients), coincides with RV diastolic stiffness, the presence of RV fibrosis and diastolic stiffness.

Part 2 – Novel insights in (assessing) treatment response in pulmonary arterial hypertension

There are several question that remain to be answered regarding monitoring and follow-up of PAH-patients. Regarding the prognostic importance of RV function and volumes, it could be argued that CMR should be the modality of choice to guide treatment decisions. However, in the current guidelines, a right heart catheterization (RHC) is recommended.

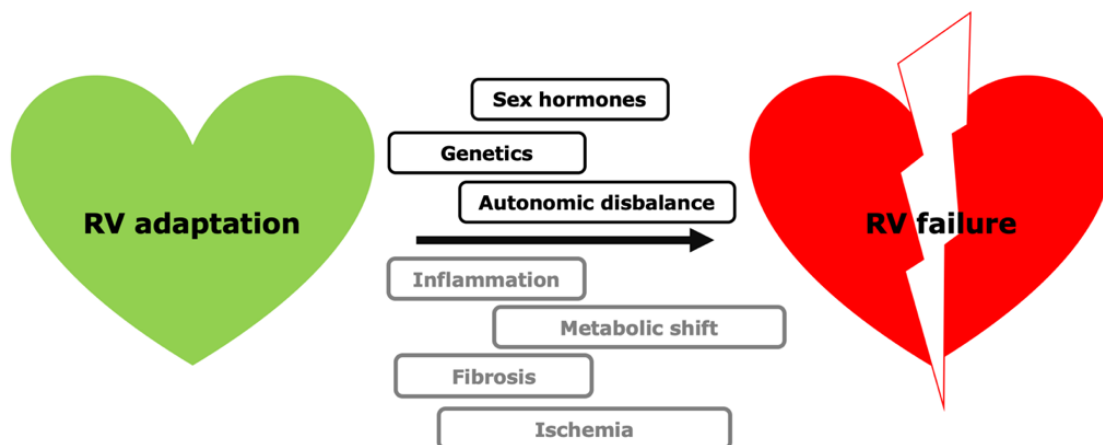
As a first step, in **chapter 6**, we compared non-invasive and invasive risk assessment in PAH-patients during follow-up. We demonstrated that non-invasive risk assessment at 1 year of

follow-up is at least equal to risk assessment based on invasive hemodynamic and functional measurements. These results confirm the clinical value of non-invasive imaging during routine follow-up in PAH.

Patients with idiopathic PAH and a reduced diffusion capacity of the lung for carbon monoxide (DLCO) have a worse survival compared to IPAH patients with a preserved DLCO.(10) Whether this survival difference can be explained by a differential response to PAH-specific medication is unknown. Therefore, in **chapter 7**, we investigated the hemodynamic and cardiac response to PAH-specific medication in IPAH patients with and without a severely reduced DLCO. We concluded that IPAH patients with a severely reduced DLCO show a similar response to PAH-specific medication in terms of hemodynamics, cardiac function and exercise capacity as IPAH patients with a preserved DLCO.

Noninvasive imaging techniques play an essential role in diagnosing PAH and monitoring disease progression. Therefore, in **chapter 8**, we provide an overview of the imaging techniques involved in the diagnostic process and follow-up of PAH patients.

Figure 9.1 – Factors affecting RV adaptation and RV failure, as described in this thesis



FUTURE PERSPECTIVES

The pressure-overloaded right ventricle in pulmonary hypertension

Collecting and connecting the dots.

In the first part of this thesis, we investigated three factors affecting the transition of right ventricular (RV) adaptation towards RV failure. In **chapter 2, 3** and **4**, we respectively investigated the effects of the Bone Morphogenetic Protein Receptor type 2, the reduced parasympathetic activity and role of sex on RV adaptation in pulmonary arterial hypertension (PAH). Obviously, numerous other factors are hypothesized and studied to play a role in this process (figure 1). (11–15) This might be of great interest, as identifying key-players in this RV

adaptation and RV failure might lead to the future development of therapies preserving RV function and halting the progression towards RV failure. However, to eventually develop these new therapies, a better understanding of the chain of events in the transition from RV adaptation towards RV failure is needed. Which process plays a role at what time point? And moreover, are the observed changes in these processes causes, consequences or bystanders in the transition towards RV failure?

As a first step studies large longitudinal cohort studies in PH-patients (of all categorized groups) are warranted. Ideally, these patients would be studied from the date of diagnosis until the occurrence of an event (death or lung transplantation). During the course of disease, patients should undergo a right heart catheterization (RHC), cardiac magnetic resonance imaging (CMR) and venipuncture to obtain biomarkers on regular timepoints with a short time interval (maximum interval: one year). Alongside the standard hemodynamics and pressures collected during RHC, pressure curves should be registered. This way, load-independent measures of RV contractility and RV diastolic stiffness can be determined according to the single-beat method of Sunagawa.(16–18) With the results of these studies, we do not only gain valuable further insights of the transition of RV adaption towards RV failure in the different subgroups, but also can compare the similarities and differences in RV adaptation between the subgroups.

Unfortunately, it is complex to study human RV tissue during the process of RV adaptation towards RV failure. RV tissue of PAH-patients is usually gathered after a combined heart-lung transplant or death and is therefore only representative of RV failure and not RV adaptation. However, there might be a new kid on the block. Our group developed a patient-specific three dimensional cell model from patient derived induced pluripotent stem cells (iPSCs).(19) It would be very interesting to identify the processes occurring in RV-cells during different levels of pressure-overload. As these cells are patient-derived and thus patient-specific, it would be intriguing to compare chronic pressure-overloaded RV-cells of PAH-patients with and without BMPR2 mutations. Furthermore, it would be possible to further compare male and female cardiomyocytes, in line with **chapter 4**. However, whether the results of this complex and time-consuming method can be extrapolated to the pressure-overloaded RV of PAH-patients is yet to be established.

Another interesting technique to obtain further insights in the chain of events in PAH is positron emission tomography (PET-CT). PET-CT makes it possible to detect pathophysiological processes and establish the degree of activity of these processes, using tracers. In example, Ashek et al. recently showed that dynamic ¹⁸FLT PET imaging can be used to report hyperproliferation in the pulmonary vasculature in PAH-patients.(20) Such a tool would allow tailored use of medicine to individual PAH-patients regarding the pulmonary vasculature. However, PET-CT also proved to be of great value to further understand the

transition from RV adaptation towards RV failure. In 2011, Wong et al. were able to demonstrate that oxygen efficiency is reduced in more advanced RV failure, thereby indicating that mitochondrial dysfunction might play a role in the failing RV. (21,22) Other studies, showed that the uptake of free fatty acids is decreased, whereas the uptake of glucose is increased. (23,24)

A promising future application of PET-CT in the field of PH is the use of tracers to image the neurohormonal disbalance in the RV by the use of [11C]-CGP12177 and [11C]-HED as markers. Despite the encouraging results of pre-clinical studies restoring the autonomic disbalance, survival and RV function did not improve in clinical studies. (25–28) Using [11C]-HED as a marker of pre-synaptic adrenergic activity, Rijnierse et al. were able to demonstrate that β -blockage did not affect local RV sympathetic nerve activity, RV wall tension and RV function. (29) Before new treatment studies targeting the neurohormonal disbalance take place, it is of utmost importance to identify which patients would benefit from restoring the sympathetic/parasympathetic balance. For a start, it would be of interest to compare [11C]-CGP12177 and [11C]-HED uptake between PAH-patients with RV adaptation and PAH-patients with RV failure.

Unraveling the remaining questions regarding the Bone Morphogenetic Protein Receptor type 2 Mutation in Pulmonary Arterial Hypertension

The effects of the BMPR2-mutation on RV adaptation

In **Chapter 2** we investigated the effects of the BMPR2 mutation on the RV of PAH-patients. In this study we found that despite a similar afterload, RV function is more severely decreased in PAH-patients carrying a BMPR2 mutation compared to PAH-patients without a BMPR2 mutation. We found no alterations RV adaptation and in in TGF- β and BMP-induced SMAD phosphorylation in the cardiomyocytes of PAH-patients with or without BMPR2 mutation. Pre-clinical studies using a transgenic rodent model of PAH with mutant BMPR2 showed that RV lipotoxicity and fatty acid oxidation impairment might play an important role. (30,31) To eliminate the bias of end-stage human cardiac tissue, the previously mentioned RV three dimensional cell model can be used. It would be interesting to study RV lipotoxicity and fatty acid oxidation on this RV-specific cell model.

The BMPR/TGF- β balance as a potential treatment target

The BMPR2 pathway is not only downregulated in PAH-patients carrying the BMPR2 mutation, but also in PAH-patients without the BMPR2 mutation. (32) This fact makes the BMPR2/TGF- β balance an attractive treatment target. Using an high-throughput screen of nearly 4000 US Food and Drug Administration (FDA)-approved drugs, FK506 (Tacrolimus) was identified as a potent BMPR2 activator. (33) FK506 proved to be safe and well tolerated in PAH-patients, and a preliminary analysis of the randomized controlled trial showed promising results in end-

stage PAH. (34,35) However, the efficacy of FK506 is yet to be established (NCT01647945). Other potential strategies to correct the impaired BMPR2 signaling are the use of chloroquine and BMP9. (36–38) In vitro studies showed that chloroquine increases BMPR2 receptor density at the cell surface by slowing down lysosomal degradation of BMPR2 (chloroquine) and restoring full-length protein (ataluren).(39–41) Future studies should reveal the potential effects of these drugs on pulmonary vascular remodeling and RV adaptation in PAH.

Incomplete penetrance of the BMPR2-mutation

Only 14% of the male and 42% of the female BMPR2 mutation carriers will eventually develop PAH. (42) This incomplete penetrance leads to uncertainty and frustration in BMPR2 mutation carriers and their families. In addition, the incomplete penetrance leads to a reasonable doubt regarding genetic counseling in suspected families. White et al. described investigating the incomplete penetrance as 'looking for a needle in the haystack'.(43) Nowadays, it is hypothesized that a 'second-hit' is needed to decrease the BMPR2 signaling beneath a certain threshold to develop PH.(1) Inflammation, additional gene mutations and sex hormones are named as potential second hits. (44–48) However, large epidemiological studies assessing the incomplete penetrance are lacking. Ideally, a large cohort study should be conducted including all patients diagnosed with the BMPR2 mutation without PAH to determine potential risk factors to develop PAH in BMPR2 mutation carriers.

Naturally, it is also of utmost important to recognize the development of PAH in BMPR2 mutation carriers at an early stage. It is known that BMPR2-mutation carriers developing PAH have an abnormal response of pulmonary artery pressures during exercise.(49,50) Future studies should reveal hemodynamic, RV or biomarkers able to recognize PAH in BMPR2 carriers at an early stage. In our center, the AmsterdamUMC location VU Medical Center, the DOLPHIN-GENESIS study currently includes unaffected BMPR2-mutation carriers with the aim to provide better understanding of the development of pulmonary vascular disease in these patients, using PET-CT, liquid biopsy, cardiopulmonary exercise testing, stress echocardiography, RHC and CMR.

The use of non-invasive imaging in the follow-up of pulmonary arterial hypertension

In the current guidelines, a RHC is recommended to guide treatment decisions during the follow-up of PAH patients.(51) In **Chapter 6**, we found that non-invasive risk assessment at 1 year of follow-up is at least equal to a risk assessment based on invasive hemodynamic measurements. Furthermore, Huis in 't Veld et al. showed that a standardized treatment strategy with RV ejection fraction (RVEF) measured by CMR as treatment goal. If RVEF deteriorated, PAH-specific therapy was escalated. This way, RVEF could be improved and patients remained clinically stable.(52) Moreover, an earlier study of van de Veerdonk et al. showed that changes in RV volumes and RV function are important indicators predicting clinical deterioration.(53) Taking these studies together provides rationale to use CMR in routine clinical care for PAH patients. Future studies should first focus on defining an optimal

CMR-based treatment strategy, after which a randomized controlled clinical trial should be conducted comparing the CMR-based treatment strategy versus the current hemodynamics based strategy. If non-inferior, the CMR-based treatment strategy is preferred regarding its non-invasive nature.

REFERENCES

- Andruska A, Spiekerkoetter E. Consequences of BMPR2 Deficiency in the Pulmonary Vasculature and Beyond: Contributions to Pulmonary Arterial Hypertension. *Int J Mol Sci* [Internet]. 2018 Aug 24 [cited 2019 Nov 20];19(9). Available from: <https://www.ncbi.nlm.nih.gov/pmc/articles/PMC6165502/>
- Brittain EL, Pugh ME, Wheeler LA, Robbins IM, Loyd JE, Newman JH, et al. Shorter survival in familial versus idiopathic pulmonary arterial hypertension is associated with hemodynamic markers of impaired right ventricular function. *Pulm Circ*. 2013 Sep;3(3):589–98.
- Sztrymf B, Coulet F, Girerd B, Yaici A, Jais X, Sitbon O, et al. Clinical outcomes of pulmonary arterial hypertension in carriers of BMPR2 mutation. *Am J Respir Crit Care Med*. 2008 Jun 15;177(12):1377–83.
- Jacobs W, van de Veerdonk MC, Trip P, de Man F, Heymans MW, Marcus JT, et al. The right ventricle explains sex differences in survival in idiopathic pulmonary arterial hypertension. *Chest*. 2014 Jun;145(6):1230–6.
- Naeije R, van de Borne P. Clinical relevance of autonomic nervous system disturbances in pulmonary arterial hypertension. *Eur Respir J*. 2009 Oct;34(4):792–4.
- Ciarka A, Doan V, Velez-Roa S, Naeije R, van de Borne P. Prognostic significance of sympathetic nervous system activation in pulmonary arterial hypertension. *Am J Respir Crit Care Med*. 2010 Jun 1;181(11):1269–75.
- Lataro RM, Silva CAA, Fazan R, Rossi MA, Prado CM, Godinho RO, et al. Increase in parasympathetic tone by pyridostigmine prevents ventricular dysfunction during the onset of heart failure. *Am J Physiol Regul Integr Comp Physiol*. 2013 Oct 15;305(8):R908–916.
- Okazaki Y, Zheng C, Li M, Sugimachi M. Effect of the cholinesterase inhibitor donepezil on cardiac remodeling and autonomic balance in rats with heart failure. *J Physiol Sci JPS*. 2010 Jan;60(1):67–74.
- Durand MT, Becari C, de Oliveira M, do Carmo JM, Silva CAA, Prado CM, et al. Pyridostigmine restores cardiac autonomic balance after small myocardial infarction in mice. *PLoS One*. 2014;9(8):e104476.
- Trip P, Nossent EJ, de Man FS, van den Berk LAH, Boonstra A, Groepenhoff H, et al. Severely reduced diffusion capacity in idiopathic pulmonary arterial hypertension: patient characteristics and treatment responses. *Eur Respir J*. 2013 Dec;42(6):1575–85.
- Dewachter L, Dewachter C. Inflammation in Right Ventricular Failure: Does It Matter? *Front Physiol* [Internet]. 2018 Aug 20 [cited 2019 Nov 22];9. Available from: <https://www.ncbi.nlm.nih.gov/pmc/articles/PMC6109764/>
- van der Bruggen CEE, Tedford RJ, Handoko ML, van der Velden J, de Man FS. RV pressure overload: from hypertrophy to failure. *Cardiovasc Res*. 2017 Oct 1;113(12):1423–32.
- Andersen Stine, Nielsen-Kudsk Jens Erik, Vonk Noordegraaf Anton, de Man Frances S. Right Ventricular Fibrosis. *Circulation*. 2019 Jan 8;139(2):269–85.
- Archer SL, Fang Y-H, Ryan JJ, Piao L. Metabolism and bioenergetics in the right ventricle and pulmonary vasculature in pulmonary hypertension. *Pulm Circ*. 2013;3(1):144–52.
- Talati M, Hemnes A. Fatty acid metabolism in pulmonary arterial hypertension: role in right ventricular dysfunction and hypertrophy. *Pulm Circ*. 2015 Jun;5(2):269–78.
- Sunagawa K, Yamada A, Senda Y, Kikuchi Y, Nakamura M, Shibahara T, et al. Estimation of the hydromotive source pressure from ejecting beats of the left ventricle. *IEEE Trans Biomed Eng*. 1980 Jun;27(6):299–305.
- Brimioulle S, Wauthy P, Ewalenko P, Rondelet B, Vermeulen F, Kerbaul F, et al. Single-beat estimation of right ventricular end-systolic pressure-volume relationship. *Am J Physiol Heart Circ Physiol*. 2003 May;284(5):H1625–1630.
- Rain S, Handoko ML, Trip P, Gan CT-J, Westerhof N, Stienen GJ, et al. Right ventricular diastolic impairment in patients with pulmonary arterial hypertension. *Circulation*. 2013 Oct 29;128(18):2016–25, 1–10.
- Llucà-Valldeperas A, Smal R, Kurakula K, Dijke P ten, Bogaard HJ, Vonk-Noordegraaf A, et al. Development of a patient-specific 3-Dimensional cell model to study right heart failure. *J Mol Cell Cardiol*. 2018 Jul 1;120:48.
- Ashek A, Spruijt OA, Harms HJ, Lammertsma AA, Cupitt J, Dubois O, et al. 3'-Deoxy-3'-[18F]Fluorothymidine Positron Emission Tomography Depicts Heterogeneous Proliferation Pathology in Idiopathic Pulmonary Arterial Hypertension Patient Lung. *Circ Cardiovasc Imaging*. 2018;11(8):e007402.
- Wong YY, Ruiter G, Lubberink M, Raijmakers PG, Knaapen P, Marcus JT, et al. Right ventricular failure in idiopathic pulmonary arterial hypertension is associated with inefficient myocardial oxygen utilization. *Circ Heart Fail*. 2011 Nov;4(6):700–6.
- Wong YY, Westerhof N, Ruiter G, Lubberink M, Raijmakers P, Knaapen P, et al. Systolic pulmonary artery pressure and heart rate are main determinants of oxygen consumption in the right ventricular myocardium of patients with idiopathic pulmonary arterial hypertension. *Eur J Heart Fail*. 2011 Dec;13(12):1290–5.

23. Matsushita T, Ikeda S, Miyahara Y, Yakabe K, Yamaguchi K, Furukawa K, et al. Use of [123I]-BMIPP myocardial scintigraphy for the clinical evaluation of a fatty-acid metabolism disorder of the right ventricle in chronic respiratory and pulmonary vascular disease. *J Int Med Res*. 2000 Jun;28(3):111–23.
24. Nagaya N, Goto Y, Satoh T, Uematsu M, Hamada S, Kuribayashi S, et al. Impaired regional fatty acid uptake and systolic dysfunction in hypertrophied right ventricle. *J Nucl Med Off Publ Soc Nucl Med*. 1998 Oct;39(10):1676–80.
25. Bogaard HJ, Natarajan R, Mizuno S, Abbate A, Chang PJ, Chau VQ, et al. Adrenergic receptor blockade reverses right heart remodeling and dysfunction in pulmonary hypertensive rats. *Am J Respir Crit Care Med*. 2010 Sep 1;182(5):652–60.
26. de Man FS, Handoko ML, van Ballegoij JJM, Schaliij I, Bogaards SJP, Postmus PE, et al. Bisoprolol delays progression towards right heart failure in experimental pulmonary hypertension. *Circ Heart Fail*. 2012 Jan;5(1):97–105.
27. van Campen JSJA, de Boer K, van de Veerdonk MC, van der Bruggen CEE, Allaart CP, Raijmakers PG, et al. Bisoprolol in idiopathic pulmonary arterial hypertension: an explorative study. *Eur Respir J*. 2016;48(3):787–96.
28. Bandyopadhyay D, Bajaj NS, Zein J, Minai OA, Dweik RA. Outcomes of β -blocker use in pulmonary arterial hypertension: a propensity-matched analysis. *Eur Respir J*. 2015 Sep 1;46(3):750–60.
29. Rijniere MT, Groeneveldt JA, van Campen JSJA, de Boer K, van der Bruggen CEE, Harms HJ, et al. EXPRESS: Bisoprolol therapy does not reduce right ventricular sympathetic activity in pulmonary arterial hypertension patients. *Pulm Circ*. 2019 Aug 14;2045894019873548.
30. Talati MH, Brittain EL, Fessel JP, Penner N, Atkinson J, Funke M, et al. Mechanisms of Lipid Accumulation in the Bone Morphogenetic Protein Receptor Type 2 Mutant Right Ventricle. *Am J Respir Crit Care Med*. 2016 15;194(6):719–28.
31. Hemnes AR, Brittain EL, Trammell AW, Fessel JP, Austin ED, Penner N, et al. Evidence for right ventricular lipotoxicity in heritable pulmonary arterial hypertension. *Am J Respir Crit Care Med*. 2014 Feb 1;189(3):325–34.
32. Atkinson Carl, Stewart Susan, Upton Paul D., Machado Rajiv, Thomson Jennifer R., Trembath Richard C., et al. Primary Pulmonary Hypertension Is Associated With Reduced Pulmonary Vascular Expression of Type II Bone Morphogenetic Protein Receptor. *Circulation*. 2002 Apr 9;105(14):1672–8.
33. Spiekerkoetter E, Tian X, Cai J, Hopper RK, Sudheendra D, Li CG, et al. FK506 activates BMPR2, rescues endothelial dysfunction, and reverses pulmonary hypertension. *J Clin Invest*. 2013 Aug;123(8):3600–13.
34. Spiekerkoetter E, Sung YK, Sudheendra D, Scott V, Rosario PD, Bill M, et al. Randomised placebo-controlled safety and tolerability trial of FK506 (tacrolimus) for pulmonary arterial hypertension. *Eur Respir J [Internet]*. 2017 Sep 1 [cited 2019 Nov 22];50(3). Available from: <https://erj.ersjournals.com/content/50/3/1602449>
35. Spiekerkoetter E, Sung YK, Sudheendra D, Bill M, Aldred MA, van de Veerdonk MC, et al. Low-Dose FK506 (Tacrolimus) in End-Stage Pulmonary Arterial Hypertension. *Am J Respir Crit Care Med*. 2015 Jul 15;192(2):254–7.
36. Morrell NW, Bloch DB, ten Dijke P, Goumans M-JTH, Hata A, Smith J, et al. Targeting BMP signalling in cardiovascular disease and anaemia. *Nat Rev Cardiol*. 2016 Feb;13(2):106–20.
37. Sitbon O, Gombert-Maitland M, Granton J, Lewis MI, Mathai SC, Rainisio M, et al. Clinical trial design and new therapies for pulmonary arterial hypertension. *Eur Respir J [Internet]*. 2019 Jan 24 [cited 2019 Nov 22];53(1). Available from: <https://www.ncbi.nlm.nih.gov/pmc/articles/PMC6351342/>
38. Morrell NW, Aldred MA, Chung WK, Elliott CG, Nichols WC, Soubrier F, et al. Genetics and genomics of pulmonary arterial hypertension. *Eur Respir J [Internet]*. 2018 Jan 1 [cited 2019 Dec 22]; Available from: <https://erj.ersjournals.com/content/early/2018/10/11/13993003.01899-2018>
39. Drake KM, Dunmore BJ, McNelly LN, Morrell NW, Aldred MA. Correction of nonsense BMPR2 and SMAD9 mutations by ataluren in pulmonary arterial hypertension. *Am J Respir Cell Mol Biol*. 2013 Sep;49(3):403–9.
40. Dunmore BJ, Drake KM, Upton PD, Toshner MR, Aldred MA, Morrell NW. The lysosomal inhibitor, chloroquine, increases cell surface BMPR-II levels and restores BMP9 signalling in endothelial cells harbouring BMPR-II mutations. *Hum Mol Genet*. 2013 Sep 15;22(18):3667–79.
41. Long L, Ormiston ML, Yang X, Southwood M, Gräf S, Machado RD, et al. Selective enhancement of endothelial BMPR-II with BMP9 reverses pulmonary arterial hypertension. *Nat Med*. 2015 Jul;21(7):777–85.
42. Larkin EK, Newman JH, Austin ED, Hemnes AR, Wheeler L, Robbins IM, et al. Longitudinal analysis casts doubt on the presence of genetic anticipation in heritable pulmonary arterial hypertension. *Am J Respir Crit Care Med*. 2012 Nov 1;186(9):892–6.
43. White R, James, Morrell Nicholas W. Understanding the Low Penetrance of Bone Morphogenetic Protein Receptor 2 Gene Mutations. *Circulation*. 2012 Oct 9;126(15):1818–20.
44. Fessel JP, Chen X, Frump A, Gladson S, Blackwell T, Kang C, et al. Interaction between bone morphogenetic

protein receptor type 2 and estrogenic compounds in pulmonary arterial hypertension. *Pulm Circ.* 2013 Sep;3(3):564–77.

45. Austin ED, Cogan JD, West JD, Hedges LK, Hamid R, Dawson EP, et al. Alterations in oestrogen metabolism: implications for higher penetrance of familial pulmonary arterial hypertension in females. *Eur Respir J.* 2009 Nov;34(5):1093–9.

46. Cogan Joy, Austin Eric, Hedges Lora, Womack Bethany, West James, Loyd James, et al. Role of BMPR2 Alternative Splicing in Heritable Pulmonary Arterial Hypertension Penetrance. *Circulation.* 2012 Oct 9;126(15):1907–16.

47. Viales RR, Eichstaedt CA, Ehlken N, Fischer C, Lichtblau M, Grünig E, et al. Mutation in BMPR2 Promoter: A “Second Hit” for Manifestation of Pulmonary Arterial Hypertension? *PLoS One.* 2015;10(7):e0133042.

48. Eichstaedt C, Song J, Viales RR, Benjamin N, Harutyunova S, Fischer C, et al. Clinical manifestation of hereditary pulmonary arterial hypertension by a “second hit” mutation in the genes BMPR2 and EIF2AK4. *Eur Respir J [Internet].* 2016 Sep 1 [cited 2019 Nov 22];48(suppl 60). Available from: https://erj.ersjournals.com/content/48/suppl_60/PA1885

49. Trip P, Vonk-Noordegraaf A, Bogaard HJ. Cardiopulmonary exercise testing reveals onset of disease and response to treatment in a case of heritable pulmonary

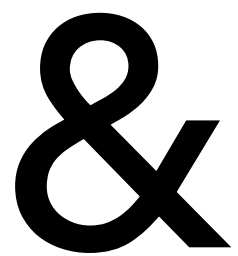
arterial hypertension. *Pulm Circ.* 2012 Jul;2(3):387–9.

50. Grünig E, Janssen B, Mereles D, Barth U, Borst MM, Vogt IR, et al. Abnormal pulmonary artery pressure response in asymptomatic carriers of primary pulmonary hypertension gene. *Circulation.* 2000 Sep 5;102(10):1145–50.

51. Galiè N, Humbert M, Vachiery J-L, Gibbs S, Lang I, Torbicki A, et al. 2015 ESC/ERS Guidelines for the diagnosis and treatment of pulmonary hypertensionThe Joint Task Force for the Diagnosis and Treatment of Pulmonary Hypertension of the European Society of Cardiology (ESC) and the European Respiratory Society (ERS): Endorsed by: Association for European Paediatric and Congenital Cardiology (AEPC), International Society for Heart and Lung Transplantation (ISHLT). *Eur Heart J.* 2016 Jan 1;37(1):67–119.

52. Huis In 't Veld AE, Van de Veerdonk MC, Spruijt O, Groeneveldt JA, Marcus JT, Westerhof N, et al. EXPRESS: Preserving right ventricular function in patients with pulmonary arterial hypertension: single centre experience with a cardiac magnetic resonance imaging-guided treatment strategy. *Pulm Circ.* 2019 Jan 11;2045894018824553.

53. van de Veerdonk MC, Marcus JT, Westerhof N, de Man FS, Boonstra A, Heymans MW, et al. Signs of right ventricular deterioration in clinically stable patients with pulmonary arterial hypertension. *Chest.* 2015 Apr;147(4):1063–71.



NEDERLANDSE SAMENVATTING
LIST OF PUBLICATIONS
CURRICULUM VITAE
DANKWOORD

Cathelijne E.E. van der Bruggen

NEDERLANDSE SAMENVATTING

Pulmonale arteriële hypertensie is een ziekte die wordt gekenmerkt door progressieve vernauwing van de kleine longvaten. Door deze vernauwing is er sprake van een hogere weerstand van het longvaatbed, wat dientengevolge weer leidt tot een verhoogde druk (hypertensie) aldaar. De vernauwing van de kleine longvaten wordt veroorzaakt door een combinatie van abnormale proliferatie (vermenigvuldiging), hypertrofie (toename in grootte) en vasoconstrictie (het samenknijpen van de longvaten). De cellen die dit met name veroorzaken zijn de cellen die direct in contact staan met de bloedstroom (endotheelcellen) en de gladde spiercellen die zich één laag daaronder bevinden.

De rechterhartkamer heeft als functie het zuurstofarme bloed dat vanuit het lichaam terugstroomt door te pompen naar de longen, zodat daar opnieuw zuurstof kan worden opgenomen. Door de verhoogde druk in het longvaatbed ontstaat er een toegenomen werkdruk voor de rechterhartkamer. Hierdoor wordt er minder bloed per tijdseenheid door de longen gepompt, waardoor er een verminderde toevoer van bloed en dus zuurstof aan de weefsels van het lichaam ontstaat. Patiënten met pulmonale arteriële hypertensie ervaren hierdoor klachten van vermoeidheid, flauwvallen en kortademigheid (bij inspanning).

De rechterhartkamer zal bij blootstelling aan de hoge drukken diverse aanpassingsmechanismen gebruiken. In eerste instantie zal er wandverdikking plaatsvinden (hypertrofie), waardoor er meer knijpkracht zal ontstaan. Na verloop van tijd zal dit compensatiemechanisme tekort schieten en vindt er verwijding (dilatie) plaats van de rechterhartkamer. Deze verwijding is een voorloper van het uiteindelijke falen van het rechterventrikel, met overlijden tot gevolg. De prognose van patiënten met pulmonale arteriële hypertensie wordt dan ook grotendeels bepaald door de functie van de rechterhartkamer, terwijl het eigenlijk een ziekte is die zich primair in de longen bevindt. Daarom is het van belang meer inzicht te verkrijgen in de aanpassing van de rechterhartkamer bij pulmonale arteriële hypertensie patiënten.

Deel 1; Aanpassingen van de rechterhartkamer in pulmonale arteriële hypertensie

Het belang van de rechterhartkamer in pulmonale arteriële hypertensie is al veel beschreven. Hierbij is naar voren gekomen dat het voor de prognose van de patiënt minder belangrijk is in welke mate de druk in het longvaatbed verhoogd is, maar wel hoe de rechterkamer hierop reageert. Zo heeft een deel van de patiënten een licht verhoogde druk in het longvaatbed maar een hevig aangedane rechterhartkamer, en heeft een ander deel een sterk verhoogde druk in het longvaatbed maar nog een goed functionerende rechterhartkamer. Het doel van **deel 1** van dit proefschrift is dan ook om meer inzicht te verkrijgen in het aanpassingsvermogen van de rechterhartkamer, en welke factoren hierop van invloed zijn.

In **hoofdstuk 2** kijken we naar de effecten van de BMPR2-mutatie op de functie van de rechterhartkamer. De BMPR2-mutatie is de meest voorkomende genetische mutatie in pulmonale hypertensie patiënten. In aangedane families heeft circa 80% een mutatie in het BMPR2-gen, en in de algemene populatie pulmonale arteriële hypertensie patiënten heeft 11-40% de BMPR2- mutatie. Patiënten met een BMPR2-mutatie krijgen op jongere leeftijd de ziekte, en vaak in ernstigere mate. Tevens hebben zij een slechtere prognose dan patiënten zonder BMPR2-mutatie. In dit hoofdstuk vergelijken we de functie van de rechterhartkamer in patiënten met en zonder mutatie. We laten zien dat patiënten met BMPR2-mutatie, ondanks dat zij dezelfde verhoogde drukken als patiënten zonder BMPR2-mutatie hebben, toch een slechtere rechterhartfunctie hebben. Om uit te zoeken wat hieraan ten grondslag ligt is er op microscopisch en moleculair niveau gekeken naar hartspiercellen van overleden of getransplanteerde pulmonale arteriële hypertensie patiënten.

Hoofdstuk 3 richt zich op de rol van het autonoom (onwillekeurig) zenuwstelsel in pulmonale arteriële hypertensie. Het autonoom zenuwstelsel bestaat uit twee delen; 1) het sympathisch zenuwstelsel, dat het lichaam zodanig beïnvloedt dat er activiteiten kunnen worden verricht (het zogenaamde '*gaspedaal*' of '*fight or flight*' mechanisme), en 2) het parasympathisch zenuwstelsel, dat het lichaam zodanig beïnvloedt dat er rust en herstel kan plaatsvinden ('*rempedaal*'). Bij pulmonale arteriële hypertensie patiënten is er sprake van overactiviteit van het sympathisch zenuwstelsel. In het begin van de ziekte is dit voordelig, want deze reactie zorgt er in het begin voor dat het hart tegen de verhoogde drukken in kan pompen. Op de lange termijn zorgt deze overactiviteit echter voor een slechtere overleving. In dit hoofdstuk laten we zien dat de verminderde activiteit van het parasympathisch zenuwstelsel een negatief effect heeft op de rechterhartkamer. Dit werd bevestigd met onderzoek van harten van overleden of getransplanteerde pulmonale arteriële hypertensie patiënten. Tevens laten we zien dat het medicamenteus stimuleren van het parasympathisch zenuwstel een positief effect heeft op de rechterkamerfunctie bij een diermodel (ratten) met pulmonale hypertensie.

Pulmonale arteriële hypertensie is een ziekte die tweemaal zo vaak voorkomt bij vrouwen ten opzichte van mannen. De overleving van mannen is echter significant slechter dan die van vrouwen. Uit onderzoek blijkt dat dit komt door een verminderd aanpassingsvermogen van de rechterhartkamer. In **hoofdstuk 4** werd in een groot Nederlands cohort gekeken naar geslachtshormonen en rechterhartfunctie. Ook werd er gekeken naar hartspiercellen van mannelijke en vrouwelijke pulmonale arteriële hypertensie patiënten. We vonden een link tussen mannelijke geslachtshormonen (androgenen) en een slechtere rechterhartkamer bij mannelijke pulmonale arteriële hypertensie patiënten. Daarnaast liet onderzoek naar hartspiercellen van overleden of getransplanteerde pulmonale arteriële hypertensie patiënten een ernstiger beeld zien (meer celdood en meer verdwenen longvaten) bij vrouwelijke patiënten dan bij mannelijke patiënten. Dit wekt de suggestie dat ondanks dat de vrouwelijke

rechterhartkamer langer met een sterk verhoogde druk in het longvaatbed kan omgaan, maar bij overlijden of transplantatie dan wel een ernstiger aangedaan beeld laat zien.

In **hoofdstuk 5** vergeleken we middels een literatuuroverzicht verschillende aanpassingsmechanismen van de rechterhartkamer bij een verhoogde werkdruk. In dit overzicht proberen we inzicht te verkrijgen in het proces van een aangepaste rechterhartkamer naar een falende rechterhartkamer. Waarom faalt de rechterhartkamer bij de ene patiëntengroep snel, en bij de andere groep niet? Om antwoord op deze vraag te krijgen kijken we naar drie verschillende soorten pulmonale hypertensie, met allemaal dezelfde mate van een verhoogde druk in het longvaatbed, maar met zeer verschillende prognoses. We laten zien dat een goed aangepaste rechterhartkamer, zoals gezien wordt bij pulmonale hypertensie patiënten met het Eisenmenger syndroom, wordt gekenmerkt door een goede knijpkracht, hypertrofie, weinig verlittekening en goede vullings-mogelijkheden. Een slecht aangepaste hartkamer, zoals gezien wordt bij pulmonale hypertensie patiënten met sclerodermie, wordt gekenmerkt door weinig reserve in knijpkracht, verlittekening en een verhoogde stijfheid.

Deel 2; Nieuwe inzichten in het (verkrijgen van het) effect van de behandeling en de monitoring hiervan in pulmonale arteriële hypertensie

Hoewel het aanpassingsvermogen van de rechterhartkamer de prognose van pulmonale arteriële hypertensie patiënten bepaalt, zijn er op dit moment geen medicijnen beschikbaar die direct effect hebben op de rechterhartkamer. De huidige beschikbare medicatie richt zich op het verminderen van de druk in het longvaatbed door het verwijderen van de longvaten. Tot nu toe is er geen medicijn gevonden dat de ziekte kan genezen.

In **deel 2** van dit proefschrift wordt gekeken naar de effecten van de huidige behandelmethodes op de rechterhartkamer. Tevens wordt er onderzocht hoe deze effecten van behandeling het beste kunnen worden gemonitord.

Tot op heden is de gouden standaard voor zowel de diagnose als de verdere monitoring van pulmonale arteriële hypertensie een rechterhart-katheterisatie. Gedurende dit invasieve onderzoek wordt er middels een katheter via de hals of lies de druk gemeten in de rechterhartkamer en de longvaten. Daarnaast vindt er in gespecialiseerde centra een MRI van het hart plaats, om op deze manier zowel de functie als de verwijding van de rechterhartkamer te meten. In **hoofdstuk 6** tonen wij aan dat alleen een MRI van het hart gedurende de follow-up van pulmonale arteriële hypertensie patiënten evenveel prognostische informatie geeft als zowel een MRI én een rechterhart-katheterisatie samen.

In **hoofdstuk 7** richten wij ons op pulmonale arteriële hypertensie patiënten met een verminderde zuurstof opnamecapaciteit van de longen (DLCO). De zuurstof opnamecapaciteit van de longen wordt met name beïnvloed door de dikte en het oppervlakte

van het membraan waarover het zuurstoftransport plaatsvindt. Voorbeelden van ziekten die zorgen voor een verminderde zuurstof opnamecapaciteit zijn longfibrose en longemfyseem. Bij pulmonale arteriële hypertensie is de zuurstof opnamecapaciteit meestal normaal. In een groeiende groep patiënten wordt echter een sterk verlaagde zuurstof opnamecapaciteit gevonden. Deze groep patiënten heeft een slechtere overleving dan pulmonale arteriële hypertensie patiënten met een goede zuurstof opnamecapaciteit. Of dit deels wordt verklaard door een slechtere respons op de huidige pulmonale arteriële hypertensie medicatie was voorheen niet bekend. Wij vonden in deze studie dat deze patiënten zowel in hartfunctie als in longvaat-drukken hetzelfde reageerden op de vaatverwijders. Ook ondervonden deze patiënten geen nadelige effecten van de vaatverwijders qua zuurstofgehalte in het bloed, waardoor er geen reden is om patiënten met pulmonale arteriële hypertensie en een lage zuurstof opnamecapaciteit deze medicatie te onthouden.

In **hoofdstuk 8** wordt een overzicht gegeven van de huidige beeldvormende technieken die gebruikt worden bij de diagnose en monitoring van pulmonale hypertensie.

Concluderend laat dit proefschrift zien dat er verschillende factoren een rol spelen in het aanpassingsvermogen van de rechterhartkamer op de verhoogde drukken ten gevolge van de vernauwing van de kleine longvaten. Verder onderzoek zal moeten uitwijzen of de mechanismen die hieraan ten grondslag liggen kunnen worden gebruikt als aangrijpingspunt voor nieuwe medicijnen die kunnen zorgen voor een betere overleving voor deze patiënten. Daarnaast hebben we laten zien dat in de toekomst een invasief onderzoek zoals een rechterhartkatheterisatie mogelijk minder frequent noodzakelijk is bij de monitoring van pulmonale arteriële hypertensie patiënten door het gebruik van een MRI van het hart. Verder onderzoek is hiervoor nodig.

LIST OF PUBLICATIONS

Interplay of sex hormones and long-term right ventricular adaptation in a Dutch pulmonary arterial hypertension cohort – van Wezenbeek J*, Groeneveldt* & Llucià-Valdeperas*, **van der Bruggen CE**, Jansen SMA, Smits AJ, Smal R, van Leeuwen R, dos Remedios C, Keogh A, Humbert M, Dorfmueller P, Mercier O, Guignabert C, Niessen HWM, Handoko ML, Marcus JT, Meijboom LJ, Oosterveer FPT, Westerhof BE, Heijboer AC, Bogaard HJ, Vonk Noordegraaf A, Goumans MJ, de Man FS. Submitted

The value of hemodynamic measurements or cardiac MRI in the follow-up of patients with idiopathic pulmonary arterial hypertension – **van der Bruggen CE**, Handoko ML, Bogaard HJ, Marcus JT, Oosterveer FPT, Meijboom LJ, Westerhof BE, Vonk Noordegraaf A, de Man FS. Chest 2020

Bisoprolol therapy does not reduce right ventricular sympathetic activity in pulmonary arterial hypertension patients – Rijnierse MT, Groeneveldt JA, van Campen JSJA, de Boer K, **van der Bruggen CE**, Harms HJ, Raijmakers PG, Lammertsma AA, Knaapen P, Bogaard HJ, Westerhof BE, Vonk Noordegraaf A, Allaart CP, de Man FS. Pulmonary Circulation 2020

Right ventricular load and function in chronic thromboembolic pulmonary hypertension: Differences between proximal and distal chronic thromboembolic pulmonary hypertension – Ruigrok D, Meijboom LJ, Westerhof BE, Huis in 't Veld AH, **van der Bruggen CE**, Marcus JT, Nossent EJ, Vonk Noordegraaf A, Symersky P, Bogaard HJ. American Journal of Respiratory and Critical Care Medicine 2019

Contribution of impaired parasympathetic activity to right ventricular dysfunction and pulmonary vascular remodeling in pulmonary arterial hypertension – Bos D, **van der Bruggen CE**, Kurakula K, Xiaoqing S, Casali KR, Casali AG, Rol N, Szulcek R, dos Remedios C, Guignabert C, Dorfmueller P, Humbert M, Goumans MJ, Bogaard HJ, Vonk-Noordegraaf A, de Man FS, Handoko ML. Circulation 2018

Right ventricular pressure overload; from hypertrophy to failure – **van der Bruggen CE**, Tedford RJ, ML Handoko, van der Velden J, de Man FS. Cardiovascular research 2017

Treatment Response in patients with idiopathic pulmonary arterial hypertension and a severely reduced diffusion capacity – **van der Bruggen CE**, Spruijt OA, Nossent EJ, Trip P, de Man FS, Marcus JT, Bogaard HJ, Vonk Noordegraaf A. Pulmonary Circulation 2017

The real face of Borderline Pulmonary Hypertension in Connective Tissue Disease – **van der Bruggen CE**, Nossent EJ, Grünberg K, Bogaard HJ, Vonk Noordegraaf A. Ann Am Thorac Soc 2016

Response by van der Bruggen et al to Letter Regarding Article, “Bone Morphogenetic Protein Receptor Type 2 Mutation in Pulmonary Arterial Hypertension: ‘A view on the right ventricle’” – **van der Bruggen CE**, Happé CM, Goumans MJ, Bogaard HJ, Vonk Noordegraaf A, de Man FS. Circulation 2016

Bisoprolol in idiopathic pulmonary arterial hypertension: an explorative study – van Campen JSJA, de Boer K, van de Veerdonk MC, **van der Bruggen C**, Allaart CP, Raijmakers PG, Heymans MW, Marcus JT, Harms HJ, Handoko ML, de Man FS, Vonk Noordegraaf A, Bogaard HJ. Eur Respir J. 2016

Assessment of right ventricular systolic function in patients with precapillary pulmonary hypertension using simple echocardiographic parameters: a comparison with cardiac magnetic resonance imaging - Spruijt OA, Di Pasqua MC, Bogaard HJ, **van der Bruggen C**, Oosterveer F, Marcus JT, Vonk-Noordegraaf A, Handoko ML. Journal of Cardiology 2016

Bone Morphogenetic Protein Receptor Type 2 Mutation in Pulmonary Arterial Hypertension, A view on the Right Ventricle – **van der Bruggen C**, Happé CM, Dorfmueller P, Trip P, Spruijt OA, Rol N, Hoevenaars FP, Houweling AC, Girerd B, Mercier O, Humbert M, Handoko ML, van der Velden J, Vonk Noordegraaf A, Bogaard HJ, Goumans MJ, de Man FS. Circulation 2016

Pulmonary hypertension; from diagnosis to monitoring. – **van der Bruggen C**, Spruijt OA, Meijboom LJ, Vonk Noordegraaf A. ERS Monograph Imaging 2016

Clinical relevance of right ventricular diastolic stiffness in pulmonary hypertension. – Trip P, Rain S, Handoko ML, **van der Bruggen C**, Bogaard HJ, Marcus JT, Boonstra A, Westerhof N, Vonk-Noordgraaf A, de Man FS. Eur Respir J. 2015

Characteristics of Pulmonary Arterial Hypertension in affected carriers of a mutation located in the cytoplasmic tail of bone morphogenetic protein receptor type 2. – Girerd B, Coulet F, Jaïs X, Eyries M, **van der Bruggen C**, de Man F, Houweling A, Dorfmueller P, Savale L, Sitbon O, Vonk-Noordegraaf A, Soubrier F, Simonneau G, Humbert M, Montani D. Chest 2015

ORAL PRESENTATIONS

2016 - Thalys-meeting, Paris, France

2014 - ATS (American Thoracic Society), San Diego, United States of America

2014 - TGF- β meeting, Leiden, The Netherlands

2014 - Thalys-meeting, Paris, France

2013 - Cardiac Function & Adaptation course, Nederlandse Hartstichting -Papendal, The Netherlands

POSTER PRESENTATIONS

2016 - GSK scientific seminar 'Connecting expertise in a rare disease' – Copenhagen, Denmark

2016 - Amsterdam Cardiovascular Sciences Symposium, Amsterdam, The Netherlands

2016 - ATS (American Thoracic Society), San Francisco, United States of America

2015 - AHA (American Heart Association), Orlando, United States of America

2015 - ERS (European Respiratory Society), Amsterdam, The Netherlands

2014 - Rembrandt Symposium of the Rembrandt Institute of Cardiovascular Science, Leiden, The Netherlands

2013 - Rembrandt Symposium of the Rembrandt Institute of Cardiovascular Science, Leiden, The Netherlands

2013 - ERS (European Respiratory Society), Barcelona, Spain

DANKWOORD

Na 8.5 jaar is het moment eindelijk daar; ik mag het dankwoord gaan schrijven! Iets waar ik lang naar uitgekeken heb; want wat is het een voorrecht om juist op deze meest gelezen pagina's van dit (gedrukte) proefschrift iedereen te mogen bedanken die direct én indirect aan de totstandkoming van dit proefschrift heeft bijgedragen. De tijd dat ik aan dit proefschrift heb mogen werken was een onvergetelijke, leerzame en soms ook moeilijke tijd, die ik voor geen goud had willen missen.

Als eerste een woord van dank aan de patiënten met deze relatief zo onbekende ziekte. De patiëntendagen, 'Heb Hart voor Longen' weekenden en het contact gedurende de MRI-avonden hebben mij altijd enorm gemotiveerd en geïnspireerd. Jullie kracht en doorzettingsvermogen zijn een voorbeeld voor velen.

Prof. dr. A. Vonk Noordegraaf, beste Anton. Zo'n tien jaar geleden, het moet midden 2011 geweest zijn, mocht ik bij jou op sollicitatiegesprek komen voor een baantje als student-assistent. Dat we een decennium later nu hier zouden staan, had ik op dat moment nog niet durven hopen. Onder jouw vleugels promoveren (en misschien ook wel een beetje volwassen worden) was een uiterst goede leerschool waar ik nog elke dag profijt van heb. Ik bewonder jouw passie, betrokkenheid en vechtlust voor patiënten, snelle denken, oneindige stroom ideeën, fysiologisch redeneren en kritische blik enorm. Niet zelden liep ik na onze onderzoeksbespreking jouw kamer uit in een staat van verwarring, lichte paniek en tegelijkertijd enthousiasme over de nieuwe ideeën. Uiteindelijk heeft het tot hele mooie resultaten geleid waar we trots op kunnen zijn! Dank voor het vertrouwen, het geduld en betrokkenheid!

Dr. F.S. de Man, lieve Frances. Mijn dank voor jou is niet in een paar zinnen uit te drukken; daar zou weer een nieuw boekje voor nodig zijn (maar laten we dat maar niet doen..). Maar misschien is het eigenlijk ook wel heel simpel; zonder jou was dit boekje er niet. Heel af en toe komt er iemand op je levenspad die de wegen daarna verandert, en voor mij ben jij dat. Jij geloofde in mij lang voordat ik dat zelf deed en hebt mij altijd heel veel vertrouwen gegeven, en daar ben ik je ontzettend dankbaar voor. En wat hebben we samen veel bereikt! Met jouw visie, doorzettingsvermogen, perfectionisme en wil om altijd het hoogste te bereiken kun je bergen verzetten en ik denk dat we dat bijvoorbeeld met ons BMPR2-stuk ook wel een beetje gedaan hebben. Ik heb genoten van ons samenwerken; je directheid, je les dat extra moeite altijd de moeite waard is, je kritische blik (zonder pokerface), het werken aan onze gezamenlijke passie voor goede figuren, maar vooral het aan één blik genoeg hebben (binnen en buiten werk). Maar buiten al deze inhoudelijke kwaliteiten ben je bovenal een van de liefste personen die ik ken. Je bent er ontzettend voor me geweest in moeilijke tijden, maakte elke werkdag samen een fijne dag en daarnaast hebben we samen ook veel bijzondere momenten gedeeld. De komst van Lizzy en Björn, de trip naar Orlando, de champagne in Parijs, de prosecco in de Mahler, etentjes met Louis en Chris en onze talloze rondjes.. Ik kijk uit naar onze nieuwe avonturen, met dit boekje dan rustig in de kast. Time to *let it go!*

Prof. dr. H.J. Bogaard, beste HJ. Vanaf het allereerste begin ben ik ontzettend blij dat je zo betrokken bent geweest bij mijn PhD-traject. Jouw positiviteit, enthousiasme, vriendelijkheid, pragmatische instelling en snelle en volledige commentaren op manuscripten zijn op meerdere fronten van grote waarde geweest. Dank!

De leden van de promotiecommissie. Prof. Dr. Chamuleau, Prof. dr. Velthuis, dr. van Balkom, dr. Bartelds en dr. Altenburg; veel dank voor het kritisch lezen van het manuscript en het plaats willen nemen in de promotiecommissie. Prof. dr. S. Kawut, thank you for participating in the reading committee.

Emeritus prof. dr. Westerhof, beste Nico. Uw betrokkenheid bij mijn PhD-traject beschouw ik als een groot voorrecht. Het grootse enthousiasme over de fysiologie en de wetenschap zelf, en met name de wil om elk getal in de resultaten écht te begrijpen is ontzettend waardevol en leerzaam geweest. Veel dank!

Dr. B. Westerhof, beste Berend. Wat was ik blij met jouw toevoeging aan het begeleidingsteam! Jouw vriendelijkheid, rust, laagdrempeligheid en originele invalshoek maakten de laatste loodjes in het VUmc nog aangenamer.

Dr. M.L. Handoko, beste Louis. Soms op de voorgrond, maar nog vaker op de achtergrond, ben je nauw betrokken geweest bij elk artikel in dit boekje. Dankjewel voor je betrokkenheid, cardiologische blik op het geheel, je hulp en gezelligheid.

Prof. dr. Goumans, beste MJ. Je bent een inspiratie voor hoe je als powervrouw toch altijd warm en betrokken kan blijven. Dank voor je tips, wijsheden en gezelligheid gedurende borrels!

Dr. J.T. Marcus, beste Tim. Bijna elke MRI die voor de onderzoeken in dit boekje is gebruikt, is door jou gemaakt. Op de vele dinsdag- en woensdagavonden die we achter het bedieningspaneel gependend hebben, heb ik veel van je mogen leren over de oneindige mogelijkheden van een cardiale MRI. Dank daarvoor.

Dr. L.J. Meijboom, beste Lilian. Dank voor de nieuwe input, expertise en gezelligheid!

CVON-PHAEDRA collega's, bedankt voor de samenwerking en gezellige PHAEDRA-dagen en weekendjes! Vooral de pikdonkere fietstocht van het enige (open) kroegje op Terschelling terug naar het hotel zal ik niet snel vergeten.

Frank, Martha en Iris; het dreamteam. Jullie zorg, passie en kennis van én voor PH-patiënten is ongeëvenaard. Martha en Iris, jullie maakten het werk op 3F altijd gezellig, om over de fantastische 'Heb Hart voor Longen' weekenden nog niet eens te spreken. Inmiddels hebben jullie je vleugels uitgeslagen naar de andere ziekenhuizen die Amsterdam rijk is, en ik wens jullie daar ontzettend veel succes! Frank, na meer dan duizend rechterhart katheterisaties ben je nog steeds net zo betrokken, oprecht geïnteresseerd, enthousiast en lief voor patiënten en PhD-studenten. Door jou heb ik zelfs een zekere sympathie voor AZ gekregen, en blijf ik ze volgen - ook al zit ik nu veilig onder de rivieren.

Beste **Ella, Ellen en Anny**. Dank voor alle administratieve hulp! Bij jullie kun je altijd terecht met allerlei problemen, en of het nu 'bloedspoed' heeft of niet.. uiteindelijk wordt het altijd opgelost. Ella, dank ook voor de mooie tijd bij de 'Inspiratie'!

Beste **Jasmijn**, mijn wetenschappelijke stage begon bij jou; met een project over PET-scans in de bèta-blokkerstudie. Nadat je me in mijn rolstoel naar een twijfelachtige uithoek van de medische faculteit had gereden, kon daar het gevecht met MATLAB en alle foutmeldingen beginnen. Ondanks dit alles ben ik mede door jouw enthousiasme toch besmet geraakt met het onderzoeksvirus. Dank daarvoor! Binnenkort weer een White Russian?

Stafleden en arts-assistenten van de afdeling Longziekten in het VUmc, dank voor de vele onderwijsmomenten en de gezelligheid. Daarnaast dank de mooie en leerzame tijd gedurende mijn semi-arts stage! Wat is het fijn om in zo'n veilige en inspirerende omgeving de eerste klinische stappen te zetten.

Dr. A. Boonstra, beste Anco. Ik kijk met heel veel plezier terug op de onderwijsmomenten, grote visites en de PH-meetings waar jij bij betrokken was. Jouw persoonlijke betrokkenheid bij patiënten en liefde voor longfysiologie blijven erg aanstekelijk.

Bart, dankjewel dat ik jouw plekje op 6D mocht innemen. Je hebt me in mijn eerste dagen als student-assistent met veel geduld geholpen met het leren herkennen van de verschillende drukcurves, waardoor het leven daarna een stuk makkelijker werd. Dank voor de mooie borrels, gezelligheid en weekendjes Berlijn en Gent!

Esther, wat bewonder ik je om je enorme kennis, perfectionisme, wilskracht en betrokkenheid. Bedankt voor de hele gezellige en leerzame samenwerking - maar meer nog voor de wijze lessen over de liefde en het leven met een glaasje wijn in de hand.

Dieuwertje, dankjewel voor de gezelligheid en de samenwerking! Ik ben erg onder de indruk van hoe je het onderzoek combineert met het klinische werk en hoe je in korte tijd zo ontzettend veel voor elkaar hebt gekregen. Ik hoop tot snel!

*Glory days well they'll pass you by,
Glory days in the wink of a young girl's eye
Glory days, glory days*

Bruce Springsteen, Born in the USA - 1984

Ik denk dat Bruce in deze zinnen de essentie van de jaren aan de Boelelaan perfect heeft gevangen - ze zijn voorbij gevlogen. Collega's werden vrienden, vrijdagmiddagborrels escaleerden niet zelden en congressen ontaardden in de mooiste verhalen. Er zijn vele onderzoekers gekomen en gegaan; maar enkele wil ik toch persoonlijk benoemen.

Als eerste mijn kamergenootjes op 6D, Paul, Pia en Justine.

Justine, hipster avant la lettre, harde werker en vooral heel fijn mens, ik heb genoten van je gezelligheid, nuchterheid, humor en relativiseringsvermogen. Bedankt voor de hele mooie tijd!

Paul, 'grote broer', en vooral grootste man met het kleinste hartje - wat hebben we een supermooie tijd gehad. Onze goede gesprekken over het leven en het werk als iedereen al naar huis was, je ham-kaas croissantjes van de bakker en met name jouw vermogen om van

het leven een feest te maken zijn fantastisch. Hoogtepunten waren de buckets bij Edel, je connecties in de Bubbels, je vis-op-het-droge zijn in het trollendoolhof en in de Suicide Circus in Berlijn, je tree met tequila-shotjes na een minstens 16-uur durende reis naar San Diego en als klap op de vuurpijl enkele dagen later onze wellicht niet geheel nuchtere zoektocht naar feestartikelen in de plaatselijke supermarkt om 5 uur 's nachts. Wat is het mooi dat de dromen waar we zo vaak over gefilosofeerd hebben nu voor een groot deel aan het uitkomen zijn! Door jou heb ik BHD altijd in mijn DD staan.

Mijn eerste kamergenootjes op 3F; Onno, Hans en later Anna.

Beste **Hans** aka 'the Voice', wat fijn dat jij kwam! Jouw stemgeluid was het enige wat mijn toonhoogte kon neutraliseren, ook dank namens de burens daarvoor! En hoewel Onno om duistere redenen het predikaat 'goed met computers' kreeg, ben jij de enige die daarvoor echt in aanmerking komt.

Onno/Onnie - one of the very good guys, de enige man met een eigen dansmove, katerkoning en ouwe hipster, weinig mannen hebben het zoveel uren in één kleine ruimte met mij volgehouden. Respect daarvoor. Je zou kunnen denken dat mijn stemgeluid in combinatie met jouw soms matige articulatie zou kunnen leiden tot een moeizame communicatie, maar ik denk dat we toch kunnen concluderen dat dit meer dan goed gekomen is. Vanaf het eerste moment was het vertrouwd en ik heb jouw adviezen, rust, humor en gezelligheid altijd enorm gewaardeerd. Elk willekeurig congres, weekendje weg of borrel heeft wel geleid tot een mooi verhaal, of dit nu een plotselinge bestorming van een VIP-podium was of het eindigen in een willekeurige Valenciaanse huiskamer. Dank voor alle good times, binnen maar eigenlijk ook vooral buiten muren van het VUmc. Ik kan niet wachten op een nieuwe borrel!

Anna, hoewel jouw frisse wind en daadkracht in het begin misschien wat overweldigend waren hebben we na een korte adaptatieperiode ontzettend veel gelachen en een heel gezellige tijd gehad – zowel binnen als buiten werk. Jouw enthousiasme en doorzettingsvermogen is enorm, waardoor je ook in recordtijd je boekje af hebt gekregen! Dank dat je altijd een luisterend oor wilde zijn voor alle onderzoekspirikelen, dat heeft ontzettend geholpen!

Dan 'The Dark Side' – de tweede ronde op 3F. Onno en Hans waren vertrokken, en Anna was verhuisd. Gelukkig kwamen daar twee nieuwe roomies; **Adinda en Gwen**. Het was in mijn laatste onderzoeksjaar; ook wel bekend als het jaar waarin het meest moet gebeuren – onder de grootste tijdsdruk. Het had dus erg ongezellig kunnen worden. Gelukkig was dit alles behalve het geval. Adinda; op het gebied van voedselintake en fysieke beweging zijn we nogal tegenpolen. Gelukkig op veel andere vlakken niet! Heel mooi dat ook jij nu je boekje klaar hebt! Gwennie, jouw kwaliteiten om een plant in leven te houden en de theevoorraad te beheren zijn ongekend. En samen klagen is zoveel beter dan alleen! Thanks voor de mooie tijd guys!

Lieve **AL**, homie aan de andere kant van de gipsplaat. We hebben het af en toe zwaar te verduren gehad met alle fitgirls om ons heen. Zelfs jij, met je shinende tenniscarrière, werd niet altijd serieus genomen qua sportiviteit. Gelukkig hadden wij andere kwaliteiten,

waaronder op het terras of in de Mahler zitten met een witte wijn. Dankjewel voor al het aanhoren, kletsen en vooral alle gezelligheid!

Lieve **Eveline**, jij begon zo ongeveer met je PhD toen ik al weg was, en wat is het dan toch extra bijzonder dat we dat laatste tijd zo naar elkaar toe gegroeid zijn! Eindelijk iemand die ook alle eredivisie-wedstrijden volgt (al is het dan vanaf 'de verkeerde kant'), ook kan genieten van obscure sporten bij Studio Sport, een wereldvoorraad memes heeft én met name ook een grote voorliefde heeft voor de après-ski playlist! *Lalalalalala baby give it up, give it up...* Ik hou van je energie, de fles in je bureau-la voor het eerste vrijmibo shotje, wijsheden en vooral je vriendschap (#samesies)! Dank!

Ik wil ook graag de andere (oud-)klinische onderzoekers en collega's van 3 en 4F heel erg bedanken voor de samenwerking en goede tijd; **Suzan, Luuk, Jurjan, Azar, Chermaine, Jelco, Jeroen, Jessie, Josien, Liza, Mariëlle, Natalia, Romane, Samara en Wouter**. En natuurlijk mag de pre-klinische kant hier niet bij ontbreken: **Deni** (Queen of Caipirinha's), **Michiel, Emmy, Robert, Sun, Pan, Rowan, Sylvia, Silvia, José en Babu**. Thanks!

En dan denk ik aan Brabant....

Na al die tijd boven de rivieren was de tijd gekomen om terug te keren naar het land waar de G geen pijn aan je oren doet en het bourgondische leven hoogtij viert.

Als eerste wil ik **prof. dr. Smeenk, dr. van Balkom, dr. Wielders, drs. Aldenkamp, dr. van den Borne, dr. J. Creemers, drs. Schakenraad, drs. Rietdijk en alle long-assistenten van het Catharina Ziekenhuis** bedanken. Vanaf het eerste moment heeft het werken in Eindhoven als een warm bad gevoeld en dat komt vooral door de zeer laagdrempelige sfeer, het teamgevoel en de persoonlijke betrokkenheid. Daarnaast is er altijd interesse geweest voor 'mijn boekje'. Dank daarvoor! Ook wil ik jullie heel erg bedanken voor de steun na mijn val op onze ski-reis (na welgeteld 4 uur op Oostenrijkse bodem). De dierenavond zullen we nog steeds een keer moeten inhalen! Jullie bezoek in het ziekenhuis, de autorit naar het vliegveld, de vlucht naar huis (speciale dank voor dr. van Balkom) en de enorme betrokkenheid daarna heeft veel voor mij betekend!

De maatschap Interne Geneeskunde en alle arts-assistenten; bedankt voor de fantastische tijd tot nu toe! De geweldige ski-reis (deze keer zonder botbreuken), vrijmibo's en het enorme groepsgevoel (wat alleen maar werd versterkt gedurende de COVID-periode) maakten dat ik afgelopen jaar elke dag met veel plezier naar werk ben gegaan. Wat een fijne groep mensen! Dank voor de steun en betrokkenheid, ook toen mijn fysieke gestel het tijdelijk liet afweten!

Oh, I get by with a little help from my friends

Mm, I get high with a little help from my friends

Mm, gonna try with a little help from my friends

- Beatles, Sgt. Pepper's Lonely Hearts Club Band, 1967

Ook al kan ik niet iedereen bij naam noemen, ik wil ook zeker een paar 'matties' buiten de muren van het VUmc bedanken voor hun afleiding en luisterend oor.

Team Zachte G

Lieve **Karlijn, Vivian en Lisette** – we go way back. Ik vind het zo leuk en bijzonder om elkaar volwassen te hebben zien worden en iedereen zijn eigen pad te zien vinden in het leven. En ook al worden veel dingen anders, de belangrijkste dingen veranderen gelukkig nooit! Dankjewel voor jullie luisterend oor en de vele mooie momenten! Liefde!

Lieve **Carina**, het is nu bewezen dat vriendschap op het eerste gezicht bestaat –een gemeenschappelijke geschiedenis helpt hier alleen maar bij. Gelukkig hebben we nog veel meer gemeenschappelijk. Dankjewel voor de puppy-liefde, tennisavondjes, de heerlijke avondjes aan de borrel of met BZV, en vooral voor je vriendschap. Lieve **Michelle/Mies**, tennis- en wijnmattie. Onze ABBA-avond was zonder twijfel een van de mooiste avonden van 2020. Ik hoop snel te genieten van je balkonlampje! Lieve **Lisanne/Lies**, de Jut van m'n Jul. Het is een feest om met jou te werken, te borrelen en je altijd fosfaat te zien suppleren. Op naar meer! Ook nog even speciale dank aan **Michelle, Sophie en Marion** – de beste collega's en vrijmi-maatjes die je wensen kan!

Lieve VVO, lieve **Marjolein** aka Lama, **Caïa** en **Sylvester** – grootste levensgenieters en Bourgondiërs van Eindhoven en omstreken. Na twee weken vooropleiding zaten we om voor mij nog steeds onduidelijke redenen samen in een app-groepje en was besloten dat we vrienden waren. Daar ben ik nog steeds dagelijks gelukkig om! Sharing is caring is naar een nieuw niveau getild, er is meer dan eens gehuild (of getuft, Lama) van het lachen, maar jullie waren er ook zomaar ineens voor me toen het leven wat moeilijker was én bij de laatste loodjes van dit boekje. Dat waardeer ik echt enorm!

Lieve **Milou**, dat een bijzondere gemeenschappelijke patiënt, een paar vrij inefficiënte maar erg gezellige ochtendvisites en een beetje 'Savage Love' tot deze vriendschap zou leiden.. dat hadden we denk ik allebei niet verwacht. Vanaf moment één zit het goed en wat is het leuk om zo veel gemeen te hebben, het leven af en toe van een heel andere kant te bekijken en van dezelfde dingen te genieten (behalve AYNIL dan). Dankjewel voor de hele fijne gesprekken (gemiddelde duur: 8 uur), je inzichten en je kritische blik bij de Nederlandse Samenvatting. Ik kijk uit naar onze toekomstige avonturen! (en misschien echt een keer een serie kijken?)

Team boven de Rivieren

Lieve **Joanne**, we hebben elkaar ontmoet op de allereerste dag van de studie en vanaf toen had het lot ons aan elkaar verbonden. Meerdere gezamenlijke studiegroepjes, een bijzondere verpleegstage en 2x per toeval op dezelfde etage in Uilenstede wonen later, was het maar goed dat we toch al besloten hadden vriendinnen te worden. Wat is het bijzonder dat we daarna ook nog eens beiden student-assistent werden van de PH-onderzoeksgroep en dat we daarna allebei aan een promotie-avontuur begonnen. Het was heel fijn en vertrouwd om dit allemaal te kunnen delen. Samen hebben we inmiddels veel mooie en onvergetelijke momenten meegemaakt en ik ben ervan overtuigd dat er nog vele zullen volgen. Onze vriendschap is me heel dierbaar!

Lieve **Yvette en Maartje** aka de 1.60 clan. Dank voor de gezelligheid en de steun tijdens de theetjes en lunches in Utrecht en omgeving. Wat is het fijn om vriendinnen te hebben die precies door dezelfde promotie-struggles gaan!

Lieve **Madde**, coschap-vriendin van het eerste uur maar nog veel belangrijker; mijn allerfavorietste vrijmibo-maatje. Hoe de week ook was, als het vrijdag vier uur-bieruur was en we met een Félix in de hand zaten, was alles meteen vergeten. Ik kan nog altijd nagenieten van alle verhalen met bijbehorende foto's, maar ik kijk ook enorm uit naar het creëren van nieuwe. Thanks voor de good times en het er zijn tijdens de bad times! En heel veel succes met jouw PhD, superleuk dat je ook onderweg bent!

Lieve **Esther**, heel veel succesvolle en minder succesvolle culturele uitspattingen later weet ik nog steeds niet wat ons grootste talent is. Ik weet ook niet of dat nu juist een goed of een slecht teken is. Dank voor alle afleidende wijntjes, etentjes en fijne avonden.

Chris, waar een memorabel nachtje in de Opium in Barcelona wel niet toe kan leiden! We hebben ons PhD-traject voor een groot deel samen doorlopen, en ik kan zeker zeggen dat je daarin mijn steun en toeverlaat bent geweest. *'Life begins at the end of your comfort zone'*; maar in deze spreuk is zeker geen rekening gehouden met mijn lab-avontuur met de kleuringen voor de BMPR2 studie. Het woord 'life' zou je in dit geval voor vele woorden kunnen vervangen, maar ik denk dat 'crying' het meest toepasselijk zou zijn. Door jouw positiviteit, vindingrijkheid en vooral vermogen om alles gezellig te maken is het toch nog goed gekomen en ik ben heel trots op het resultaat! En of het nu gaat om congressen, roadtrips (Florida!), oneindige vrijdagmiddagborrels, feestjes, avondjes Paradiso of Tivoli of om grootse plannen maken; met jou is alles leuker! Op naar nog vele homemade pizza's, tripjes en concerten!

'Dancing queens, young and sweet, only seventeen (++++)'

Lieve ~~cocktail, champagne,~~ drankvriendinnen, lieve **Pia, Gerrina & Lonneke**. Onze vriendschap is misschien wel het mooiste en meest waardevolle gevolg van mijn onderzoekstijd. Zoals Willeke Alberti, Paul de Leeuw en Lonneke weleens zingen; *'Samen zijn, is samen lachen, samen huilen, leven door dicht bij elkaar te zijn'*, en ik denk dat onze vriendschap zo perfect wordt samengevat. Met jullie is het leven een feest, of we nu een cocktailavond hebben, on tour zijn, minstens 5 uur in het ABBA-museum doorbrengen of wanneer we voor de zoveelste keer chagrijnig worden aangekeken in een random restaurant of café vanwege onze decibellen (fijn om een groepje vriendinnen te hebben waarin mijn lach zeker niet de meest luidruchtige is). Maar nog meer waardeer ik dat jullie er altijd voor me zijn, bij elke breakdown of tegenslag, onafhankelijk van tijd of afstand. Zonder jullie was alles anders, en daar kan ik jullie niet genoeg voor bedanken!

Lieve **Lonny**, Thank God dat je nog één plekje over had op je sociaal-leven-vriendenlijst! Ik werd zomaar ineens in jullie cocktailgroepje opgenomen voor ons champagne-tripje, en vanaf de eerste minuut waren we vriendinnen; alsof het nooit anders was geweest. Dankjewel voor de enorme hulp gedurende de moeilijke momenten (ik hoef hier mijn huisje maar rond te kijken..), gebrek aan pokerface wanneer ik dat nodig had, lieve kaartjes en vooral alle good

times. Jij bent de grootste doorzetter die ik ken en kijk heel erg uit naar alles wat de toekomst ons gaat brengen!

Lieve **Sherry**, hoewel jij initieel telkens als ik op 6D kwam werken ineens ging thuiswerken, is het gelukkig toch nog goed gekomen! En hoe! Want wat is er beter dan samen het leven vieren met een vrouw die de meest indrukwekkende drankkast van heel de Vinex en wijde omgeving heeft, en ook nog eens een eigen cocktail heeft? (de 'Pornstar Gerrini' welteverstaan) Onze dagen en avondjes (samen met Geert) zijn altijd een feest. En als jij achter mijn keuzes staat, voelt het altijd beter. Ik ben blij dat dat vertrouwen wederzijds is, en dat ik op onze vakantie vorig jaar zo ongeveer twee uur in Der Wagen mocht rijden (☺). Je weet ook niet half hoe ik het waardeer dat je altijd zo enorm voor me klaar staat. En als jij erbij bent heb ik altijd het idee dat alles goed komt, dus ik ben ontzettend blij dat je naast me wil staan op deze dag! *The winner takes it all!*

Lieve **Pi**, in 2011 begon dit avontuur als jouw student-assistent. Na daarna jouw wetenschappelijke stage-student te zijn geweest, werden we collega's en uiteindelijk vriendinnen (al was ik daar wat eerder van overtuigd dan jij, ik wist dat maar aan onze respectievelijk Groningse en Brabantse inborst..). Wat is het een geluk om iemand te vinden die zo hetzelfde in het leven staat en die zo van dezelfde (kleine) dingen kan genieten! En over genieten gesproken.. het eindeloos dansen in Buenos Aires, de full Rio experience, de nachttrein in Moskou, roadtrippen in Andalusië en California of onze 'retraites' – het zijn stuk voor stuk memories for a lifetime! Maar waar we ook zijn, het concept is hetzelfde; een wijntje - de lekkerste hapjes van de kaart - drie keer met onze ogen knipperen en dan is ineens het restaurant/café leeg, gaan de lichten aan en is er weer een avond voorbij gevlogen. Zonder jouw kritische vragen, matig enthousiaste reacties op menig van mijn eigen ideeën ('tsja, je moet het zelf weten') en enorme steun gedurende de 'lows' zou dit boekje niet zijn wat het nu is geworden. Ik geniet enorm van je eerlijkheid, (tijdelijk) zeer belangrijke principes en overtuigingen, onze reisjes en belevenissen, onze creatieve hobby's, onze gesprekken, maar boven alles van jouw vriendschap – want ik ken niemand met een groter hart dan jij. Op naar alle nieuwe highs, lows en in between!

De bakermat

Lieve **Sandra en Mat**, jullie zijn me ontzettend dierbaar. Dankjewel voor alle kaartjes, appjes en natuurlijk de fijne herinneringen.

Lieve **familie**, bedankt voor alle betrokkenheid, gezelligheid en afleiding. Ik kijk er nu al naar uit dat de Landdagen en neven- en nichtjesweekenden weer kunnen plaatsvinden!

Lieve **Jan**, jij overleed in mijn onderzoekstijd. Dat er zes jaar later bij de 'Eeuwig Licht'-actie in het Philips Stadion nog meerdere lichtjes voor jou brandden zegt denk ik genoeg; je wordt niet vergeten. Lieve **Roel**, dat er eerder een boek over mij was dan door mij komt door jou; en dat blijft voor altijd!

Lieve **Querine**, *you changed my ways.*

Dit is een (t)huis waar liefde woont

- Guus Meeuwis, Morgen 2015

Lieve **papa en mama** / het fundament, zonder jullie was ik nergens. Ondanks jullie drukke levens en carrières hebben jullie ons altijd op de eerste plaats gezet en ons een hele warme en veilige thuishaven gegeven. Jullie hebben mij altijd alle vrijheid en kansen gegeven om me te kunnen ontwikkelen tot wie ik nu ben, al was en is het soms een uitdaging om een vrij eigenwijze dochter te hebben. Gelukkig maken de daarbij horende discussies al mijn keuzes meer beargumenteerd en krijgen ze daardoor meer waarde. Ik hou van jullie!

Lieve **mama**, wat is het bijzonder om zowel als longarts in spé als nu met deze promotie in jouw voetsporen te mogen treden. Ik hoop dat ik nog in vele opzichten, op professioneel en nog belangrijker op persoonlijk gebied, jouw voorbeeld mag volgen. Dankjewel voor je buitengewone liefde, enorme betrokkenheid, het altijd al tien stappen vooruit denken en les dat je als je iets maar écht wilt, je dat kan bereiken. Lieve **papa**, *ik lijk steeds meer op jou*. Wat is het bijzonder om iemand te hebben die zo hetzelfde in elkaar zit en waarmee je dezelfde hobby's en passies kan delen. Dankjewel dat je er al bijna 30 jaar echt áltijd voor me bent.

Lieve **Phil**, grote kleine broer, maar vooral grootste held; jij bent alles wat ik niet ben en daar bewonder ik je enorm om. Al sinds jongs af aan zijn we twee handen op één buik en dat is altijd zo gebleven. Ik ben heel dankbaar dat je zo dicht bij me staat en vind het superbijzonder hoe jij altijd voor anderen en ook voor mij klaar staat – in het geval van alle promotie-perikelen, maar ook in alle andere aspecten van het leven. Dat betekent ontzettend veel voor mij! Ik ben zo trots op jou!

Dan last but not least **mijn oma's**, aan wie dit boekje is opgedragen. Het is een groot voorrecht dat jullie al zo lang deel uitmaken van mijn leven en dat ik jullie zo goed heb mogen leren kennen. Jullie zijn het ultieme voorbeeld van (veer)kracht, betrokkenheid, doorzettingsvermogen, eigenwijsheid, humor en warmte. In jullie tijd was het niet vanzelfsprekend dat je als vrouw mocht 'doorstuderend', maar jullie hebben me vaak verteld dat jullie dit zo ontzettend graag hadden gedaan. Dat ik hier op deze dag mag staan is dan ook door én voor jullie. Liefde!

CURRICULUM VITAE

On the 5th of October, 1991, Cathelijne Emma Elisabeth van der Bruggen was born in the small town of Veghel, the Netherlands. After completing secondary school (cum laude) at the Dr. Knippenbergcollege in Helmond, she left Noord-Brabant behind and started medical school at the Vrije Universiteit in Amsterdam. After obtaining her bachelor of medicine and having worked as a nursing aid at the Viecuri hospital in Venlo, Cathelijne decided to pursue her PhD before continuing her training to become a medical doctor. In May 2013, she started her PhD in the field of Pulmonary Hypertension under the supervision of Frances de Man, Harm Jan Bogaard and Anton Vonk Noordegraaf. In 2017 she continued her medical training and obtained her degree in August 2019. Directly after graduation Cathelijne started working as a resident at the department of Pulmonary Medicine of the Catharina Ziekenhuis in Eindhoven under supervision of prof. dr. Smeenk and dr. van Balkom. In December 2019, she started her training to become a pulmonologist at the Catharina Ziekenhuis at the department of Internal Medicine under supervision of dr. Konings and dr. Ammerlaan.

